Client: Nederlandse Aardolie Maatschappij

Arup Project Title: Groningen 2013

Seismic Risk Study - Earthquake Scenario-Based Risk Assessment

REP/229746/SR001

Issue | 29 November 2013

Job number 229746
External ref EP201311204035

Arup bv
PO Box 57145
1040 BA
Amsterdam
The Netherlands
www.arup.com

ARUP

Contents

Appendices

Executive Summary

Introduction and Aim of This Report

This report presents the results of an earthquake scenario-based seismic risk assessment undertaken by Arup for NAM to investigate the risk to buildings and the life safety of building occupants associated with induced seismicity in the Groningen region of the Netherlands.

This report forms part of a wider scope of services related to the structural upgrading strategy for buildings in the Groningen region, described in a series of reports by Arup (2013).

- Structural Upgrading Strategy [1];
- Seismic Risk (this report);
- Structural Upgrading Study [2]; and
- Implementation Study [3].

The seismic risk study is in support of the required studies outlined in the letter of Minister Kamp to the Dutch Parliament of 11 February 2013.

Scenario Earthquake Risk Assessment Methodology

For this risk assessment a study area has been defined that covers the Groningen gas field. A database has been compiled for buildings in this study area along with the simplified engineering characteristics for each building, estimated usage of the buildings, estimated occupancy rates and a preliminary interpretation of their potential seismic fragility . There are approximately 250,000 buildings in the study area with a total population of approximately 500,000 with approximately 200,000 people in the city of Groningen alone.

Four earthquake scenarios have been considered:

- A magnitude M_w =5 earthquake;
- A magnitude M_w =3.6 earthquake;
- A magnitude M_w =4 earthquake; and
- A magnitude M_w =4.5 earthquake.

An earthquake scenario of $M_w \geq 5$ in this report is estimated to have a probability of occurring of less than 10% in the next 10 years[1]. The smaller magnitude earthquakes have higher probabilities of occurring in the Groningen area.

---

[1] NAM indicates: *"The 'Report to the Technical Guidance Committee (TBO) on Production Measures; Part 1: Depletion Scenarios and Hazard Analysis' reports that although considerable progress was made in the understanding of the seismic hazard, significant uncertainty remains at present. The predictions of the seismic hazard range are believed to be conservative and NAM has initiated a further data acquisition program to obtain additional field data, and a studies program to reduce the uncertainty. A Mw≥5 earthquake scenario in this report is estimated to have a probability of occurring of less than 10% in the next 10 years.*

Further datagathering and further studies in the next years will be executed in order to reduce the uncertainty range and may well in the future further reduce the hazard. For example, it is expected

For each of these earthquake scenarios the distribution of ground shaking hazard in terms of peak horizontal ground acceleration (PGA) has been determined. The distribution and amplitude of the ground shaking and the relevant fragility functions that are assigned to each building are then used to estimate the amount of potential building damage in the study area. Building damage is classified into five damage states: slight damage (DS1), moderate damage (DS2), extensive damage (or substantial to heavy) (DS3), complete (or very heavy) damage (DS4), and collapse (or destruction) (DS5). The distribution and numbers of buildings damaged (to each damage state) is then summarised and reported.

There is a strong correlation between the level of building damage and the expected number and severity of injuries to the occupants of the buildings. Therefore the number of buildings in each damage state and the population in each of the buildings is used to estimate the potential number and severity of casualties in an earthquake scenario. Casualties are classified into four levels: SL1 injuries which require basic medical aid; SL2 injuries which require greater medical care but are not life threatening; SL3 injuries are life threatening if not treated; and SL4 injuries in which an individual is mortally injured or instantaneously killed.

The earthquake scenario risk assessment results presented in this report provide an estimate of what could happen in a number of single possible future earthquakes of given magnitudes in the Groningen region. The scenario assessments do not provide an estimate of the cumulative damage and casualties that could potentially arise from all possible future induced earthquakes during the life of the gas field and after.

Scenario Earthquake Risk Assessment Results

The numbers of buildings estimated to be damaged to different damage states (DS1 to DS5) in each of the four main earthquake scenarios (M_w =3.6, 4, 4.5 and 5) using median PGA ground motion input values are summarised in Figure 1.

that geomechanical studies, explicitly modelling faults, can demonstrate a physical upper bound to the maximum magnitude."

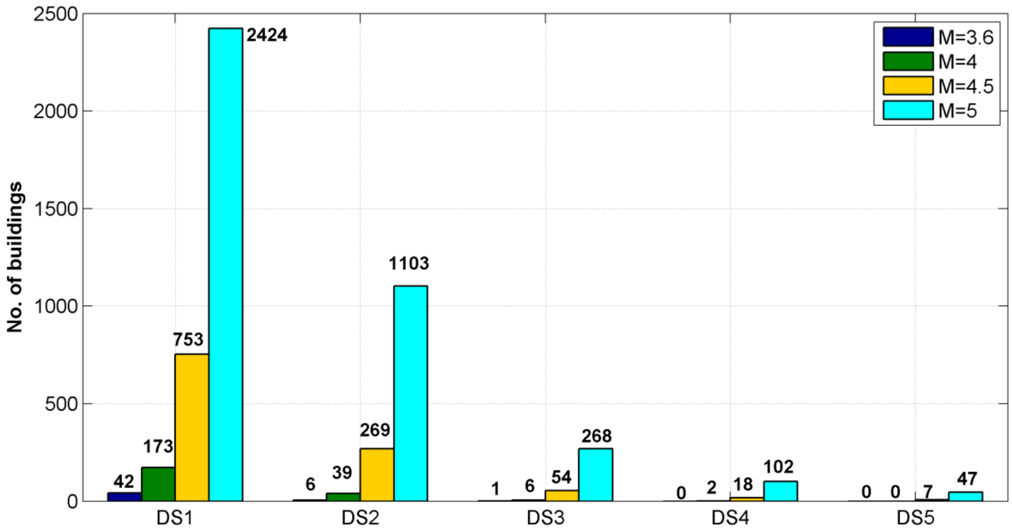

Figure 1 Summary of estimated number of buildings damaged to each damage state (DS1to DS5) for earthquake scenarios with magnitude M_w =3.6, 4, 4.5 and 5 using median (50th percentile) PGA input values.

The estimated number of buildings that will potentially be damaged is expected to increase significantly with increasing magnitude of the earthquake. For a smaller magnitude earthquake, such as the M_w=4 earthquake scenario, it is expected that hundreds of buildings will be slightly damaged, tens of buildings will be moderately damaged and less than 10 buildings will be extensively damaged. In the event of an earthquake of magnitude M_w =5, it is expected that thousands of buildings will be slightly or moderately damaged, hundreds of buildings extensively to completely damaged and approximately 50 buildings will collapse.

The number of potential casualties that are estimated to be caused by each of these scenario earthquakes is also expected to increase significantly with increasing magnitude. The numbers of casualties estimated to occur in each of the four main earthquake scenarios (M_w =3.6, 4, 4.5 and 5) are summarised in Figure 2 below. For a smaller magnitude earthquake, such as a M_w =4 earthquake scenario, it is expected that 2 or 3 people will be injured. In the event of an earthquake of magnitude M_w =5, it is expected that approximately one hundred people will potentially be injured with almost ten life threatening injuries or direct fatalities.

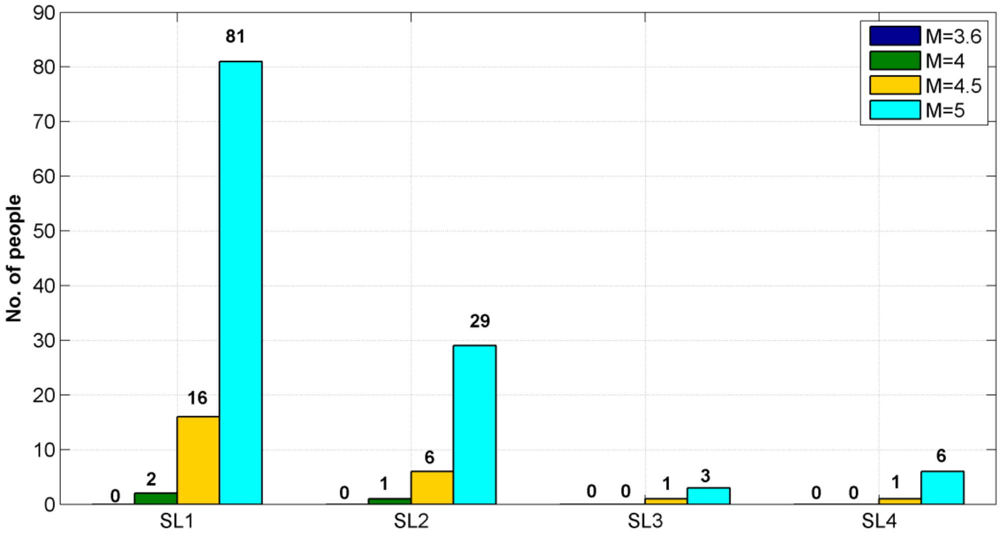

Figure 2 Summary of estimated number of casualties to severity of injury (SL1to SL4) for earthquake scenarios with magnitude M_w =3.6, 4, 4.5 and 5 using median (50th percentile) PGA input values.

It is emphasised that these risk assessment results are preliminary and work is still in progress. There are very significant uncertainties in the input parameters to the risk assessment calculations. There are significant uncertainties in seismic hazard ground motion PGA values, the fragility functions assigned to the buildings and therefore the estimation of the amount of potential building damage and also uncertainty in the estimation of casualties given the expected levels of building damage. Considerable effort is on-going through research and development tasks to reduce the uncertainty in all areas.

In order to investigate the potential impact of these large uncertainties on the risk assessment calculation results a series of sensitivity analyses have been undertaken and the findings from these sensitivity analyses are also described in the report. The sensitivity analyses include investigation of the effect of the uncertainty and spatial variability of the seismic hazard ground motion PGA values (16th and 84th percentiles). Sensitivity analyses have also been undertaken to investigate the effect of assigning different fragility functions to account for the uncertainty in the performance of the Groningen region building stock under seismic ground shaking. In particular, the effect of use of alternative fragility functions to account for the potential effect of shorter duration ground shaking on the expected level of building damage has been investigated.

The numbers of buildings estimated to be damaged to different damage states (DS1 to DS5) in each of the four main earthquake scenarios (M_w =3.6, 4, 4.5 and 5) using uniformly higher 84th percentile PGA ground motion input values (rather than the median or 50th percentile PGA values) are summarised in Figure 3. The estimated numbers of damaged buildings using this uniformly higher level of PGA is significantly higher but cannot be considered unrealistically high at this stage. These analyses do serve to emphasise how sensitive the results are to changes in input values.

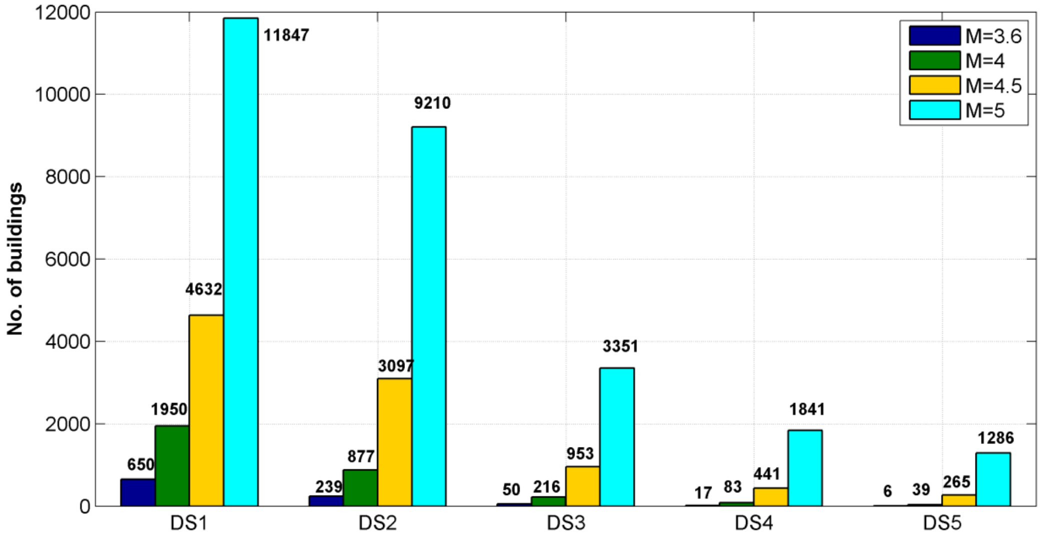

Figure 3 Summary of number of buildings damaged to each damage state (DS1to DS5) for earthquake scenarios with magnitude M_w =3.6, 4, 4.5 and 5 using 84th percentile (median +1 sigma) PGA input values.

The number of potential casualties that are estimated to be caused by each of the scenario earthquakes but using the uniformly higher 84th percentile PGA ground motion input values (rather than the median or 50th percentile PGA values) are summarised in Figure 4. The estimated numbers of casualties is also significantly higher but cannot be considered unrealistically high.

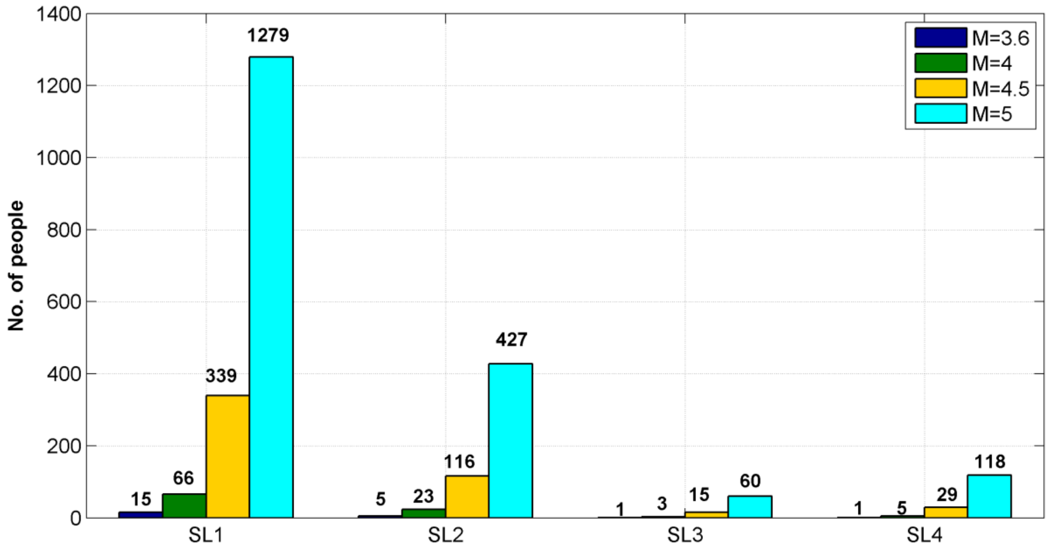

Figure 4 Summary of estimated number of casualties to severity of injury (SL1to SL4) for earthquake scenarios with magnitude M_w =3.6, 4, 4.5 and 5 using 84th percentile (median +1 sigma) PGA input values.

Sensitivity analyses have also been undertaken to investigate the effect of assigning different fragility functions to account for the uncertainty in the performance of the Groningen region building stock under seismic ground shaking. Three sets of fragility functions are used. The Arup fragility functions are based on empirical damage statistics from earthquakes elsewhere in the world calibrated for the Groningen region building stock. The fragility functions adopted by Pinho and Crowley use shake table test data from elsewhere in the world calibrated for the Groningen region building stock (Pinho and Crowley "unmodified"). Pinho and Crowley also developed fragility functions amended to account for the potential effect of small magnitude earthquake / short duration ground motions on the performance of Groningen region building stock (Pinho and Crowley "duration modified"). The comparison of the number of buildings that are estimated to be damaged in an earthquake scenario with M_w=5 using the median or 50th percentile PGA values and the higher 84th percentile PGA values and with the different fragility function sets are summarised in Figure 5 and Figure 6.

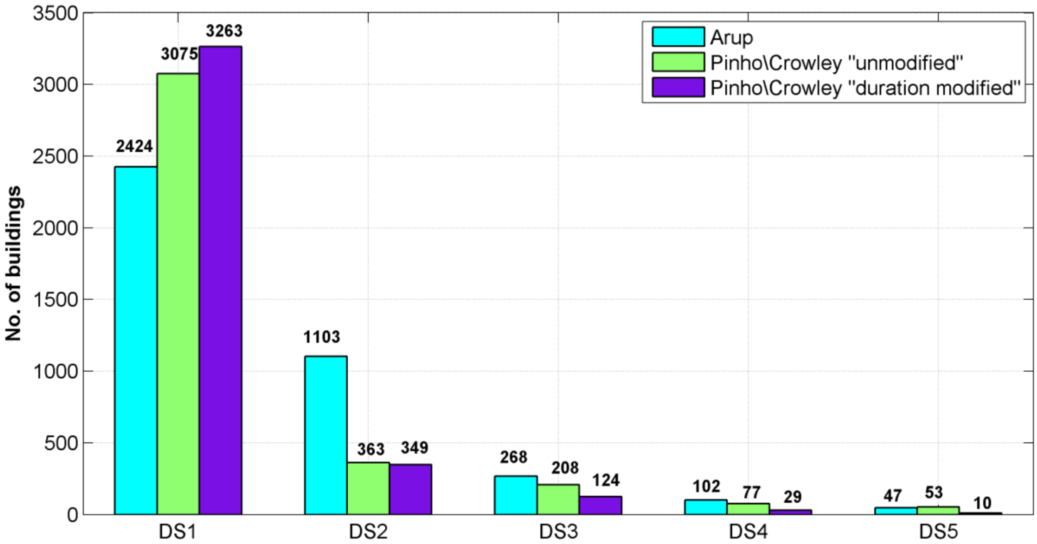

Figure 5 Summary of estimated number of buildings damaged to each damage state (DS1to DS5) for an earthquake scenario with magnitude M_w = 5 using median (50th percentile) PGA input values and comparing the results obtained using different sets of fragility functions proposed by Arup, Pinho and Crowley "unmodified" and Pinho and Crowley "duration modified" for Groningen region building stock.

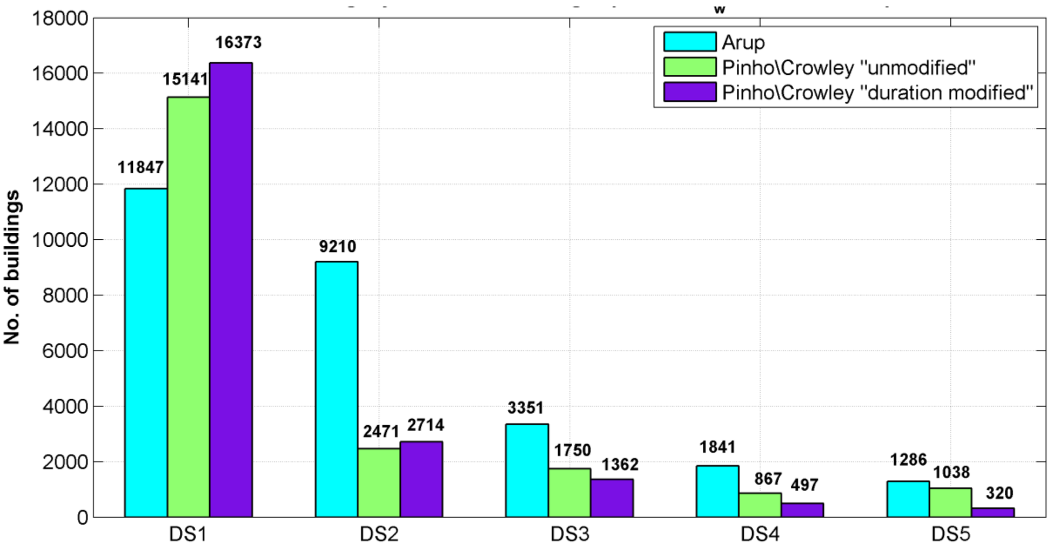

Figure 6 Summary of estimated number of buildings damaged to each damage state (DS1to DS5) for an earthquake scenario with magnitude M_w = 5 using 84th percentile PGA input values and comparing the results obtained using different sets of fragility functions proposed by Arup, Pinho and Crowley "unmodified" and Pinho and Crowley "duration modified" for Groningen region building stock.

The comparison of the number of casualties estimated to occur in an earthquake scenario with M_w =5 using the median or 50th percentile PGA values and the higher 84th percentile PGA values and with the different fragility function sets are summarised in Figure 7 and Figure 8.

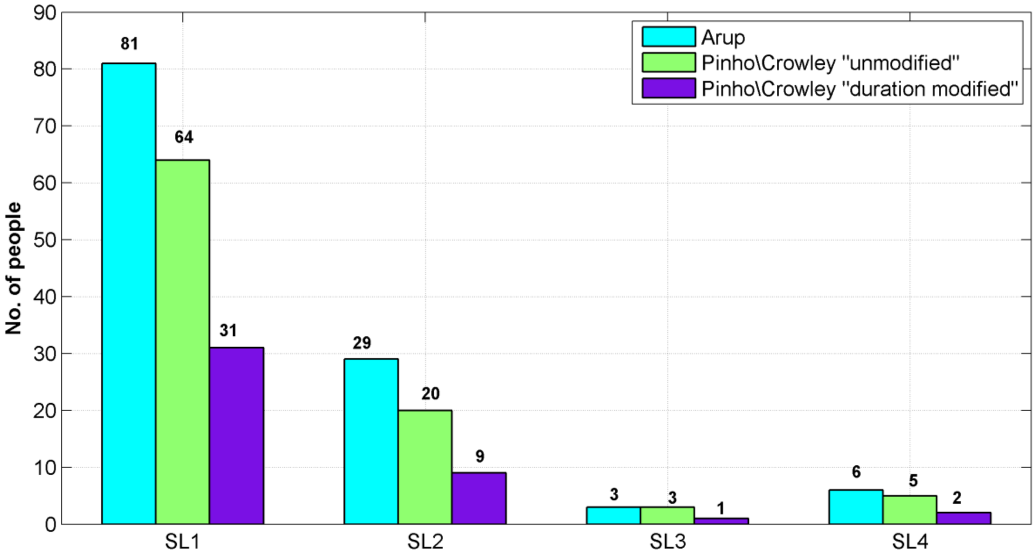

Figure 7 Summary of estimated number of casualties to severity of injury (SL1to SL4) for an earthquake scenario with magnitude M_w = 5 using median (50th percentile) PGA input values and comparing the results obtained using different sets of fragility functions proposed by Arup, Pinho and Crowley “unmodified” and Pinho and Crowley “duration modified” for Groningen region building stock.

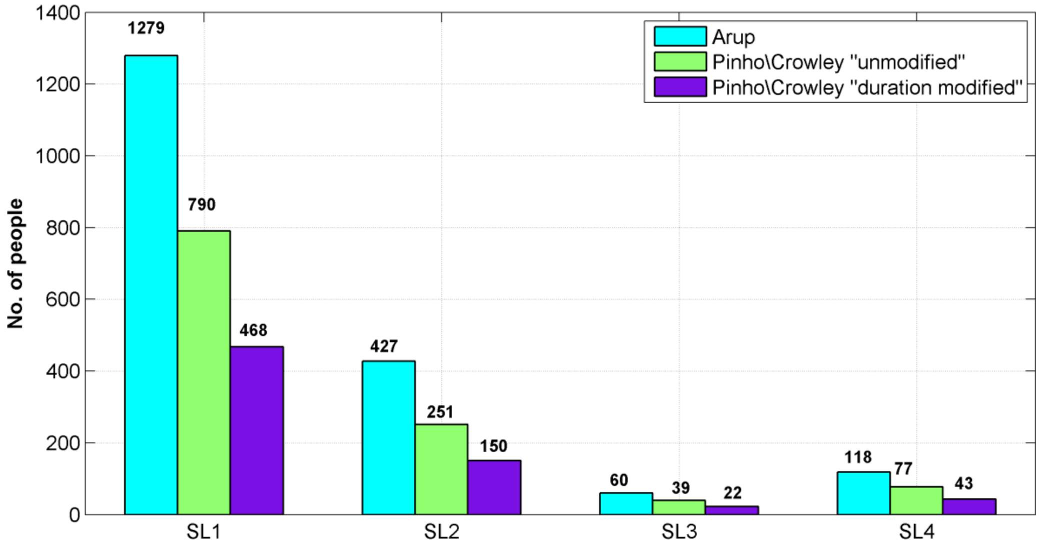

Figure 8 Summary of estimated number of casualties to severity of injury (SL1to SL4) for an earthquake scenario with magnitude M_w = 5 using 84th percentile PGA input values and comparing the results obtained using different sets of fragility functions proposed by Arup, Pinho and Crowley “unmodified” and Pinho and Crowley “duration modified”for Groningen region building stock.

It is not possible at this stage to judge which set of fragility functions is most suitable for the Groningen region building stock and, therefore, three separate sets of fragility functions have been used to represent the uncertainty of the expected building performance under earthquake ground shaking. It is recommended that the range of results using these three separate sets of fragility functions be considered as providing a reasonable estimate of expected number of damaged buildings and casualties.

It is emphasised throughout this report that there is considerable uncertainty in the input parameters for the risk assessment and therefore there will be significant uncertainty in the estimated numbers of potentially damaged buildings and numbers of potential casualties presented for different earthquake scenarios. It is therefore recommended that the range of results be considered as providing a good indication of the possible levels of damage and numbers of casualties that could occur in future earthquakes in the Groningen region.

The scenario earthquake risk assessment using the median PGA values as input (see Figure 1 and Figure 2) are considered to provide a reasonable estimate of the potential building damage and number of casualties. These median results appear to be consistent with the levels of damage and casualties resulting from similar magnitude tectonic earthquakes elsewhere in the world. However, median PGA values by their very nature mean that the ground shaking could be higher or lower.

If the variability of the input ground motion is used (i.e. possible higher or lower PGA values) and the range of possible fragility functions are used then the estimated levels of damage and casualties are higher. These higher building damage and casualty estimates are possible but appear to be higher than observed levels of damage and casualties from tectonic earthquakes of similar magnitude elsewhere in the world.

Uncertainty Reduction

A key aspect of on-going risk management work is uncertainty reduction through research and development. Key areas for uncertainty reduction include; improved understanding of the ground motion hazard including the amplitude, frequency content and duration; improved understanding of the effect of the local geology on the earthquake ground motions; improved definition and classification of the building structural typologies in the region; improved understanding of the vulnerability of the building stock to ground shaking; improved estimation of the amount of building damage that can potentially occur by better understanding of the response of the buildings to potentially higher frequency and shorter duration ground motions; and improved casualty estimation methodology using building damage and casualty statistics from elsewhere in the world but that are most relevant to the situation in the Groningen region.

Risk Management

The findings from this risk assessment study can be used to inform risk management decisions. Unreinforced masonry buildings constitute 75% to 85% of the building stock in the Groningen region and therefore particular attention should be given to understanding, and improving when necessary, the performance of these buildings under earthquake ground shaking. The risk analyses indicate it is not only the older unreinforced masonry buildings but also the newer unreinforced masonry buildings that contribute most to the risk. Severe injury and potential loss of life is predominantly associated with building collapse and therefore strengthening of buildings particularly the unreinforced masonry buildings for collapse prevention should form a key component of the risk management strategy. The risk assessment results can also be used to help identify the priorities for risk management activities. Priority should be given to buildings in highest risk areas (high hazard x high exposure x high vulnerability) along with buildings of high importance (e.g. hospitals), high occupancy (e.g. schools), and high cultural value (e.g. churches and museums) as well as facilities where there may be secondary hazards (e.g. chemicals storage facilities) and facilities where systems failure might have adverse cascading impacts (e.g. failure of electrical distribution or water supply).

1 Introduction

1.1 Background

Arup has been appointed by Nederlandse Aardolie Maatschappij B.V. (NAM) to carry out consultancy services in relation to induced seismicity hazard and risk assessment, and the design of strengthening measures for buildings in the Groningen region of the Netherlands.

Arup is a global firm of professional consultants. This report has been commissioned by NAM, and produced using information, instructions and directions from NAM. However the findings reached are the product of our independent professional judgement, on the basis of our scientific knowledge at the date of writing this report.

For the original scope of work for the earthquake scenario-based risk assessment, Arup were requested to consider a study area with a 15 km radius around the epicentre of the August 2012 Huizinge earthquake. As more information became available on the location of induced earthquakes in the Groningen region the scope of work was increased and the study area was expanded to cover the full extent of the Groningen gas field. The spatial extent of the extended study area is also shown on Figure 9. In this report the extended study area is adopted only for the purposes of the damage estimation, while the initial building database (15 km radius) is adopted for the casualty estimation. The compilation of all required information on all buildings and the occupants in the extended study area is still in progress.

The Netherlands has large on-land gas reservoirs, which have been exploited since the 1960s. Numerous small magnitude (≤ 3.6 M_w) and shallow (< 4 km) earthquake events have been induced as a result of this gas exploitation (van Eck et al, 2006). The location of earthquakes events is in the north of the Netherlands and predominantly associated with the Groningen gas field which is the largest of the gas fields in the region (see Figure 10). The induced earthquakes have caused damage to buildings in the region and are the subject of concern to the population.

This report describes the results of the earthquake scenario-based risk assessment for the Groningen region being undertaken by Arup for NAM. Scenario earthquake risk assessments provide an estimate of what could happen in terms of building damage and casualties in single possible future earthquakes of a given magnitude (e.g. what could happen in a magnitude M_w=5 earthquake located near the town of Huizinge). The scenario earthquake risk assessments do not provide an estimate of the cumulative damage and casualties that could potentially arise from all possible future induced earthquakes during the life of the gas field and after.

Figure 9 Groningen region location plan.

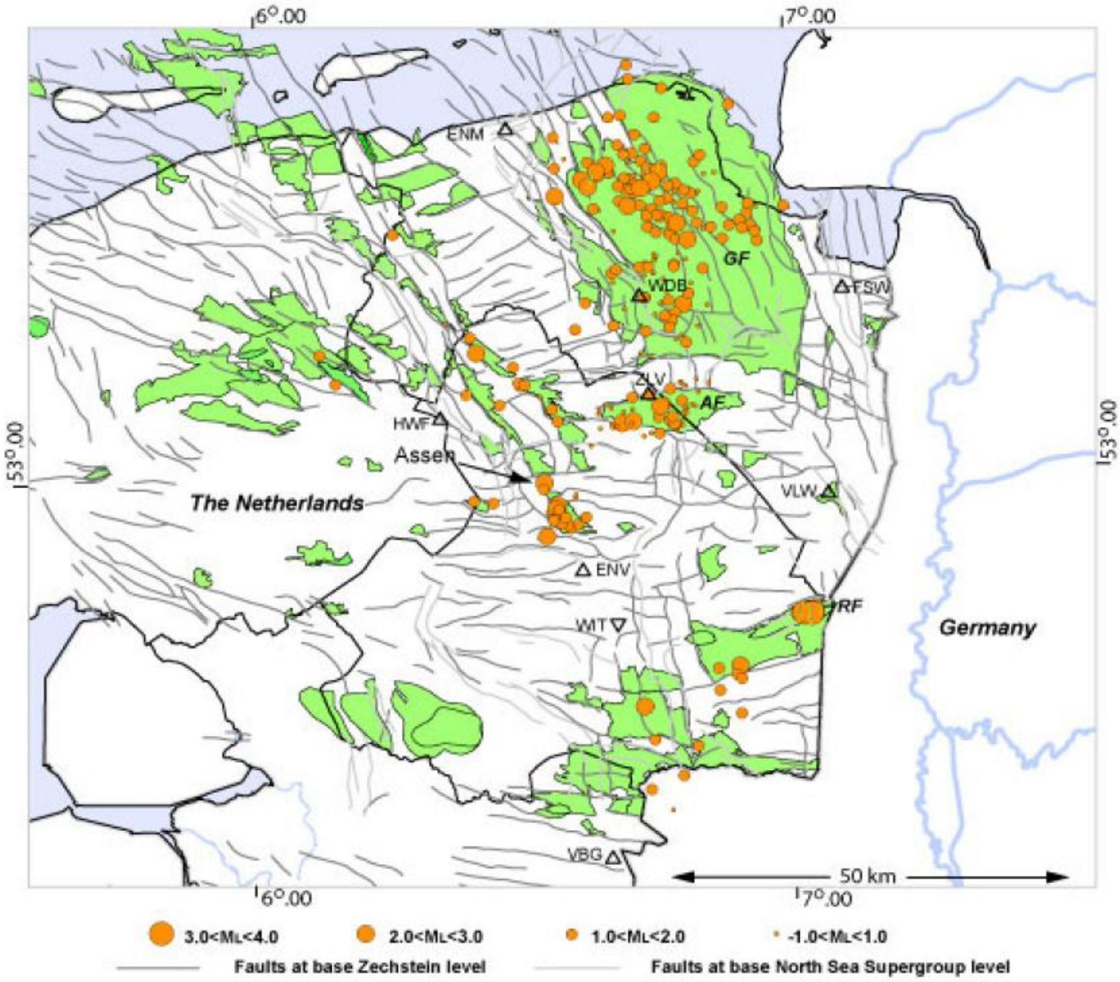

Figure 10 Seismicity of the Groningen region (from Van Eck et al., 2006).

1.2 Seismic Risk Assessment Methodology

The seismic risk assessment methodology can be divided into four main components:

- Seismic hazard assessment;
- Building exposure assessment;
- Building vulnerability assessment; and
- Building risk calculation.

This report provides a summary of the scenario-based methodology that has been used for the initial damage assessment only and provides a description of the proposed methodology to be undertaken in the future to enhance the risk assessment.

Figure 11 explains the relationship between the basic components of hazard, exposure and vulnerability considered in determination of seismic risk. Each of these components is discussed in more detail in the following sections of this report.

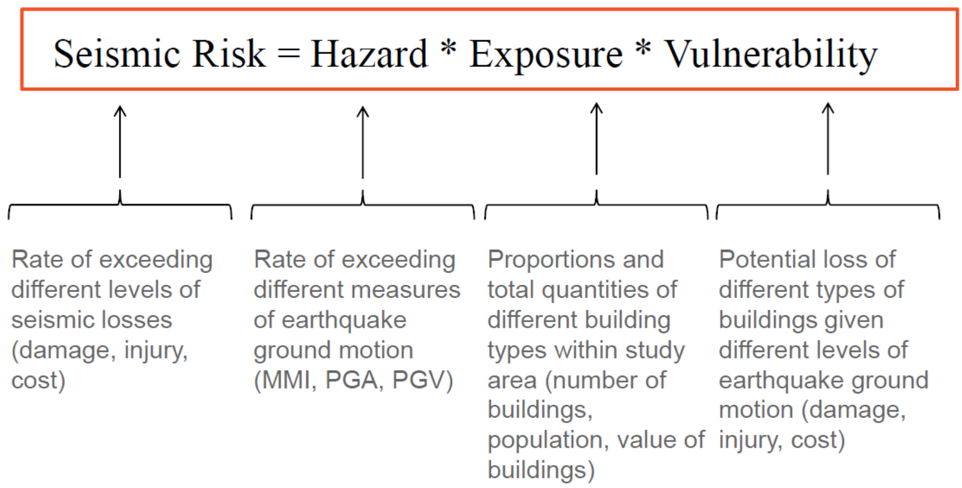

Figure 11 Seismic risk calculation.

1.3 Outline of This Report

The report is divided into main sections that match the main components of the risk assessment methodology followed by presentation of the initial risk calculation results and then a summary with recommendations for future work.

- Seismic hazard;
- Building exposure;
- Building vulnerability;
- Building risk calculation;
- Risk assessment results; and
- Conclusions and recommendations.

2 Seismic Hazard

2.1 Introduction

This section of the report describes the methodologies that have been used to determine the ground motion hazard from induced earthquakes in the Groningen region.

The Royal Netherlands Meteorological Institute (KNMI) has monitored the induced seismicity in the region since 1986 [2] and reports on the induced seismic hazard in the region have been published by van Eck et al. (2006) and Dost et al. (2012). KNMI is one of the organisations providing an estimate of the induced seismic hazard for the Groningen region.

There are traditionally two principal ways of estimating seismic hazard:

- Deterministic seismic hazard assessment (DSHA); and
- Probabilistic seismic hazard assessment (PSHA).

A full description of these methods is given in Reiter (1990) and McGuire (2004).

Deterministic seismic hazard methodology determines the seismic hazard from a scenario earthquake with assumed magnitude and location. This methodology does not allow the likelihood of this event actually occurring to be determined. Probabilistic seismic hazard methodology allows the probability of events to be determined and is usually applied to the seismic hazard associated with tectonic earthquakes with a fundamental assumption of the methodology being that the earthquake events are random or time independent. This assumption does not apply in the case of induced seismicity. Studies undertaken separately by NAM (e.g. van Elk & Doornhof, 2012; Bourne and Oates, 2013) have demonstrated that there is a correlation between the induced seismicity in the Groningen region and production from the gas field beneath. The distribution of induced seismicity is found to be non-random and time dependent.

An alternative probabilistic methodology has therefore been proposed by Bourne and Oates (2013) for NAM to reassess the probabilities of induced earthquakes due to gas production from the Groningen field using Monte Carlo methodology to generate large statistically representative catalogues of induced earthquake simulations (in space and time) for the region and to combine these with published earthquake ground motion prediction equations to estimate the probability of ground motion shaking at the surface.

Both deterministic and probabilistic methods are used in earthquake loss estimation. For example the California Geological Survey recently published their seismic loss estimates for California and both scenario-based deterministic ground motions and probabilistic seismic hazard were used (Chen et al. 2013). The California Geological Survey used median ground motions in their earthquake scenario analyses.

[2] Monitoring of induced seismic events by KNMI since 1986.
http://www.knmi.nl/research/seismology/ind_seism_hazard.html

2.2 Deterministic Seismic Hazard Assessment

The deterministic earthquake scenario-based methodology incorporates the following components:

- Definition of an earthquake scenario in terms of earthquake magnitude, depth and distance; and
- Definition of appropriate ground motion prediction equation(s), GMPE, to calculate the ground motion level resulting from the scenario earthquake. The ground motions can be modelled either deterministically (e.g. using median values only) or probabilistically (e.g. using the standard deviation on the GMPE to account for potential variability in the ground motions).

2.2.1 Earthquake Scenarios

KNMI has identified the locations of eight induced earthquakes in the Groningen region with magnitude greater than M_w=3 (see Table 1 and Figure 12), for selection of the locations of the scenario earthquakes.

Table 1 Location of the past eight earthquakes used as epicentres by KNMI (pers. comm. by Dost on 13/06/2013).

Name	**Date**	**Magnitude (M_w)**	**Lat (ºN)**	**Lon (ºE)**
Hoeksmeer	24/10/2003	3.0	53.295	6.792
Stedum	10/11/2003	3.0	53.325	6.69
Westeremden	08/08/2006	3.4	53.325	6.697
Westeremden	30/10/2008	3.1	53.337	6.72
Zeerijp	08/05/2009	2.9	53.354	6.762
Hoeksmeer	27/06/2011	3.4	53.299	6.8
Huizinge	16/08/2012	3.6	53.345	6.672
Zandeweer	07/02/2013	3.2	53.389	6.667

Arup has selected three of the eight earthquake epicentre locations provided by KNMI to undertake the deterministic risk assessment scenario-based calculations. The three earthquake scenario events that have been undertaken are:

- A M_w = 5.0 event located at Huizinge at a 3km depth;
- A M_w = 5.0 event located at Zandeweer; and
- A M_w = 5.0 event located at Hoeksmeer.

The 'Report to the Technical Guidance Committee (TBO) on Production Measures; Part 1: Depletion Scenarios and Hazard Analysis' reports that although considerable progress was made in the understanding of the seismic hazard, significant uncertainty remains at present. The predictions of the seismic hazard range are believed to be conservative and NAM has initiated a further data acquisition program to obtain additional field data, and a studies program to reduce the uncertainty. An earthquake scenario of M_w≥5 in this report is estimated to have a probability of occurring of less than 10% in the next 10 years (Bourne et al., 2013).

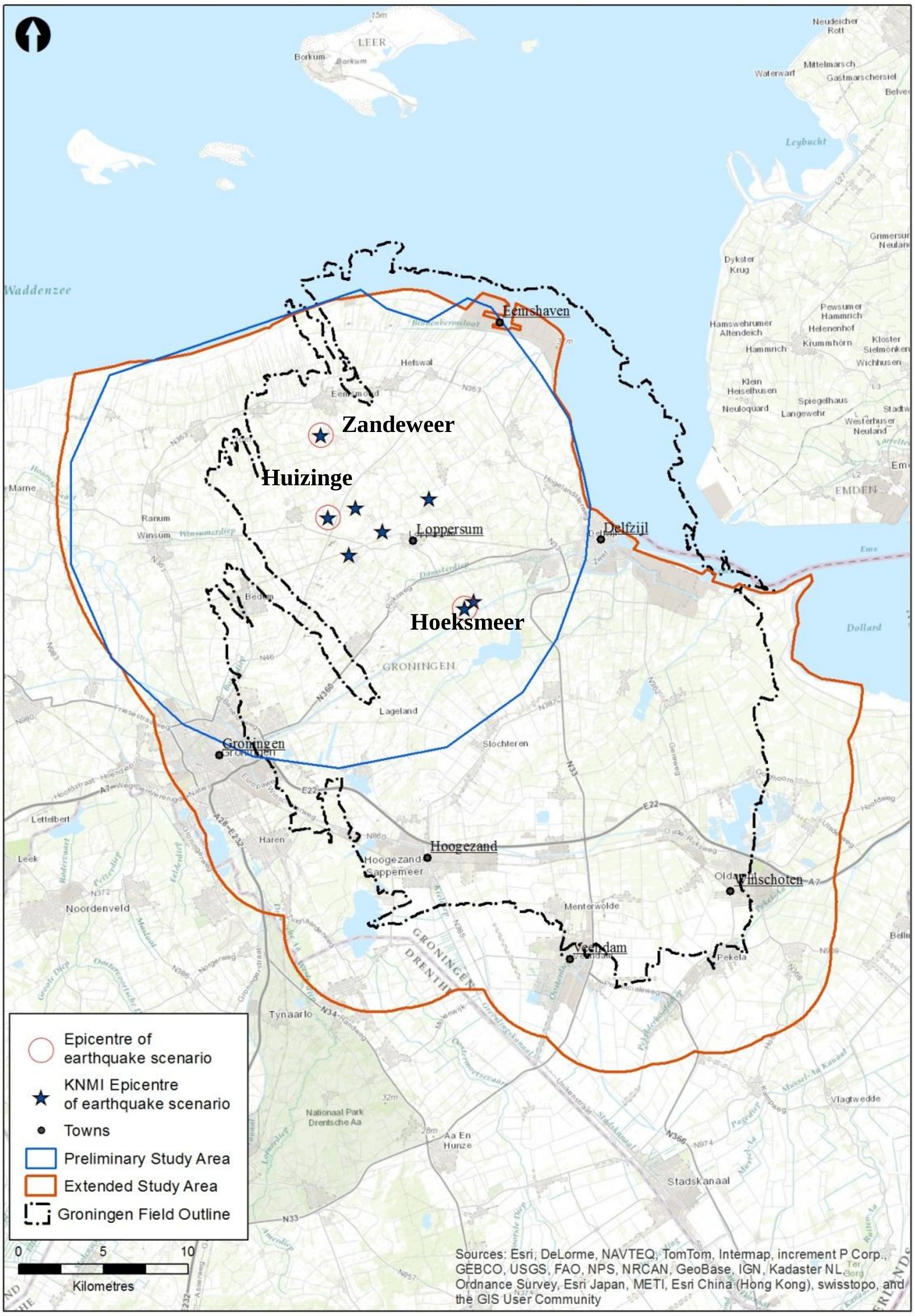

Figure 12 Location of the eight earthquake epicentres identified by KNMI (blue stars). The red circles highlight those events adopted in the scenario-based risk assessment by Arup.

The locations of the epicentres of the three earthquake scenario events are highlighted by red circles in Figure 12. The M_w=5 event with an epicentre located at Huizinge serves as a basis for comparison with other scenarios for the sensitivity analyses. The other two earthquake epicentre locations were chosen in order to have a good geographical coverage of the central portion of the study area.

The scenario earthquake calculations have been repeated for different magnitudes:

- A M_w=3.6 event located at Huizinge;
- A M_w = 4 event located at Huizinge, and
- A M_w = 4.5 event located at Huizinge.

2.2.2 Ground Motion Prediction Equations

Ground-motion prediction equations (GMPEs) allow the calculation of ground motion parameters of engineering interest, such as peak ground acceleration (PGA), peak ground velocity (PGV), or response spectral values as a function of a few independent parameters (magnitude, source-to-site distance, site classification, fault mechanism, etc.). The uncertainty in the GMPE is represented by the standard deviation (σ_{tot}) from the median values.

The selection and application of the GMPEs for the region is described in a separate study by Bommer (2013). The study by Bommer recommends the use of the recently published GMPEs by Akkar, Sandikkaya and Bommer (2013). Bommer (2013) proposed a modification of the GMPEs at low magnitudes (M<4) based on an analysis of residuals from the recorded Dutch earthquakes. This modification is not adopted herein since the main scope of the report is scenario earthquakes of M = 3.6–5.

A GMPE can generally be written with the form:

$$\ln PGA_{es} = \mu_{es} + \delta B_e + \delta W_{es}$$

where:

- $\ln PGA_{es}$ is the natural logarithm of the ground motion parameter observed at site *s* during earthquake *e*, and μ_{es} is the mean of the logarithm of the PGA predicted by the GMPE.
- δB_e are the between-event (or *inter-event*) residuals, which represent the average source effect not captured by magnitude, style-of-faulting and source depth. The residuals are the amounts by which each individual observation differs from the mean model given by μ_{es}. They are normally distributed with zero mean and standard error τ: $\delta Be \sim N(0, \tau)$.
- δW_{es} are the within-event (or *intra-event*) residuals, normally distributed with zero mean and standard error ϕ: $\delta W_{es} \sim N(0, \phi)$. They represent azimuthal variations in source, path, and site effects that cannot be captured by a distance metric and a site-classification based on the average shear-wave velocity.

The sum of $\delta B_e + \delta W_{es}$ represents the total residual, i.e. the misfit between observation and the mean prediction. The two components (*inter-* and *intra-*events) are uncorrelated, so that the total standard deviation from the mean (*sigma*) of the ground motion model is $\sigma_{tot} = \sqrt{\tau^2 + \phi^2}$.

In the earthquake scenario risk assessment calculations presented in this report three ground motion levels are considered:

- 50th percentile (median ground motion): $PGA_{median} = \exp(\mu_{es})$;

- 84th percentile: $PGA_{84-perc.} = \exp(\mu_{es} + \sigma_{tot}) = PGA_{median} \times \exp(\sigma_{tot})$; and
- Mean ground motion: $PGA_{mean} = PGA_{median} \times \exp(\sigma_{tot}^{2} / 2)$.

Appendix E provides a short description of the definition of the statistical parameter used in this report (e.g. mean, median percentile) in particular in the cases of the normal and lognormal distributions. An implicit assumption in these three cases is that the ground motion variability is fully correlated and thus the same number of standard deviations (σ, "sigma") is used for all the buildings. However, a real earthquake would be expected to lead to some local areas with lower than median ground motion, and other areas with higher than median ground motion. The ground motion is expected in reality to be spatially correlated. Two close areas are expected to experience the same or similar ground motion level, while areas far from one another are not correlated and will experience a different level of ground motion.

For a given earthquake, the ground motion *inter-event* variability (τ) is the same: i.e. the same number of τ, is applied to all the buildings of the dataset – this number of standard deviations is expressed as ε_τ. However, the ground motion *intra-event* variability is dependent on the site and can vary from site to site: i.e. the number of ϕ, can vary from building to building – this number of standard deviations is expressed as ε_ϕ.

In order to investigate this variability and spatial correlation of ground motion in the scenario earthquake calculations, analyses have been undertaken for two extreme cases:

- The ground motion variability among the sites is fully correlated ($\rho = 1$): all the sites experience the same number of *sigma* above/below the mean, and
- The ground motion variability among the sites is fully uncorrelated ($\rho = 0$): all the sites experience the same number of τ above/below the mean and a different number of *intra*-event residual. So that the same ε_τ but a different ε_ϕ, randomly chosen such that $\varepsilon_\phi \sim N(0,1)$, is applied to all the buildings.

Figure 13 below shows the concepts of ground motion variability and spatial correlation. The first rows shows the attenuation of the ground motion with distance of the Akkar *et al.* (2013) GMPEs for the median (50th percentile) in red, for the 16th and 84th percentiles in green and for the 5th and 95th percentiles in blue. The black squares represent locations at which the PGA values are computed. When the median (ε=0) ground motion is computed, Figure 13 (a), the black squares are aligned along the red curves (leftmost plot). The corresponding PGA map is shown in the left plot of the bottom row. The two central plots, Figure 13 (b), show an example of fully correlated ground motion variability with ε =1.2. The top central plot shows the black squares aligned along about the 84th percentile and the bottom plot shows the corresponding PGA values distribution. Finally the two right plots, Figure 13 (c), represent examples of fully uncorrelated ground motion PGA values, for which ε_τ is 0.25 and ε_ϕ is randomly computed at each site. The black squares are no longer aligned with an individual GMPE percentile line but each building location is shown to experience a different level of sigma above/below the median. The corresponding PGA spatial distribution is shown in the right bottom panel. Although the general pattern still shows the attenuation with distance, some local areas with higher PGA values and others with lower PGA values can be identified.

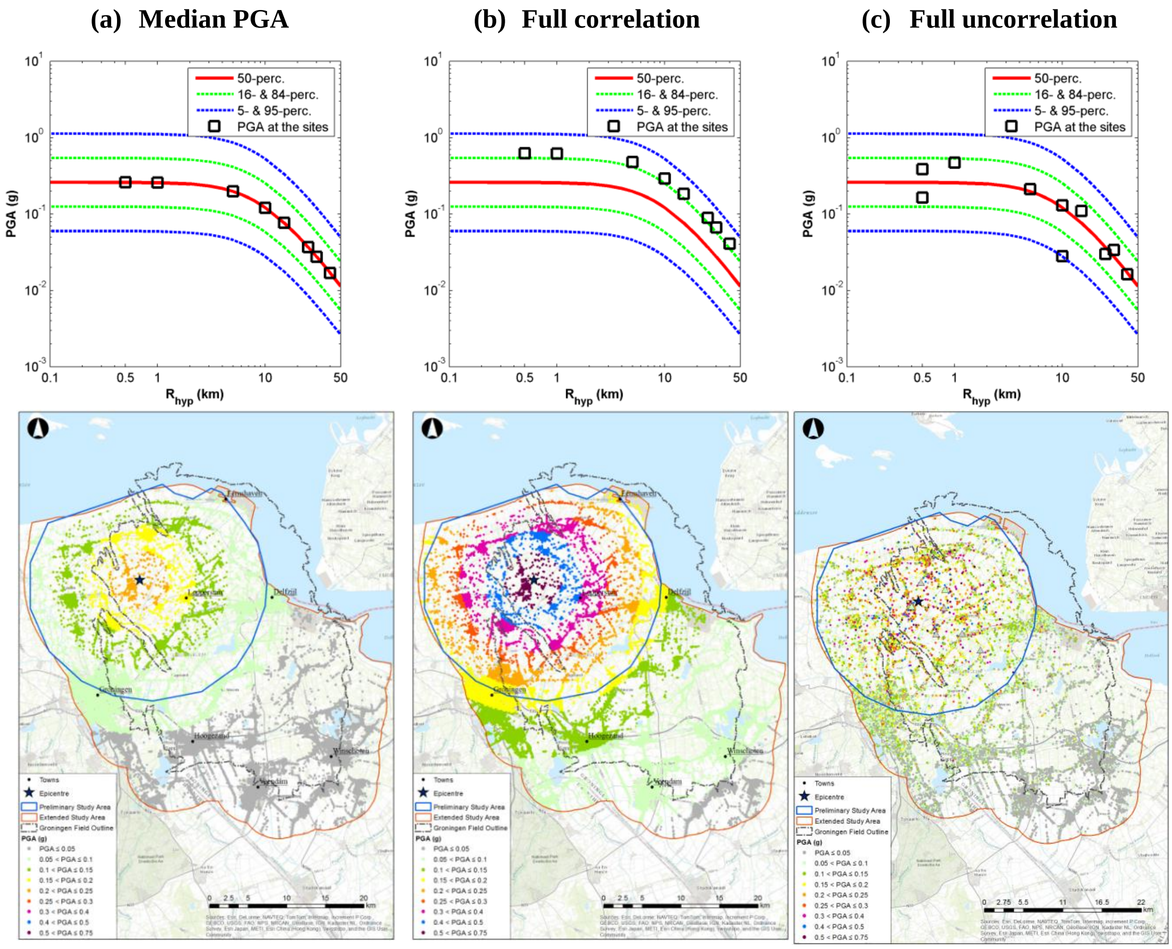

Figure 13 Comparison of ground motion prediction analyses with fully correlated and fully uncorrelated treatment of the ground motion uncertainty.

A Monte Carlo simulations approach is used to investigate the ground motion variability, where the number of simulations N_{sim} was chosen such that the final results are stable (N_{sim}=50, 100, 1000, 2500, 5000, 10000).

The steps below are followed:

1. Computation of the seismic hazard:

   In the fully correlated case:
   - Compute ε from a standard normal distribution, $N(0,1)$;
   - At all the buildings locations: $PGA_{building} = PGA_{median} \exp(\varepsilon \times \sigma_{tot})$;
   - Count the number of buildings in each damage state through the fragility functions.

   In the fully uncorrelated case:
   - Compute ε_{τ} from a standard normal distribution $N(0,1)$;
   - Compute one ε_{ϕ} for each building of the dataset from standard normal distribution;
   - At each building location: $PGA_{building} = PGA_{median} \exp(\varepsilon_{\tau} \times \tau + \varepsilon_{\phi,building} \times \phi)$;
   - Count the number of buildings in each damage state through the fragility functions.
2. Repeat step 1. N_{sim} times.

3. Compute the median number of buildings per damage state N_{sim} simulations.

2.3 Probabilistic Seismic Hazard Assessment – Poisson Process Methodology

KNMI has undertaken probabilistic seismic hazard assessments for the induced seismicity in the Groningen region assuming a Poisson process for the estimation of the earthquake ground motion hazard (Dost et al., 2012).

A probabilistic seismic hazard assessment combines the elements of seismic source zones, earthquake recurrence and the ground motion prediction equations to produce hazard curves in terms of level of ground motion with an associated annual frequency of being exceeded. The key elements of a probabilistic seismic hazard assessment include:

- Seismic source zones to define the spatial variation of earthquake activity. These source zones are based on the distribution of observed seismic activity together with geological and tectonic factors and represent areas where the seismicity is assumed to be homogenous; i.e. there is an equal chance that a given earthquake will occur at any point in the zone.
- Earthquake recurrence to define the level of activity within a particular source zone. There are, generally, more small (low-magnitude) earthquakes than large (higher magnitude) earthquakes. Again observed seismicity is used to determine the earthquake recurrence relationships.
- Ground-motion predictive equations (GMPEs) to define what ground motion should be expected at location A due to an earthquake of known magnitude at location B. Generally, ground-motion equations are derived from observations from past earthquakes and also provide a measure of the variability of the ground motion parameter.

This methodology is based on that originally proposed by Cornell (1968), modified to include variability and uncertainty in the various input parameters.

It is understood that an updated probabilistic seismic hazard assessment for the Groningen region is in preparation by KNMI but the results from the updated study by KNMI were not available to Arup at the time of reporting.

It should be noted that the probabilistic seismic hazard assessment methodology is usually applied to the seismic hazard associated with tectonic earthquakes with a fundamental assumption of the methodology being that the earthquake events occur in a time independent way – e.g. the probability of an earthquake of a certain size occurring this year is the same as next year. This fundamental assumption does not apply in the case of induced seismicity, in which this probability is changing over time. Studies undertaken separately by NAM (e.g. van Elk & Doornhof, Nov 2012) have demonstrated that there is a correlation between the induced seismicity in the Groningen region and production from the gas field beneath. The induced seismicity is found to be non-random and time dependent.

2.4 Probabilistic Seismic Hazard Assessment - Monte Carlo Methodology

An alternative probabilistic methodology has been proposed by Stephen Bourne and Steve Oates of Shell (Bourne and Oates, 2013) to reassess the probabilities of induced earthquakes. They describe the correlation between the induced seismicity in the Groningen region and the measured strain in the reservoir and overburden interpreted to be associated with gas extraction / production from the gas field. The induced seismicity is found to be time dependent – i.e. earthquake occurrence probability changes with time.

Monte Carlo methodology is used to generate statistically representative catalogues of simulated induced earthquakes (in space and time) for the region that represent the seismic moment release predicted to be associated with the measured rates of strain in the region. These earthquake catalogues are combined with earthquake ground motion prediction equations to estimate the probability of ground motion shaking at the surface.

The seismic hazard findings using the Monte Carlo methodology are described by Bourne and Oates (2013). Examples of the PGA hazard maps, prepared using this methodology, are provided in Figure 14. It is understood that considerable research and development work is on-going to update this analysis in the future. It is proposed that the induced seismic hazard levels determined using this updated Monte Carlo methodology along with updated building fragility functions will be used in the detailed seismic risk assessment studies to be undertaken for the Groningen project in the future.

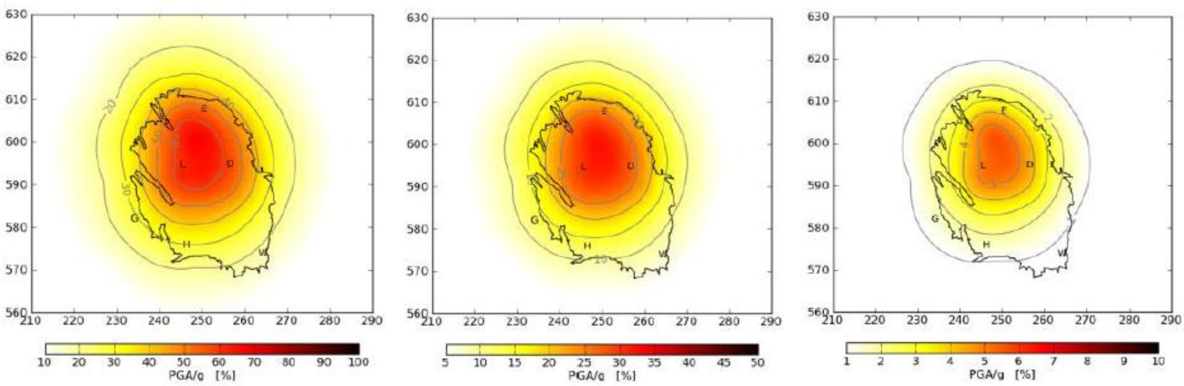

Figure 14 PGA hazard maps for the 10 years from 2013 to 2023 with a 2%, 10% and 50% chance of exceedance (from Bourne and Oates, 2013).

2.5 Influence of Ground Conditions on Ground Motion Hazard Levels

Earthquake ground motions are strongly influenced by ground conditions. One of the key inputs in a seismic hazard assessment is the interpretation of the local ground conditions and determination of their potential impact on the amplitude of the ground shaking. The interpretation and modelling of the ground conditions is important as weak soils can significantly reduce or amplify earthquake ground motions depending on the amplitude and characteristics of the incoming ground motions. For this reason a parameter providing a simplified classification for the ground conditions is normally included in the form of the ground motion prediction equations. It should be noted that the Dost et al. (2004) GMPEs is based on ground motion records measured directly on the local ground conditions and therefore implicitly included the effect of local ground conditions. The Akkar et al. (2013) GMPEs used in the earthquake scenario risk calculations in this report are not based on local Groningen ground conditions but do include a ground conditions classification factor to take ground conditions into account.

TNO has undertaken an initial review of the geotechnical and geological data for the Groningen region. They have derived a map showing the mean shear wave velocity over the top 30m, known as V_{S30}, for the Groningen region (see Figure 15). This shows that the region broadly has a V_{S30} of about 200m/s with local variations occurring particularly to the southeast of the study area. TNO (2003) calculate that the local soil effects can approximately double to quadruple the amplitude of the ground motions measured at the surface.

Anecdotal observations by the public with regard to variation in the amplitude of ground motions indicate that the public perception is that local ground conditions have a strong influence on earthquake ground shaking. The investigation of these issues will require a study of the near surface geological conditions and the geotechnical properties of the soils across the entire Groningen region. The Netherlands is in the fortunate position that a large amount of ground investigation information is available online in pre-existing databases. In this risk assessment study, the local site amplification due to ground conditions has been taken into consideration using the soil amplification factor within the Akkar et al. (2013) GMPE, assuming V_{s30}=200 m/s across the entire study area.

A preliminary study is also being undertaken by Arup to investigate the characteristics of the local ground conditions and the influence on seismic site response and liquefaction potential. The preliminary findings support the early results of TNO that the ground conditions are shown to strongly amplify ground motions and it is recommended that further work is undertaken to investigate this issue on a regional scale. Initial liquefaction analyses indicate that discrete layers of sand and silt in the region are potentially susceptible to liquefaction under the expected ground motion hazard levels caused by earthquakes with magnitude M_w= 5 that could potentially occur in the region.

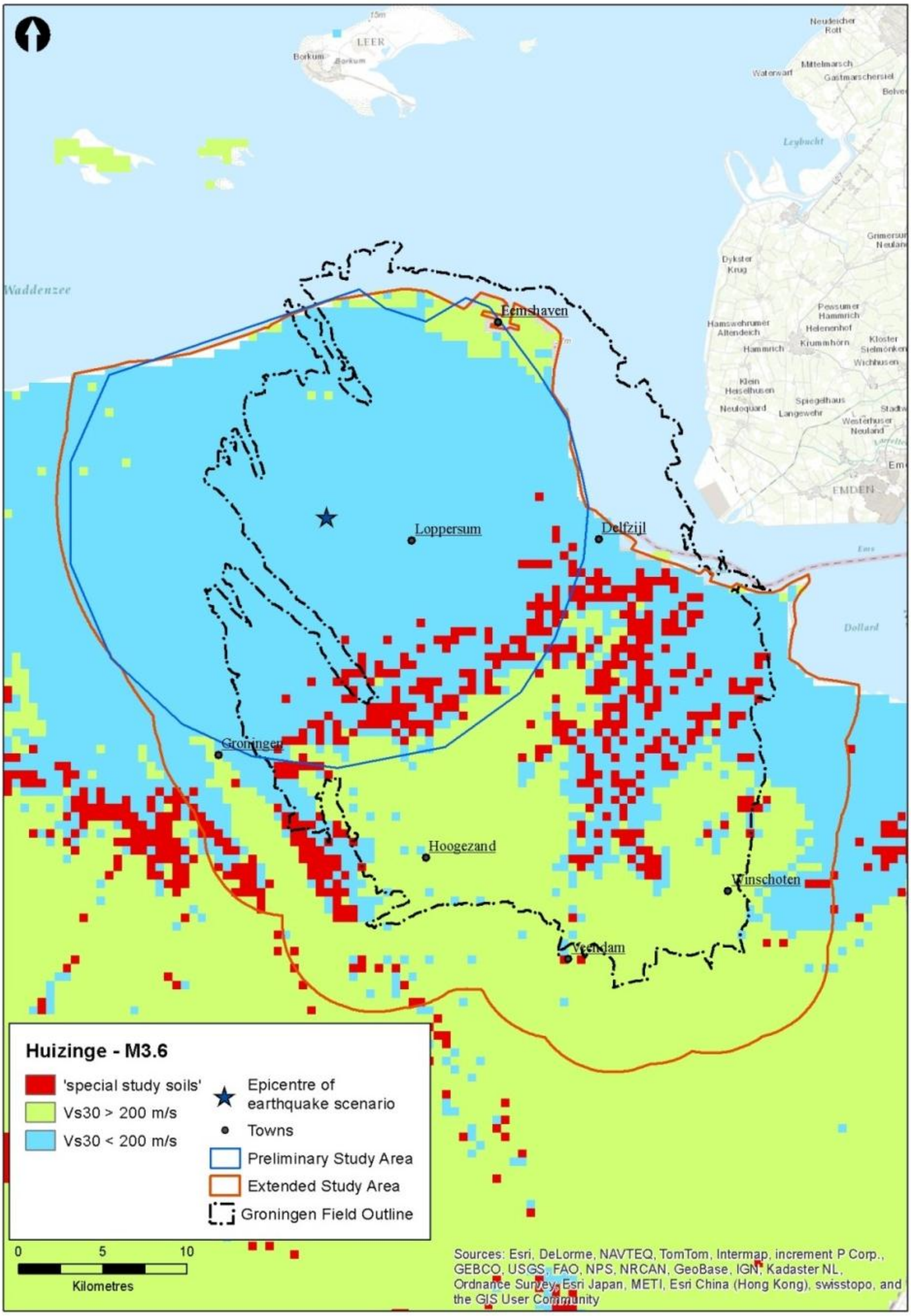

Figure 15 Preliminary ground conditions V_{s30} Map for Groningen region (TNO pers. comm. 2013).

3 Building Exposure

3.1 Introduction

This section of the report describes the compilation of the initial building exposure database for the Groningen region.

The original scope of work for Arup required the compilation of building data for a study region with a 15 km radius around the epicentre of the Huizinge earthquake (blue outline on Figure 16). It was later proposed that the study region be expanded to investigate the seismic risk over a wider area related to the extent of the Slochteren gas field and the seismic hazard level findings of the Monte Carlo methodology probabilistic seismic hazard assessment (Bourne and Oates, 2013). The new study area, red outline on Figure 16, includes the preliminary area and extends 5 km beyond the boundaries of the gas field (dashed black line on the figure below).

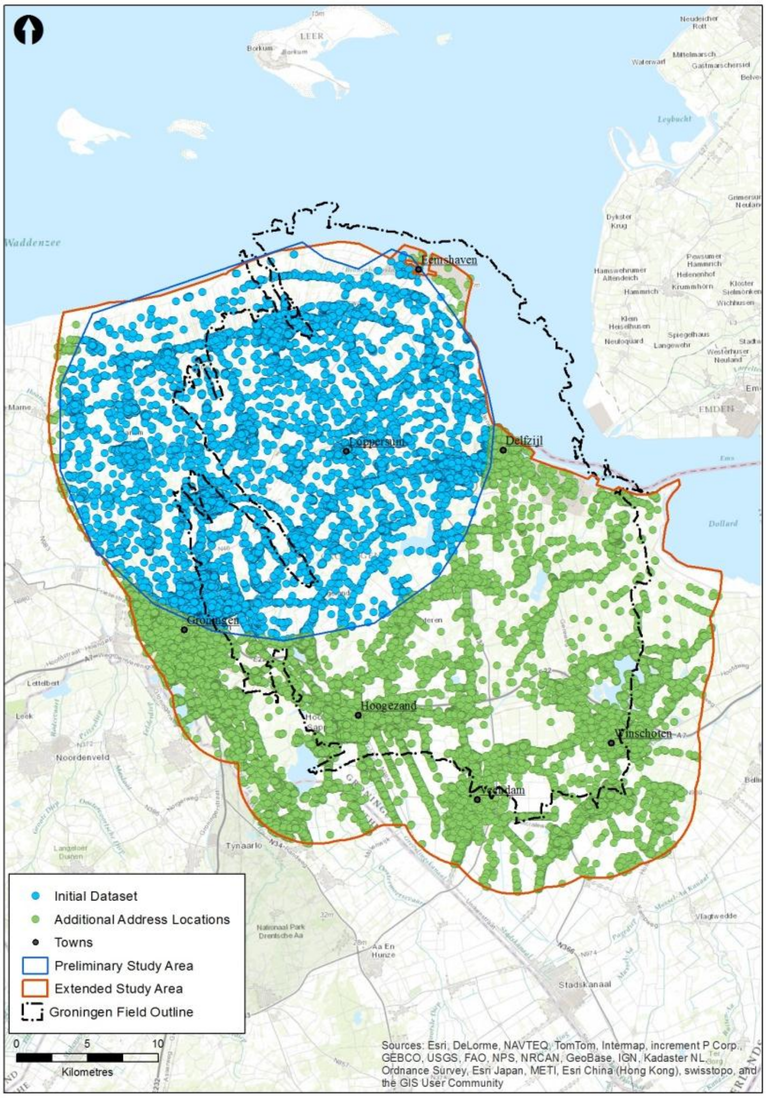

Figure 16 Extended and initial study area with 15 km radius around Huizinge. Individual building locations in the initial study area are shown by blue points, while the green points represent the addresses locations added in the extended database.

Expansion of the building database for the extended study area is in progress. A preliminary version of the extended database is used in this study to assess the number of damaged buildings. Note that the term “preliminary” is herein used since the assembling of the database for the extended study is still in progress and quality assurance checks have not yet been completed.

The initial building database (within the 15 km radius) included approximately 65,000 individual buildings while the extended database includes approximately 250,000 buildings of which approximately 100,000 do not have addresses and associated information. These latter buildings are thought to be mainly barns and sheds and therefore unoccupied. However, further work is on-going to consistently classify all the buildings.

The building (exposure) database is compiled in Geographical Information System (GIS) software and contains data from a range of different sources. The following categories of building data were obtained for compilation into the initial building database: location, address, usage, landscape height, occupancy and property value. Part of this input has been used to estimate building heights, number of floors, building categories (construction material and type), day time and night time occupancy.

3.2 Building Location and Address

The number and location of the buildings in the study area have been obtained from the BAG data, or Basisregistratie Adressen en Gebouwen [Kadaster, July 2013]. This contains data layers for the building outlines, addresses and other data layers.

Two further separate datasets have been obtained containing data on the building addresses within the study area. Population data has been obtained from Bridgis. The DataLand dataset provides detailed information on building typology, usage, value and the year a building was built for these addresses. Appendix A1 illustrate typical examples of the address point analysis, highlighting the main difficulties encountered

3.3 Building Usage

Buildings are classified by usage to evaluate occupancy at different times of the day. Mixed use buildings occur where commercial use occurs at street level with residential use above. The usage categories adopted in the database classification are displayed in Table A.1 in Appendix A.

3.4 Building Height and Number of Floors

The building height data is derived from the Actueel Hoogtebestand Nederland (AHN) [Rijkswaterstaat, Het Waterschapshuis, 2013]. The AHN is a digital height map for the Netherlands, developed from laser scan data. From the height data in this digital map in combination with the building shapes from the topographic map, an estimation is made of the number of floors for each building.

3.5 Building Type

A building type classification is assigned to each building. The estimated construction material (e.g. unreinforced masonry, reinforced concrete, timber, steel) is an important component of this classification, together with the estimated number of floors, and building age. The definitions of the building typologies for the risk assessment are classified in the Table A.2 in Appendix A for the initial and extended database and a summary is shown in Figure 17. The figure shows the proportions of the buildings in the two databases (y-axis), and the actual numbers as labels for each bar on the histogram.

Unreinforced masonry is the dominant building type in the region, estimated to comprise approximately 90 % of the building stock of the initial building database (within 15 km radius) and 75% to 80% of the preliminary extended building database. The second largest building material type is reinforced concrete which comprises around 5% of the building stock in the initial building database (within 15 km radius) and 4% in the preliminary extended database. Wood and steel frame buildings comprise less than 0.5% of the building stock.

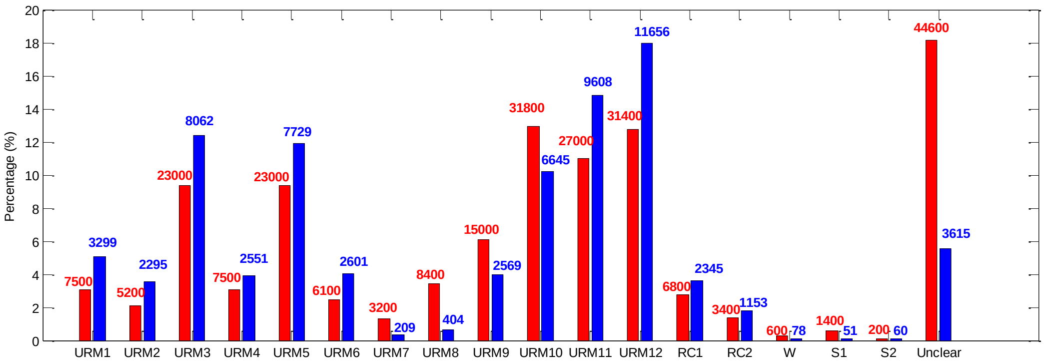

Figure 17 Building typology distribution in study area.

The geographical distribution of the building types are shown in Figure A.3 in Appendix A.

3.6 Building Database Gap Analysis

It is emphasised that the checking and quality assurance of the database for the initial study area and the extended building database is in progress. An important part of developing a database of this type is making sure that the data accurately represents the actual situation on the ground. Spot checks of the database have been undertaken by undertaking street surveys by Arup staff and reviews of discrete areas using satellite imagery and Google Street View. Checks have also been undertaken by comparing data from different independent datasets. Discrepancies in the database have been identified and further work is required to resolve these issues.

4 Building Vulnerability

4.1 Introduction

This section of the report describes the compilation of the initial vulnerability/fragility functions for the building stock in the Groningen region.

Vulnerability is defined in this report as the degree of loss to a given element at risk (i.e. a building) resulting from a given level of hazard (e.g. amplitude of earthquake ground motion shaking). The measure of loss used depends on the element at risk and may be measured in terms of a description of the amount of damage, the number of people injured or killed, or the cost of repair. In this report, only building damage and human casualties are reported.

The vulnerability terminology used in this report has been subdivided between the term "fragility" used to describe the potential damage and the term "loss" to describe the potential injuries or fatalities.

4.2 Fragility Functions

There are three primary categories of fragility functions:

- Empirical: based on damage observation statistics collected following earthquakes and shake table testing;
- Analytical: based on structural modelling and analysis using computer models of buildings and infrastructure; and
- Judgement-based: based on the experience and judgement of experts.

Each of these categories has limitations and benefits. Empirical equations are based on real observations. When sufficient data are available, the empirical method is often thought to be the most reliable, since it uses real observations of damage and therefore has the best chance of capturing the real uncertainty and variability.

In this earthquake scenario-based risk assessment work, empirical fragility functions have been used. These empirical functions are based on earthquake damage data observed elsewhere in the world and therefore require calibration with local earthquake damage observations. It is intended that these functions will be calibrated in future with the detailed analytical work undertaken on numerical models of buildings that is being carried out by Arup as part of the Structural Upgrading work stream for the Groningen project and described in a separate report (Arup, 2013).

Fragility functions are typically specific to a particular building typology classification. The classification will include building material and structural system as these are the most important parameters for identifying the vulnerability / fragility of a building. If sufficient data and meta-data are available, building classifications for fragility functions may also differentiate between other factors such as: building age, number of storeys, floor system (rigid or flexible diaphragms), and the presence of wall-floor ties (for masonry buildings).

For this initial study, building typology classifications have been defined based on the distribution of observed typologies in the building stock but also based on the availability of suitable existing fragility functions in the literature. The representative typology classes that have been selected for analytical modelling in the Arup Structural Upgrading work stream have also been taken into consideration.

At this stage the same fragility functions for many of the masonry typology classes have been assigned. However, when results are available from the analytical modelling being undertaken by the Structural Upgrading work stream, it is anticipated that this may allow the fragility functions of different building classes to be further distinguished and existing fragility functions modified.

4.3 Ground Motion Intensity Measure

Damage assessment requires a consistent measure of the level of ground shaking – ideally one that is well-correlated with damages to buildings. Appendix B describes in more detail the possible ground motion measures to be used in the damage estimation.

In this initial risk assessment, PGA is adopted as the primary measure of ground motion hazard level, although conversions between different macroseismic measures and PGA are used to allow a wider pool of fragility relationships to be considered. The use of PGA as the ground motion hazard measure is a pragmatic choice because the majority of suitable published fragility functions are in terms of PGA. However, it is anticipated that other ground motion measures may in fact provide improved correlation with damage observations and this requires further investigation.

4.4 Damage Classification

The damage classifications from the (EMS-98; European Seismological Scale, 1998) are used. These classifications have the advantage that they are well defined for different types of buildings and have been used in many other studies across Europe. The classification of damage to masonry buildings and reinforced concrete buildings in the EMS-98 are illustrated in Figures B.1 and B.2 in Appendix B.

4.5 Selection of Fragility Functions

4.5.1 Empirical Fragility Functions

Empirical fragility functions are typically developed for geographical locations and building typologies for which damage data have been collected following earthquakes. Generally, multiple earthquake events are considered so that the data are not too specific to the unique characteristics of a particular earthquake. There are no sets of fragility functions for damage state DS1 to DS5 developed specifically for Dutch buildings, as very few earthquakes causing damage have been experienced. Where damage data are available (such as from the recent earthquakes in the Groningen area), they tend to be for relatively low levels of damage (slight damage restricted to cracking of masonry walls or cracking of plaster within the interior of buildings) rather than the higher levels of damage that is expected in the epicentral area of a future potentially larger sized earthquake.

To overcome this lack of earthquake damage data, initial selection of fragility functions was carried out based on available functions for masonry buildings, as this allowed comparison with damage data from Dutch earthquakes. To this end, use was made of the Global Earthquake Model (GEM), an international project to develop and improve methods and tools for seismic risk assessment (see Appendix B3).

The criteria specified in Appendix B4 were used to reduce the pool of potential relationships to a manageable number. In summary, only those equations based on a dataset with intensity measures including PGA, PGV, macroseismic intensity or PSI and that could reliably be extrapolated to the low ground motion values of interest were considered.

All functions were converted to a consistent ground motion intensity measure, PGA, as follows:

- PSI was converted to PGA using the relationship in Spence et al. (1992): $\log_{10}(PGA) = 2.04 + 0.051 \times PSI$, with PGA in cm/s^2 and taking account of the error on the regression and the differences in the definitions used for PGA (see Appendix B5).
- Other macroseismic intensity values (EMS/MMI/MCS) were converted to PGA using an inversion of the relationship in Wald et al. (1999): $MMI = 3.66\times \log_{10}(PGA) – 1.66$.

The latter is a one way regression, which technically should not be inverted. However, this conversion could have legitimately been applied directly to estimated PGA values to obtain a map of MMI to use with the unconverted fragility relationship. Given that this would give identical loss calculations, the theoretical objection to inverting regression relationships need not be applied here. Arup has considered other equations for conversion between MMI and PGA but these have been presented in a separate technical note.

- Finally the following fragility functions were considered:
- Rota et al. (2008);
- Coburn and Spence (2002); and
- Spence et al. (2011).

4.5.2 Fragility Functions from Shake Table Testing

Empirical fragility functions can also be developed on the basis of experimental testing, particularly on a shake table. This allows much more control over the input characteristics of the earthquake shaking. The characteristics of the physical building model can also be well controlled, and therefore an accurate (albeit usually reduced scale) representation of local building stock can be built and tested. The primary disadvantage is that it is expensive to carry out a large number of shake table tests and therefore it is difficult to capture the full spread of variability in a particular building class. For this reason, experimental evidence may not be sufficient to develop a full set of fragility functions, and will often be supplemented by either empirical data (of the type discussed in the previous section) and/or analytical modelling.

Experimental data was used by Pinho (2013) and Pinho and Crowley (2013) in their development of fragility functions for Groningen, discussed in Section 4.9.

4.6 Calibration of Fragility Functions

In order to calibrate the three sets of fragility curves short-listed by Arup for the risk assessment, empirical damage data from the Roermond earthquake of M_w =5.4 (M_L=5.8) that occurred on 13 April 1992 (refer to Appendix B6.1) and from the Huizinge earthquake of 16 August 2012 (M_w=3.6) (refer to Appendix B6.2) was used.

It is stressed that there is a trade-off here between making use of the existing functions that have been developed based on data from a number of events, albeit for building stock that may not be representative of the Netherlands, and using limited data (limited in both number and in the range of damage and ground motion intensity levels) available from Dutch earthquakes. As mentioned earlier, in future work it is intended to also use analytical models of Dutch buildings to calibrate the empirical fragility functions.

It should also be noted that the Roermond and Huizinge earthquakes predominantly caused damage to masonry buildings. For the levels of ground motion under consideration for this project, damage to reinforced concrete, steel and timber buildings, may be expected if they are present in the epicentral area and subject to ground shaking. Unfortunately, the limited Roermond and Huizinge damage data available cannot be used to calibrate the fragility functions for the concrete, steel and timber buildings (except to check that the selected functions should not predict significant damage under the levels of shaking observed in Roermond and Huizinge, as this would contradict observation). It is therefore preferred to calibrate “sets” or “families” of fragility functions with available functions that cover the full range of adopted building typologies (i.e. a set of functions developed by the same authors using the same dataset), which can be validated based on the masonry data alone, and trust that the reinforced concrete buildings (and those of other materials) will be well-represented.

Table 2 and Table 3 display the percentages of buildings in each damage state according to the Roermond and Huizinge earthquake respectively. It is noted that in the case of the Huizinge earthquake, a subset of buildings, for which observed values of PGA were available at eight recording stations, was considered in this analysis (see Appendix B6.2). This allows a direct and more reliable correlation between damage and measured ground motion amplitude (in terms of PGA).

Table 2 Percentages of buildings suffering damage larger or equal to damage state during the Roermond earthquake.

Age	Intensity	PGA (g)	DS1	DS2	DS3
URM Pre 1920	VI	0.126	32.60%	1.60%	0.00%
	VII	0.236	35.40%	6.50%	0.30%
URM 1920 - 1960	VI	0.126	7.00%	0.00%	0.00%
	VII	0.236	11.00%	1.30%	0.00%
URM after 1960	VI	0.126	3.00%	0.00%	0.00%
	VII	0.236	1.60%	0.30%	0.00%

Table 3 Percentages of buildings suffering damage larger or equal to a damage state DS, during the Huizinge earthquake.

Station	PGA (g)	DS1	DS2
'HKS'	0.009	8.7%	0.0%
'WIN'	0.012	5.9%	0.7%
'STDM'	0.026	4.7%	0.0%
'KANT'	0.038	0.0%	0.0%
'WSE'	0.043	8.4%	0.0%
'GARST'	0.057	10.7%	0.0%
'MID1'	0.060	5.6%	0.2%

Figure 18 shows the comparison between shortlisted fragility functions for masonry buildings only with damage data from the 1992 Roermond and 2012 Huizinge earthquakes.

Damage statistics after the Roermond earthquake are presented for 40 locations by Pappin et al. (1994). The locations suffered either macroseismic intensity I_{MSC}= VI (corresponding to *PGA*=0.13 g) or I_{MCS}=VII (*PGA*=0.24 g). For each location, the probabilities of the buildings to be slightly or moderately damaged (DS1 or DS2) were computed and are shown with circles in Figure 18.

The damage statistics for the Huizinge earthquake are compiled from damage reports from eight areas surrounding instrument locations where PGA values were measured. It has therefore been possible to determine the percentage of buildings damaged to different damage states at a range of PGA values.

Damage statistics were also determined from the surveys of buildings undertaken by Arup in May 2013. The damage statistics from these surveys is summarized in Table 4. The surveys demonstrated that damage was observed during and after the earthquake both for URM buildings Pre 1920 and for URM buildings built during the 60s-70s even for very low PGA values. However, only small samples of buildings in 3 locations were surveyed. Thus, even though the results are shown for reference, the damage levels are not considered reliable for calibration purposes.

Table 4 Damage statistics based on the survey undertaken by Arup in May 2013.

City	URM	R_{epi} (km)	PGA (m/s^2)	PGA obs (m/s^2)	DS1 (%)	DS2 (%)
Loppersum	<1920	6.28	0.51	-	61.5	3.8
Bedum	1920-1960	7.4	0.45	-	19.1	0.0
Middelstum	>1960	1.29	0.79	0.5	0.0	0.0

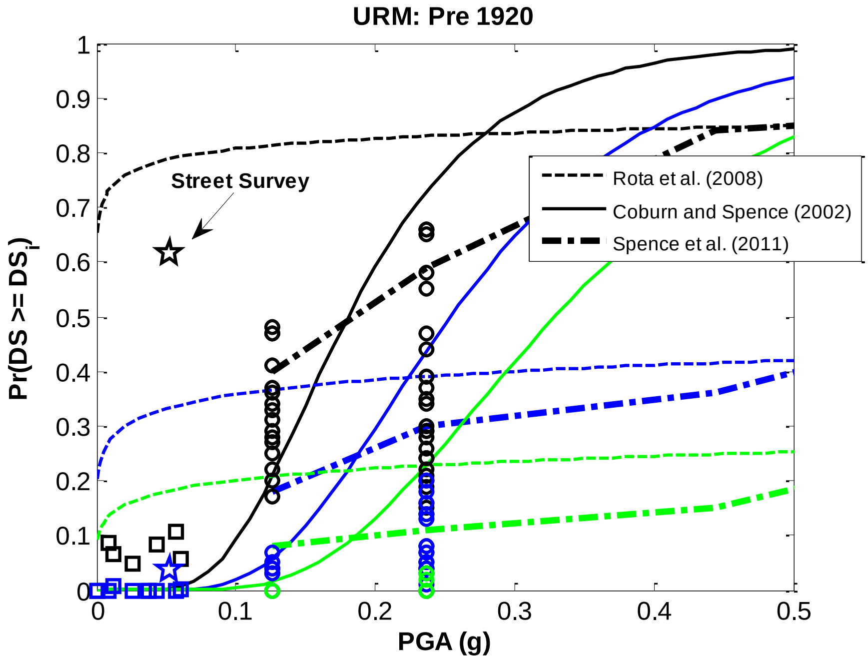

Figure 18 Comparison between selected vulnerability curves and data from Roermond (circle) and Huizinge (squares) earthquakes. Dashed lines refer to Rota et al. (2008) fragility functions, solid lines to Coburn and Spence (2002) and thick dashed lines to Spence.

It is clear that none of the plotted relationships perfectly describes damage observed in the previous Dutch earthquakes. Furthermore, there is significant scatter in the proportions of damage observed, making it difficult for any one relationship to fit the data well. The following observations can be drawn:

- Rota et al. (2008) predict excessively high levels of damage at low PGA values and significantly increasing levels of damage are not shown to occur with increasing PGA levels. The shape of the functions is strongly influenced by the fact that buildings are reported to be already damaged before the earthquake.
- Coburn and Spence (2002) show the expected shape for a fragility function (a lognormal distribution against PGA). The original curves are a function of the intensity PSI, and conversions provided by the authors were used to plot them versus PGA accounting for the uncertainty. See Appendix B6 for more details.
- Spence et al. (2011) are not analytical distributions and it is difficult to “adjust” them to the observed data.

While the Huizinge data are not consistent with any of the fragility functions, the fit of the Roermond data with the Coburn and Spence (2002) functions is reasonable. Moreover such functions have the advantage that they can easily be modified to better agree with the observed data. For these reasons, the Coburn and Spence (2002) fragility functions for masonry buildings have been selected (see Appendix B6). A more accurate comparison between the chosen fragility functions and the data from the Roermond (circles) and the Huizinge (squares) earthquakes for the URM Pre 1920 is presented in Figure 19. To account for the uncertainty in the estimation of PGA values at the 40 locations of the Roermond earthquake, the comparison is carried out both using the conversion between intensity and PGA, as before, and using the PGA values from the USGS Shakemaps (USGS, 1992). The latter provide predictions of peak ground motion parameters (including peak accelerations) observed ground motion, fault characteristics and ground motion prediction equations. Note that for the Roermond earthquake no recordings were available, thus the maps are only based on the ground motion prediction equations. It is highlighted that, as stated in the Shakemap Manual, for all maps and products the maximum value observed on the two horizontal components of motion is provided. Hence the PGA values from the Shakemaps are converted to the geometric mean component applying the conversion factor by Beyer and Bommer (2006).

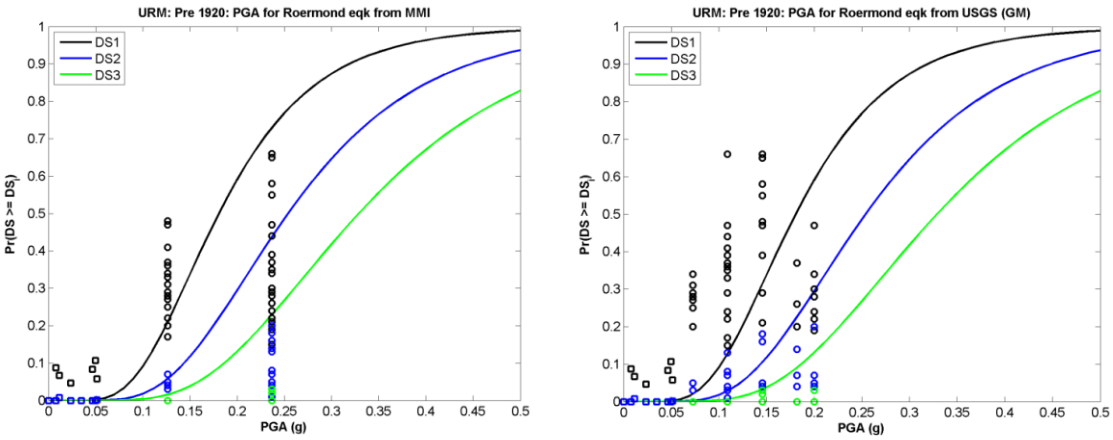

Figure 19 Comparison between the fragility functions proposed in this study and the data from the Roermond (circles) and the Huizinge (squares) earthquakes for the URM Pre 1920. Left panel: geometric mean PGA values, PGA_{GM}, for the Roermond earthquake are computed converting MMI to PGA_{GM}. Right panel panel: PGA_{GM} for the Roermond earthquake are extrapolated from the USGS Shakemaps with (right) conversions to geometric mean.

A description of the method adopted to modify the fragility functions for more modern buildings is illustrated in Appendix B6. Herein, the comparison of the URM 1920-1960 buildings modified fragility functions with the Roermond data is shown (Figure 20).

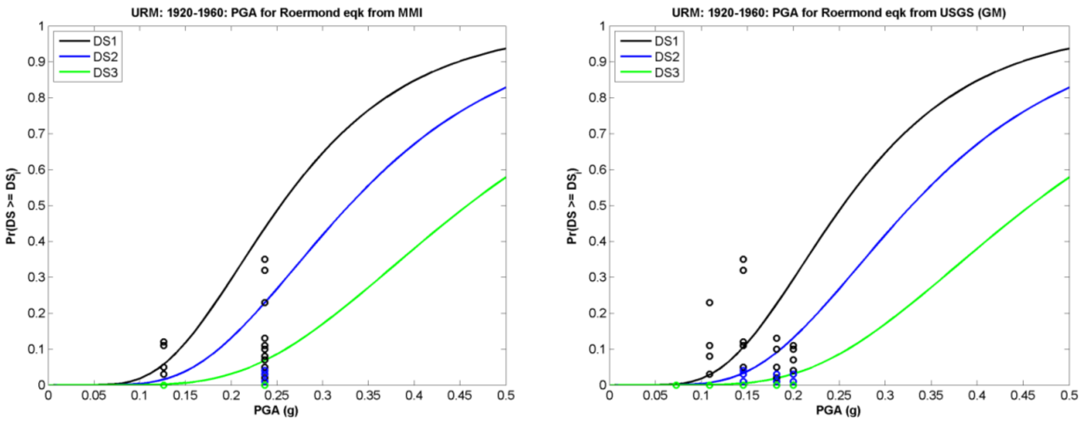

Figure 20 Comparison between the fragility functions proposed in this study and the data from the Roermond (circles) and the Huizinge (squares) earthquakes for the URM 1920-1960. Top panel geometric mean PGA values, PGA_{GM}, for the Roermond earthquake are computed converting MMI to PGA_{GM}. Bottom panel: PGA_{GM} for the Roermond

earthquake are extrapolated from the USGS Shakemaps with (right) conversions to geometric mean.

4.7 Building Collapse Damage State

Collapse state fragility functions are typically based on very limited amounts of data from past earthquakes because the numbers of collapsed buildings is typically a small proportion of the overall numbers of damaged buildings. As with other damage states the fraction of the building stock that collapses will vary according to the materials and structural types. Typically, it is the older most fragile buildings that collapse, such as unreinforced masonry and poorly engineered reinforced concrete. However, there are exceptions to this trend such as when the frequency of earthquake ground motions coincides with the fundamental period of particular buildings leading to resonance in the building and amplification of shaking and potentially leading to collapse. This effect on medium rise reinforced concrete buildings occurred in the Mexico City earthquake of 1985 (EEFIT, 1985).

The loss estimation methodology HAZUS (FEMA, 2013) indicates that the proportion of fully collapsed buildings can be estimated as a constant proportion of those buildings in the DS4 damage state. This proportion varies for each building typology. The building collapse rates shown in Table 5 have also been used to determine the number of buildings damaged to DS4 and DS5 damage states for consistency with the later use of HAZUS methodology for casualty estimation.

Table 5: Collapse rates to define damage state DS5 collapse fragility functions.

Building class	Collapse rate (%)
URM	15
RC1	13
RC2	10
W	3
S1	8
S2	5

The original DS4 and DS5 damage state functions are used for the estimation of the number of collapsed buildings. However, revised DS4-Hazus and DS5-Hazus functions are used for estimation of numbers of damaged buildings when these numbers are used only for casualty estimation (i.e. potential injuries and fatalities).

4.8 Fragility Functions for Groningen Region

This section of the report provides the definition of the fragility functions developed for the different building types of Groningen region. For each of the main building categories identified in the Groningen area, a table with the median PGA and the sigma of the natural logarithm of PGA_{GM} is reported as well as a figure that displays the fragility functions for damage states DS1 to DS5. The function obtained by applying the collapse rates from HAZUS to the fragility function of DS4 is also shown (dashed red curve) for each category but not provided in the tables.

4.8.1 Fragility Functions for Unreinforced Masonry Buildings

A discussion on the calibration and modification of the fragility functions from Coburn and Spence (2002) for use in the Groningen region is provided in Appendix B6. The original functions of Coburn and Spence (2002) did not include any distinction for the age of the buildings, thus a shift of the median values of the functions to larger values of PGA for modern buildings is applied to account for the expected slightly improved buildings performance of more recently constructed buildings (see Appendix B6).

The adopted functions are shown in Figure 21 and parameters of the lognormal distribution of PGA are given in Table 6. The proposed revision to the fragility functions includes the removal of the step in the damage state DS1 fragility function at low PGA values adopted in the initial risk assessment to capture the damage statistics from the Huizinge earthquake. A comparison between the fragility functions adopted in the initial risk assessment and those used in this study is provided in Appendix B7.

Table 6 Final parameters (means and standard errors) used for the URM fragility functions.

	URM: pre 1920		**URM: 1920-1960**		**URM: Post 1960**	
	PGA (g)	$\sigma_{\ln PGA}$	**PGA (g)**	$\sigma_{\ln PGA}$	**PGA (g)**	$\sigma_{\ln PGA}$
DS1	0.181	0.443	0.254	0.443	0.329	0.443
DS2	0.254	0.443	0.329	0.443	0.370	0.443
DS3	0.329	0.443	0.458	0.443	0.532	0.443
DS4	0.397	0.443	0.583	0.443	0.694	0.443
DS5	0.484	0.443	0.753	0.443	1.308	0.443

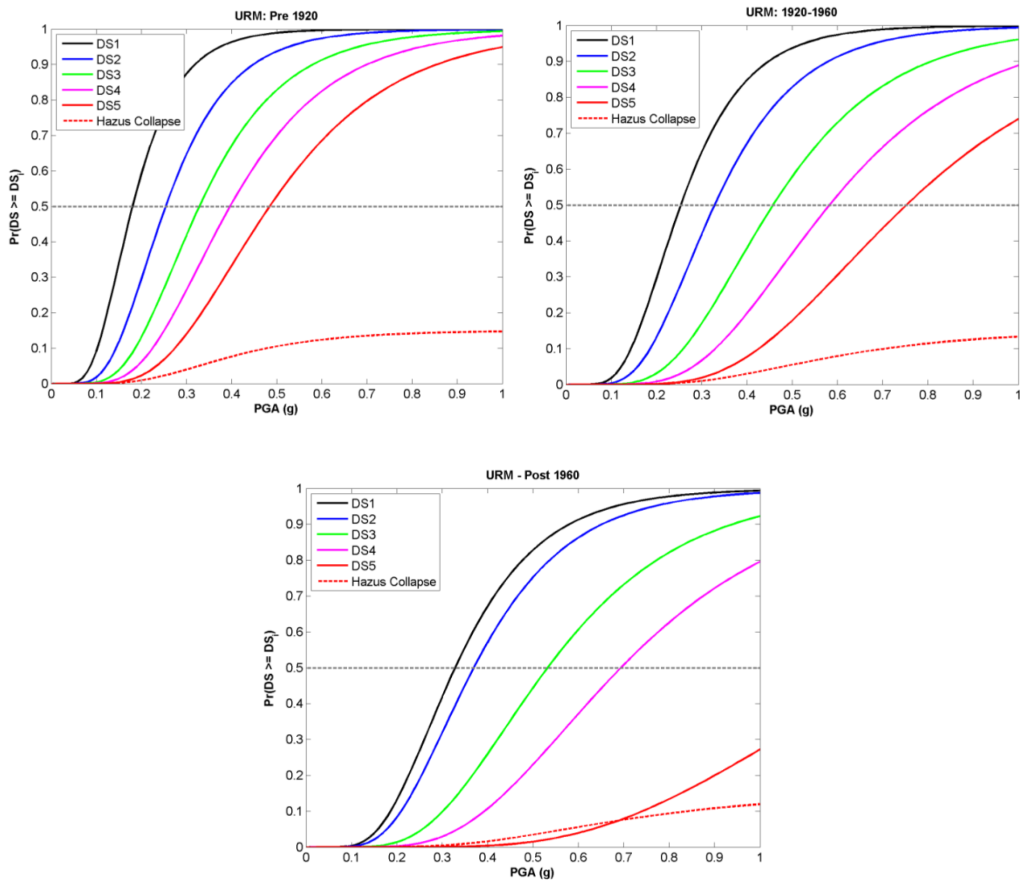

Figure 21 Fragility functions for buildings developed by Arup (Arup/CB2002) for the five damage states. The curve obtained by applying the collapse rates from HAZUS to the fragility function of DS4 is also shown (dashed red curve).

4.8.2 Fragility Functions for Reinforced Concrete Buildings

Fragility functions are provided for reinforced concrete (RC) buildings although no Netherlands specific earthquake damage data is available to calibrate and modify these functions. Fragility functions for reinforced concrete were taken the Arup UK seismic risk study (Ove Arup & Partners, 1993). These UK fragility functions for reinforced concrete buildings were developed in a consistent format with the Coburn and Spence (2002) fragility functions for unreinforced masonry and other typologies. Parameters for the reinforced concrete fragility curves are shown in Table 7. The curves for the two categories differ only for damage state DS5, since the proportions provided by HAZUS (FEMA, 2013) depend on the height of the buildings (dashed lines in the two plots).

It should be noted that the RC fragility curves are predominantly based on damage to RC moment frame buildings, whereas most RC buildings in the Groningen area are expected to be shear wall buildings. This suggests that the adopted fragility curves are likely to be very conservative (i.e. predict higher damage states) for Groningen RC buildings. This conservatism is particularly evident comparing the median collapse (DS5) PGA from RC buildings, i.e. ~0.5, and that from the modern URM buildings, i.e. ~1.3. The set of fragility functions for RC buildings should be amended when results from analytical modelling become available. However, this conservatism is not expected to significantly affect the risk assessment calculations because the number of reinforced concrete buildings in the region is relatively small (~4-5% of the total building stock).

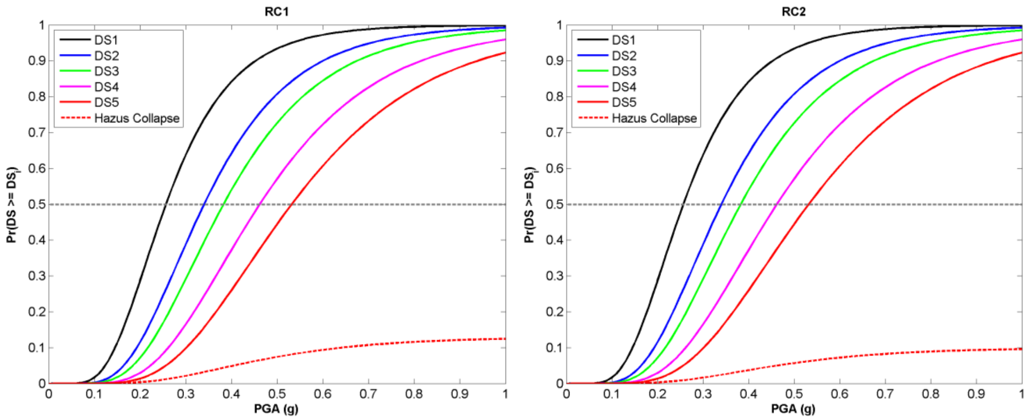

Figure 22 Fragility functions for Reinforced Concrete buildings with less than three storeys (RC1, left) and three storeys or more (RC2, right) developed by Arup (Arup/CB2002) for the five damage states. The curves obtained by applying the collapse rates from HA.

Table 7: Median PGA (g) and sigma of the natural log of PGA_{GM} for the fragility functions of RC1 and RC2 buildings.

	Median PGA (g)	**Sigma (lnPGA)**
DS1	0.257	0.443
DS2	0.341	0.443
DS3	0.383	0.443
DS4	0.462	0.443
DS5	0.532	0.443

4.8.3 Fragility Functions for Steel Frame Buildings

Steel buildings comprise only 0.2% of the total building stock. Steel buildings are generally expected to be less vulnerable to earthquake shaking than masonry and reinforced concrete buildings. Steel building fragility functions were taken from the Arup UK seismic risk study (Ove Arup & Partners, 1993). These UK fragility functions for steel buildings were developed in a consistent format with the Coburn and Spence (2002) fragility functions for unreinforced masonry and other typologies.

The fragility functions for steel are shown in Figure 23. The parameters for the steel fragility functions are shown in Table 8.

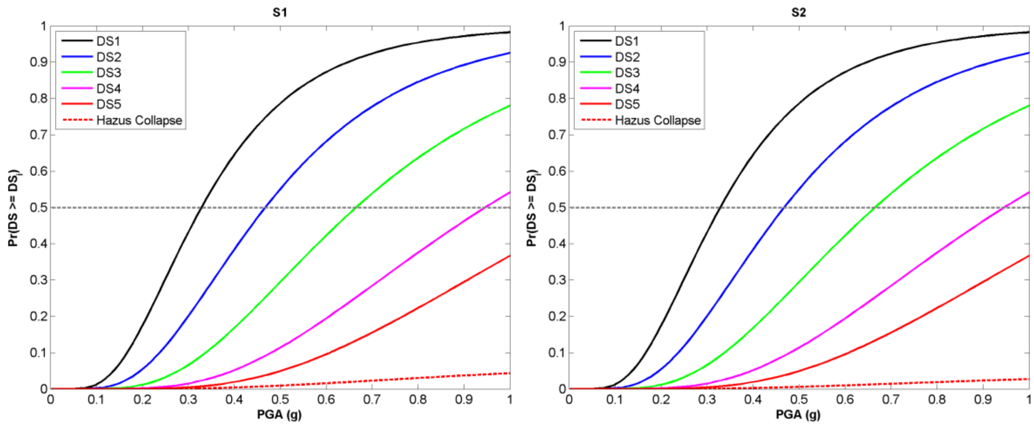

Figure 23 Fragility functions for Steel buildings with a height lower than 15 m (S1, left) and higher than 15 m (S2, right) developed by Arup (Arup/CB2002) for the five damage states. The curve obtained by applying the collapse rates from HAZUS to the fragility.

Table 8 Median PGA (g) and sigma of the natural log of PGA_{GM} for the fragility functions of S1 buildings.

	Median PGA (g)	Sigma (lnPGA)
DS1	0.329	0.528
DS2	0.468	0.528
DS3	0.665	0.528
DS4	0.946	0.528
DS5	1.197	0.528

4.8.4 Fragility Functions for Wood Buildings

Wood buildings comprise only ~1% of the total building stock in the region. Wood buildings are primarily old wooden barns that are attached to masonry farm houses. Where the barns have masonry walls or have masonry facades they have been classified as unreinforced masonry. For the initial risk assessment it has been assumed that the fragility of wooden buildings is equivalent to pre-1920 unreinforced masonry fragility functions. The proposed revision to the fragility functions includes the removal of the step in the damage state DS1 fragility function at low PGA values.

The fragility functions are shown in Figure 24. The parameters for the wood buildings fragility functions are shown in Table 9.

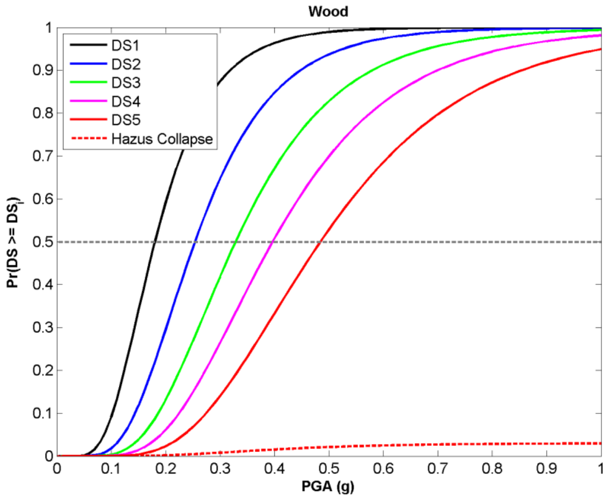

Figure 24 Fragility functions adopted in this study for wooden buildings.

Table 9 Median PGA (g) and sigma of the natural log of PGA_{GM} for the fragility functions of timber buildings.

	Median PGA (g)	**Sigma (lnPGA)**
DS1	0.181	0.443
DS2	0.254	0.443
DS3	0.329	0.443
DS4	0.397	0.443
DS5	0.484	0.443

4.9 Pinho and Crowley (2013) Fragility Functions

Pinho and Crowley (2013) also proposed fragility functions for unreinforced masonry buildings in Groningen. They also observe that limited damage data for Dutch building stock are available from past earthquakes, as was also noted in Section 4.5.2. They also note that most available empirical fragility functions for masonry structures in Europe have been calibrated on damage data from Mediterranean construction, and they conclude that they may therefore not be applicable to Dutch building stock.

Pinho and Crowley therefore take as a baseline a set of fragility functions developed by Bothara et al. (2010), which are based on experimental testing of scale models of masonry buildings in New Zealand, the assumption now being that given the fact that New Zealand masonry construction is similar to Dutch construction. Bothara et al. obtained the mean value of fragility curves from the experimental programme, and the standard deviation of the curves from other studies for masonry buildings elsewhere in the world. Pinho and Crowley observe that the Bothara functions compare reasonably well with the damage data collected for pre-1920s masonry buildings in the Roermond earthquake. They then adjust the fragility functions for the other two age categories of masonry buildings using the Roermond data, preserving the ratios between the fragility functions, using a similar procedure to that described in Section 4.6 and Appendix B6. The resulting fragility functions are described as “Pinho/Crowley-original” in the comparisons in Figures 28-30 (green curves) and are compared with the fragility functions proposed by Arup (light blue curves).

Pinho and Crowley (2013) also provide a preliminary estimate of the potential effect of shorter ground motion duration on building fragility (see Section 4.10). Based on a literature review and nonlinear dynamic analysis results, they conclude that the median collapse PGA can be increased by 40% due to the shorter expected duration of ground motions in the Groningen area when compared to typical damaging earthquakes (for which damage data have been collected, and which were used as the input to shake table testing, such as that of Bothara et al.). Since this is expected to have more of an effect on collapse than other damage states, Pinho and Crowley propose that the increase is 30% on the DS4 median PGA, 20% on DS3, 10% on DS2 and no change in DS1. The resulting fragility curves are described as “Pinho/Crowley-short” (for “short duration”) in the comparisons in Figures 28-30 (dashed violet curves).

There are no available published fragility curves that satisfy all the requirements for the risk assessment of Netherlands and Groningen region specific buildings reported here (i.e. based on earthquake damage to local building stock for an appropriate range of ground motion acceleration levels) and therefore there remains considerable uncertainty on the actual fragility of Groningen building stock. Therefore, the risk calculations have also been carried out using the set of Arup fragility functions described in Section 4.8 and both the unadjusted Pinho and Crowley fragility curves (Pinho and Crowley – original), and those adjusted for ground motion duration (Pinho and Crowley-short) (see Section 6).

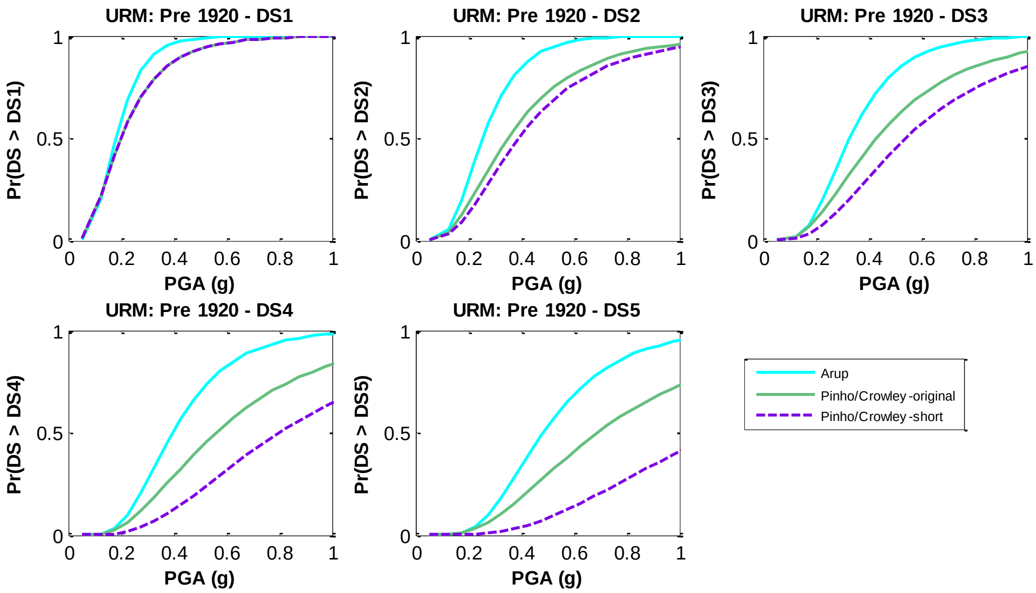

Figure 25 Comparison between the fragility functions proposed by Arup, those proposed by Pinho and Crowley (Pinho/Crowley-original) and those modified by Pinho and Crowley to account for the short duration of the ground motion (Pinho/Crowley-short) for the URM Pre 1920 buildings.

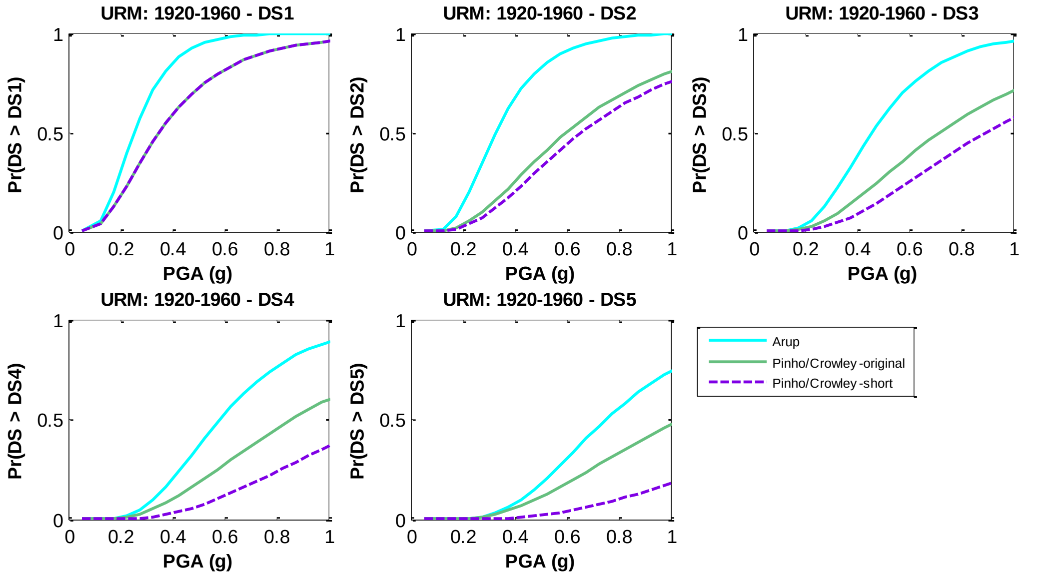

Figure 26 Comparison between the fragility functions proposed by Arup, those proposed by Pinho and Crowley (Pinho/Crowley-original) and those modified by Pinho and Crowley to account for the short duration of the ground motion (Pinho/Crowley-short) for the URM 1920-1960 buildings.

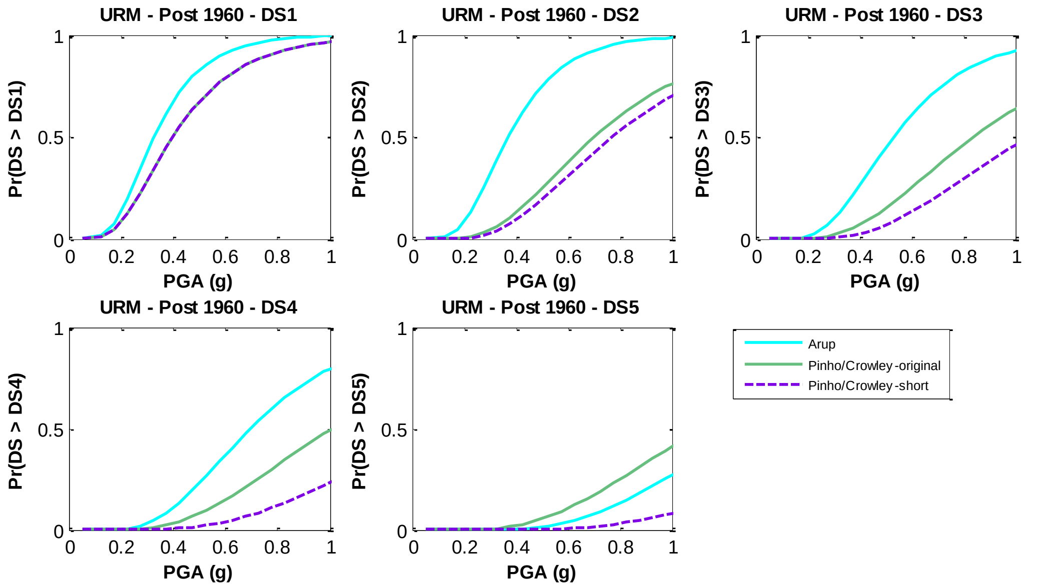

Figure 27 Comparison between the fragility functions proposed by Arup and those proposed by Pinho and Crowley for the URM Post 1960 buildings.

Pinho and Crowley (2013) have proposed fragility functions for URM buildings only and therefore for all the other buildings (reinforced concrete, steel and wood) the Arup fragility functions described in Section 4.8 are used.

4.10 Fragility Function Uncertainty

There are several sources of uncertainty and variability in the development and use of empirical fragility functions for seismic risk assessment. Some of these sources of uncertainty are listed below.

1. There is real variation in the performance of individual buildings within a building class subjected to the same level of ground motion (this is reflected in the standard deviation of the fragility function).
2. Buildings on which damage data was collected are not representative of buildings to which fragility functions are to be applied.
3. Data collection may introduce bias if damage states are unclear or inconsistent, or collection locations are not randomised.
4. Ground motion values associated with collected damage data may not be predicted or measured correctly. Furthermore, if damage data are grouped into ranges (e.g. over a whole town or city block) then ground motion may vary within that range.
5. Characteristics of earthquake ground motion (other than the PGA considered as the measure of ground motion intensity here, such as ground motion duration) may influence the damageability of the earthquake. If damage data are taken from earthquakes with different characteristics, then this will introduce bias.
6. Different regression analysis methods used by researchers to fit functions to empirical data give different results. Different functional forms fit to the same data will also be different.

Items 1 and partially 4 are taken into account through the fact that the fragility function is probabilistic, with a standard deviation that includes both the real variability in damage data in the data set and some of the uncertainty when this data is combined together. If this variability did not exist, fragility functions would be vertical lines, indicated 100% probability of collapse at a particular level of PGA.

Items 2, 3, partially 4, 5 and 6 are mitigated by careful selection of empirical data to use, supplemental analytical/experimental studies to understand effects of certain variables on damage estimates, and by the inclusion of multiple fragility curves in a logic tree approached, as discussed in Section 5.4. This has been partially carried out here, by including results for both the Arup fragility functions and Pinho and Crowley fragility functions, including duration adjustments (item 5 above). This does not fully explore the range of uncertainties, however, as both studies used data from the Roermond earthquake to calibrate models (which did not cause any damage beyond DS3) and the same functional form (log-normal) for the relationships.

Ground motion duration has been identified as a key input into the fragility functions (item 5), and, as noted in the previous section, has been taken into account in a preliminary study in the fragility functions of Pinho and Crowley. Ground motions from the magnitude 5 earthquake scenarios considered here are expected to be shorter duration than those from earthquakes from which earthquake damage data are typically collected. The collapse performance of masonry buildings has been shown to be duration dependent, and therefore typical fragility curves in the literature would require adjustment for short durations. A preliminary Arup study into the effect of duration is presented in Appendix C, which shows a smaller effect of duration than that shown by Pinho and Crowley (2013) (around 20% increase in the PGA to cause collapse, compared with 40% increase). For both the Arup and Pinho and Crowley duration studies, the numerical model on which these studies were calibrated needs to be verified by experimental models, and the studies need to be expanded to a wide range of masonry building types in the area, before the effect of duration can be reliably estimated.

Other sources of uncertainty, particularly those relating to the specific characteristics of Groningen building stock (item 2), are also being addressed by on-going studies. Analytical models that have been developed for masonry buildings in the area (presented in the Arup Structural Upgrading study) show a wide variation in the behaviour of different typologies of building, whereas the masonry fragility functions used in the risk assessment study are classified only based on building age. For example, analytical results for terraced and semi-detached houses show higher vulnerability than other building types, whereas in the present risk assessment the same fragility curves have been used for these typologies. As noted with regard to item 1 on the list above, the variability in fragility for different buildings within a classification is taken into account in the standard deviation on the fragility curve, and therefore represents a range of possible values for buildings in the overall population.

The Structural Upgrading study shows a range of results, depending on analysis method adopted, but the results using the most detailed structural analysis method (time history analysis) indicate PGAs required to cause partial collapse (approximately equivalent to DS4) of around 0.45g (terraced house model) and > 0.5g (villa model). This is not inconsistent with the DS4 fragility functions in Figure 24, which are intended to represent the range of URM buildings in the Groningen area.

Going forward, fragility functions will be further refined based on the following:

- The Cambridge Global Consequences Database will be used to collect further international data that is more closely related to the Groningen context;
- Detailed analytical models from the Structural Upgrading study will be used to get a better estimate of the variation in PGAs to reach each damage state for specific building typologies, and to further separate sub-typologies of buildings that should be identified in the building database and separated in the risk calculations;
- Statistical sensitivity studies on the building stock in the area will used to identify the range of potential building geometries to explore the effect of this on structural response and building fragility functions. Initial studies on the variation in wall opening sizes on a subset of buildings in Loppersum are presented in the Structural Upgrading study report.

4.11 Fragility Functions for Strengthened Buildings

Analytical modelling work is on-going to develop fragility functions for buildings that have been retrofitted by structural engineering measures. It is anticipated that the structural engineering measures will very significantly reduce the number of buildings that will experience moderate, extensive, complete damage and collapse.

5 Risk Calculation

5.1 Introduction

This section of the report describes the risk calculation methodology for estimation of building damage and for estimation of casualties.

5.2 Building Damage Calculation

The probability of having damage state, Pr(DS=DS_i) with i=1…5, given the occurrence of a peak ground acceleration PGA= a_j, can be estimated directly from the fragility functions as shown in Figure 28.

Consequently the number of buildings in each damage state is easily computed from the number of buildings subject to a certain acceleration and the probability that given such an acceleration level the buildings will have suffered a certain level of damage. The details and the equations for this calculation are illustrated below.

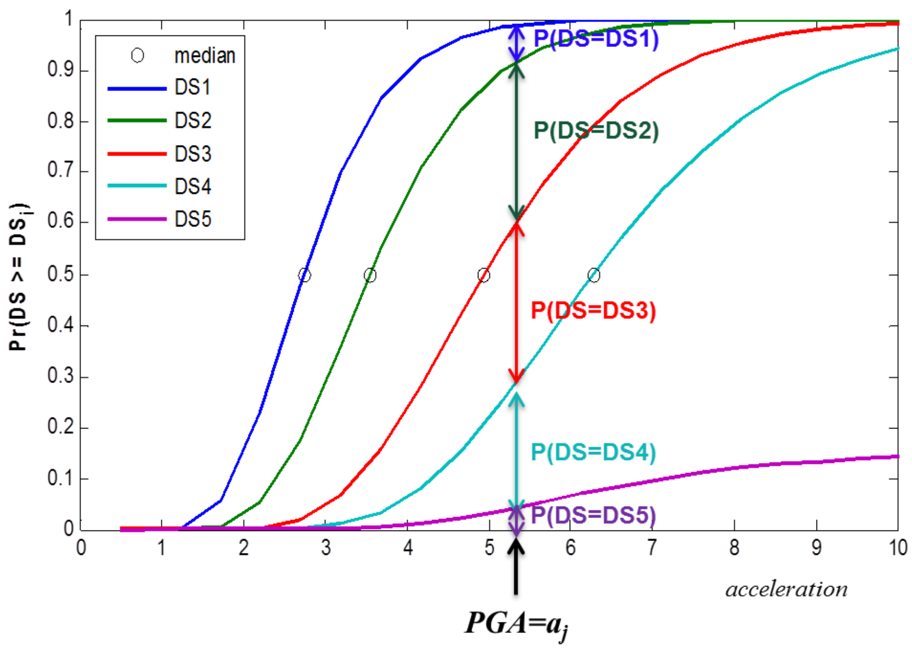

Figure 28 Scheme of the computation of the damage state probability given PGA=aj, and a set of fragility functions.

The probability of having damage state (DS_i with i=1…5) given the occurrence of a peak ground acceleration PGA= a_j, can be estimated directly from the fragility functions:

$$P(DS = DS_i \mid PGA = a_j)_{BCL} = P(DS \geq DS_i \mid PGA = a_j)_{BCL} - P(DS \geq DS_{i+1} \mid PGA = a_j)_{BCL}$$

The number of potential buildings of building class BCL_k that will experience damage state DS_i, $N_{b,}(DS_{i,} BCL_k)$, is computed as:

$$N_b(DS_i, BCL_k) = \sum_{j=1}^{N_a} P(DS = DS_i \mid PGA = a_j)_{BCL_k} \times N_b(a_j, BCL_k)$$

where N_a is the number of acceleration value for a certain scenario and $N_{b,}(a_j,BCL_k)$, is the number of buildings of class BCL_k subjected to $PGA=a_j$.

The total number of buildings in DS_i is simply the sum over all the building classes:

$$N_b(DS_i) = \sum_{j=1}^{N_{BCL}} N_b(DS_i, BCL_k)$$

where N_{BCL} is the total number of building classes (8 in this risk analysis), and $N_b(DS_i)$ is the total number of buildings in DS_i.

5.3 Casualty Estimation

HAZUS (FEMA, 2013) provides the methodology for the estimation of casualties based on the assumption that there is a strong correlation between the level of damage and the number and severity of the casualties.

Severity levels (SL) are defined as:

- SL 1: injuries that require basic medical aid and could be administered by paraprofessionals. They would need bandages or observations.
- SL 2: injuries requiring a greater level of medical care and use of medical technology (x-rays or surgery) but not expected to progress to a life threatening status.
- SL 3: injuries posing immediate life threatening conditions if not adequately treated.
- SL 4: instantaneously killed or mortally injured.

The number of casualties of a severity level *n*, *SL1 to SL4,* is the product of:

- The number of buildings in the damage states for each building class, *BCL*: $N_b(DS_i, BCL_k)$.
- The distribution of the population among the building classes and usage type. An average number of people per building class and usage is used: $\overline{N}_{people}(BCL_k)$.
- The proportion of people that will be indoor (*IN*) and outdoor (*OUT*) during the occurrence of the earthquake (Table 10). Indoor and outdoor population are estimated as proportions of the total population, depending on the usage of the buildings (e.g. residential, commercial, industrial, etc.).

Hence, for each damage state and building type, the numbers of casualties of severity level SL1, 2, 3 and 4 can be computed as:

$$N_{people,IN}(SL_n, DS_i, BCL_k) = N_b(DS_i, BCL_k) \times \overline{N}_{people}(BCL_k) \times \Pr_{IN}(SL = SL_n \mid DS_i) \times IN$$
$$N_{people,OUT}(SL_n, DS_i, BCL_k) = N_b(DS_i, BCL_k) \times \overline{N}_{people}(BCL_k) \times \Pr_{OUT}(SL = SL_n \mid DS_i) \times OUT$$

The indoor and outdoor casualty rates, $Pr(SL{=}SL_n|DS_i)$, are provided by HAZUS (FEMA, 2013) and are shown in Table 11 and Table 12 respectively, as a function of building typology and damage state.

Table 10 Proportions of people expected to be indoor and outdoor during the day and during the night (HAZUS, FEMA 2013).

USAGE	INDOOR		OUTDOOR	
	Night	Day	Night	Day
Residential	100%	70%	0%	30%
Commercial	100%	99%	0%	1%
Industrial	100%	90%	0%	10%
Agricultural	100%	99%	0%	1%
Religion/Non Profit	0%	99%	0%	1%
Government	0%	99%	0%	1%
Education	0%	90%	0%	10%

Table 11 Indoor Casualty rates by Model Building type and damage states (based on HAZUS, FEMA 2013).

Building Type	Severity level	DS1	DS2	DS3	DS4	DS5
URM	SL1	0.05%	0.35%	2%	10%	40%
	SL2	0%	0.4%	0.2%	2%	20%
	SL3	0%	0.001%	0.002%	0.02%	5%
	SL4	0%	0.001%	0.002%	0.02%	10%
RC1/RC2	SL1	0.05%	0.25%	1%	5%	40%
	SL2	0%	0.03%	0.1%	1%	20%
	SL3	0%	0%	0.001%	0.01%	5%
	SL4	0%	0%	0.001%	0.01%	10%
Wood	SL1	0.05%	0.25%	1%	5%	40%
	SL2	0%	0.025%	0.1%	1%	20%
	SL3	0%	0%	0.001%	0.01%	3%
	SL4	0%	0%	0.001%	0.01%	5%
Steel: S1/S2	SL1	0.05%	0.2%	1%	5%	40%
	SL2	0%	0.025%	0.1%	1%	20%
	SL3	0%	0%	0.001%	0.01%	5%
	SL4	0%	0%	0.001%	0.01%	10%

Note that the casualty rates in Table 11 for collapsed buildings (DS5) are lower for SL3 severity than for SL4 severity casualties, for all building types. This is a function of the definition of severity levels in HAZUS (FEMA 2013), and indicates that in collapsed buildings, fewer people are expected to suffer immediate life threatening injuries than those who are instantaneously killed or mortally injured.

Table 12 Outdoor Casualty rates by Model Building type and damage states (based on HAZUS, FEMA 2013).

Building Type	Severity level	DS1	DS2	DS3	DS4	DS5
URM	SL1	0%	0.15%	0.6%	5%	5%
	SL2	0%	0.015%	0.06%	2%	2%
	SL3	0%	0.0003%	0.006%	0.4%	0.4%
	SL4	0%	0.0003%	0.0006%	0.6%	0.6%
RC1	SL1	0%	0.05%	0.1%	2%	2%
	SL2	0%	0.005%	0.001%	0.5%	0.5%
	SL3	0%	0%	0.001%	0.1%	0.1%
	SL4	0%	0%	0.0001%	0.1%	0.1%
RC2	SL1	0%	0.05%	0.2%	2.2%	2.2%
	SL2	0%	0.005%	0.02%	0.7%	0.7%
	SL3	0%	0%	0.002%	0.2%	0.2%
	SL4	0%	0%	0.0002%	0.2%	0.2%
Wood	SL1	0%	0.05%	0.3%	2%	2%
	SL2	0%	0.005%	0.03%	0.5%	0.5%
	SL3	0%	0.0001%	0.003%	0.1%	0.1%
	SL4	0%	0.0001%	0.0003%	0.05%	0.05%
Steel S1	SL1	0%	0.05%	0.1%	2%	2%
	SL2	0%	0.005%	0.01%	0.5%	0.5%
	SL3	0%	0%	0.001%	0.1%	0.1%
	SL4	0%	0%	0.0001%	0.01%	0.01%
Steel S2	SL1	0%	0.05%	0.2%	2.2%	2.2%
	SL2	0%	0.005%	0.02%	0.7%	0.7%
	SL3	0%	0%	0.002%	0.2%	0.2%
	SL4	0%	0%	0.0002%	0.02%	0.2%

6 Risk Assessment Calculation Results

6.1 Introduction

This section of the report provides a summary of the earthquake scenario-based building damage and casualty assessment results. The extended building database (see Section 3) is used for the calculation of the number of damaged buildings. Information on the distribution of population and usage of the buildings for the extended buildings database is incomplete and therefore the preliminary building database (i.e. the area within 15 km radius around Huizinge) is used for the casualty estimation. It should be emphasised that the compilation of the building database for the extended study area is work in progress and therefore subject to change. However, it is recommended that the findings of the report are considered suitable to provide a basis for prioritising future risk management work.

The first task in the risk assessment calculation is to calibrate the earthquake scenario-based building damage assessment using the observed building damage from the earthquake with a magnitude M_w=3.6 which occurred in Huizinge in August 2012. The estimated building damage from this earthquake scenario is computed for comparison purposes only. For sake of brevity, this scenario is presented in Appendix D2. The calibration was followed by an estimation of building damage from an earthquake of magnitude M_w=5 with an epicentre location in Huizinge (Section 6.2).

Sensitivity analyses are carried out to test the influence on the risk results in terms of building damage and casualties of the choices made in terms of a number of key input assumptions:

- Earthquake magnitude: the risk results from four earthquake scenarios are compared with M_w =3.6, M_w =4, M_w =4.5 and M_w =5, using both the 50th and the 84th percentiles (mean +1 sigma in logarithm terms).
- Earthquake location: three earthquake scenario epicentre locations are considered (Huizinge, Zandeweer and Hoeksmeer).
- Fragility functions: three earthquake scenarios are compared with three sets of fragility functions.

Detailed results for each of these scenarios are presented in Appendix D. The sensitivity analyses are provided in this section to highlight the influence of the different input parameters (Section 6.3).

A further set of analyses is undertaken to investigate the effect of ground motion variability on the risk estimation. The ground motion spatial variability and its influence on the results are investigated through a Monte Carlo approach for the M_w =5 earthquake scenario, assuming either the ground motion is spatially uncorrelated or fully correlated. The main results are presented in Section 6.4, while more details are provided in Appendix D11.

Table 13 summarizes the scenarios considered in the following sections, as well as the corresponding maximum PGA value (PGA_{max}).

Table 13 Earthquake scenarios included in the damage assessment.

Purpose	**Case**	**Epicentre**	**M_w**	**GMPE**	**GMPE variability**	**PGA$_{max}$ (g)**	**Fragility function**
2012 Huizinge	# 0 a,b	Huizinge	3.6	ASB2013	50th perc./84 th perc.	0.082/0.171	Arup
Magnitude	# 1 a,b,c	Huizinge	5	ASB2013	50 th perc/84 th perc and mean	0.234/0.488/ 0.306	Arup
Magnitude	# 2 a,b	Huizinge	4	ASB2013	50th perc./84 th perc.	0.113/0.236	Arup
Magnitude	# 3 a,b	Huizinge	4.5	ASB2013	50th perc./84 th perc.	0.165/0.343	Arup
Epicentre	# 4	Zandeweer	5	ASB2013	50th perc.	0.234	Arup
Epicentre	# 5	Hoeksmeer	5	ASB2013	50th perc.	0.234	Arup
Fragility functions	# 6	Huizinge	5	ASB2013	50th perc.	0.234	Pinho/Crowley original
Fragility functions	# 7	Huizinge	5	ASB2013	50th perc.	0.234	Pinho/Crowley short duration
GM variability	# 8	Huizinge	5	ASB2013	Random fully correlated	(*)	Arup
GM variability	# 9	Huizinge	5	ASB2013	Random fully uncorrelated	(*)	Arup

(*) 2500 scenarios are carried out for these analyses, each having a different PGA$_{max}$ according to the number of standard error included in the GMPE.

In this report, quantities of damaged buildings and human losses are reported in tables and figures to the nearest whole number of buildings and people, respectively. This allows small changes between different analysis assumptions to be reported. However, due to the probabilistic nature of the calculations, and uncertainties in seismic hazard, building fragility and exposure data, the estimated loss quantities should be considered accurate to no more than one or two significant figures. In text descriptions of results, reported numbers are generally rounded to one significant figure.

6.2 Scenario # 1: Huizinge Earthquake M_w = 5 - Median (50th percentile) PGA

Scenario #1 comprises a M_w = 5 earthquake with an epicentre located at Huizinge and with a hypocentral depth of 3 km. The earthquake is assumed to have a point source and median ground motion PGA values have been used.

The distribution of ground motions in terms of median PGA caused by this scenario earthquake are shown in Figure 29.

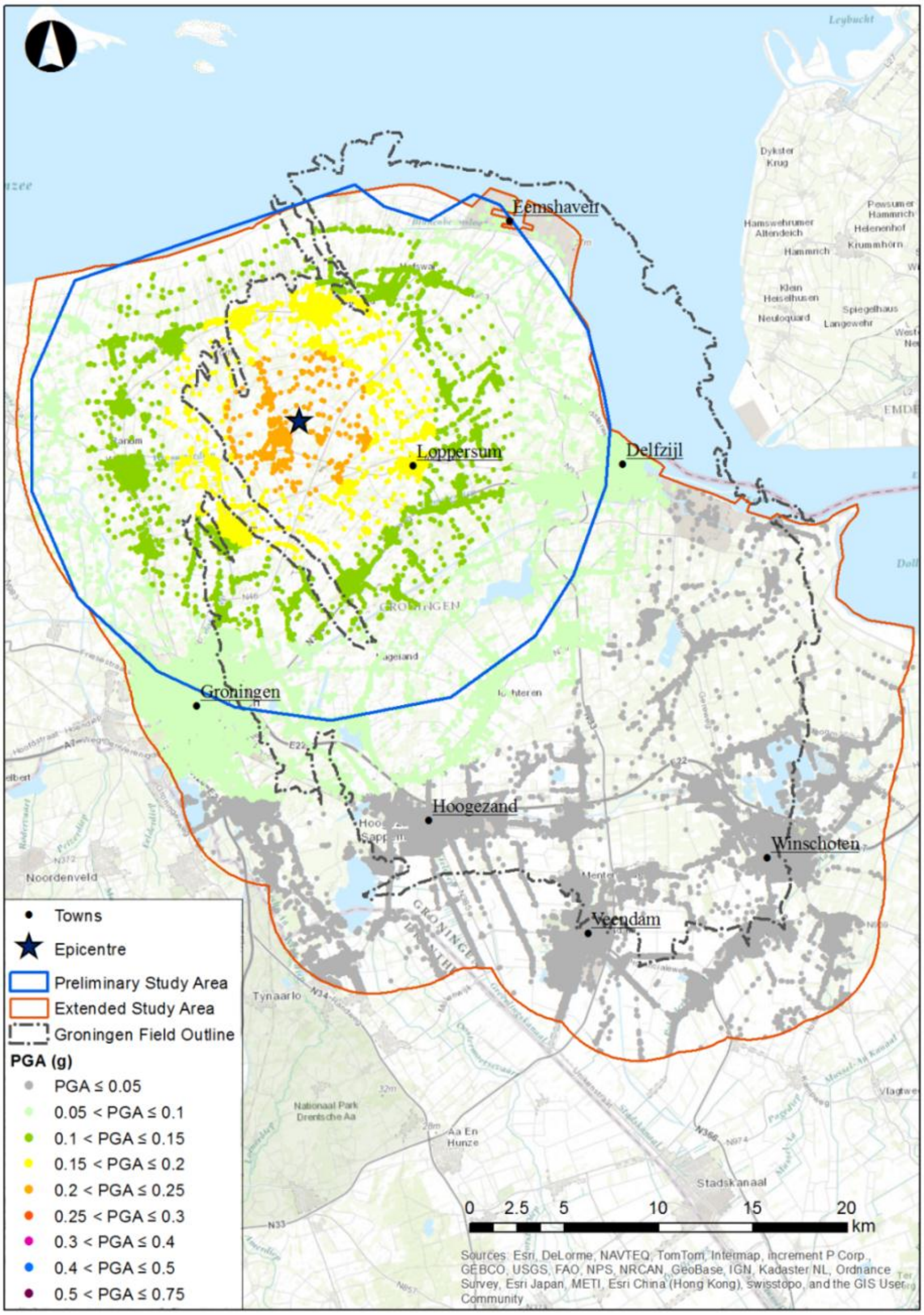

Figure 29 Median peak ground acceleration (PGA) estimated for an earthquake of M_w=5 and depth H=3 km with epicentre in Huizinge. The GMPE by Akkar et al. (2013) is used.

6.2.1 Number of Buildings Exposed

The number of buildings that are subjected to different levels of ground motion, in terms of PGA, are summarised in Table 14.

Table 14: Number of buildings subjected to ground motion (*PGA* in g) in scenario #1 - Huizinge M_w = 5 earthquake using the 50th percentile of the GMPE.

Building Type	$0 \leq PGA < 0.05$	$0.05 \leq PGA < 0.1$	$0.1 \leq PGA < 0.15$	$0.15 \leq PGA < 0.2$	$0.2 \leq PGA < 0.25$
URM: Pre 1920	4307	15735	2352	1412	442
URM: 1920-1960	24395	44534	4411	3132	648
URM: Post 1960	26545	49134	6552	4501	644
RC1	1796	4192	473	315	37
RC2	749	2494	69	62	4
Wood	253	156	109	50	21
S1	478	705	132	62	13
S2	61	121	5	1	2

6.2.2 Building Damage

The calculated number of buildings of different typologies damaged in this scenario are summarised in Table 15 and Figure 30. The numbers of damaged buildings are reported for each damage state: DS1 (slight damage), DS2 (moderate damage), DS3 (extensive damage), DS4 (complete damage) and DS5 (collapse).

In this scenario the calculated damage is dominated by slight and moderate damage to older unreinforced masonry buildings. However approximately 270 buildings suffer damage DS3, 100 are completely damaged by the earthquake and 47 buildings, mainly belonging to URM pre-1920 typology, are estimated to collapse.

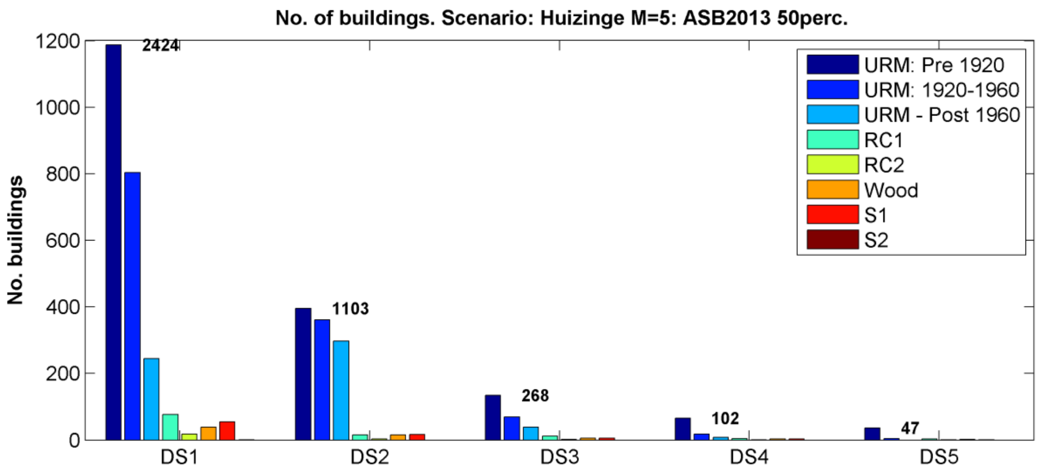

Figure 30 Number of buildings in damage state DS1, DS2, DS3, DS4 and DS5 according to their building typology class for the Huizinge M_w = 5 earthquake scenario.

Table 15: Number of buildings damaged in Huizinge M_w = 5 earthquake scenario

Huizinge (#1)	DS1	DS2	DS3	DS4	DS5
50th percentile	2424	1103	268	102	47

6.2.3 Casuality Estimation

The methodology proposed by HAZUS (FEMA, 2013) is followed for the estimation of the casualties. To this end, the number of buildings in damage states DS4 and DS5 is re-computed following the HAZUS guidelines: the number of collapsed buildings is a proportion of the buildings that suffer complete damage. This proportion depends on the building typology and is called Collapse Rate (see Section 4.7. It is important to highlight that the casualty estimation is performed adopting the 15 km radius study area (blue outlines in Figure 29). Figure 31 presents the numbers of buildings in each damage state for the 15 km radius building database area when the 50th percentile PGA values are used. The damage states DS4 and DS5 are computed both using the fragility functions and with the HAZUS Collapse Rates (DS4 – H and DS5 – H). The HAZUS methodology leads to 21 collapsed buildings and 125 completely damaged buildings. These numbers, DS4 – H and DS5 – H, are used only for the casualty estimation purposes.

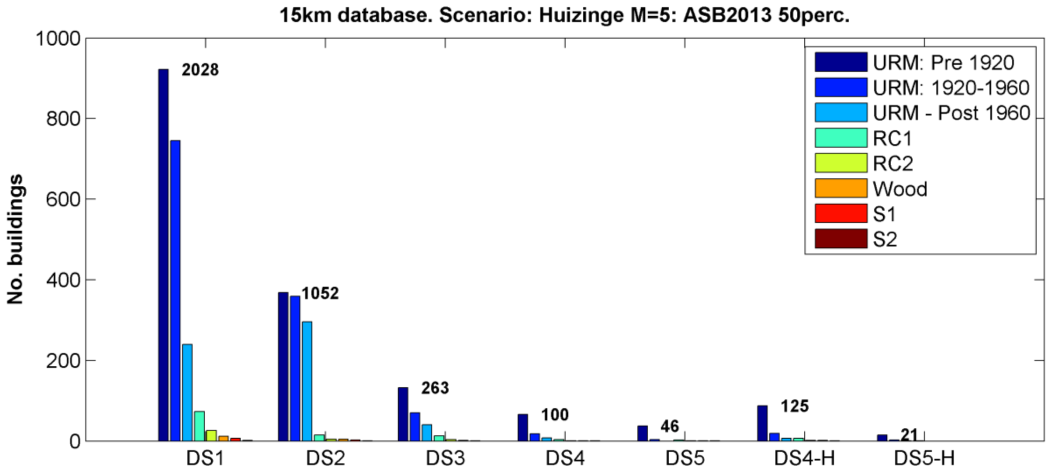

Figure 31: Number of buildings in damage state DS1, DS2, DS3, DS4 and DS5 according to their building class for the Huizinge M_w = 5 earthquake scenario. DS4 – H and DS5 – H represent the number of buildings computed using the HAZUS methodology for loss estimation purposes. Labels in the plot present the total number of buildings in each damage state.

The numbers of casualties in terms of the severity of injury are summarised on the top panel of Figure 32 for the occurrence of the Huizinge M_w = 5 scenario event during the day and on the bottom panel for the occurrence of the event during the night. The figure shows the number of people that would suffer injury severity levels (SL) 1 to 4 in damage states DS1, DS2, DS3, DS4 (HAZUS) and DS5 (HAZUS). 113 people are estimated to be slightly-to-seriously injured with approximately 6 potential fatalities during the day and 104 injured and 5 potential fatalities during the night. This shows that casualty estimates are relatively unaffected by when the scenario earthquake occurs.

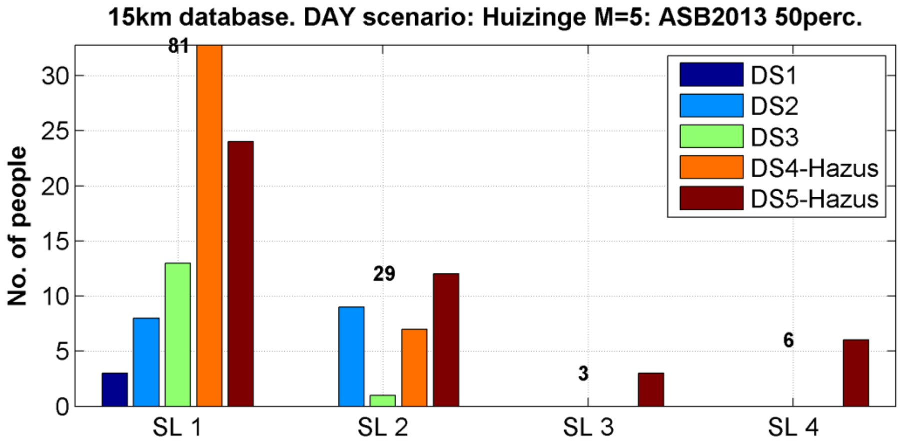

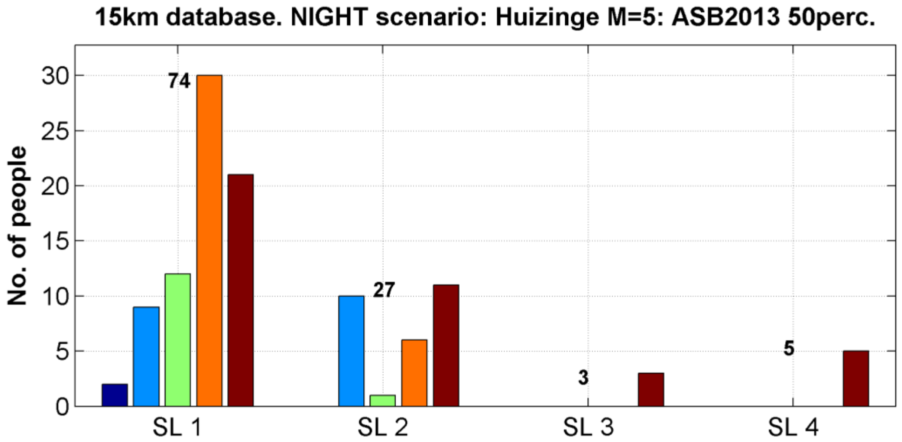

Figure 32 Estimated number of casualties in severity levels SL1, SL2, SL3 and SL4 associated with damage states DS1, DS2, DS3, DS4 and DS5, due to the occurrence of the Huizinge $M_w = 5$ earthquake scenario during the day (2 pm), top panel, and during the night (2 am), bottom panel.

6.3 Sensitivity Analyses

This section describes the sensitivity analyses undertaken to investigate the effect of the PGA percentile (Section 6.3.1), of the earthquake magnitude (Section 6.3.2), earthquake location (Section 6.3.4) and to the selected fragility functions (Section 6.3.5) on the risk assessment results. Detailed results are presented in Appendix D.

6.3.1 Comparison between the 50th Percentile, the 84th Percentile and the Mean PGA Scenarios M_w = 5

84th percentile PGA values at the building locations are shown in Figure 33 and the mean PGA values are shown in Figure 34.

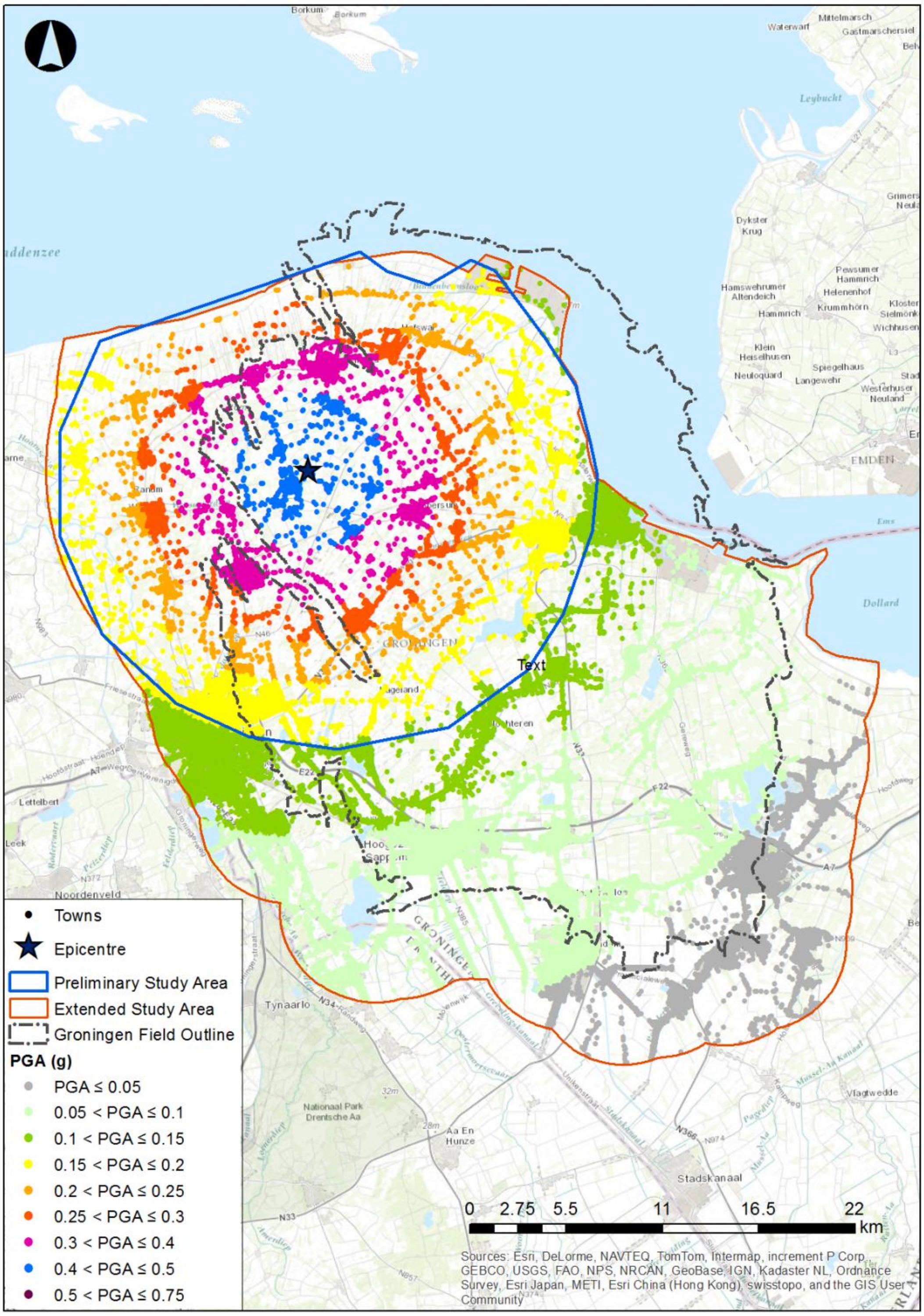

Figure 33 84th percentile peak ground acceleration (PGA) estimated for an earthquake of M_w=5 and depth H=3 km with epicentre in Huizinge. The GMPE by Akkar et al. (2013) is used.

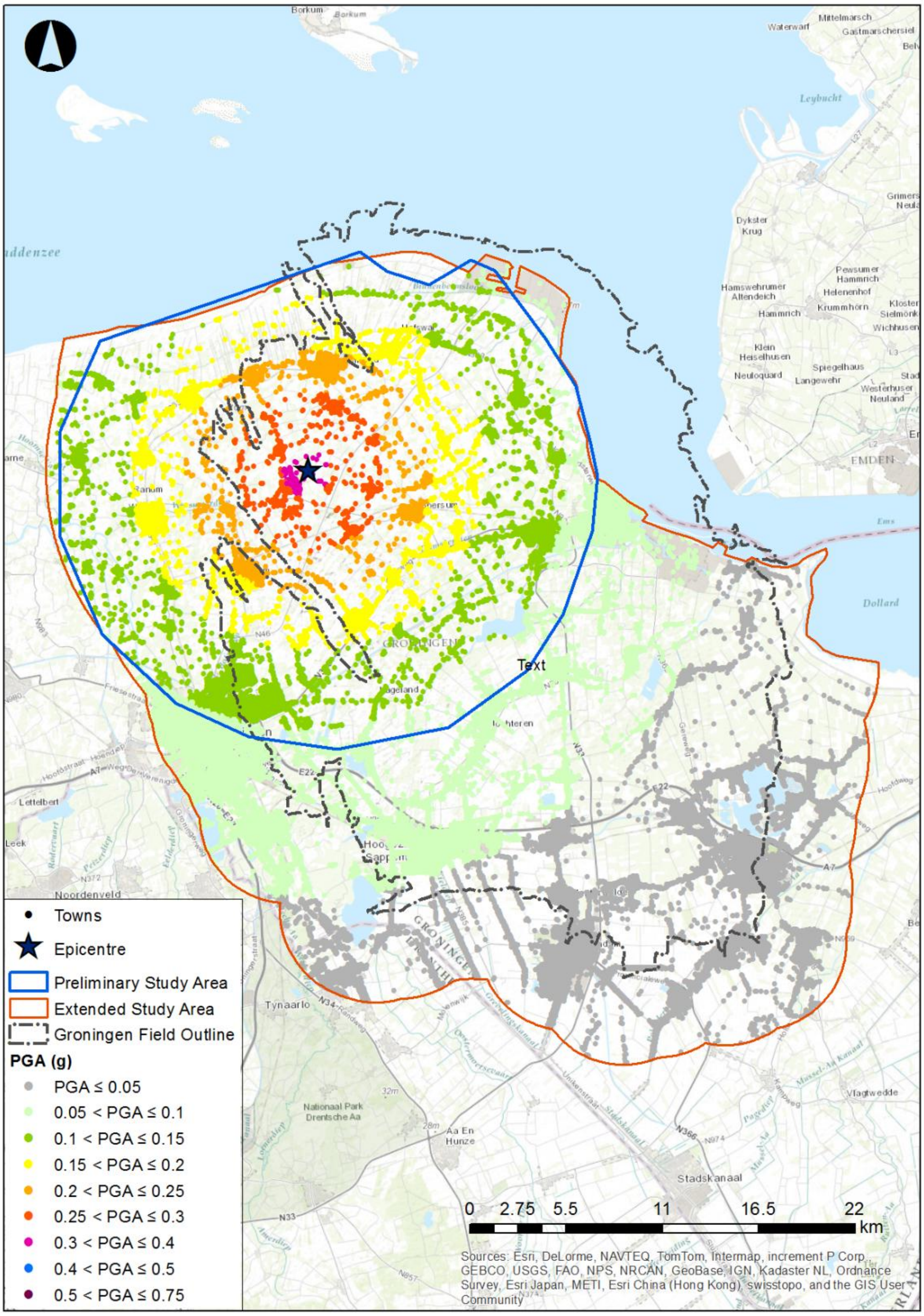

Figure 34 Mean peak ground acceleration (PGA) estimated for an earthquake of M_w=5 and depth H=3 km with epicentre in Huizinge. The GMPE by Akkar et al. (2013) is used.

A comparison of the estimated number of damaged buildings associated with the median (50th percentile), the 84th percentile and the mean PGA values is provided in Table 16 and on Figure 35. The median PGA values result in 47 collapsed buildings while the mean PGA values result in 201 collapsed buildings. As expected the 84th percentile PGA values provide an extreme scenario with 1286 collapsed buildings.

Table 16: Number of buildings damaged in Huizinge M_w = 5 earthquake scenario

	DS1	DS2	DS3	DS4	DS5
50th percentile	2424	1103	268	102	47
84th percentile	11847	9210	3351	1841	1286
Mean	4366	2738	802	355	201

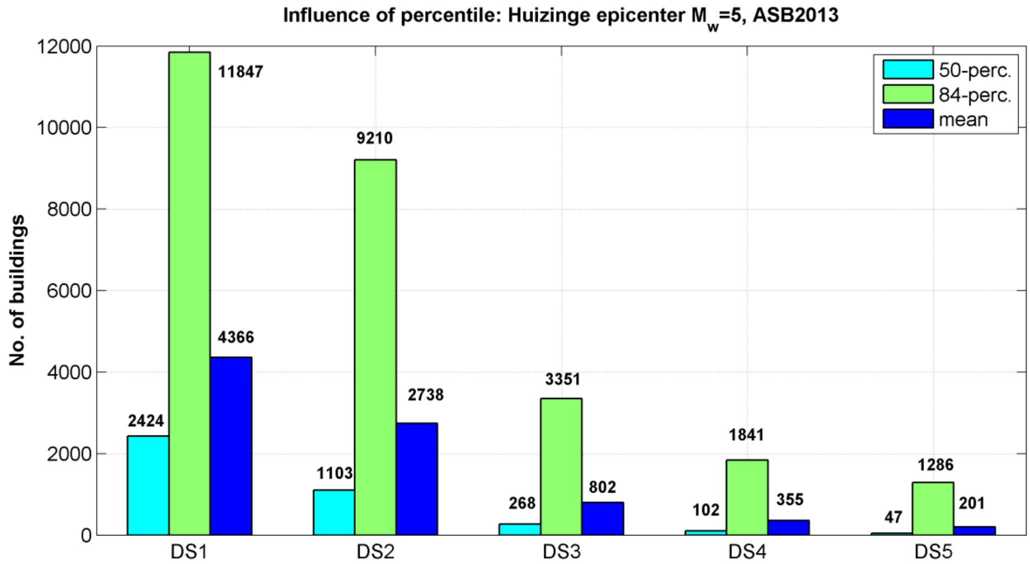

Figure 35: Comparison of the number of buildings in damage state DS1, DS2, DS3, DS4 and DS5 for the Huizinge M_w = 5 earthquake scenario using the 50th, the 84th percentiles and the mean of the GMPE.

Figure 36 and Figure 37 show the comparison of the expected number of casualties obtained with the 50th, 84th percentiles and the mean PGA values when the earthquake occurs during the day and during the night respectively.

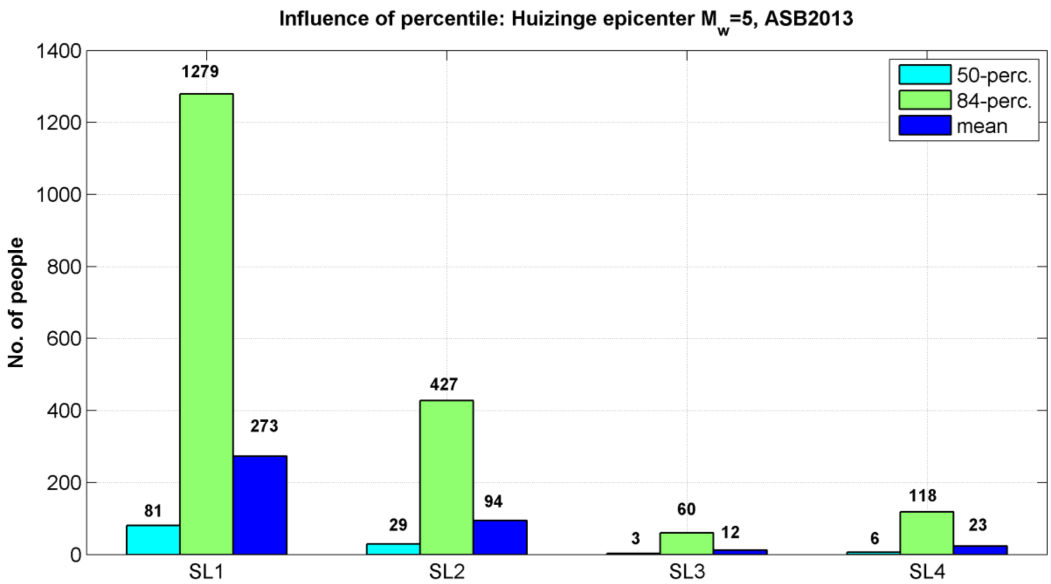

Figure 36 Comparison of the estimated number of casualties for the Huizinge M_w = 5 earthquake scenario occurring during the day using 50th, the 84th percentiles and the mean of the GMPE.

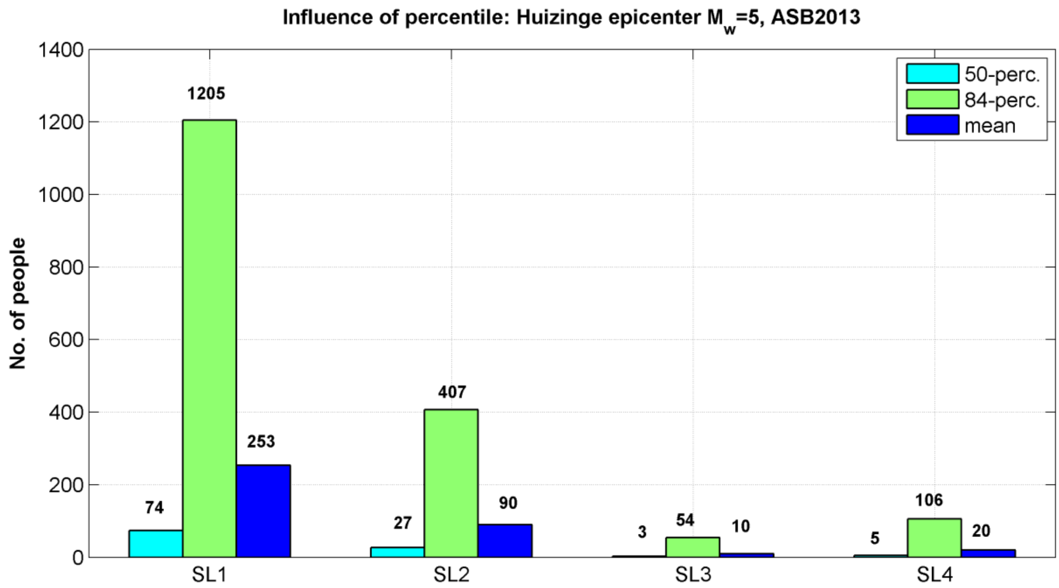

Figure 37 Comparison of the estimated number of casualties for the Huizinge M_w = 5 earthquake scenario occurring during the night using the 50th, the 84th percentiles and the mean of the GMPE.

The results highlight how sensitive the scenario-based risk assessment is to the level of ground motion used for the computation of the seismic hazard. A more in-depth analysis of the ground motion variability is presented in Section 6.4.

6.3.2 Comparison of the Results for the Four Earthquake Scenarios with Magnitude M_w = 3.6, 4, 4.5 and 5 (50th percentile PGA values)

The detailed analyses for the four earthquake magnitude results are presented in Appendix D. The Huizinge M_w=5 earthquake scenario (scenario #1) is taken as reference and the risk assessment is carried out for magnitude M_w=4 (scenario #2, Appendix D4) and 4.5 (scenario #3, Appendix D5). A comparison of the results for the 50th percentile PGA values is presented below. Appendix D10 presents the same comparisons for the 84th percentile PGA values among the four earthquake magnitude scenarios.

The results of the four earthquake scenarios in terms of damaged buildings are compared in Table 17 and Figure 38. Table 18 and Table 19 show the estimated number of casualties for the four earthquake scenarios. The risk results both in terms of damage and casualties indicate that expected losses are very sensitive to the magnitude, as expected.

Table 17: Comparison of the four earthquake scenarios with magnitude 3.6, 4, 4.5 and 5 in terms of number of buildings damaged to damage states DS1 to DS5. The extended database is used.

Scenario	Location	Magnitude	DS1	DS2	DS3	DS4	DS5
#0	Huizinge	3.6	42	6	1	0	0
#2	Huizinge	4	173	39	6	2	0
#3	Huizinge	4.5	753	269	54	18	7
#1	Huizinge	5	2424	1103	268	102	47

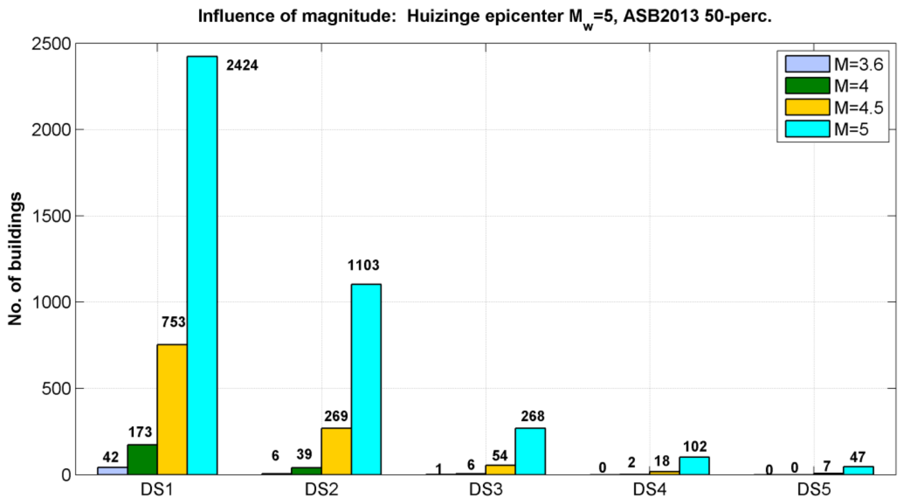

Figure 38 Comparison of the four earthquake scenarios with magnitude M_w=3.6, 4, 4.5 and 5 in terms of number of buildings damaged to damage states DS1 to DS5.

Table 18 Comparison of the estimated number of casualties for the four earthquake scenarios with magnitude M_w=3.6, 4, 4.5 and 5, assuming the occurrence of the earthquake during the day.

Scenario	Location	M_w	SL1	SL2	SL3	SL4
#0	Huizinge	3.6	0	0	0	0
#2	Huizinge	4	1.8	0.7	0	0
#3	Huizinge	4.5	16	6	0	1
#1	Huizinge	5	81	29	3	6

Table 19 Comparison of the estimated number of casualties for the three earthquake scenarios with magnitude M_w=3.6, 4, 4.5 and 5, assuming the occurrence of the earthquake during the night.

Scenario	Location	M_w	SL1	SL2	SL3	SL4
#0	Huizinge	3.6	0	0	0	0
#2	Huizinge	4	1.6	0.6	0	0
#3	Huizinge	4.5	14	6	0	1
#1	Huizinge	5	74	27	3	5

Careful review of the damage reports obtained after the 2012 Huizinge earthquake has revealed that some of the reports are duplicated, some are related to damage from other earthquakes and some are potentially related to pre-existing damage. Hence, the number of damaged buildings associated with the Huizinge earthquake may be lower than the number of damage reports and a direct comparison with the estimated number of damaged buildings obtained with this risk assessment is not possible.

6.3.3 Comparison of the Results for the Earthquake Scenarios with Magnitude M_w=3.6, 4, 4.5 and 5 (84th percentile PGA values)

The results for the four earthquake scenarios in terms of damaged buildings are compared in Table 20 and Figure 39. Table 21 and Table 22 show the estimated number of casualties for the four earthquake scenarios but using the 84th percentile of the ground motion PGA values.

Table 20 Comparison of the four earthquake scenarios with magnitude M_w=3.6, 4, 4.5 and 5 in terms of number of buildings damaged to damage states DS1 to DS5.

Scenario	Location	Magnitude	DS1	DS2	DS3	DS4	DS5
#0	Huizinge	3.6	617	231	49	17	6
#4	Huizinge	4	1636	830	210	82	39
#5	Huizinge	4.5	4206	3035	947	440	264
#1	Huizinge	5	11847	9210	3351	1841	1286

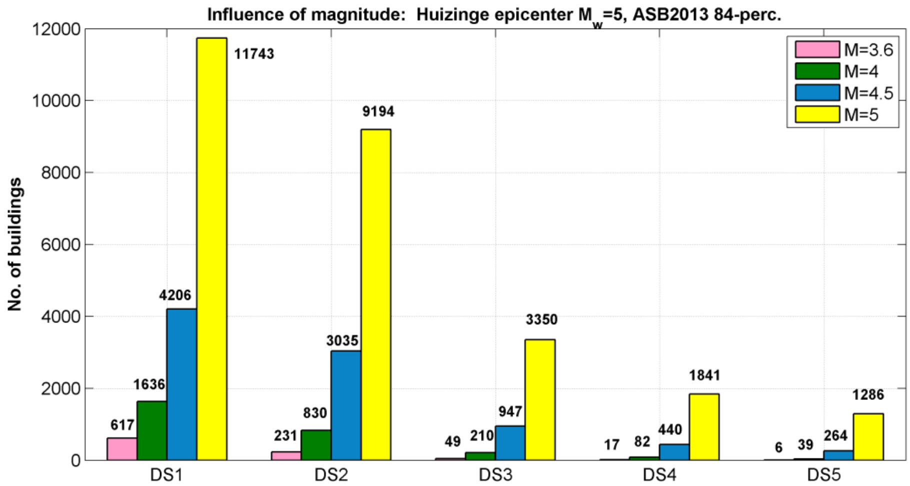

Figure 39 Comparison of the four earthquake scenarios with magnitude 3.6, 4, 4.5 and 5 in terms of number of buildings damaged to damage states DS1 to DS5.

Table 21 Comparison of the estimated number of casualties for the four earthquake scenarios with magnitude 3.6, 4, 4.5 and 5, assuming the occurrence of the earthquake during the day.

Scenario	Location	M_w	SL1	SL2	SL3	SL4
#0	Huizinge	3.6	15	5	1	1
#2	Huizinge	4	66	23	3	5
#3	Huizinge	4.5	339	116	15	29
#1	Huizinge	5	1279	386	50	118

Table 22 Comparison of the estimated number of casualties for the four earthquake scenarios with magnitude 3.6, 4, 4.5 and 5, assuming the occurrence of the earthquake during the night.

Scenario	Location	M_w	SL1	SL2	SL3	SL4
#0	Huizinge	3.6	13	5	0	1
#2	Huizinge	4	60	22	2	4
#3	Huizinge	4.5	314	111	13	26
#1	Huizinge	5	1205	407	54	106

The earthquake scenarios casualty estimates using the 84th percentile PGA values as input are found to be conservative with the estimated number of casualties interpreted to be higher than expected. The magnitude M_w =3.6 scenario with 84th percentile PGA results in 18 slight (SL1) to moderate (SL2) injuries and an estimated single potential fatality. This result is higher than the actual casualties associated with the August 2012 Huizinge earthquake. However, as noted previously, it is recommended that these higher casualty estimates are taken into consideration.

6.3.4 Comparison of Results for the Three Earthquake Epicentre Locations (50th percentile PGA values)

This section compares the results the sensitivity analyses undertaken to investigate the effect of changes of the earthquake location. To this end, the Huizinge scenario (scenario #1, Section 6.2) is taken as the reference and the risk assessment is carried out for two more locations: Zandeweer to the north of Huzinge (Appendix D6) and Hoeksmeer (Appendix D7) to the south. The 50th percentile PGA values are used in the calculations.

The risk results for the three earthquake scenarios in terms of damaged buildings are compared in Table 23 and in Figure 40. Table 24 and Table 25 show the number of casualty for the three earthquake scenario locations.

The damage results for each of the scenarios in terms of damaged buildings are similar, indicating that the building stock is relatively evenly distributed across the study area. The casualties' estimates are slightly lower in the case of the Hoeksmeer earthquake scenario due to the relative position of the epicentre and the preliminary study area used for casualty estimation.

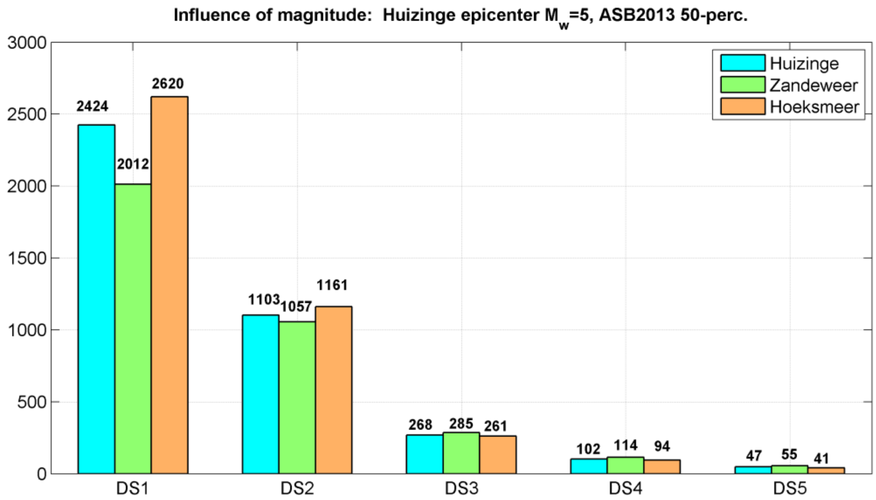

Figure 40: Comparison of the three M_w=5 earthquake scenarios in terms of number of buildings damaged to damage states DS1 to DS5. The extended database is used.

Table 23: Comparison of the three earthquake scenarios in terms of number of buildings damaged to damage states DS1 to DS5. The extended database is used.

Scenario	Epicentre	M_w	DS1	DS2	DS3	DS4	DS5
#1	Huizinge	5	2424	1103	268	102	47
#4	Zandeweer	5	2012	1057	285	114	55
#5	Hoeksmeer	5	2620	1161	261	94	41

The casualty estimates for the three earthquake scenario locations are also very similar indicating that the population is relatively evenly distributed across the study area.

Table 24: Comparison of the estimated number of casualties for the three M_w=5 earthquake scenarios, assuming the occurrence of the earthquake during the day.

Scenario	Epicentre	M_w	SL1	SL2	SL3	SL4
#1	Huizinge	5	81	29	3	6
#4	Zandeweer	5	90	31	4	7
#5	Hoeksmeer	5	65	23	3	5

Table 25: Comparison of the estimated number of casualties for the three M_w=5 earthquake scenarios, assuming the occurrence of the earthquake during the night.

Scenario	Epicentre	M_w	SL1	SL2	SL3	SL4
#1	Huizinge	5	74	27	3	5
#4	Zandeweer	5	81	30	3	6
#5	Hoeksmeer	5	58	22	2	4

6.3.5 Comparison of the Results Using the Three Families of Fragility Functions (50th percentile PGA values)

This section describes the sensitivity analyses undertaken to investigate the effect of the selection of the fragility functions on the risk assessment results. The M_w=5 Huizinge earthquake scenario is taken as the reference (Section 6.2). The risk assessment is then repeated using the fragility functions by Pinho and Crowley (scenario #6, Appendix D8) and the modified fragility functions to account for potential effects of ground motion short duration (scenario #7, Appendix D9). The median 50th percentile and the 84th percentile PGA values are used in the calculations. In this section the comparison is carried out for the median PGA values, while Appendix D10.1 present the comparisons using the 84th percentile PGA values.

The risk assessment results in terms of damaged buildings for the earthquake scenario computed with the three sets of fragility functions with the 50th percentile PGA values are compared in Table 26 and in Figure 41. Table 27 and Table 28 show the estimated number of casualties. Table 26 Comparison of the earthquake scenario of Huizinge M=5 using the three families of fragility functions in terms of number of buildings damaged to damage states DS1 to DS5.

Scenario	Location	Fragility functions	DS1	DS2	DS3	DS4	DS5
#1	Huizinge	Arup	2424	1103	268	102	47
#6	Huizinge	Pinho/Crowley “duration unmodified”	3075	363	208	77	53
#7	Huizinge	Pinho/Crowley “duration modified”	3263	349	124	29	10

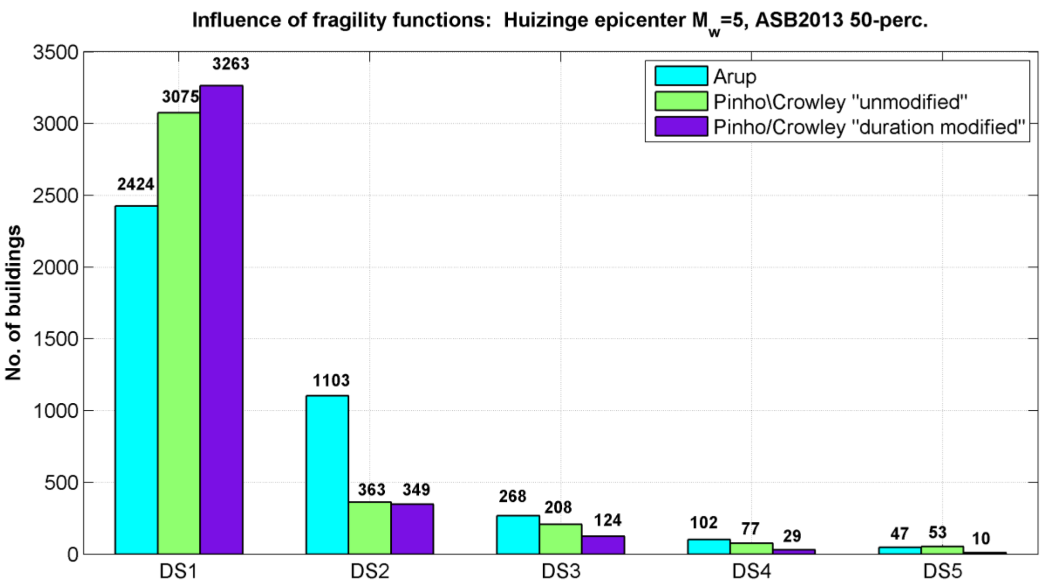

Figure 41 Comparison of the earthquake scenario of Huizinge M_w =5 using the three families of fragility functions in terms of number of buildings damaged to damage states DS1 to DS5.

The risk results from the Arup and Pinho and Crowley “duration unmodified” fragility functions are similar while the estimated number of damaged buildings and consequently the estimated number of injured people decreases when the effects of duration are accounted for in the fragility functions.

The estimated number of slightly damaged buildings (DS1) is similar with the three sets of fragility functions. The estimated number of moderately damaged (DS2) is significantly lower when using the Pinho and Crowley fragility functions. The estimated number of extensively damaged buildings is approximately 270 when the Arup fragility functions are used, approximately 210 in the case of the Pinho and Crowley “duration unmodified” fragility functions and decreases to 124 when the Pinho and Crowley “duration modified” fragility functions are adopted. The estimated number of completely damaged buildings is approximately 100 with Arup fragility functions set, approximately 80 in the case of the Pinho and Crowley “duration unmodified” fragility functions and decreases to approximately 30 when the Pinho and Crowley “duration modified” fragility functions are adopted. The number of collapsed buildings estimated with the Arup fragility functions is similar to that estimated with the Pinho and Crowley “duration unmodified” fragility functions (approximately 50) while only ten buildings are estimated to collapse with the Pinho and Crowley “duration modified” fragility functions.The estimated number of casualties using the Pinho and Crowley “duration modified” fragility functions is approximately one third (30%-40%) of the estimated casualties using the Arup fragility functions. The estimated number of casualties using the Pinho and Crowley “duration unmodified” fragility functions is approximately two thirds (60%-70%) of the estimated casualties using the Arup fragility functions for SL1 and SL2, but the number of severe injuries estimated with the Arup and with the Pinho and Crowley “duration unmodified” fragility functions is similar.

Table 27 Comparison of the estimated number of casualties for the earthquake scenario of Huizinge M_w=5 using the three families of fragility functions, assuming the occurrence of the earthquake during the day.

Scenario	Location	Fragility functions	SL1	SL2	SL3	SL4
#1	Huizinge	Arup	81	29	3	6
#6	Huizinge	Pinho/Crowley “duration unmodified”	64	20	3	5
#7	Huizinge	Pinho/Crowley “duration modified”	31	9	1	2

Table 28 Comparison of the estimated number of casualties he earthquake scenario of Huizinge M=5 using the three families of fragility functions, assuming the occurrence of the earthquake during the night.

Scenario	Location	Fragility functions	SL1	SL2	SL3	SL4
#1	Huizinge	Arup	74	27	3	5
#6	Huizinge	Pinho/Crowley “duration unmodified”	56	17	2	4
#7	Huizinge	Pinho/Crowley “duration modified”	21	7	1	1

6.4 Investigating the Ground Motion Variability

A further set of analyses is undertaken to better understand the influence of the ground motion variability on the risk estimation results. The details of the methodology have been described in Section 2.2.2. Examples of PGA maps derived with the fully correlated and the fully uncorrelated Monte Carlo cases for the M_w=5 Huizinge earthquake scenario and details on the Monte Carlo analyses are presented in Appendix D11. The analysis shows that a relatively small number of Monte Carlo simulations (2500) is sufficient to obtain a good estimate of the numbers of damaged buildings. Hence, a set of 2500 Monte Carlo simulations is used to carry out the casualty estimation within the study area (15 km radius) for the case of fully uncorrelated and fully correlated ground motion variability.

It is noted that both hypotheses represent extreme cases and the expected realistic ground motion experienced during an earthquake is spatially correlated to an extent which will depend on the distance between the buildings: ground motions recorded close to one another are expected to be closely correlated, while distant recordings are uncorrelated. The two cases herein analysed are two bounding cases. Moreover, in this study the ground motion variability distribution is sampled in an unbounded way (i.e. very large or very small ground motions are sampled from this distribution). In the uncorrelated case, this distribution is sampled 10,000s of times per analysis, and therefore this leads to extreme cases with PGA values over three standard deviations above the mean. Therefore, the result with some amount of spatial correlation taken into account would be expected to be closer to the fully correlated case, as it is not as influenced by the extreme values of ground motion. Median results (50th percentiles) from the Monte Carlo analysis are compared with the median results from the deterministic median PGA values as input.

The results are compared in Figure 42 in terms of median (50^{th} percentile) number of damaged buildings obtained in the assumption of full uncorrelation (green bars) and full correlation (blue bars).

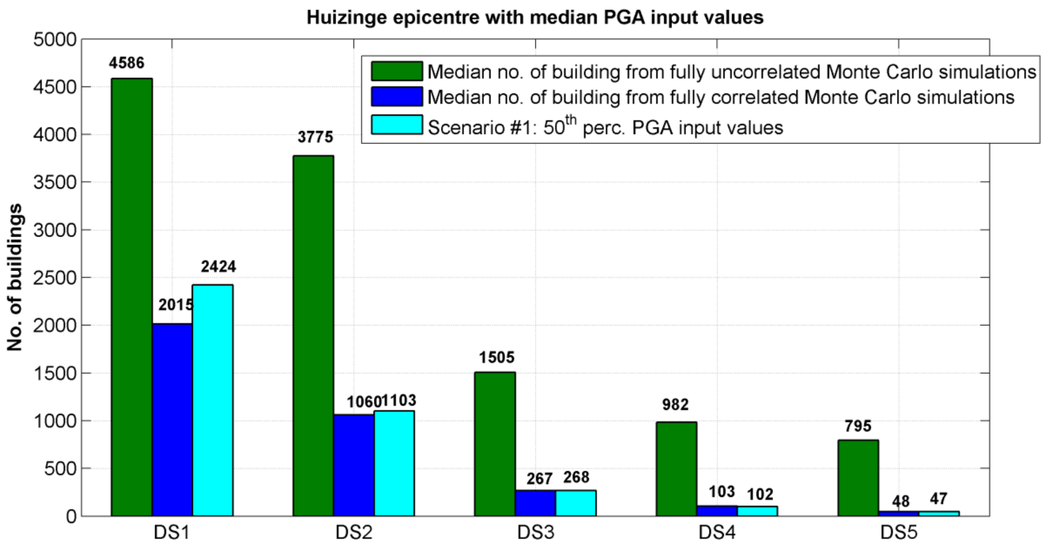

Figure 42 Comparison of the median (50^{th} percentile) number of damaged buildings obtained from the Huizinge M_w=5 scenario with the Monte Carlo simulation for the fully correlated case (blue), fully uncorrelated case (green). The numbers of damaged building obtained with the median PGA input values are shown for comparison.

Figure 43 compares the results obtained in terms of casualty estimation. It is highlighted that while in the uncorrelated case about 60 potential fatalities are estimated, in the case of the fully correlated PGA variability the estimated median number of potential fatalities is about 7. The estimated median (50^{th} percentile) number of damaged buildings and potential casualties obtained with the fully correlated spatial distribution of PGA values as input to the Monte Carlo simulations are consistent with the number of damaged buildings estimated using the median (50^{th} percentile) input PGA values of the GMPE.

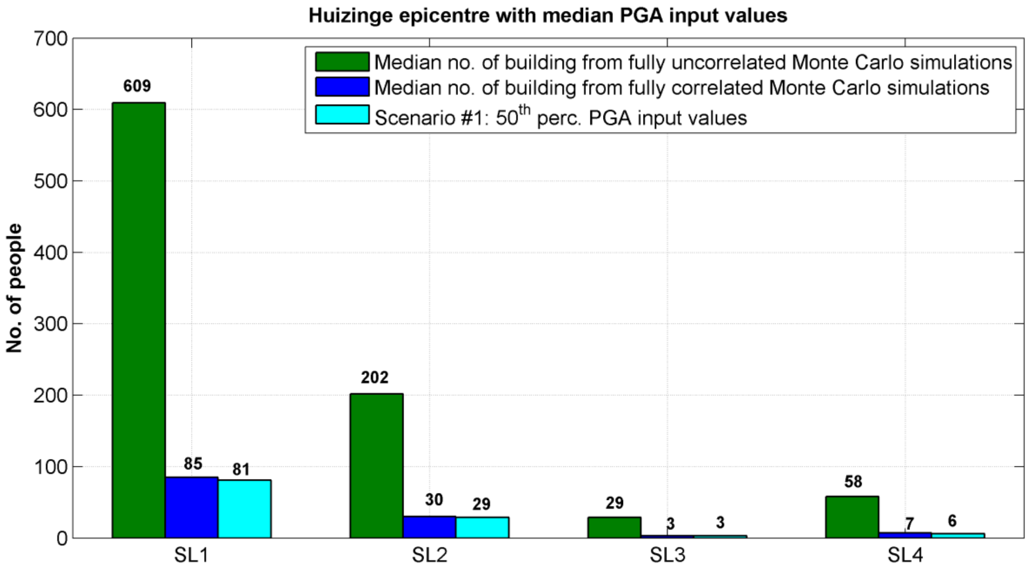

Figure 43 Comparison of the median (50^{th} percentile) numbers of casualties obtained from the Huizinge M_w=5 scenario with the Monte Carlo simulation for the fully correlated case (blue), fully uncorrelated case (green). The numbers of casualties obtained with the median PGA input values are shown for comparison.

6.4.1 Sensitivity of the Results to the Fragility Functions

A sensitivity analysis is undertaken to investigate the influence of the selected fragility functions on the mean number of damaged buildings obtained through the Monte Carlo simulations. As for the previous section, a set of 2500 Monte Carlo simulations and fully uncorrelated ground motion variability are assumed.

The results are presented in terms of median (50^{th} percentile) numbers of damaged buildings (Figure 44) and median number of casualty estimation assuming the occurrence of the M_w=5 earthquake scenario during the day (Figure 45).

The results are sensitive to the fragility functions used in the risk assessment as described previously. In particular, the number of estimated collapsed buildings and numbers of estimated fatalities is less if the Pinho and Crowley (2013) duration modified fragility functions are used compared to the Arup fragility functions. At this stage it is unknown which fragility functions best represent the likely performance of Groningen building stock under seismic loading and it is recommended that the range of results is considered.

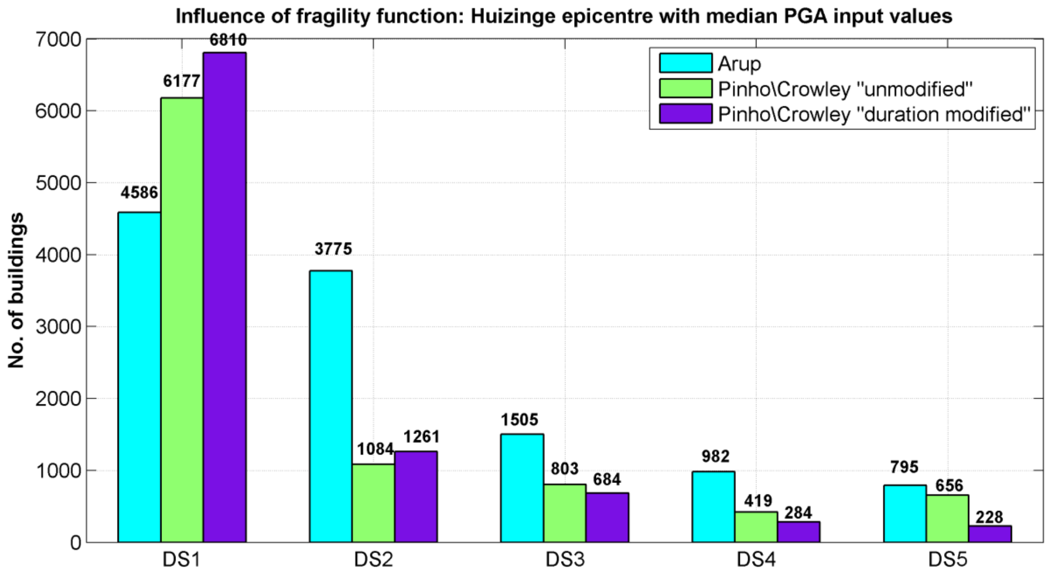

Figure 44 Comparison of the median (50th percentile) number of damaged buildings obtained from the Huizinge M_w=5 scenario using the three sets of fragility functions.

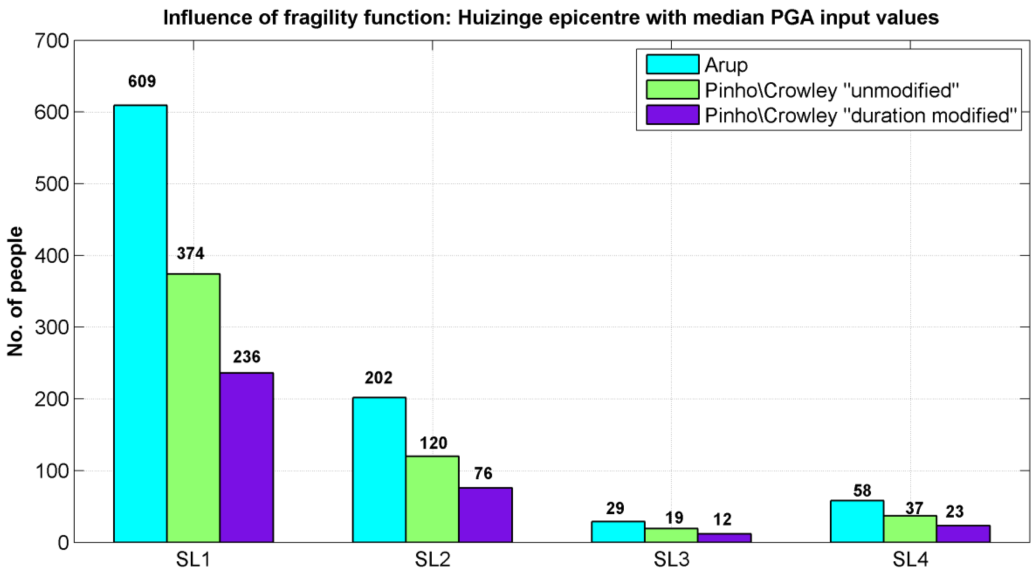

Figure 45 Comparison of the median (50th percentile) number of casualties obtained from the Huizinge M_w=5 scenario using the three sets of fragility functions.

6.5 Summary of the Risk Assessment Results

Potential building damage estimates (and subsequently the potential casualty estimates for the building occupants) are sensitive to the level of ground shaking (e.g. measured in PGA) expected at each building location. A given magnitude of earthquake that can potentially occur in the future can produce a range of possible PGAs at each building location. Therefore, to answer questions like, “how many buildings are expected to be damaged in a M_w=5 earthquake?”, a range of possible outcomes, some more likely than others, must be considered. The probability distribution of these outcomes describes how likely each of them are to occur, given the scenario earthquake event.

There are many different ways of describing such a probability distribution. The ‘median’ describes the value which has a 50% chance of being exceeded (and a 50% chance of not being exceeded) given the occurrence of the scenario earthquake event. Other ‘percentile’ values can also be reported. For example, the 16th percentile is exceeded with 84% probability (100% minus 16%), and is therefore likely (although not certain) to be a low estimate of what would occur in an earthquake, while the 84th percentile is exceeded with only 16% probability (100% minus 84%), and therefore is likely (although not certain) to be a high estimate. These particular percentiles (16th and 84th) are often reported, as they represent the median minus and plus one standard deviation from the median.

The ‘mean’ is what would be obtained if a representative number of possible scenario earthquake events were observed, and the average calculated. For a skewed probability distribution (in which disproportionately large values are possible but with a very small probability), the mean is larger than the median, i.e. the mean value has less than 50% chance of being exceeded. Estimates of building damage in earthquakes have a skewed probability distribution so the mean is much larger than the median. Nevertheless, the “median” and the “mean” are commonly used measures to represent possible values from a probability distribution. By themselves, however, the ‘median’ and the ‘mean’ are not adequate to describe what could potentially occur even in a single scenario earthquake – and a range of possible results provides the best understanding.

A summary of the risk results in terms of expected number of damaged buildings for a M_w=5 earthquake scenario is provided in Table 29 while the results in terms of casualties are summarised in Table 30. The numbers highlight the large uncertainty included in the analysis and in particular the large influence that the standard deviation of the GMPE, i.e. the considered percentile, has on the final results.

The results with the 50th percentile PGA values show a number of collapsed buildings that ranges from 10 to 55 and a number of potential fatalities that ranges from 2 to 6. When the 84th percentile PGA values are instead considered the expected number of collapsed buildings varies approximately from 300 to 1290 while the number of potential fatalities from 40 to 120.

Table 29 Number of damaged buildings computed with an earthquake of magnitude M_w=5 with different assumptions on epicentre location, percentile of the GMPE and fragility function.

Case	Epicentre	M_w	GMPE variability	Fragility function	DS1	DS2	DS3	DS4	DS5
# 1 a	Huizinge	5	50 th perc	Arup	2424	1103	268	102	47
# 1 b	Huizinge	5	84 th perc.	Arup	11847	9210	3351	1841	1286
# 1 c	Huizinge	5	Mean	Arup	4366	2738	802	355	201
# 4	Zandeweer	5	50th perc.	Arup	2012	1057	285	114	55
# 5	Hoeksmeer	5	50th perc.	Arup	2620	1161	261	94	41
# 6 a	Huizinge	5	50th perc.	Pinho/Crowley unmodified	3075	363	208	77	53
# 6 b	Huizinge	5	84 th perc.	Pinho/Crowley unmodified	15141	2471	1750	867	1038
# 7 a	Huizinge	5	50th perc.	Pinho/Crowley duration modified	3263	349	124	29	10
# 7 b	Huizinge	5	84 th perc.	Pinho/Crowley duration modified	16373	2714	1362	497	320
# 8	Huizinge	5	Random ρ=1 (N_{sim}=2500, 50th perc.)	Arup	2015	1060	267	103	48
# 9	Huizinge	5	Random ρ=0 (N_{sim}=2500, ρ=0, 50th perc.)	Arup	4586	3775	1505	982	795
# 9	Huizinge	5	Random ρ=0 (N_{sim}=2500, ρ=0, 50th perc.)	Pinho/Crowley unmodified	6177	1084	803	419	656
# 9	Huizinge	5	Random ρ=0 (N_{sim}=2500, ρ=0, 50th perc.)	Pinho/Crowley duration modified	6810	1261	684	284	228

Table 30 Number of casualties estimated in case of an earthquake of magnitude M_w=5 with different assumptions on the epicentre location, the on epicentre location, percentile of the GMPE and fragility function.

Case	Epicentre	M_w	GMPE variability	Fragility function	SL1	SL2	SL3	SL4
# 1 a	Huizinge	5	50 th perc	Arup	81	29	3	6
# 1 b	Huizinge	5	84 th perc.	Arup	1279	427	60	118
# 1 c	Huizinge	5	Mean	Arup	273	94	12	23
# 4	Zandeweer	5	50th perc.	Arup	90	31	4	7
# 5	Hoeksmeer	5	50th perc.	Arup	65	23	3	5
# 6 a	Huizinge	5	50th perc.	Pinho/Crowley unmodified	64	20	3	5
# 6 b	Huizinge	5	84 th perc.	Pinho/Crowley unmodified	790	251	39	77
# 7 a	Huizinge	5	50th perc.	Pinho/Crowley duration modified	31	9	1	2
# 7 b	Huizinge	5	84 th perc.	Pinho/Crowley duration modified	468	150	22	43
# 8	Huizinge	5	Random ρ=1 (N_{sim}=2500, 50th perc.)	Arup	85	30	3	7
# 9	Huizinge	5	Random ρ=0 (N_{sim}=2500, ρ=0, 50th perc.)	Arup	789	261	39	77
# 9	Huizinge	5	Random ρ=0 (N_{sim}=2500, ρ=0, 50th perc.)	Pinho/Crowley unmodified	502	162	26	51
# 9	Huizinge	5	Random ρ=0 (N_{sim}=2500, ρ=0, 50th perc.)	Pinho/Crowley duration modified	319	104	16	31

6.6 Comparison with Observations from Other Earthquakes

In order to provide a “sense check” on the initial earthquake scenario-based building damage risk results, a brief desk study has been undertaken to compare the severity of damage and injuries caused by earthquakes of approximately magnitude M_w ~ 5 to 5.5 elsewhere in the world. It should be noted that a number of earthquakes in the table below have magnitudes above M_w =5 to 5.8 range and it would be beneficial to expand this brief review to include more events and in particular induced earthquake events. A brief summary of the findings from observations of damage and injuries from these selected earthquakes is provided in Table 31.

Table 31 Comparison of risk results with observations from earthquakes elsewhere in the world.

Location	Date	M	Depth (km)	Damage and Loss Description	Reference
Kentucky, USA	1980	M_L 5.2	8	Slight damage to 306 buildings.	USGS[1]
Liege, Belgium	1983	M_L 4.9	4	Slight damage to approximately 13000 buildings. 25 partially or totally destroyed. 2 fatalities and a few injuries. Repair cost was approximately $ 80Million.	Jongmans and Campillo (1990) EEFIT (1985)
Newcastle, Australia	1989	M_L 5.6	15	50,000 buildings damaged. Over 160 injuries and 13 fatalities.	Geoscience Australia[2]
Roermond, Netherlands	1992	M_L 5.8 M_w 5.4	21	Slight damage to 1000s and moderate damage to 10s of buildings. €125 Million economic damage. 1 indirect fatality (heart attack) and 45 injuries.	Pappin et al. (1994)
Mionica, Serbia	1998	M_L 5.5	10	60 schools damaged. 3 houses destroyed. 1 fatality and 17 injuries.	NGDC [3]
Molise, Italy	2002	M_W 5.8	10	Over 3600 unsafe buildings (likely to be demolished) and 30 deaths, approximately 100 injured and ~2300 homeless.	Mola et al. (2003)
Kraljevo, Serbia	2010	M_w 5.5	10	$150million economic losses. Over 100 injuries and 2 fatalities.	Daniell et al. (CATDAT, 2010)
Lorca, Spain	2011	M_w 5.1	1	4035 buildings in EMS-98 grade 2, 1328 buildings in grade 3, 689 in grade 4 and 329 buildings in grade 5. 9 fatalities, 3 heavy injuries and ~400 slight injuries.	Daniell et al. (CATDAT, 2011) Donaire-Avila et al. (2012)
Oklahoma, USA	2011	M_w 5.6	5	Slight to complete damage. 14 houses collapsed. 2 slight injuries.	USGS[1]

[1] http://earthquake.usgs.gov/earthquakes/; [2] http://www.ga.gov.au/hazards.html
[3] http://www.ngdc.noaa.gov/nndc/struts/results?eq_0=5505&t=101650&s=13&d=22,26,13,12&nd=display

6.6.1 Liege, Belgium Earthquake 1983

On the 8th November 1983 the region of Liege in Belgium experienced a magnitude M_L=4.9 earthquake. The event was strongly felt across the city of Liege and caused slight damage to thousands of buildings (approximately 13000) and complete damage or collapse to 25 buildings. The principal types of damage were failure of chimneys, vertical cracks between façade and cross wall and shear cracking in the walls. Modern and well-constructed buildings were generally undamaged. Two people were killed and a few people injured (Jongmans and Campillo, 1990). Images of the type of damage that occurred during this event are shown in Figure 46.

Figure 46 Observations of extensive damage and partial collapse of buildings caused by the Liege, Belgium 1983 earthquake (from EEFIT 1983).

6.6.2 Roermond, Netherlands Earthquake 1992

On the 13th April 1992 the region of Roermond in the Netherlands experienced a magnitude M_L=5.8 (M_w=5.4) earthquake. This was the strongest earthquake ever recorded in the Netherlands and one of the strongest in Northwest Europe. This was a tectonic earthquake and not an induced event associated with gas extraction. The event was strongly felt across the Netherlands, Germany and Belgium and into France and even to the south of England.

Images of the type of damage that occurred during this event are shown in Figure 47.

Figure 47 Observation of slight to extensive damage to buildings and failure of a canal slope as a result of the Roermond, Netherlands 1992 earthquake.

6.6.3 Lorca, Spain Earthquake 2011

On the 11th May 2011 the town of Lorca in Spain experienced a magnitude Mw=5.1 earthquake. The event is reported to have a hypocentral depth of only 1km. The maximum recorded PGA was of 0.36 g and the mean significant duration of the ground motion (time between the 5% and 95 % of Arias Intensity) was about 1 sec over the available recordings.

The event was strongly felt in Southern Spain and caused significant damage to the town of Lorca where most of the damaged buildings were reinforced concrete frame structures and reinforced concrete waffle slab. According to the data provided by the Lorca council, 6416 of the 7852 buildings of the city were checked, and the observed damage measured with the EMS-98 scale (see Appendix B2) was distributed as follows: 4035 buildings in grade 2, 1328 buildings in grade 3 damage, 689 in grade 4 and 329 buildings in grade 5, which collapsed or were demolished after the earthquake (Donaire-Avila et al., 2012). The earthquake caused 9 fatalities, 3 heavy injuries and ~400 slight injuries (Daniell et al., 2011).

Images of the type of damage that occurred during this event are shown in Figure 48.

Figure 48 Observations of complete damage and collapse of an old unreinforced masonry church building caused by the Lorca, Spain 2011 earthquake.

6.6.4 Lessons Learned from Previous Earthquakes

There have been very few damaging earthquakes in the Netherlands in modern times and therefore there is very little information on which to base the expected performance of local Netherlands and particularly local Groningen buildings under earthquake ground shaking. In particular there is little information on damage and casualties related to small to moderate magnitude earthquakes. Similarly there is very little information on which to investigate how the population in the Groningen region will respond during a more significant earthquake event than experienced to date and how many people might be injured. It is therefore essential to take advantage of lessons learned from earthquakes elsewhere in the world particular regarding lessons for life safety.

There is unfortunately surprisingly little consistent data on earthquake injuries worldwide. For human casualty estimation the key factors are building type, level of structural damage, non-structural damage and secondary hazards (Coburn and Spence, 1992). A broad range of other factors are also important including building height, construction quality, specific non-structural elements and contents, location relative to other buildings, as well as local ground conditions and potential for secondary ground related hazards. A consistent finding from post-earthquake studies is that increasing age of the building occupants is associated with higher mortality in earthquakes. Women have also been found to be more vulnerable than men. These and other socio-cultural factors associated with gender and age are particularly important to take into account during risk communication (Petal, 2011).

So and Pomonis (2012) describe casualty rates for use in loss estimation and it is clear that care must be taken in extrapolating casualty rates from a wide range of earthquake magnitudes and from different building typologies. So and Pomonis provide fatality rates for different types of masonry. They report that European masonry building with wooden floors had 9 to 12% fatality rates in collapsed buildings. Structural masonry (low rise) is reported to have fatality rates of 6 to 8% and structural masonry to have fatality rates of 13 to 16%. However, Ferreira et al. (2011) report that for masonry buildings the chance of survival in a collapsed building is higher than within a collapsed reinforced concrete building.

Post-earthquake data generally indicates that being inside a building is more hazardous than being outside a building. This applies particularly for rural environments. However, there is less data from dense urban environments where there is higher building density and narrow streets (Petal, 2011). Ferreira et al. (2013) provide a correlation between earthquake magnitude and numbers of fatalities which emphasises the importance of population density on fatality levels. For a magnitude M=5 earthquake the fatalities are shown to vary between less than 1 to 2 at low population density to near 100 fatalities at higher population density.

It is recommended that further work is undertaken to compile useful information on lessons learned from earthquakes to inform risk management decisions on the Groningen project.

7 Conclusions and Recommendations

This section of the report provides a high level summary of the findings of the scenario earthquake risk assessment for the Groningen region.

Recommendations are provided for future work to progress from the earthquake scenario-based building damage assessment presented in this report to the proposed detailed quantitative risk assessment of induced seismicity risk in the Groningen region.

7.1 Conclusions of Risk Assessment Results

Earthquake scenario risk assessment calculations have been undertaken for the Groningen region for a range of potential earthquake scenarios with magnitudes from M_w =3.6 to M_w =5 and earthquake risk estimates are presented in terms of potential numbers of damaged buildings and potential numbers of casualties. These risk estimates represent what damage and casualties are estimated to occur in the event of individual induced earthquakes within the Groningen region. These results do not represent the cumulative damage and casualties that could potentially result from all possible earthquakes over the life of the gas field.

The number of buildings that will potentially be damaged and the number of associated casualties is expected to increase significantly with increasing magnitude of the potential future earthquakes. For a smaller magnitude earthquake, such as an M_w =4 earthquake event (using median PGA values as input) it is expected that hundreds of buildings will be slightly damaged, tens of buildings will be moderately damaged and fewer than 10 buildings will be extensively damaged. In the event of an earthquake of magnitude M_w =5 (using median PGA values as input) it is expected that thousands of buildings will be slightly or moderately damaged, hundreds of buildings extensively to completely damaged and approximately 50 buildings will collapse. For the smaller magnitude earthquake event it is expected that 2 or 3 people could be injured. In the event of an earthquake of magnitude M_w =5, it is expected that hundreds of people will potentially be injured with almost ten life threatening injuries or direct fatalities.

If instead of using uniformly the median (50^{th} percentile) or 84^{th} percentile PGA values as input to the risk assessment calculation, the full potential variability in the ground motion PGA values is taken into consideration then the risk estimation results are significantly larger. The assessment of the full potential variability of the ground motion PGA is described in Section 6.4. For example, In the event of an earthquake of magnitude M_w =5 (using full variability in PGA values as input) it is expected that 8,000 to 9,000 buildings will be slightly or moderately damaged, 1,300 to 3,200 buildings extensively to completely damaged and approximately 370 to 1200 buildings will collapse. It is estimated that 470 to over a 1000 people could be injured with 45 to over 100 life threatening injuries or direct fatalities. These significantly higher estimates are believed to be conservative but cannot be discounted at this stage. These analyses serve to emphasise how sensitive the results are to changes in input values but also serve to emphasise the need for urgency.

There is considerable uncertainty in all aspects of the risk assessment methodology. In particular, the ground motion hazard caused by the induced seismicity is uncertain and subject to change. The vulnerability / fragility of the buildings in the Groningen region to earthquake ground motion is still under investigation and also subject to change. In order to deal with this high level of uncertainty, risk calculations have been prepared using median ground motion PGA values and then sensitivity analyses have been undertaken to investigate the impact of changing the input values (e.g. increasing the PGA values or using alternative fragility functions) on the risk estimation results.

7.2 Recommendations for Future Risk Assessment Research and Development Work

It is recognised that each aspect of the initial earthquake scenario-based building damage assessment can be improved and the methodology made more robust. These improvements are necessary to provide a better understanding of the risk, its distribution geographically and in time, but also to better understand the level of uncertainty in the risk results. This improvement may also lead to an enhanced understanding of what is contributing most to the risk results (e.g. which building structural types, which locations, which building usage types and perhaps type of occupants). These enhancements are essential to provide a better understanding with regard to how best to manage the risk.

7.2.1 Uncertainty Reduction by Research and Development

A key aspect of on-going risk management work will be uncertainty reduction through research and development. Key areas for uncertainty reduction include:

- Improved understanding of the ground motion hazard including the amplitude, frequency content and duration;
- Improved understanding of the effect of the local geology on the ground motions;
- Improved definition and classification of the building structural typologies in the region;
- Improved understanding of the vulnerability of the building stock to ground shaking;
- Improved estimation of the amount of building damage that can potentially occur by better understanding of the response of the buildings to potentially higher frequency and shorter duration ground motions; and
- Improved casualty estimation methodology using building damage and casualty statistics from earthquakes elsewhere in the world but that are most relevant to the situation in the Groningen region.

7.2.2 Seismic Hazard

The risk assessment described in this report presents results for discrete earthquake scenarios only. It is proposed that a detailed quantitative risk assessment will also be undertaken in the future. It is recommended that both scenario earthquake analyses and probabilistic seismic hazard analyses are taken forward for the quantitative risk assessment.

The detailed quantitative risk assessment should include:

- Earthquake ground motion hazard levels determined using probabilistic seismic hazard analysis methodology and input from the geomechanical model for the gas field with expert input from colleagues at KNMI and NAM.
- In addition to ground motion prediction equations for peak values, the selection and implementation of ground motion prediction equations for response spectral values should be studied to allow determination of seismic hazard response spectra.

An improved understanding of the local geology and the effect on the earthquake ground motions is desirable. Region specific geological maps and geotechnical data should be used to derive regional maps showing the distribution of seismic site response factors.

The instrumentation and monitoring programme proposed by NAM would allow fundamental data on the characteristics of the earthquake ground motions in the region to be collected. It is recommended that the following issues are taken into consideration:

- Seismological instruments would allow improved accuracy of the location, depth and characteristics of the induced earthquake events.
- Free-field strong-motion instruments would provide an increased number of earthquake ground motion recordings. It is recommended that the probabilistic hazard maps are used to inform the placement of these instruments.
- It is recommended that borehole arrays are installed at selected locations to confirm seismic site response within the ground conditions within the region.
- Instrument arrays should be installed on typical, critical and historical buildings and critical infrastructure to determine the response of these structures to seismic ground motions. Other instruments such as tilt and crack meters may also be considered for selected buildings. Where buildings are to be instrumented it is important that a good understanding of the ground conditions and free-field ground motion is also obtained.
- A data management system with data analytics and automated reporting will be required to manage the large volume for interpretation and to inform decision making in a timely manner. It is recommended that an organisation with experience on seismic strong-motion instrumentation and monitoring, and recent experience of monitoring buildings and infrastructure under earthquake loading, is consulted to ensure lessons are learned from recent earthquakes.

7.2.3 Building Exposure

The building database used for the risk assessment is still under development and includes data gaps and assumptions related to building structural type, building usage, building occupancy and building cost. These gaps have been filled by making reasonable, informed decisions using the statistics derived from adjacent buildings or the statistics of the entire building database. For example, where the building structural type is unknown it is assumed that the building could be a range of possible structural types with appropriate weightings based on the statistics of all buildings of the same usage type. Building inspections at a number of towns in the region have also been undertaken to validate assumptions and fill data gaps.

For the future detailed risk assessment considerably more effort would be required to resolve the data gaps and assumptions to reduce uncertainty where possible. This additional work has started and a programme for rapid visual assessment of all buildings is being undertaken across the region to validate the key characteristics of the buildings in the Groningen region.

7.2.4 Building Vulnerability

The fragility functions for the buildings in the Groningen region have been calibrated using limited observations of building damage caused by earthquakes that have occurred in the region and elsewhere in the Netherlands. Further work is recommended to process the statistics of damage observations from other earthquakes in the region or neighbouring areas and to calibrate these building damage statistics with those compiled by other organisations particularly TNO. This aspect of the research would benefit from even closer interaction with TNO.

Work is also on-going to calibrate the fragility functions with findings from detailed analytical models of buildings of region specific building types. The analytical models can be used to investigate the effect of the region specific earthquake ground motion characteristics including amplitude, frequency and duration, as well as the effect of the ground conditions and sub-structure and the effect of the particular characteristics of the building materials and forms of construction.

The instrumentation and monitoring of buildings will also provide important data on the performance of Groningen buildings in response to future earthquake ground motions when and if this information will also be valuable in the calibration of fragility functions for the Groningen region buildings.

7.2.5 Risk Calculation

Improved methodology for estimation of the amount of building damage that may potentially be caused by Groningen region earthquakes is required. Improved definition of the hazard from induced seismicity along with an improved understanding of the response of the building types to potentially higher frequency and shorter duration ground motions is also required. In particular improved definition of the collapse rate of buildings is required as this is a critical factor for casualty estimation.

Improved casualty estimation methodology using loss statistics that are most relevant to the situation in the Groningen region is also required. This will require improved detail on the population and demographics in the region as well as improved understanding on the correlation of casualties and building damage that are specific to the characteristics of building types in the Groningen region.

7.2.6 Risk Management by Engineering by Strengthening of Buildings

The work being undertaken with regard to proposed engineering and strengthening of buildings is described in a series of separate reports by Arup (Arup, 2013):

- Structural Upgrading Strategy;

- Seismic Risk Assessment - Earthquake Scenario-Based Risk Assessment for Building Damage (this report);
- Structural Upgrading Study; and
- Implementation Study.

It is recommended that the risk assessment calculations are repeated in the future using fragility functions that represent the enhanced building performance expected following (based on numerical analysis of typical buildings in the Groningen region before and after implementation of building strengthening measures). These calculations would show the cost / benefit of implementing the building strengthening programme and will be important in identifying when the induced seismicity risk is as low as reasonably practical in accordance with Netherlands risk acceptance criteria.

References

[1] REP/229746/ST001 Structural Upgrading Strategy, Arup, Amsterdam (29-11-2013).

[2] REP/229746/SU003 Structural Upgrading Study, Arup, Amsterdam (29-11-2013).

[3] REP/229746/IS001 Implementation Study, Arup, Amsterdam (29-11-2013).

[4] Akkar, S., Sandikkaya, M.A. and Bommer, J.J. (2013). "Empirical Ground-Motion Models for Point- and Extended-Source Crustal Earthquake Scenarios in Europe and the Middle East". Accepted for publication in *Bulletin of Earthquake Engineering.*

[5] Arup (2013). Project Groningen 2013. Building Strengthening Reports.

[6] Baker, J. W., and Jayaram, N. (2008). "Correlation of spectral acceleration values from NGA ground motion models". *Earthquake Spectra*, 24(1): 299-317.

[7] Beyer and Bommer (2006). "Relationships between median values and between aleatory variabilities for different definitions of the horizontal component of motion." *Bulletin of the Seismological Society of America*, 96(4A), 1512–1522.

[8] Bommer, J. J. and Martínez-Pereira, A. (1999). "The effective duration of earthquake ground motion". *Journal of Earthquake Engineering,* 3: 127–172.

[9] Bommer, J. J., Stafford, P. J., and Alarcón, J. E. (2009). "Empirical equations for the prediction of the significant, bracketed, and uniform duration of earthquake ground motion." *Bulletin of the Seismological Society of America*, 99(6), 3217–3233.

[10] Bommer, J.J. (2013). "Selection of ground motion prediction equations". Project report.

[11] Bothara, J.K., Dhakal, R.P. and Mander, J.B. (2010). "Seismic performance of an unreinforced masonry building: An experimental investigation". *Earthquake Engineering and Structural Dynamics*, 39(1):45-68.

[12] Bradley, B. A. (2010). "A generalized conditional intensity measure approach and holistic ground-motion selection". *Earthquake Engineering and Structural Dynamics,* 39(12): 1321-1342.

[13] Bradley, B. A. (2011). "Correlation of significant duration with amplitude and cumulative intensity measures and its use in ground motion selection". *Journal of Earthquake Engineering*, 15(6):

[14] Bridgis Geoservices BV, Geodata. Retrieved: March 2013, from: http://www.bridgis.nl/product/geodata/

[15] Chen, R., Branum, D.M., Willis, C.J., (2013). "Annualised and earthquake scenario loss estimations for California". *Earthquake Spectra* 2013 (in press), http://dx.doi.org/10.1193/082911EQS210M

[16] Coburn, A. and Spence, R. (1992). *Earthquake Protection*, John Wiley, 1992, ISBN 0 471 91833 4.

[17] Coburn, A. and Spence, R. (2002). *Earthquake Protection*, John Wiley and Sons Ltd, 2nd Edition, 420 pp.

[18] Cornell, A.C. (1968). Engineering seismic risk analysis. *Bulletin of the Seismological Society of America*, Vol 58, pp1583-1606.

[19] Daniell, J.E., Khazai, B., Wenzel, F., Vervaeck, A. [2011a] "The CATDAT damaging earthquakes database", *Nat. Hazards Earth Syst. Sci*., 11, 2235-2251. Year in review 2010 and 2011 in http://earthquake-report.com

[20] J. Donaire-Avila, A. Benavent-Climent, A. Escobedo, E. Oliver-Saiz, A.L. Ramírez-Márquez, M. Feriche, (2012) "Damage assessment on building structures subjected to the recent near-fault earthquake in Lorca (Spain)". 15th World Conference on Earthquake Engineering, 15WCEE, Lisboa (Portugal).

[21] Dost, B., Goutbeek, F., van Eck, T., Kraaijpoel, D., 2012. "Monitoring induced seismicity in the North of the Netherlands: status report 2010", KNMI scientific report; WR 2012-13

[22] Dost, B., Van Eck, T. and Haak, H. (2004). "Scaling of peak ground acceleration and peak ground velocity recorded in the Netherlands". *Bollettino di Geofisica Teorica ed Applicata*. Vol 45, No. 3, pp 153-168.

[23] EEFIT (1985) "The Liege Earthquake 1983 – Damage Inspection Report". http://www.istructe.org/resources-centre/technical-topic-areas/eefit/ .

[24] EFFIT (1985). "The Mexican earthquake of 18th September 1985. EEFIT". http://www.istructe.org/resources-centre/technical-topic-areas/eefit/ .

[25] European Seismological Commission (1998). "European Macroseismic Scale 1998, EMS-98". Editor: G. Grunthal, Luxembourg.

[26] FEMA (2013). "Hazus-MH 2.0. Multi-hazard loss estimation methodology. Technical Manual". www.fema.gov/hazus. Access June 2013.

[27] Ferreira, M.A., Oliveira, C.S., Mota de Sá, F. (2011). "Estimating human losses in earthquake models: a discussion". In *Human Casualties in Earthquakes*. Editors: Spence, R., So, E., and Scawthorn, C., pp. 255-266. ISBN 978-90-481-9454-1.

[28] Hancock, J., Watson-Lamprey, J. A., Abrahamson, N. A., Bommer, J. J., Markatis, A., McCoy, E., and Mendis, R. (2006). "An improved method of matching response spectra of recorded earthquake ground motion using wavelets." *Journal of Earthquake Engineering*, 10(Special Issue 1), 67–89.

[29] Het Waterschapshuis, Actueel Hoogtebestand Nederland. Retrieved: March 2013, from: http://www.ahn.nl/

[30] Ibarra, L. F., Medina, A. M. and Krawinkler, H. (2005). "Hysteretic models that incorporate strength and stiffness deterioration", *Earthquake Engineering and Structural Dynamics*, 34(12): 1489-1511.

[31] Jongmans, D., and Campillo, M. (1990) "The 1983 Liege Earthquake: damage distribution and site effect". *Earthquake Spectra*, Vol. 6(4), 713-737.

[32] Kadaster (2013), Basisregistratie Topografie. Retrieved: March 2013, from: http://www.kadaster.nl/web/Themas/Registraties/BRT.htm

[33] McGuire, R. K. (2004). "Seismic hazard and risk analysis", Earthquake Engineering Research Institute, Oakland, CA.

[34] Musson, R. M. W., Grunthal, G. and Stucchi, M. (2010). "The comparison of macroseismic intensity scales". *Journal of Seismology*, Vol. 14, pp. 413-428.

[35] National Institute of Standards and Technology, NIST (2011). "Selecting and Scaling Earthquake Ground Motions for Performing Response-History Analyses". Report No. NIST GCR 11-917-15.

[36] Ove Arup & Partners (1993). *Earthquake Hazard and Risk in the UK.*

[37] Pappin, J. W., Coburn, A. R. and Pratt, C. R. (1994). "Observations of damage ratios to buildings in the epicentral region of the 1992 Roermond earthquake, the Netherlands". *Geologie en Mijnbouw*, Vol. 73, pp. 299-302.

[38] Pappin, J.W., Free, M.W., Vesey, D.G., (2005) "Methodology to study the seismic risk to buildings in a modern high ise city in a region of moderate seismicity". *Proceedings of 2UEE*, Japan, 2005

[39] Petal (2011). "Earthquake casualties Research and public education". In *Human Casualties in Earthquakes*. Editors: Spence, R., So, E., and Scawthorn, C., pp. 25-50. ISBN 978-90-481-9454-1.

[40] Pinho, R. (2013) "Preliminary fragility functions for unreinforced masonry building types within the Groningen region". Presented at Seismic Hazard Workshop, 5/8/2013.

[41] Pinho, R. and Crowley, H., (2013) "Preliminary fragility functions for unreinforced masonry building types within the Groningen region". Version 2. 25 September 2013.

[42] Reiter, L. (1990). "Earthquake Hazard Analysis: Issues and Insights". Columbia University Press, New York.

[43] Rota, M., Penna, A., Strobbia, C. and Magenes, G. (2008). "Derivation of empirical fragility curves from Italian damage data". Research Report No. ROSE-2008/08, IUSS Press, Pavia, Italy.

[44] Rossetto, T., Ioannou, I., and Grant, D. N. (2012). "Existing empirical vulnerability and fragility functions: compendium and guide for selection". Draft report for Global Earthquake Model, dated January 2012.

[45] So, E.K.M. and Pomonis, A., (2012) "Derivation of globally applicable casualty rates for use in earthquake loss estimation models". *15th World Conference of Earthquake Engineering, 15WCEE*, Lisboa, 2012.

[46] Spence, R.J.S, Coburn, A.W., Pomonis, A. and Sakai, S. (1992). "Correlation of ground motion with building damage: The definition of a new damage-based seismic intensity scale". *10th World Conference of Earthquake Engineering Research Institute,* Madrid.

[47] Spence, R., So, E. and Scawthorn, C. (2011). *Human Casualties in Earthquakes: Progress in Modelling and Mitigation*, Springer, 322 pp.

[48] TNO (2003) Seismisch hazard van geinduceerde aardbevingen - Rapportage fase 1. Wassing, B.B.T., Maljers, D., Westerhoff, R.S., Bosch, J.H.A. and Weerts, H.J.T. Report NITG 03-185-C.

[49] USGS (1992) Advanced National Seismic System (ANSS), ShakeMap, Global Region, Maps of ground shaking and intensity for event 199204130120, Roermond, Netherlands, Edition: Map Version 1.1; Code Version 3.2.1 GSM Geospatial_Data_Presentation_Form: Map. Online_Linkage: http://earthquake.usgs.gov/eqcentre/shakemap

[50] Vamvatsikos, D. and Cornell, C. A. (2001). "Incremental dynamic analysis". *Earthquake Engineering and Structural Dynamics,* 31(3): 491-514.

[51] van Eck T., F.H. Goutbeek, H.W. Haak and B. Dost, (2006). "Seismic hazard due to small-magnitude, shallow-source induced earthquakes in the Netherlands". *Engineering Geology*, **87**, 105-121.

[52] van Elk, J., and Doornhof, D., (2012). "Study and Data Acquisition Plan for Induced Seismicity in Groningen". Planning Report.

[53] Wald, D. J., Quitoriano, V., Heaton, T. H. and Kanamori, H. (1999). “Relationship between Peak Ground Acceleration, Peak Ground Velocity, and Modified Mercalli Intensity for Earthquakes in California”. *Earthquake Spectra*, Vol. 15, No. 3, pp. 557-564.

Tables

Figures

Appendix A

Building Exposure Data & Classification

A1 Building Location and Address

Typical examples of the address point dataset overlaid on satellite imagery of portions of the study region are shown in Figure A. 1 and Figure A. 2 below. The single address points are represented by blue dots on these figures. Closer inspection reveals that although most of the building address points are coincident with a building, there are buildings visible that do not have a building address point or there are address points where there is no longer a building. In addition, there are single address points for locations where there are a number of buildings. This tends to occur for farm address points where a single address is provide for the farm house and associated barns and other farm buildings. Similarly, a single address point occurs for industrial facilities made up of several buildings. A gap analysis was undertaken to identify and resolve these issues.

A2 Building Usage

Buildings are classified by usage to evaluate exposed occupancy at different times of the day. Mixed use buildings occur where commercial use occurs at street level with residential use above. The usage categories adopted in the database classification are displayed in table A.1.

Table A.1 Initial building occupancy categories.

Occupancy Category
Residential
Commercial – retail, banks
Commercial – medical office, hospital
Commercial – other
Industrial – factory, warehouse
Agriculture - farm
Religious - church
Government – offices
Emergency response – police, fire, etc.
Education – schools, universities

Figure A. 1 Typical example of Address Points dataset overlain on satellite imagery for a portion of study area. Blue dots show Address Points that are aligned with buildings. Red dots show Address Points that are not aligned with buildings and indicate a gap in the data that requires resolution.

Figure A. 2 Typical example of Address Points dataset overlain on satellite imagery for a portion of study area. Blue dots show Address Points that are aligned with buildings. Red polygons show Address Points that are not aligned with buildings. In addition, single Address Points can be seen to be associated with multiple buildings.

A3 Building Type

Each building is assigned a building type classification. A combination of datasets, surveys by Arup and others and GIS tools such as Google Street View have been used to assign the building typologies. The definition of the building typologies are summarised in Table A.2, for the 15 km dataset and for the preliminary extended database.

Figure A. 3 illustrates the geographical distribution of the dominant buildings typologies for a 250m x 250m grid square. It can be seen that unreinforced masonry buildings are distributed across the entire region with reinforced concrete buildings only being the predominant type in discrete locations within Groningen city area, Eemshaven industrial area and associated with other urban areas. There are very few grid squares within the study area where wood is the dominant building type.

It should be noted that there is no pre-existing dataset on construction material type for the region and therefore compilation of this information required the most effort and includes the highest level of uncertainty and will therefore be subject to change as additional information becomes available.

It should be emphasised that it is not always possible to accurately determine the building construction type from the outside. Entry to buildings is not always possible or practical. For buildings where a construction type could not be determined, two or more building types have been assigned to the same building with a weighting factor assigned where the building type is more likely to be one building type than another based on the distribution of building types of the same age and usage in adjacent areas.

Table A.2 Building typologies for risk assessment and distribution in the initial study area (15 km radius database) and the extended study area.

Material	Building typology	Building type	Age	Storeys /Height	15 km database Sub-total	15 km database Total (%)	Extended database Sub-total	Extended database Total
Unreinforced masonry	Detached/villa/semi-detached, flexible diaphragms	URM1	Pre 1920	1-2	3,299 (5.03%)	57,628 (89%)	7,500 (2.40%)	189,100 (77%)
		URM2		≥3	2,295 (3.5%)		5,200 (2.10%)	
		URM3	1920-1969	1-2	8,062 (12.4%)		23,000 (9.30%)	
		URM4		≥3	2,551 (3.9%)		7,500 (3%)	
	Detached/villa/semi-detached, rigid diaphragms	URM5	Post 1970	1-2	7,729 (11.9%)		23,000 (9.30%)	
		URM6		≥3	2,600 (5%)		6,100 (2.50%)	
	Terraced house, flexible diaphragms	URM7	Pre 1920	1-2	209 (0.3%)		3200 (1.3%)	
		URM8		≥3	404 (0.6%)		8400 (3.4%)	
		URM9	1920 - 1969	1-2	2,569 (4%)		15,000 (6.1%)	
		URM10		≥3	6,645 (10.2%)		31,800 (13%)	
	Terraced house, rigid diaphragms	URM11	Post 1970	1-2	9,608 (14.8%)		27,000 (11%)	
		URM12		≥3	11,656 (18%)		31,400 (12%)	
Reinforced concrete	Concrete bearing wall, rigid diaphragms	RC1	Post 1980	1-3	2,345 (3.6%)	3,498 (5.40%)	6,800 (3%)	10,200 (4%)
		RC2	Post 1970	≥4	1,153 (1.8%)		3,400 (1%)	
Wood	Wooden barns of all ages (with possible non-bearing masonry façade)	W	All	All	78 (0.1%)	78 (0.1%)	600 (0.2%)	600 (0.2%)
Steel	Lightweight steel frame structures (e.g. industrial, building footprint larger than 200 m2)	S1	Post 1960	<15 m	51 (0.1%)	111 (0.20%)	1400 (0.6%)	106 (1%)
	Other steel buildings (steel offices, residential)	S2	Post 1960	>15 m	60 (0.10%)		200 -0.10%	
Unclear	Objects with unknown functions or under construction	UNCL	All	All	3,262 (5%)	3,262 (5%)	44,600 (18%)	3,311 (18%)
Other	To be ignored: (Electricity poles, demolished and non-existing buildings, caravans, docking bays, defence buildings)	OTHER	All	All	353 (0.5%)	353 (0.5%)		
				TOTAL	**64,931**		**246,100**	

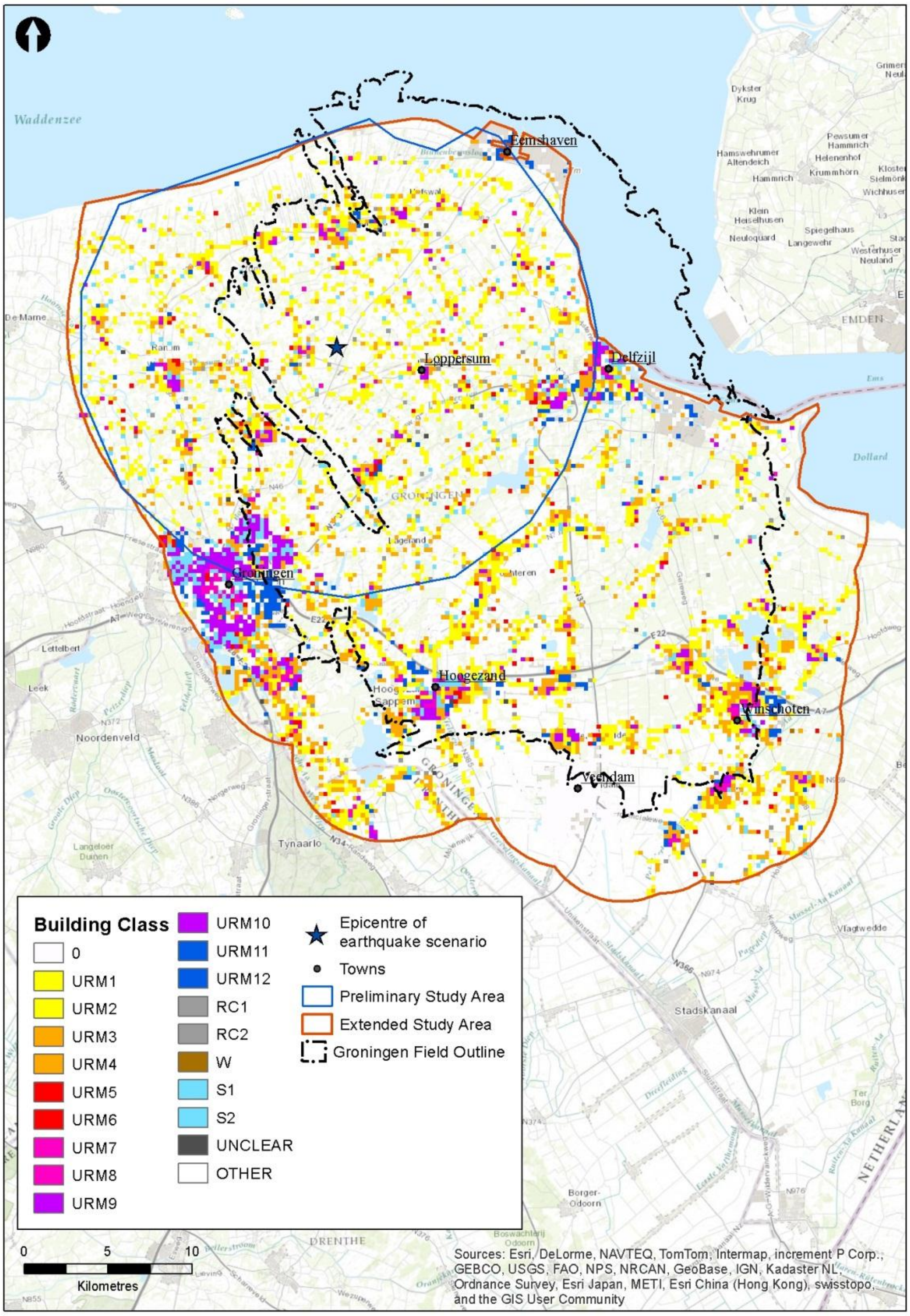

Figure A. 3 Distribution of building type within extended study area.

Appendix B

Building Vulnerability

B1 Ground Motion Intensity Measure

There are two main types of intensity measure used: macroseismic intensity indices and instrumental measures. The former are discrete scales based on observations of felt effects of shaking by humans and observed levels of damage. Common scales used are the Modified Mercalli Intensity (MMI), the European Macroseismic Scale (EMS) and Parameterless Seismic Intensity (PSI). Macroseismic intensity has the advantage that it is well correlated with damage – in fact, damage observations are used in assigning values, so the correlation should be strong. The trade-off is that ground motion prediction equations (GMPEs) are limited for macroseismic measures, and therefore conversions from instrumental measures are usually required, which introduces further uncertainty in the estimates of damage or loss.

Instrumental measures are more robust measures of ground shaking based on direct measurements – generally either peak ground acceleration (PGA) or peak ground velocity (PGV). The latter is generally considered to be better correlated with damage, but very few published equations are available which use it as the intensity measure (with the exception of Japanese studies). Response spectral values for a range of frequencies are generally considered to provide an even better correlation with observed damage.

A common problem with the development of fragility functions in terms of instrumental measures is that most earthquakes are not widely measured, and even when accelerometers are available, ground motion can vary significantly over a kilometre or so, limiting significantly the damage data that can be correlated with a measured level of shaking. It is common to instead use “instrumental” levels of ground motion based on a GMPE mean or median value prediction (based on the magnitude, location and other known characteristics of the event), but this introduces significant uncertainty in the correlation between the actual damage observations and the “theoretical” rather than measured ground motion.

B2 Damage Classification

Fragility and loss functions can differ in the way that damage is classified. However, it is important that damage descriptions are consistent and systematically applied across the fragility and loss functions (e.g. “moderate” damage should mean the same thing from the point of view of estimating damage and financial losses). It is however difficult to assure consistency in damage classification across different building types (e.g. what is the equivalent of “2 mm cracks in masonry walls” to damage of a steel building?); this should either be done using a single loss function (and therefore “moderate” damage, for example, should always be associated with a consistent level of loss across all building types) or by using loss functions applicable to each building class (in which case it does not matter that “moderate” does not mean the same thing across classes, as losses are calculated separately for each).

In this project, the damage classifications from the (EMS-98; European Seismological Scale, 1998) are used consistently. The damage classes are:

- Grade 1 – Negligible to slight damage;

- Grade 2 – Moderate damage;
- Grade 3 – Substantial to heavy damage;
- Grade 4 – Very heavy damage; and
- Grade 5 – Destruction.

These classifications have the advantage that they are well defined for different types of buildings and have been used in many other studies across Europe. The classification of damage to masonry buildings and reinforced concrete buildings in the EMS-98 are illustrated in Figure B.1 and Figure B.2.

The earthquake loss estimation methodology, referred to as HAZUS (FEMA, 2013), uses an equivalent set of damage classification terms, referred to as damage states, for estimation of losses from ground shaking:

- Damage State 1 – Slight damage;
- Damage State 2 – Moderate damage;
- Damage State 3 – Extensive damage;
- Damage State 4 – Complete damage; and
- Damage State 5 – Collapse.

In this initial study the EMS-98 and the HAZUS terms are assumed to be equivalent. Further work is required to validate this assumption.

Classification of damage to masonry buildings	
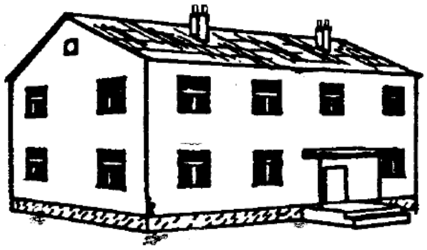	**Grade 1: Negligible to slight damage** **(no structural damage,** **slight non-structural damage)** Hair-line cracks in very few walls. Fall of small pieces of plaster only. Fall of loose stones from upper parts of buildings in very few cases.
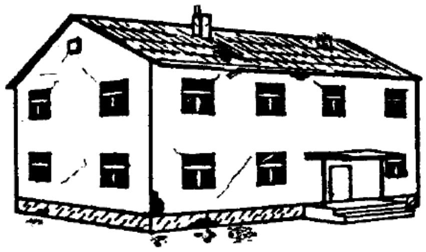	**Grade 2: Moderate damage** **(slight structural damage, moderate non-structural damage)** Cracks in many walls. Fall of fairly large pieces of plaster. Partial collapse of chimneys.
	**Grade 3: Substantial to heavy damage** **(moderate structural damage,** **heavy non-structural damage)** Large and extensive cracks in most walls. Roof tiles detach. Chimneys fracture at the roof line; failure of individual non-structural elements (partitions, gable walls).
	**Grade 4: Very heavy damage** **(heavy structural damage,** **very heavy non-structural damage)** Serious failure of walls; partial structural failure of roofs and floors.
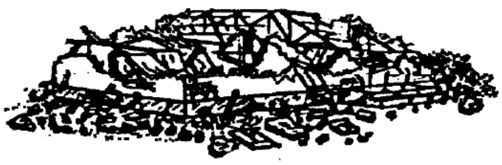	**Grade 5: Destruction** **(very heavy structural damage)** Total or near total collapse.

Figure B.1 Classification of damage to masonry buildings (EMS-98) (European Seismological Commission, 1998).

Classification of damage to buildings of reinforced concrete	
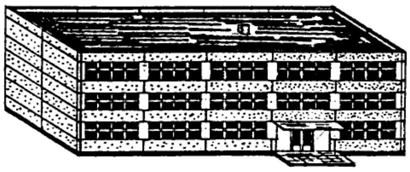	**Grade 1: Negligible to slight damage** **(no structural damage,** **slight non-structural damage)** Fine cracks in plaster over frame members or in walls at the base. Fine cracks in partitions and infills.
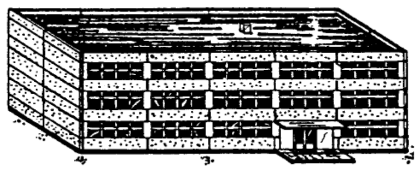	**Grade 2: Moderate damage** **(slight structural damage,** **moderate non-structural damage)** Cracks in columns and beams of frames and in structural walls. Cracks in partition and infill walls; fall of brittle cladding and plaster. Falling mortar from the joints of wall panels.
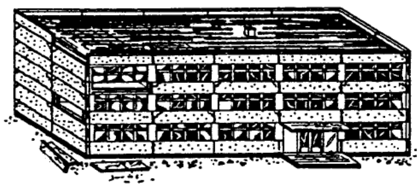	**Grade 3: Substantial to heavy damage** **(moderate structural damage,** **heavy non-structural damage)** Cracks in columns and beam column joints of frames at the base and at joints of coupled walls. Spalling of conrete cover, buckling of reinforced rods. Large cracks in partition and infill walls, failure of individual infill panels.
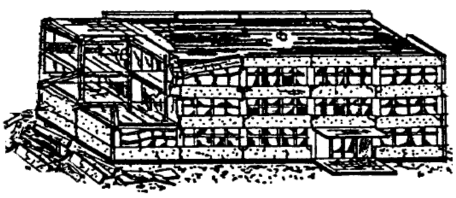	**Grade 4: Very heavy damage** **(heavy structural damage,** **very heavy non-structural damage)** Large cracks in structural elements with compression failure of concrete and fracture of rebars; bond failure of beam reinforced bars; tilting of columns. Collapse of a few columns or of a single upper floor.
	**Grade 5: Destruction** **(very heavy structural damage)** Collapse of ground floor or parts (e. g. wings) of buildings.

Figure B.2 Classification of damage to reinforced concrete buildings (EMS-98) (European Seismological Commission, 1998).

B3 Global Earthquake Model Empirical Vulnerability Compendium

The Global Earthquake Model (GEM) is an international project to develop and improve methods and tools for seismic risk assessment. They have recently produced a compendium of available empirical vulnerability, fragility and loss functions from the literature, containing 100s of relationships (Rossetto, Ioannou, and Grant, 2012). This is accompanied by a Microsoft Access database of the relationships, with extensive meta-data about their applicability. Examples of the meta-data are: building material and typology, number of storeys, age of buildings, ground motion intensity measure used, regression method and functional form used to fit the empirical data, sources of the data (earthquake events and geographical spread).

B4 Criteria for the Selection of Fragility Functions

The criteria for initial selection of fragility curves for unreinforced masonry buildings are illustrated below:

- Fragility functions based on a single earthquake were not used.
- Only the following intensity measures were considered: PGA, PGV (although no relevant relationships were available for the latter), MMI/MSK/MCS/EMS (all of which were considered to be numerically equivalent based on the recommendations of Musson et al. (2010)), and PSI.
- Relationships with bespoke or non-standard damage scales were not considered as it is difficult to get one-to-one agreement between damage scales.
- Only relationships for masonry (or specifically “brick masonry” where this was distinguished) were considered. Much of the data in the relationships that were used would come from data that included stone masonry (for example), but relationships that were specifically for stone masonry were eliminated, as were those for adobe and reinforced masonry. Relationships for EMS vulnerability class B (for flexible diaphragms) and C (for rigid diaphragms) were also considered.
- The range of interest (for PGA) was considered to be 0.05g to around 0.5g–0.9g. There are not many empirical datasets that go up to the top of this range, so relationships that could be reasonably extrapolated were preferred. A few were eliminated because they were for a minimum macroseismic intensity of VII which corresponds approximately to a PGA of 0.23g, and therefore misses a large part of the range of interest, including the levels of acceleration that were measured in Huizinge.
- Relationships that took into account number of storeys were assigned to the relevant building typologies; others were assigned to all heights.
- Relationships that took into account rigid versus flexible diaphragms were assigned to relevant building typologies; others were assigned to both diaphragm types.
- More general quality assurance criteria were also taken into consideration including preference for published equations with appropriate supporting information.

B5 Modification of the Coburn and Spence (2002) Fragility Functions

B5.1 Coburn and Spence (2002) Fragility Functions for URM

Coburn and Spence (2002) provide fragility functions as a function of the intensity measure PSI (Spence et al., 1992). The original functions for unreinforced masonry buildings are normal distributions of PSI with the parameters shown in Table B.1 and they are displayed in Figure B.3.

Table B.1 Mean, μ_{PSI}, and sigma, σ_{PSI}, of the fragility functions for unreinforced masonry buildings according to Coburn and Spence (2002).

DS	μ_{PSI}	σ_{PSI}
DS1	4.9	2.5
DS2	7.8	2.5
DS3	10.0	2.5
DS4	11.6	2.5
DS5	13.3	2.5

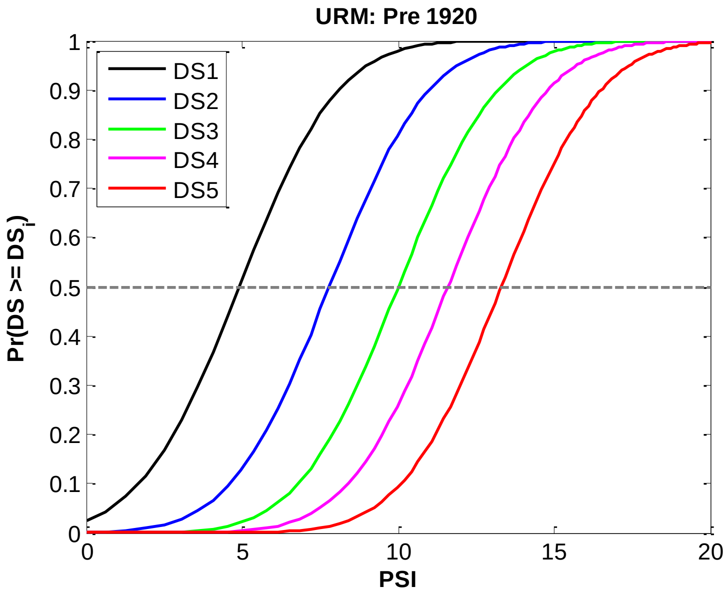

Figure B.3 Fragility curves for unreinforced masonry (URM) buildings by Coburn and Spence (2002).

B5.2 Conversion from PSI to PGA_{max}

Spence et al. (1992) provide a correlation to convert the intensity measure PSI to PGA.

- $\log_{10}(PGA_{max}) = a + b \times PSI + \varepsilon$ (1)

- where a = 2.04, b = 0.051 and ε is the error of the regression that is normally distributed with zero mean and sigma $\sigma_\varepsilon = 0.144$. The correlation provides PGA in cm/s^2, in terms of the larger horizontal component (hereinafter PGA_{max}).
- From eq. (1) it is apparent that PGA_{max} is log-normally distributed:
- $PSI \sim N(\mu_{\mathbf{PSI}}, \sigma_{\mathrm{PSI}}) \rightarrow \ln(PGA_{max}) \sim N(\mu_{\ln PGA}, \sigma_{\ln PGA}) \rightarrow PGA_{max} \sim LN(\mu_{\ln PGA}, \sigma_{\ln PGA})$.
- where "~ N" means normally distributed with the given mean and standard deviation, and "~ LN" means lognormally distributed with the given mean and standard deviation of the natural logarithm. The mean and the sigma of the natural logarithm of PGA can be easily computed, recalling the definition of the first two moments of a linear combination, z.

$$z = f(x,y) = ax + by + c$$
$$E[z] = aE[x] + bE[y] + c$$
$$Var[z] = a^2 Var[x] + b^2 Var[y] \quad (2)$$

- Where E is the expected value and Var is the variance of the variables.
- Hence in this case:

$$\ln(PGA_{\max}) = \ln(10)a + \ln(10)b \times PSI + \ln(10)\varepsilon = \bar{a} + \bar{b} \times PSI + \ln(10)\varepsilon$$
$$\mu_{\ln PGA} = E[\ln(PGA_{\max})] = \bar{a} + \bar{b} \times E[PSI] + \ln(10)E[\varepsilon] = \bar{a} + \bar{b} \times \mu_{PSI}$$
$$\sigma_{\ln PGA} = Var[\ln(PGA_{\max})] = \bar{b}^2 \times Var[PSI] + \ln(10)^2 Var[\varepsilon] = \bar{b}^2 \times \sigma_{PSI}{}^2 + \ln(10)^2 \sigma_\varepsilon{}^2 \quad (3)$$

B5.3 Conversion from PGA_{max} to PGA_{GM}

As mentioned, the correlation of eq. (1) is valid for the larger horizontal component of PGA. To convert such a measure to the geometric mean (GM) of the two horizontal components we use the relationship from Beyer and Bommer (2006). According to the latter, the ratio between the two components is:

$$\frac{PGA_{\max}}{PGA_{GM}} = 1.1 \rightarrow PGA_{GM} = \frac{PGA_{\max}}{1.1} \quad (4)$$

And the error is normally distributed with zero mean and $\sigma_{\log\frac{PGA_{\max}}{PGA_{GM}}} = 0.05$.

Neglecting the error, we can compute the mean and the sigma of PGA in terms of geometric mean as follows:

$$\mu_{\ln PGA_{GM}} = E[\ln(PGA_{GM})] = \mu_{\ln PGA_{\max}} - \ln(1.1)$$
$$\sigma_{\ln PGA_{GM}} = \sigma_{\ln PGA_{\max}} \quad (5)$$

Finally, we obtain that $PGA_{GM} \sim LN(\mu_{\ln PGAGM}, \sigma_{\ln PGAGM})$.

B6 Calibration of Fragility Functions

Empirical damage data from the Huizinge earthquake of 2012 and the Roermond earthquake of 1992 are used to calibrate selected fragility functions.

B6.1 1992 Roermond earthquake

On the 13 April 1992 the region of Roermond experienced a magnitude M_w=5.4 (M_L=5.8) earthquake. This was the strongest earthquake ever recorded in the Netherlands and one of the strongest in Northwest Europe. It should be noted that this was a tectonic earthquake and not an induced event associated with gas extraction. An earthquake intensity map for the event is presented in Figure B.4 and shows that the event was strongly felt across the Netherlands, Germany and Belgium and into France and even to the south of England.

Observations of the damage caused to buildings in the Roermond region by the earthquake are described by Pappin et al. (1994). They systematically recorded damage to buildings of different ages and building structural types at 40 locations within the earthquake epicentral region. The statistics of the building damage observations are summarised in Table A.4. Buildings were classified into three age ranges: pre-1920, 1920-1960 and post-1960. Unreinforced masonry buildings suffered the most damage during the earthquake and the damage statistics in Table B.2 refer only the unreinforced masonry buildings. The damaged buildings lie in areas with assigned macroseismic intensity of VI and VII.

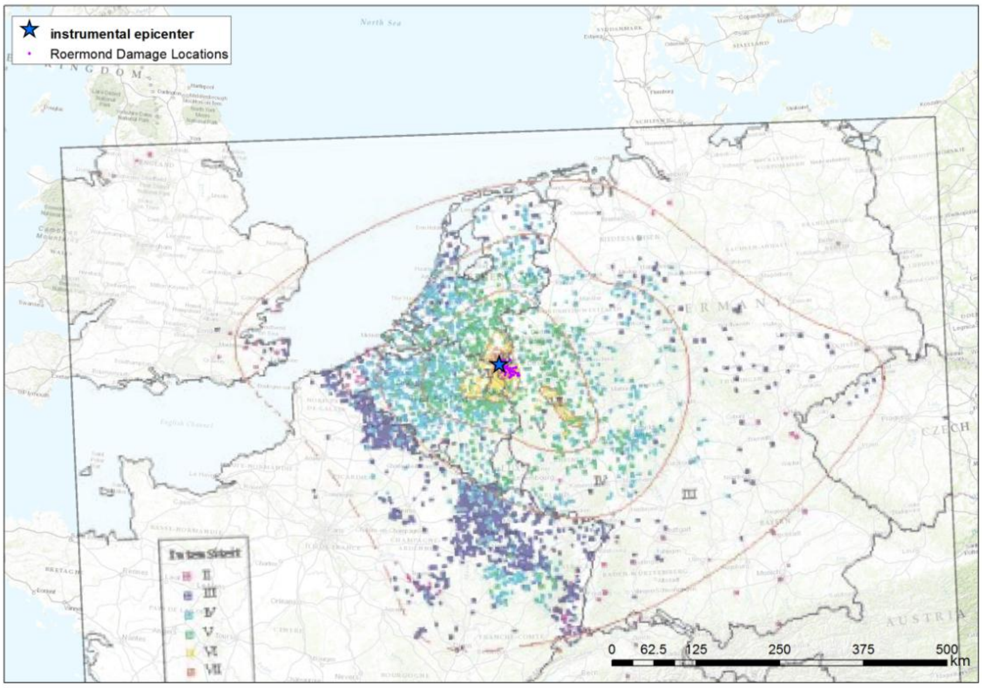

Figure B.4 Intensity map from the 1992 Roermond earthquake (M_L=5.4). The epicentre is displayed with a blue star, while the magenta points show the locations where the damage level was identified. Other coloured dots are individual intensity reports.

Table B.2: Percentages of buildings suffering damage larger or equal to a damage state

Age	Pre 1920		1920 - 1960		After 1960	
Intensity	VI	VII	VI	VII	VI	VII
PGA (m/s^2)	1.24	2.32	1.24	2.32	1.24	2.32
DS1	32.6	35.4	7.0	11.0	3.0	1.6
DS2	1.6	6.5	0.0	1.3	0.0	0.3
DS3	0.0	0.3	0.0	0.0	0.0	0.0

B6.2 2012 Huizinge earthquake

On 16th August 2012 the region of Groningen experienced a magnitude M_w=3.6 earthquake with an epicentre near the town of Huizinge in the Municipality of Loppersum (Dost et al., 2013). An earthquake intensity map for the event is presented in Figure B.9 and shows that the event was felt across the Groningen region.

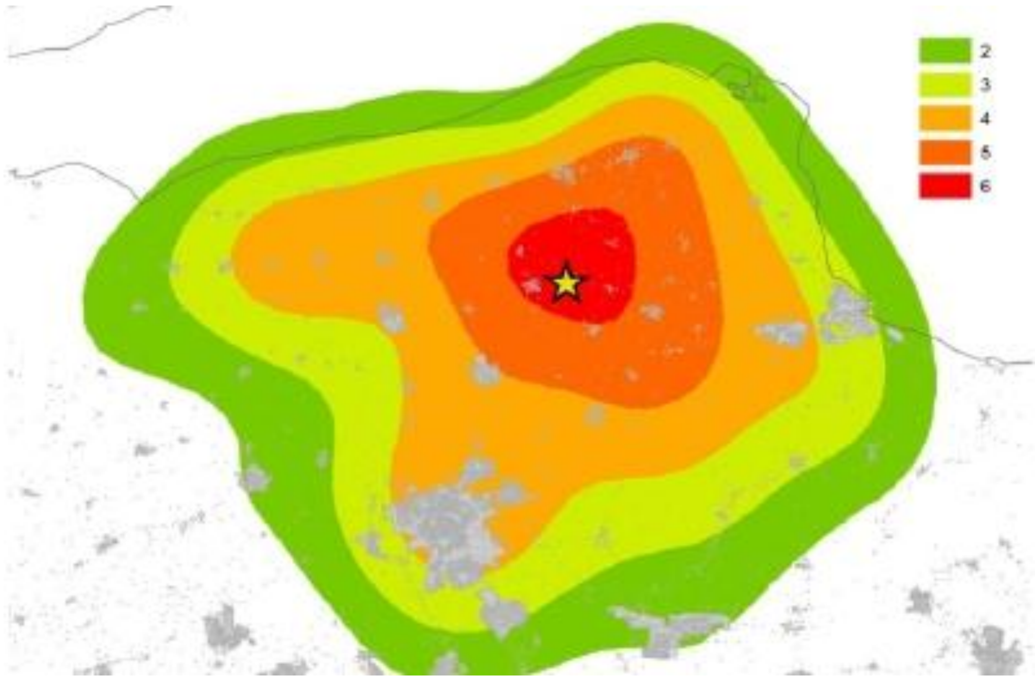

Figure B.5 Intensity map from the 2012 Huizinge earthquake (M_w=3.6). The epicentre is displayed with a yellow star.

Detailed reports of the damage to buildings caused by the 2012 Huizinge earthquake were compiled by NAM. Copies of these reports were provided to Arup and an interpretation of the damage statistics undertaken. Systematic damage classifications were assigned to each building in the studied area (all those within a 15 km radius of the Huizinge epicentre). Damage classifications were assigned based on the European Macroseismic Scale damage descriptions. All assigned damages were in the DS1 or DS2 damage levels.

In order to investigate the dependence of the distribution of building damage on peak ground acceleration (PGA) subsets of building damage statistics for areas within a 1 km radius of accelerometers have been compiled. This allowed an estimate of the correlation between the statistics of building damage and the observed PGA values (Figure B.6). No assessment of the uncertainty on the estimation of PGA is included at this stage. Statistics are shown in Table B.3.

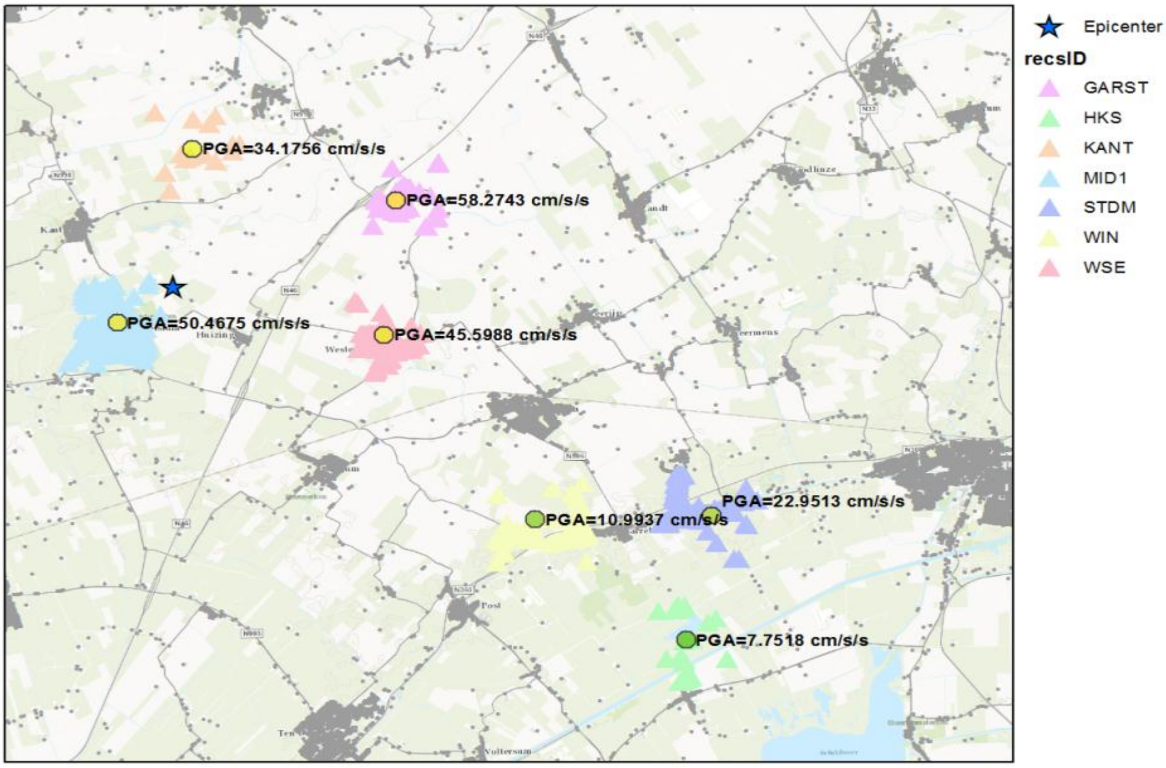

Figure B.6 Buildings included in the statistics.

Table B.3: Percentages of buildings suffering damage larger or equal to a damage state DS, during the Huizinge earthquake.

Station	PGA (g)	DS0	DS1	DS2
MID1	0.060	94.3	5.6	0.2
KANT	0.038	100	0	0
WSE	0.043	91.6	8.4	0
GARST	0.057	89.3	10.7	0
STDM	0.026	95.3	4.7	0
WIN	0.012	93.3	5.9	0.7
HKS	0.009	91.3	8.7	0

Ground motion recordings were provided by KNMI (pers comm. From Bernard Dost in February 2013).

B6.3 Calibration of Fragility Functions for URM buildings

In the 1992 Roermond earthquake, building damage data were classified by age of building. Damage data are compared with Coburn and Spence (2002) relationship for unreinforced masonry buildings in Figure B.7. Huizinge damage data are shown for the pre-1920 case only, even though a small percentage of damage was also observed for buildings built in the 60s-70s.

The curves satisfactorily fit Roermond data (circles) from pre-1920 buildings but overestimate the damage for buildings after 1920.

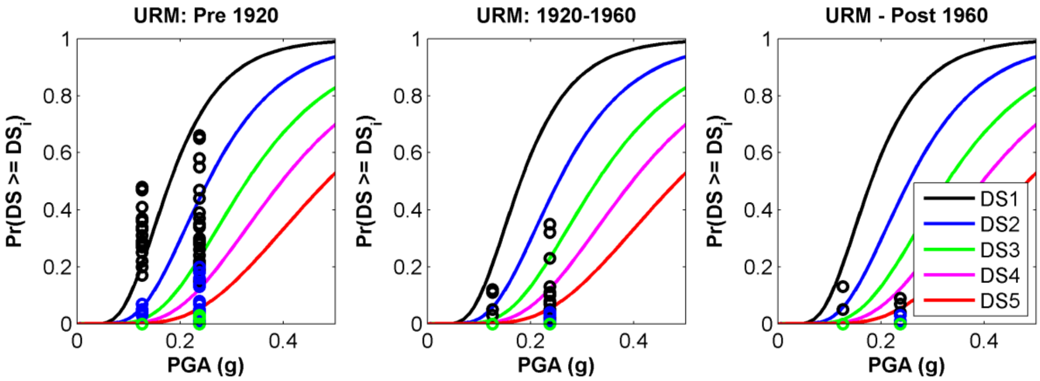

Figure B.7 Fragility curves proposed by Coburn and Spence (2002) for unreinforced masonry buildings.

In the Arup UK seismic risk study (Ove Arup & Partners, 1993), distinction was drawn between buildings in the same age categories used in the Roermond data collection. Fragility curves were developed for each age category. The fragility relationships are shown in Figure B.8. Again, the pre-1920 data is well-represented by these functions, but the later age categories over-estimated the Roermond observed damage.

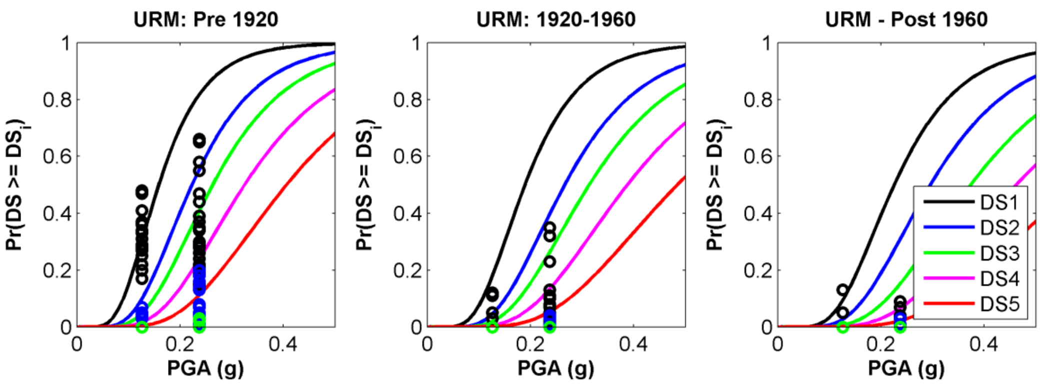

Figure B.8 Fragility functions proposed in the study carried out in United Kingdom (Ove Arup & Partners, 1993)

To better reflect the observed damage data, the curves of Coburn and Spence (2002), were adjusted within each building age category (Figure B.9):

- The Coburn and Spence (2002) curves, which do not include age distinction, were considered appropriate for buildings before 1920. No modification was made to capture the damage observed during the Huizinge earthquake under relatively low PGA values.
- For buildings built between 1920 and 1960 and for those after 1960, the DS1 and DS2 curves from Coburn and Spence (2002) were modified such that: the standard error of the distribution is kept at 2.5 (measured with respect to PSI rather than PGA), while the mean values are shifted to larger values in order to fit the data from the Roermond earthquake.
- The ratios between higher damage states with respect to DS2 (DS3/DS2, DS4/DS2 and DS5/DS2) are maintained as in the original ratios.

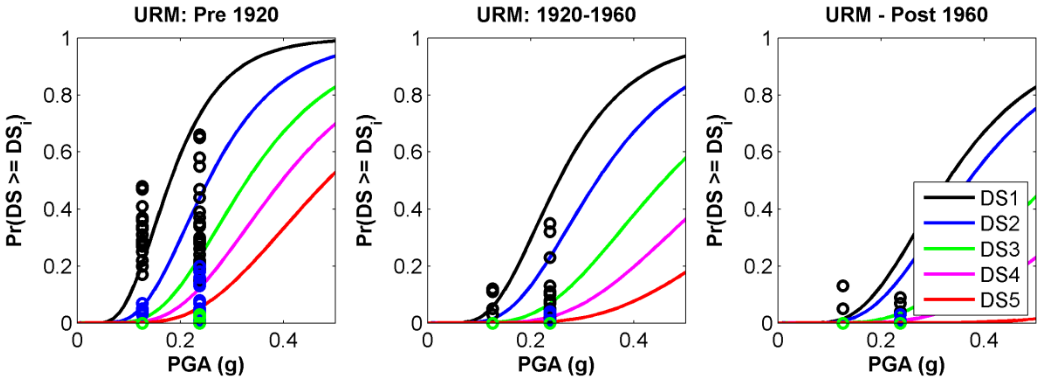

Figure B.9 Fragility functions proposed in this study.

B7 Comparison with the Fragility Functions Previously Proposed by Arup (Arup July 2013)

Figure B.10-to-Figure B.13 compare the fragility functions adopted in the initial Risk Assessment study (Arup, July 2013) and those amended in this study. The modifications include:

- The propagation of the error in the conversion from PSI and PGA_{max}
- The conversion between PGA_{max} and PGA_{GM}.
- For URM Pre 1920 and URM 1920-1960, the removal of the plateau for DS1 at low PGA values.
- The use of the actual DS5 from the fragility functions family instead of the DS5 curve obtained applying the HAZUS rates for collapse. Note that the latter are instead used in the loss estimation.

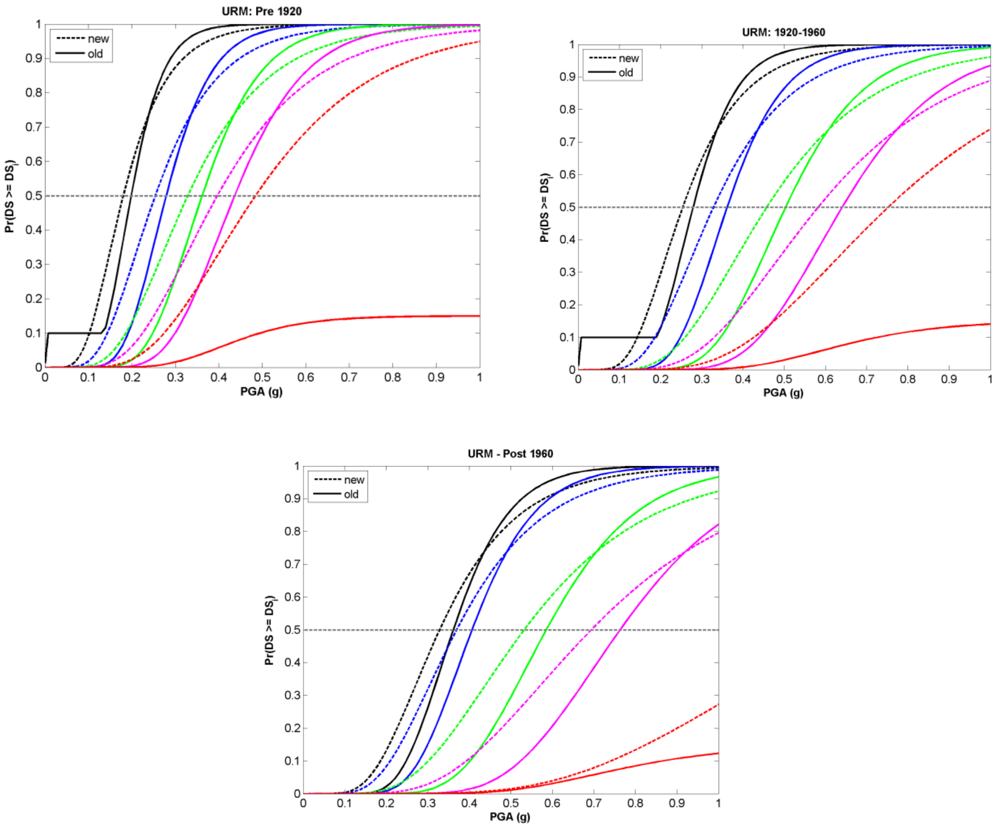

Figure B.10 Comparison between the fragility functions used in the Initial risk Assessment (Arup, July 2013), “old”, and those proposed in this report, “new” for the unreinforced masonry buildings (URM).

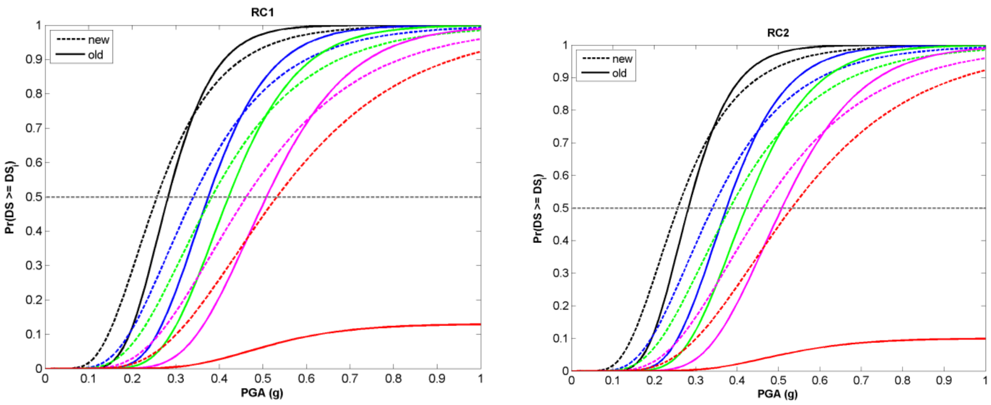

Figure B.11 Comparison between the fragility functions used in the Initial risk Assessment (Arup, July 2013), “old”, and those proposed in this report, “new” for the reinforced concrete buildings (RC).

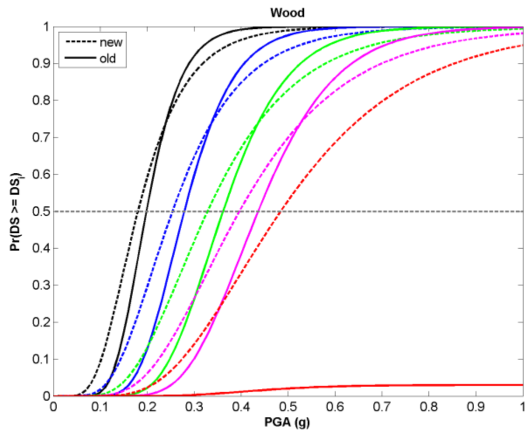

Figure B.12 Comparison between the fragility functions used in the Initial risk Assessment (Arup, July 2013), "old", and those proposed in this report, "new" for the timber buildings (Wood).

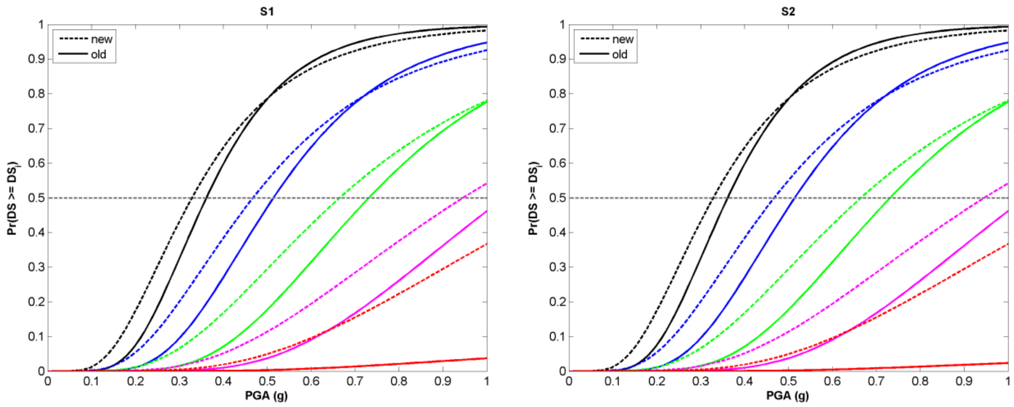

Figure B.13 Comparison between the fragility functions used in the Initial risk Assessment (Arup, July 2013), "old", and those proposed in this report, "new" for the steel buildings (S).

Appendix C

Arup Ground Motion Duration Study

C1 Arup Duration Study

Arup has conducted an initial study into the effect of duration on the structural fragility of masonry houses in the Groningen area. The goal was to compare the relative performance of a simple structural model to suites of ground motions representing (1) the shorter durations expected in the Groningen field, and (2) longer durations that would be typical of ground motions causing damage in tectonic earthquakes elsewhere in the world.

C2 Ground Motion Development

For time history analyses, ground acceleration histories are required to apply to structural analysis models. There is a very large body of literature on ground motion selection, scaling and modification (GMSM), and no consensus has yet emerged. In any case, the most appropriate GMSM methodology depends on the application – the requirement here is not just to estimate the mean response of a structure (as may be appropriate in design and assessment codes of practice) but also its statistical distribution. This means that a relatively large number of ground motions are required and their variability must be appropriate. Here, 30 ground motions are considered adequate for this purpose (NIST, 2011) and the concepts of Conditional Spectrum (NIST, 2011) and Generalized Conditional Spectrum (Bradley, 2010) are used to retain the appropriate statistical variability of the input.

Two suites of ground motions were developed for these studies, to explicitly quantify the effect of duration on structural fragility. They are referred to as the “short duration” and “long duration” suites. Each suite contains 30 single-component ground motions.

The short duration suite assumed a scenario earthquake with the following parameters:

- Moment magnitude = 4.7; hypocentral distance = 3 km – these parameters are based on the disaggregation of the P&T seismic hazard study for PGV with 2% exceedance probability in 10 years, evaluated close to Loppersum. The PGV disaggregation (rather than the PGA disaggregation which gave a magnitude of 4.2) was selected, as it was expected that the disaggregation of spectral ordinate hazard studies (if conducted in the future) would show results closer to the PGV disaggregation. Note that this is within the range of magnitudes covered in the Arup risk study.
- Epsilon = 1.5. “Epsilon” is the number of standard deviations above the median in the ground motion prediction equation. Since the peak PGA in the P&T study (the version available at the time of carrying out this work) was 0.57g, the epsilon value was back-calculated from the Akkar et al. (2013) GMPE.
- Normal faulting, V_{s30} = 200 m/s, depth to top of rupture = 3 km (in common with the P&T hazard study).

From these parameters, the Conditional Spectrum (NIST, 2011), conditioned on the PGA value from the P&T study, was developed. The Baker and Jayaram (2008) correlation between spectral ordinates was assumed, and (since PGA correlations were not available) the PGA correlation was assumed the same as the 0.01 second spectral acceleration correlation. The Conditional Spectrum retains both the median and variability of the expected response spectra, conditioned on a particular value of spectral acceleration (in this case the PGA) and scenario parameters.

The statistical distribution of ground motion duration was developed, using the 5%-75% significant duration (Bommer et al., 2009) as the duration measure. The correlation of Bradley (2011) was used between PGA and duration, taking into account that the higher-than-expected PGA values (due to epsilon > 0) are negatively-correlated with duration, and therefore significant durations are shorter than normal for a M4.7 earthquake measured at 3 km from source. The Bommer et al. (2009) prediction equation for significant duration was used, and modified by the Bradley (2011) correlation. The parameters (median and standard deviation) of the resulting lognormal distributions are shown in Table C.1.

Table C.1 Parameters of the lognormal cumulative distribution function of significant duration for different scenarios.

	M4.7, d = 3 km, ε = 0	**M4.7, d = 3 km, ε = 1.5**	**M7, d = 10 km, ε = 0**
Median(Sig. Dur.)	0.90 sec	0.61 sec	7.6 sec
Std dev (ln(Sig. Dir))	0.55	0.49	0.55

The goal was to develop a suite of 30 ground motions that retained both the distribution inherent in the Conditional Spectrum and the distribution of expected durations. For this purpose, an initial database of 91 recordings of real earthquakes was assembled from:

- the Japanese accelerometric network K-NET (http://www.kyoshin.bosai.go.jp/),
- from the Italian accelerometric archive ITACA (http://itaca.mi.ingv.it) , and
- the PEER NGA database (http://peer.berkeley.edu/peer_ground_motion_database/)

The selection was based on three main criteria for consistency with the main scenario earthquake used in the risk calculations:

- Magnitude: $4.5 \leq M_w \leq 5.5$
- Distance: $R \leq 20$ km
- Peak ground acceleration: $0.2\text{ g} \leq PGA \leq 0.3\text{ g}$

It was found that the 182 available ground motions (two horizontal components of each of the 91 recordings) generally skewed towards longer durations. Therefore, the 30 shortest of these 182 were selected. For a range of periods, the median and sample standard deviations of the natural logarithm of the spectra of these 30 ground motions were calculated, and for each period the number of sample standard deviations away from the median was retained. An individual target spectrum for each record was then developed, based on the median of the conditional spectrum and the number of standard deviations on the conditional spectrum equal to the number of sample standard deviations on the record. This process automatically retains the correlation between periods for each of these target spectra based on the spectra of the records selected.

Finally, records were spectrally matched using the program *RspMatch2005* (Hancock et al., 2006) with a loose tolerance of 25%. This means that there is some variation with respect to each target spectrum, but overall the statistics of the conditional spectrum are maintained. The cumulative distribution function (CDF) of the durations of the resulting records compared with the conditional CDF for the assumed scenario is shown in Figure C.1. The records are slightly longer in duration than the target values, but overall the correct distribution of records is reasonably maintained. The spectra of the resulting records, their sample statistics, and the target Conditional Spectrum is shown in Figure C.2. The percentiles of the Conditional Spectrum (2.5%, 16%, 50%, 84% and 97.5% are plotted) are retained to periods of at least 1 second.

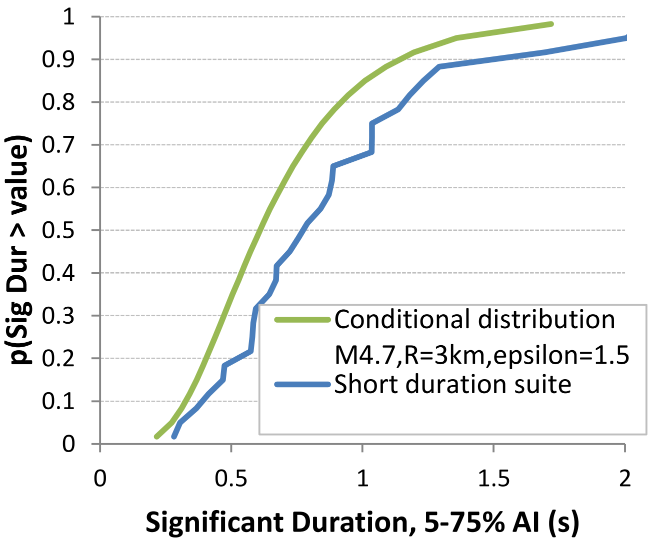

Figure C.1 Cumulative distribution function of duration for Short Duration suite.

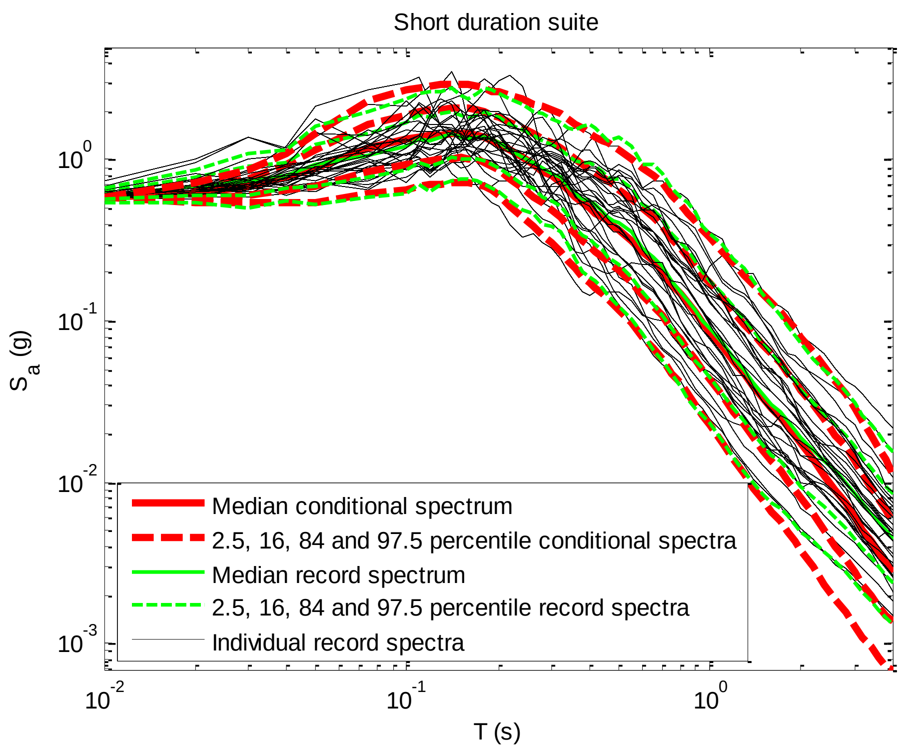

Figure C.2 Record spectra compared to Conditional Spectrum for Short Duration suite.

The process was repeated for the development of the Long Duration suite, with the following target scenario:

- Moment magnitude = 7; hypocentral distance = 10 km – these parameters are based on "typical" damaging earthquakes that may be considered in the development of fragility curves. Note however that since this study was expressly to study the importance of duration, the target conditional spectrum from the Short Duration study was retained, and the scenario was only used for the duration statistical distribution.
- Epsilon = 0.
- Normal faulting, V_{s30} = 200 m/s, depth to top of rupture = 3 km (as before).

Target duration distribution and target spectra were evaluated as before. Parameters for the former are shown in Table C.1. The median significant duration is over 10 times that of the short duration suite, and the standard deviation is slightly higher, as it is less constrained by an epsilon of 0.

Records were selected from the PEER database only, from those with moment magnitudes between 6.6 and 8, and epicentral distance from 0 to 100 km. This was reduced to a subset of 70 records with the best initial fit of the median of the target spectrum. From these 70, 30 records were selected to give a best fit of the CDF of the expected durations by finding the record with the closest duration to the following percentiles of the duration: 1.7%, 5%, 8.3%, … 91.7%, 95%, 98.3%. Individual target spectra for each record were developed as before, and spectral matching was carried out with a tighter tolerance (15%) since the records required more modification to match the targets. The resulting duration distribution and record spectra are shown in Figure C.3 and Figure C.4. The conditional distribution of the duration is matched very well. The conditional spectrum is matched well within the period range 0.01 sec to 0.5 sec, and reasonably well out to 1 second.

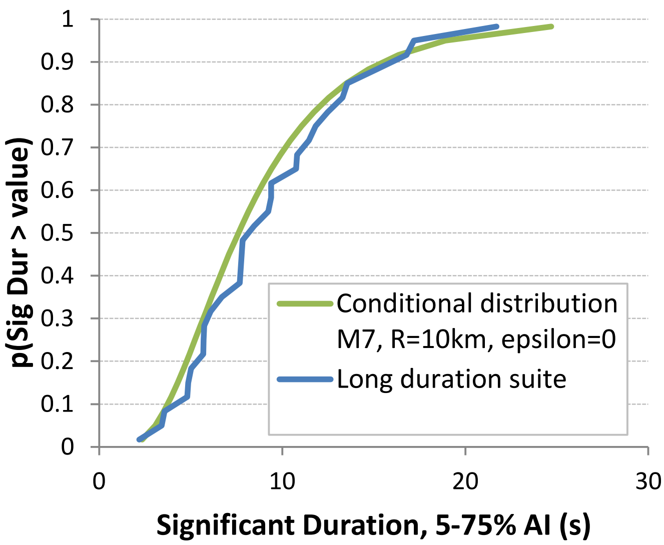

Figure C.3 Cumulative distribution function of duration for Long Duration suite

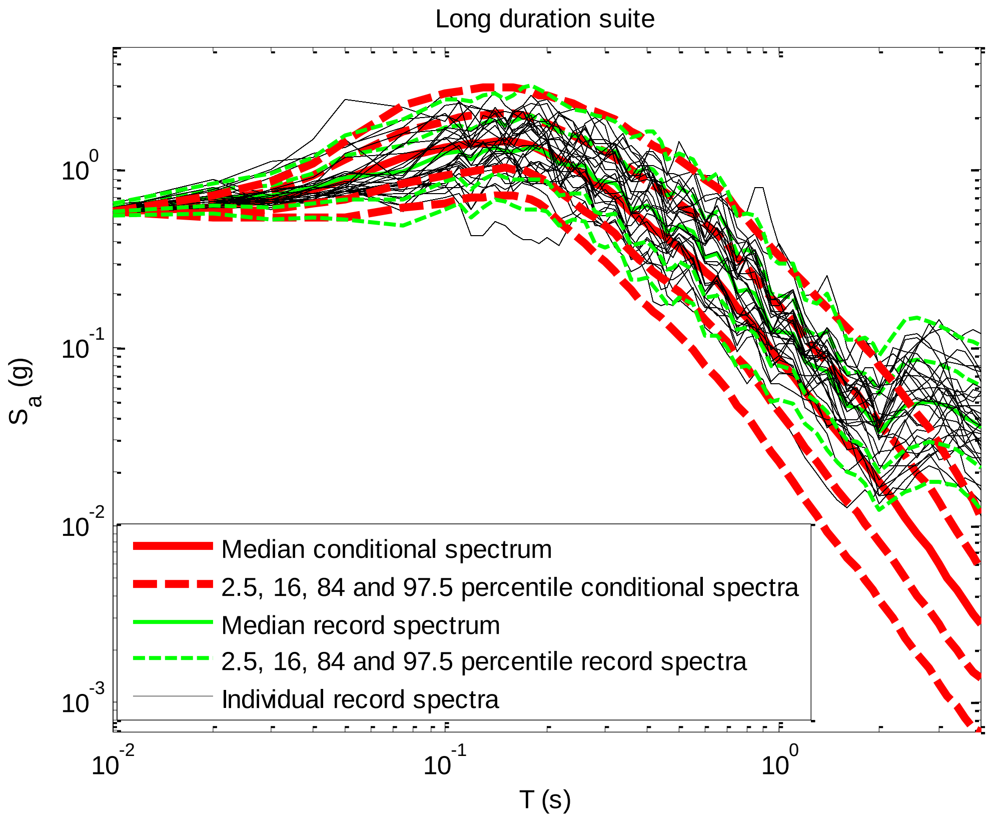

Figure C.4 Record spectra compared to Conditional Spectrum for Long Duration suite

C3 Structural Model

A single-degree-of-freedom (SDOF) hysteretic model was developed to allow a large number of time history analyses to be carried out. The model was calibrated on the 3D LS-DYNA villa model, described in the Arup Structural Upgrading report (Arup, 2013). The hysteretic model used was a modified Ibarra-Medina-Krawinkler (IMK) model, modified to reflect the degradation characteristics observed in the LS-DYNA model.

C3.1 Model description

The SDOF model that has been developed is a modified version of the hysteretic model proposed by Ibarra, Medina and Krawinkler (Ibarra et al., 2005). A brief overview of the model is provided and how this model has been modified to provide an improved correlation with the Villa model.

C3.2 Ibarra Medina Krawinkler deterioration model

The hysteretic model from IMK allows for the modelling of both strength and stiffness deterioration. The model was implemented in Mathworks MATLAB.

Full details of the material can be found in (Ibarra et al., 2005), with some of the main features included below. The monotonic curve for the bilinear model is defined by the four regions shown in Figure C.5.

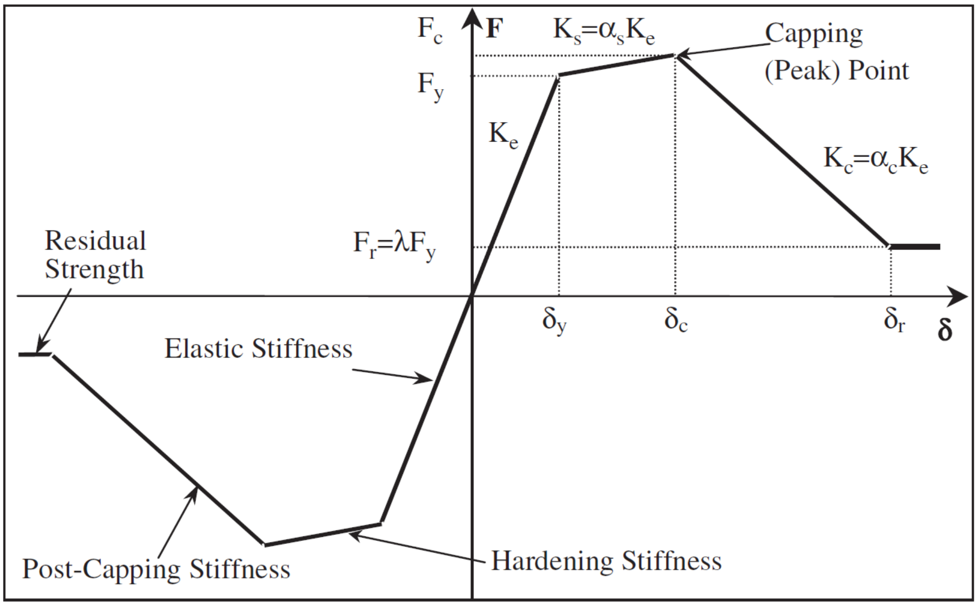

Figure C.5 Backbone curve for hysteretic models (Ibarra et al., 2005).

The model is capable of modelling four methods of cyclic deterioration once the yield stress is exceeded. These are:

1. Basic strength deterioration
2. Post-capping strength deterioration
3. Unloading stiffness deterioration
4. Accelerated reloading stiffness deterioration

When calibrating the SDOF against the Villa monotonic and backbone results, only modes 1 and 3 were mobilised. The IMK model calculates the rate of cyclic deterioration based on the level of hysteretic energy dissipated, given by the expression:

$$\beta_i = (E_i/(E_t \ - \Sigma E_j))^c$$

where E_i is the hysteretic energy for the half cycle in question, ΣE_j is the total hysteretic energy dissipated in all previous cycles (both positive and negative), and E_t is a reference energy based on twice the elastic strain energy at yield [2].

The basic strength deterioration is defined by reducing the yield strength and ratio of strain-hardening to yield stiffness to:

$$F_i = \left(1-\beta_{s,i}\right)F_{i-1} \quad \text{and} \quad \alpha_s = \left(1-\beta_{s,i}\right)\alpha_{s,i-1}$$

Unloading stiffness deterioration follows the equation:

$$K_{u,i} = \left(1-\beta_{k,i}\right)K_{u,i-1}$$

where $K_{u,i}$ and $K_{u,i-1}$ are the deteriorated unloading stiffnesses after and before excursion i [2].

C3.3 Model modifications for fragility study

The expression for calculating the damage parameter β is dependent on the hysteretic energy in excursion i, but is not linked to the *change* in peak plastic displacement. The cyclic results shown in Figure C.6 are for 3 cycles of displacement at four levels of displacement (i.e. 12 complete cycles in total). Results show that it is in the first cycle at a displacement level that the main strength and stiffness deterioration occurs, and a higher proportion of the strength and stiffness degradation occurs in the earlier levels of displacement. At displacement level 1, if the IBK method of computing damage were to be used, there would be a more even force and stiffness degradation between cycles of the same peak displacement.

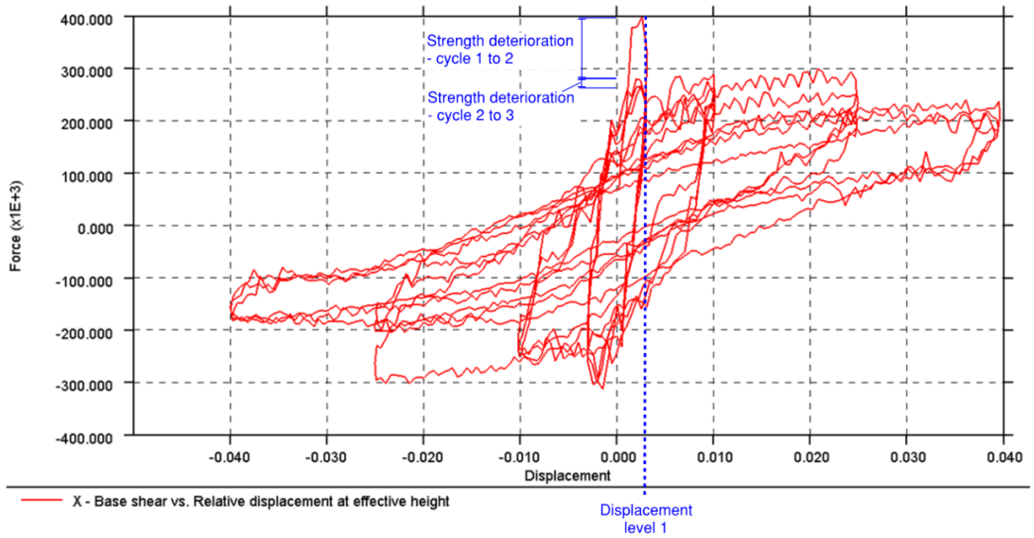

Figure C.6 Behaviour of LS-DYNA Villa model under prescribed cyclic loading.

To model the between cycle behaviour more accurately, a revised equation for β was proposed, whereby the level of damage was a function of the change in peak displacement, and given by the following equation:

$$\beta_i = \left(\frac{|\delta_{peak,i}|}{|\delta_{peak,i-1}|}\right)^c \qquad \left|\delta_{peak,i}\right| \nless \left|\delta_{peak,i-1}\right|$$

Damage is only computed if the previous absolute peak displacement, $\delta_{peak,i-1}$, is exceeded, and $\delta_{peak,i}$ is calculated when the change in displacement between timesteps changes sign. Initially $\delta_{peak,i-1}$ is set to the yield displacement, to ensure damage is only computed in the inelastic range. This leads to the majority of strength and unloading stiffness deterioration occurring in the first cycle, as shown in Figure C.7.

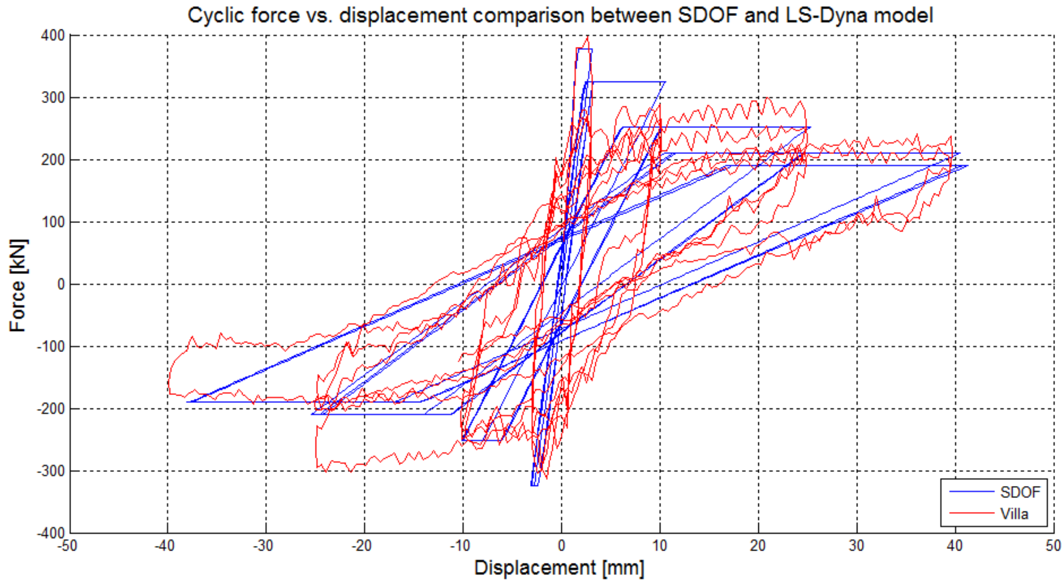

Figure C.7 Comparison of SDOF and LS-DYNA model under a prescribed cyclic motion.

C3.4 Model calibration

The model was calibrated using the following procedure:

- The monotonic backbone was calibrated on a monotonic pushover of the LS-DYNA model;
- The cyclic degradation parameters were then calibrated on the cyclic pushover analysis model (see Figure C.7);
- Mass was calibrated to give a good match of the initial period of the LS-DYNA model. The resulting mass is between the total mass of the structure, and the participating mass in the first mode, since the first mode representation is not a perfect representation of the distributed mass of the real structure;
- A small level of viscous damping was calibrated to give a good match of one dynamic analysis in LS-DYNA (with ground motion only applied in one direction to remove three-dimensional effects). This calibration is shown in Figure C.8, for a fraction of critical damping of 3% (based on the initial stiffness, which was found to give a better calibration of dynamic response). This is higher than the value of damping assumed in LS-DYNA (which was 0.5%) as it accounts for small cycle energy dissipation that is explicitly accounted for in LS-DYNA but not in the SDOF hysteretic model used.

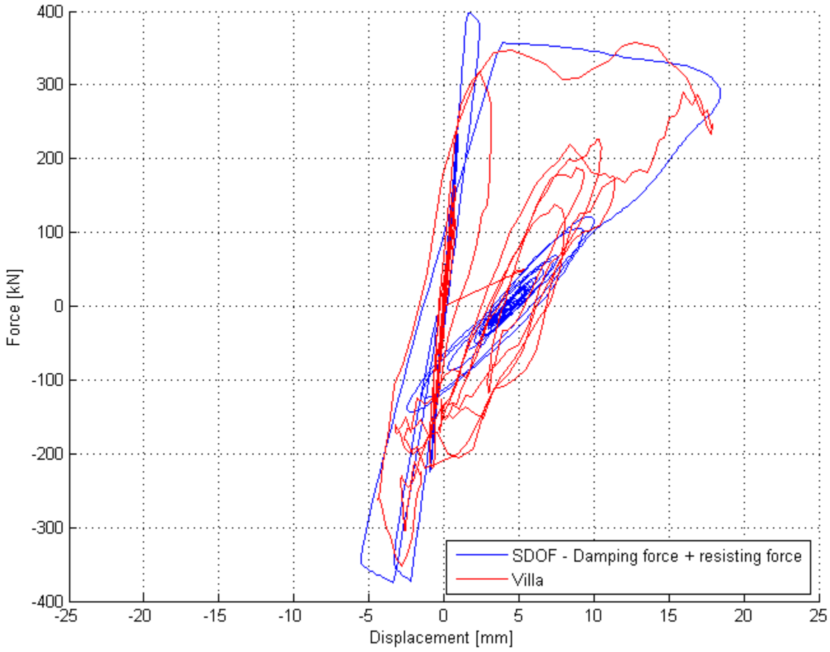

Figure C.8 Comparison of SDOF and LS-DYNA model under single-component seismic ground motion input..

C3.5 Interpretation of damage states

To determine fragility curves for the SDOF model, it must be possible to determine if a given analysis has exceeded a particular damage state, consistent with the damage states adopted in the risk assessment. For this study it was assumed that damage states could be established on the basis of peak absolute displacement only. DS1 through DS3 were established on the basis of crack widths in the LS-DYNA cyclic pushover analyses and dynamic analyses. DS4 was established based on the displacement that led to partial collapse in one dynamic analysis. DS5 was based on the monotonic pushover analyses at the level where a large reduction in capacity occurred. The displacement limits for each damage state are shown in Table C.2.

Table C.2 Definition of damage states and threshold displacements

DS	Description	Used for SDOF Fragility study	Relative displacement at effective height [mm]
1	Hairline cracks	0.1 mm cracks	1.3
2	Cracks 5–20 mm	~ 5 mm cracks	5.4
3	Cracks 20 mm or wall dislodged	~ 20 mm cracks	24
4	Complete collapse of individual wall or roof support	Substantial damage to a wall/lintel falling out	57
5	More than one wall collapsed or more than half of roof	Not attained in LS-Dyna analysis – maximum relative displacement from pushover analysis taken forward	96

C4 Incremental Dynamic Analysis Results

Incremental Dynamic Analysis (IDA) (Vamvatsikos and Cornell, 2001) was carried out on the SDOF analysis model, with ground motions scaled to PGA values from 0.05g to 4g. Each suite (short and long duration) was considered separately. For each PGA value, the proportion of records exceeding each damage state, from DS1 to DS5, was calculated. A log-normal fragility curve was fit to the data using the maximum likelihood method.

The resulting fragility curves are shown in Figure C.9. Data points are also shown for DS5 only to show the fit of the log-normal fragility curve to the data.

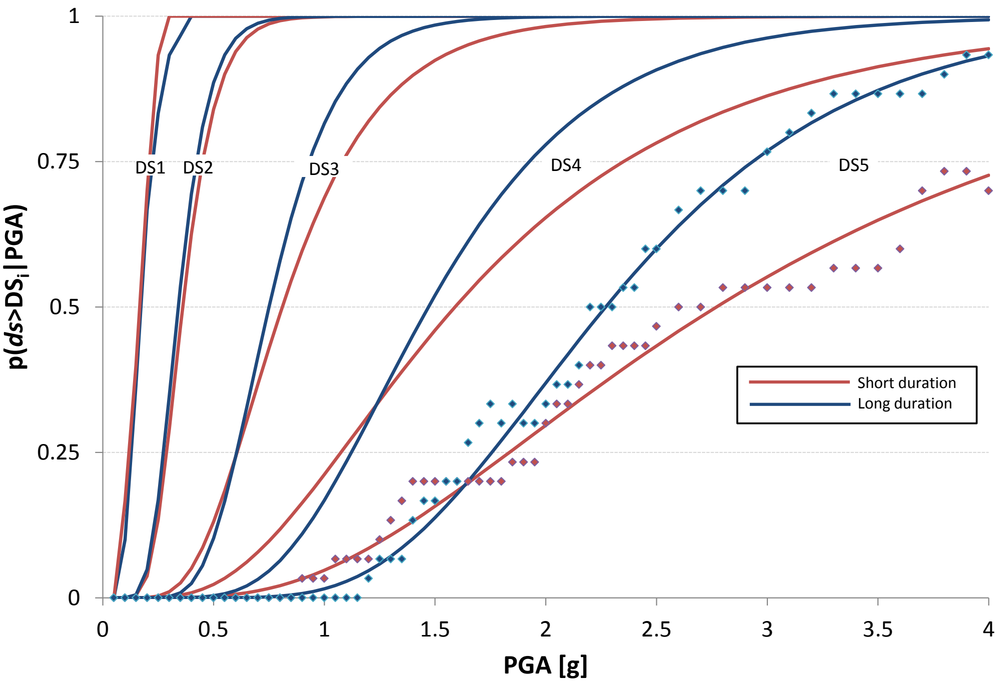

Figure C.9 Fragility curves from SDOF analyses. Lines show Maximum Likelihood fits; data points shown for DS5 only to illustrate fit of fragility curves to data.

Considering the median fragility only (shown in Table C.3), the effect of duration is small for DS1 and DS2 and increases from DS3 to DS5. The medians for short duration fragility are higher for short duration, meaning that buildings are effectively stronger in responding to shorter duration ground motions than longer duration ones (except for DS1 where the short duration PGA is negligibly smaller than the longer duration PGA). The maximum effect on DS5 damage state is a 22% increase in collapse PGA going from long duration to short duration.

Table C.3 Median fragility in PGA (g) for unidirectional input

DS	Short duration	Long duration
1	0.15	0.17
2	0.36	0.34
3	0.81	0.75
4	1.59	1.47
5	2.77	2.27

The median DS4 and DS5 fragilities are significantly higher than the PGA values associated with partial and complete collapse in the full LS-DYNA model for the villa building. There could be several reasons for this:

- The SDOF model was mainly calibrated on moderate levels of demand and the DS4 and DS5 limit states may not have been correctly identified by the displacement limits in Table C.2.
- The ground motions used in the LS-DYNA model were spectrally matched to a Eurocode 8 design spectrum, whereas those used here followed a conditional spectrum approach that would tend to be lower than the design spectrum on the average, but that explicitly accounts for the variability.
- The SDOF model is shaken monotonically whereas the LS-DYNA model is shaken with 3 components of ground motion (two horizontal, one vertical).
- Related to the last point, the ground motions used here represent an average ground motion whereas the maximum component is more likely to lead to exceeding a damage state (for example, if the collapse capacity is exceeded in either direction, then collapse would occur).

To approximately deal with the last point, it could be considered that each horizontal direction of the structure is represented by the fragility curves in Figure C.9 and that their responses are statistically independent. The accuracy of this assumption has not been investigated but it provides a starting point for assessing what the effect of multi-component input would be. Under this assumption, the probability that any damage state is exceeded under a given PGA is equal to 1 minus the probability that it is not exceeded in either direction. This can be shown to give the median fragilities in Table C.4. Note that the amount this reduces the median PGA is dependent on the standard deviation, and since the short duration suite has a higher standard deviation for DS5, this has the effect of bringing the median values closer together (difference of only 8%). This may be an artificial effect, or it may be a real effect if the response to shorter duration ground motions is actually more uncertain.

Table C.4 Median fragility in PGA (g) approximately accounting for bidirectional input.

DS	Short duration	Long duration
1	0.12	0.14
2	0.30	0.29
3	0.64	0.63
4	1.16	1.18
5	1.99	1.85

The standard deviations of the fragility curves are not reported, but they are higher for the short duration fragility curves (as noted above). This means that the long and short duration fragility curves cross over for values of acceleration below the median, therefore implying that structures are more likely to collapse (for example) for shorter duration ground motions at e.g. 1g PGA. This does not appear to be physical, and may be a result of the modelling or regression approaches.

Note that the standard deviations of the curves shown in Figure C.9 will be underestimated when applied to diverse building stock, as they only include record-to-record variability (i.e. the difference in response for different ground motions) and not the fact that different structures have different capacities.

C5 Comparison of Results and Methodology with Pinho and Crowley (2013)

As noted in the body of the report, Pinho and Crowley (P&C; 2013) adopted a similar methodology, but showed a larger dependence of collapse PGA on duration. The main differences between their study and the Arup study are the following:

- P&C used the significant duration from 5% to 95% Arias Intensity as duration measure; Arup used 5% to 75% to help to remove the effect of the surface wave train.
- P&C used a longer duration suite from 8 real records with magnitude 5.5 to 7.4, several of which were also used in the Bothara study from which they obtained the baseline fragility curves. The 5-95% significant durations ranged from around 13 seconds to 34 seconds, with a mean of 23 seconds. The Arup long duration suite comprised 30 records calibrated on the predicted 5-75% duration from a M7 earthquake at 10 km, with a target median value of 7.6 seconds. To make a proper comparison these would need to be translated into a consistent duration measure.
- P&C used a shorter duration suite with recordings from the Huizinge earthquake, which was a M3.6 earthquake (smaller than the hazard disaggregation and smaller than the maximum M5 considered in the risk assessment in this report), but with duration that exceeded the expected value from the Bommer et al. (2009) prediction equation. Arup used a short duration suite with expected durations for a M4.7 earthquake with epsilon = 1.5, but did not consider any Groningen-specific characteristics of the ground motions.
- P&C used a SDOF model calibrated on experimental response of masonry components, scaled to a base shear coefficient of 0.25. The hysteretic model includes hysteretic pinching, and in-cycle strength and stiffness degradation. It does not appear to include between-cycle strength degradation (i.e. the monotonic and cyclic response would be the same). Arup used a SDOF model calibrated on a 3D model of a single house representative of building stock in the Groningen area. The base shear coefficient was 0.5.
- P&C considered a strength-degradation based failure criterion for collapse (when capacity is reduced to 70% of its capacity. Arup considered a maximum displacement-based criterion.

One key observation is that the LS-DYNA analysis model does not appear to show the same level of strength degradation as the experimental tests on which P&C based their hysteretic response. This could be due to the fact that crushing of bricks is only taken into account in an approximate way in the LS-DYNA model, which may mean the degradation is underestimated. Alternatively, it could be because the experimental results were based on a failure mechanism (such as shear or toe crushing) which degrades more than the rocking/sliding response seen in the analysis models for Groningen buildings. As noted by Pinho and Crowley (2013), this requires further calibration on experimental testing of typical Dutch buildings and/or their components.

C6 On-going Research

Both the Arup and Pinho and Crowley (2013) studies have only been carried out for one SDOF building model, and based on limited calibration with local building stock. It is recommended that different typical buildings are calibrated with SDOF models and the studies repeated. It is also recommended that the analytical models are validated on the basis of experimental testing.

The consistency between the results of the LS-DYNA model and the SDOF model are currently under investigation.

When more detailed calibration is available, it will be possible to use the results of this study to complement the fragility curves taken from empirical literature, and not just to measure a relative effect of duration.

Appendix D

Detailed Results of the Risk Assessment Study

D1 Introduction

This Appendix provides a complete summary of all the risk assessment analyses for the earthquake scenarios considered in Section 6. For each earthquake scenario, the following results are presented:

- Distribution of PGA values at each building location;
- The number of buildings subjected to certain PGA levels;
- The number of damaged buildings to damage states DS1 (slight) to DS5 (collapse); and
- The number of estimated casualties to severity levels SL1 (slight injury) to SL4 (fatality).

The risk assessment analysis results are compared for four different earthquake magnitudes and for the range of fragility functions in the cases for which the 84th percentile PGA values are adopted to define the seismic hazard. Finally, a discussion is presented on the Monte Carlo simulations performed to investigate the effect of the spatial ground motion variability on the risk assessment results.

D2 Scenario #0,a: Huizinge Earthquake M_w=3.6 - Median (50th percentile) PGA

The scenario earthquake building damage assessment calculation is carried out for the scenario of the Huizinge earthquake of August 2012 with magnitude M_w=3.6. This section discusses the results obtained using the 50th percentile PGA values.

The median (50th percentile) PGA values at the building locations are plotted in Figure D. 1. The observed PGA values at seven recording stations (coloured triangles) are also shown in the map for comparison. It is noted that the median PGA values from the GMPE slightly over-estimate the observed PGA values at three stations in the epicentral area. However, it should be recognised that earthquake ground motions could be higher or lower in future earthquakes and more data are needed before a good understanding of the characteristics of the earthquake ground motion in the Groingen region can be achieved.

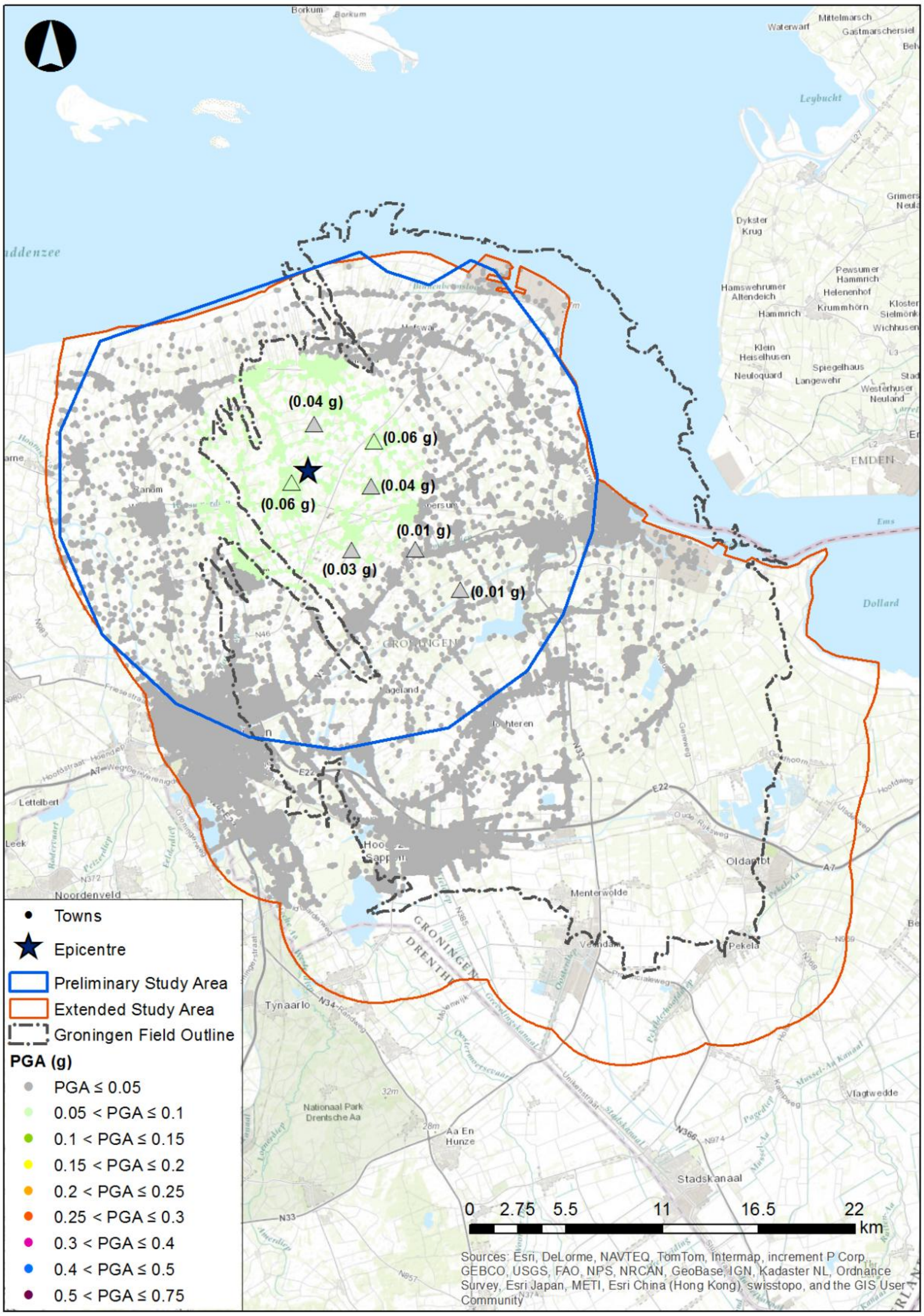

Figure D. 1 Median peak ground acceleration (PGA) estimated for an earthquake of Mw=3.6 and depth H=3 km with epicentre in Huizinge. The GMPE by Akkar et al. (2013) is used. The observed PGA values at the instrument locations (triangles) are shown for comparison.

D2.1 Number of Building Exposed

The number of buildings that are subjected to different levels of ground motion, in terms of PGA, are summarised in Table D. 1.

Table D. 1 Number of buildings subjected to median ground motion (PGA in g) in scenario #0 – 2012 Huizinge Mw = 3.6 earthquake.

Building Type	**0 ≤ PGA < 0.05**	**0.05 ≤ PGA < 0.1**
URM: Pre 1920	22745	1502
URM: 1920-1960	74257	2863
URM: Post 1960	84019	3357
RC1	6570	243
RC2	3337	42
Wood	531	60
S1	1335	54
S2	188	3

D2.2 Building Damage

The calculated number of buildings of different typologies damaged in this scenario are summarised in Figure D. 2 for the median PGA values.

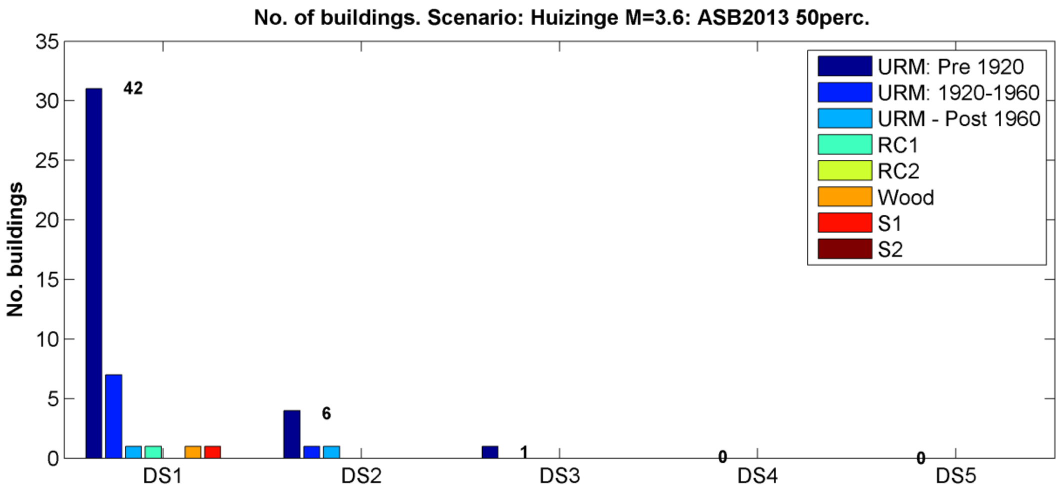

Figure D. 2 Number of buildings in damage state DS1, DS2, DS3, DS4 and DS5 according to their building class for the Huizinge Mw = 3.6 earthquake scenario. Labels in the plot present the total number of buildings in each damage state.

The numbers of damaged buildings are reported for each damage state: DS1 (slight damage), DS2 (moderate damage), DS3 (extensive damage), DS4 (complete damage) and DS5 (collapse). It is clear that given the low levels of PGA only a few buildings are expected to suffer damage. A total of 42 buildings are calculated to be slightly damaged and only 6 moderately damaged (DS2).

Approximately 3000 damage reports have been obtained following the Huizinge earthquake. In preliminary risk assessment calculations, the DS1 fragility functions for the URM Pre 1920 and URM 1920-1960 buildings were modified with a minimum threshold at 10% in order to capture the observed damage (see Appendix B7). This adjustment led to an estimate of approximately 2600 slightly damaged buildings. However this adjustment was not considered to be representative of expected building performance.

A careful review of the 3000 building damage reports for the Huizinge earthquake reveals that a large proportion of the reports actually refer to damage caused by other earthquakes or not associated with a defined earthquake. The detailed review of these building damage reports and detailed analysis of damage buildings are on-going.

D2.3 Casualty Estimation

For this scenario no buildings are estimated to suffer DS4 or DS5 (Figure D. 3). Hence, no casualties are expected.

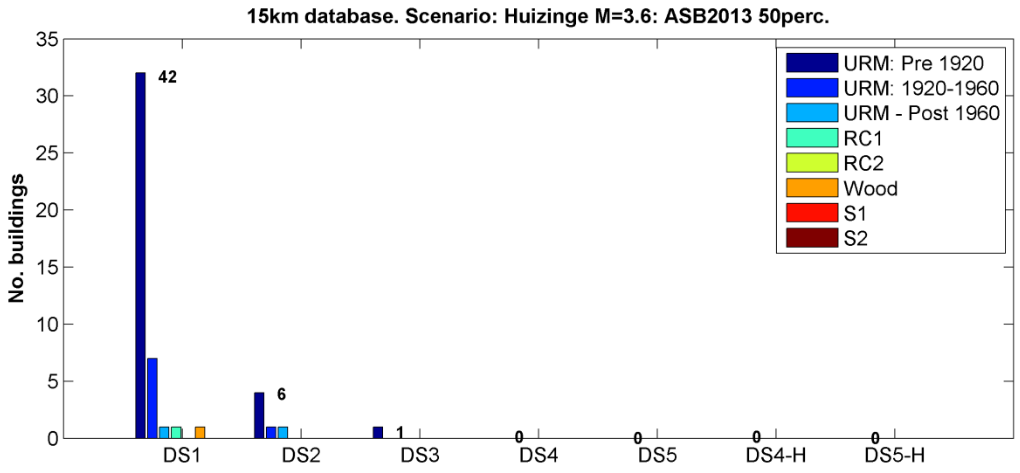

Figure D. 3 Number of buildings in damage state DS1, DS2, DS3, DS4 and DS5 according to their building class for the Huizinge M_w = 3.6 earthquake scenario. DS4 – H and DS5 – H represent the number of buildings computed using the HAZUS methodology for loss estimation purposes. Labels in the plot present the total number of buildings in each damage state.

D3 Scenario #0,b: Huizinge Earthquake M_w=3.6 – 84th percentile PGA

Figure D. 4 shows the 84th percentile (i.e. in log terms the mean +1 sigma) PGA values for the scenario of the Huizinge earthquake of August 2012 with magnitude M_w=3.6. The observed PGA values at seven recording stations are also shown on this figure for comparison. It should be noted that when the 84th percentile is considered, the PGA values appear to have an unrealistically high maximum of 0.2 g. This is high in comparison with the observed maximum PGA during the 2012 Huizinge earthquake which was approximately 0.08 g at about 1 km from the epicentre.

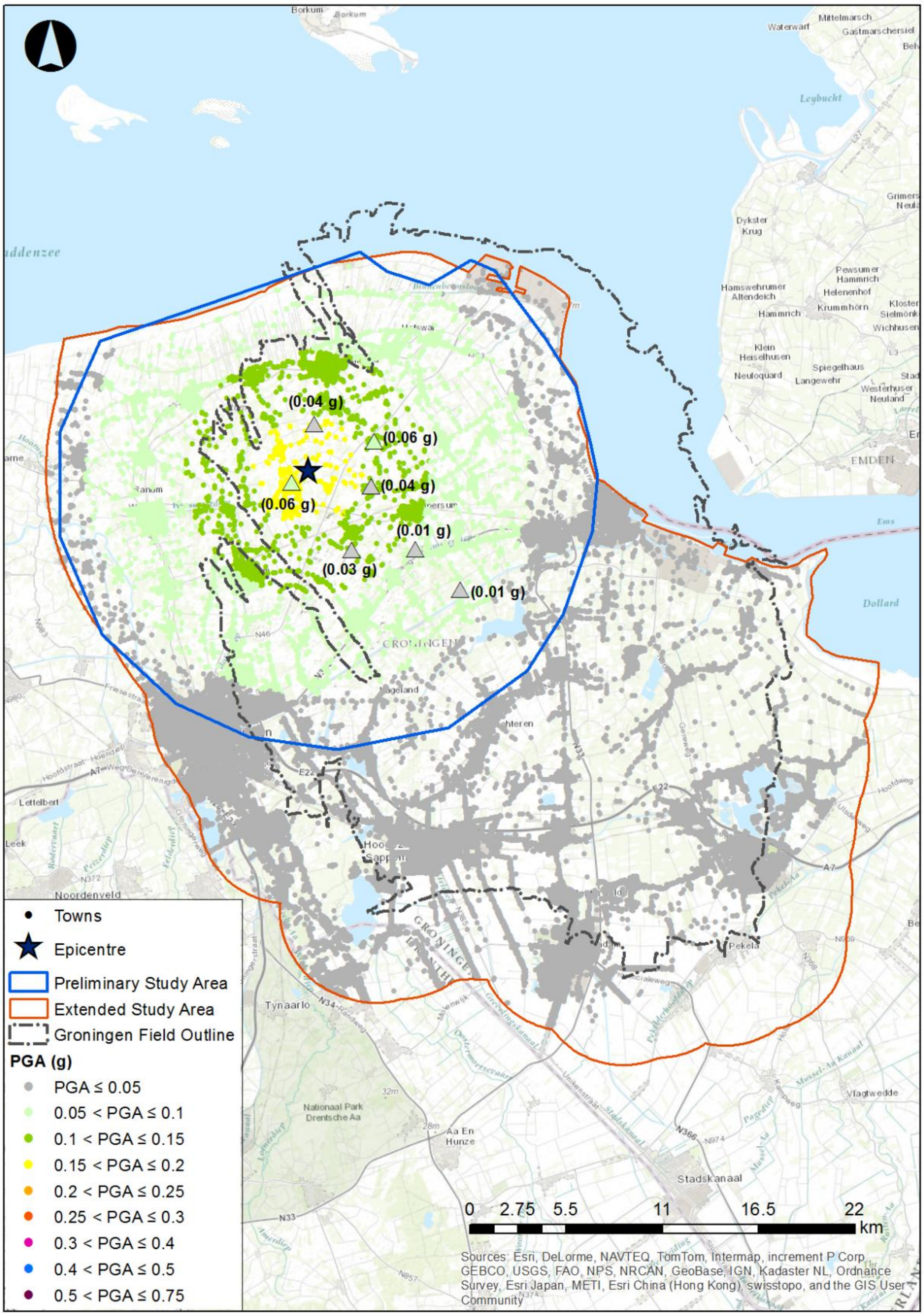

Figure D. 4 84th percentile peak ground acceleration (PGA) estimated for an earthquake of Mw=3.6 and depth H=3 km with epicentre in Huizinge. The GMPE by Akkar et al. (2013) is used. The observed PGA values at the instrument locations (triangles) are shown for comparison.

D3.1 Number of building exposed

The number of buildings that are subjected to different levels of ground motion, in terms of PGA, are summarised in Table D. 2.

Table D. 2 Number of buildings subjected to the 84th pecentile ground motion (84-perc. PGA in g) in scenario #0 – 2012 Huizinge Mw = 3.6 earthquake.

Building Type	**0 ≤ PGA < 0.05**	**0.05 ≤ PGA < 0.1**	**0.1 ≤ PGA < 0.15**	**0.15 ≤ PGA < 0.2**
URM: Pre 1920	19637	2883	1382	346
URM: 1920-1960	68341	5443	2808	528
URM: Post 1960	70775	12081	3919	601
RC1	5277	1232	271	33
RC2	3163	157	56	3
Wood	380	143	53	14
S1	1168	158	53	11
S2	181	6	1	2

D3.2 Building damage

The calculated number of buildings of different typologies damaged in this scenario are summarised in Figure D. 5. Using the 84th percentile PGA values the scenario appears very different from that obtained using the 50th percentile with 650 buildings slightly damaged, ~240 moderately damaged, 50 buildings suffering extensive damage and 17 buildings completely damaged by the earthquake. In this case approximately 6 buildings are estimated to collapse. The 84th percentile PGA values scenario therefore appears to unrealistically over-predict the damage when compared with the damage observed following the August 2012 Huzinge earthquake.

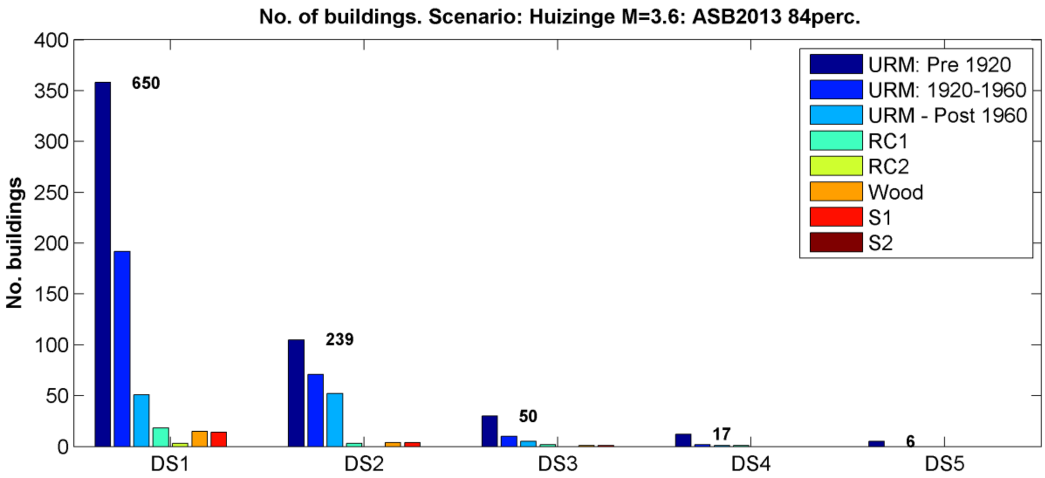

Figure D. 5 Number of buildings in damage state DS1, DS2, DS3, DS4 and DS5 according to their building class for the Huizinge Mw = 3.6 earthquake scenario computed with 84th percentile in the GMPE. Labels in the plot present the total number of buildings in each damage state.

D3.3 Casualty estimation

As for the 50th percentile, the casualty estimation is performed adopting the 15 km radius study area (blue outlines in Figure D. 4). The damage states DS4 and DS5 are computed both using the fragility functions and with the HAZUS Collapse Rates (DS4 – H and DS5 – H). This leads to a lower proportion of collapsed buildings and more buildings in damage state DS4. These numbers, DS4 – H and DS5 – H, are used only for the loss estimation purposes.

Figure D. 6 presents the numbers of buildings in each damage state for the 15 km radius database when the 84th percentile PGA values are used. It is highlighted that the numbers of buildings in DS1 and DS2 may be slightly different than those presented in Figure D. 5, since a few buildings with a non-negligible PGA outside the 15 km radius area are now not included in the calculations.

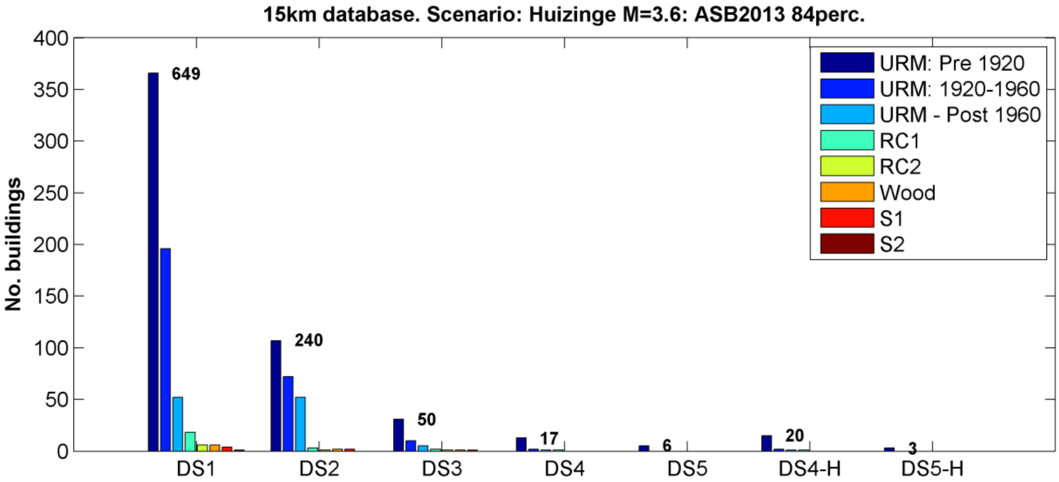

Figure D. 6 Number of buildings in damage state DS1, DS2, DS3, DS4 and DS5 according to their building class for the Huizinge Mw = 3.6 earthquake scenario computed with the 84th percentile. DS4 – H and DS5 – H represent the number of buildings computed using the HAZUS methodology for loss estimation purposes. Labels in the plot present the total number of buildings in each damage state.

The numbers of casualties in terms of the severity of injury are summarised on the top panel of Figure D. 7 for the occurrence of the Huizinge scenario event during the day and on the bottom panel for the occurrence of the event during the night. The casualty estimates for day and night are very similar. The figures show the number of people that would suffer injury severity levels (SL) 1 to 4 in damage state DS1, DS2, DS3, DS4 (HAZUS) and DS5 (HAZUS). 15 people are estimated to be slightly injured,5 moderately injured. One fatality is estimated. It is clear that these casualty estimates are larger and more severe than the actual casualties related to the Huzuinge earthquake. However, these higher estimates should not be dismissed entirely and it is recommended the low likelihood but possible occurrence of casualties even from small magnitude earthquakes is considered.

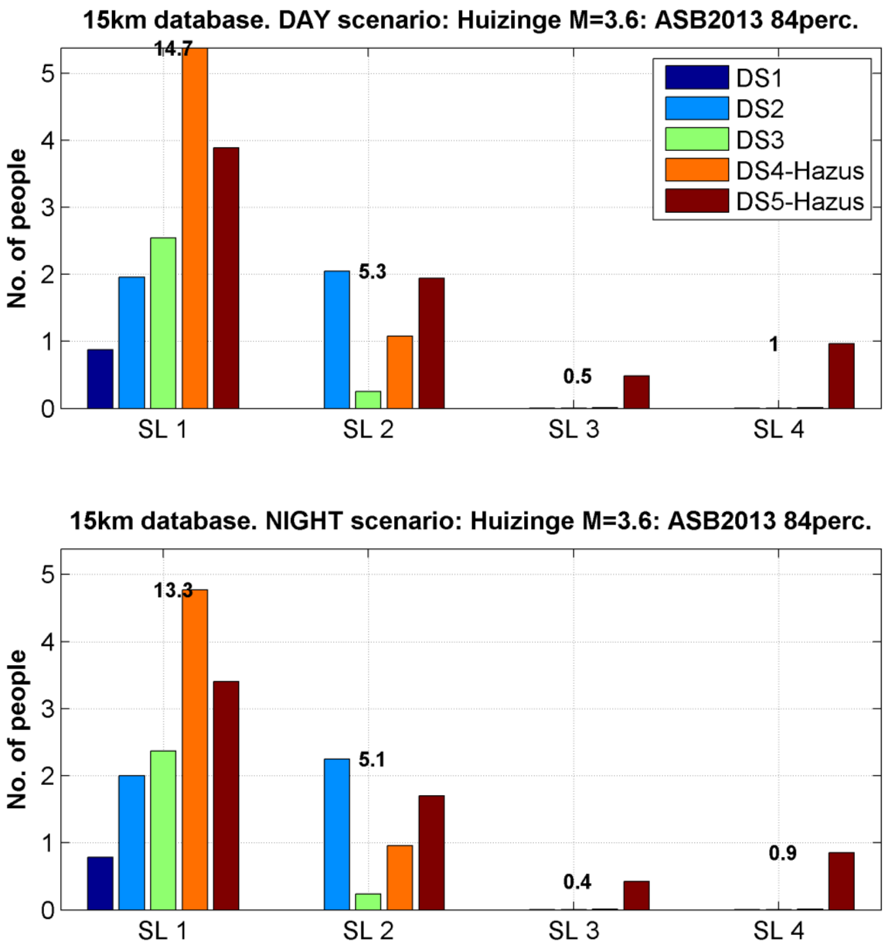

Figure D. 7 Estimated number of casualties in severity levels SL1, SL2, SL3 and SL4 associated with damage states DS1, DS2, DS3, DS4 and DS5, due to the occurrence of the Huizinge Mw = 3.6 earthquake scenario during the day (2 pm), top panel, and during the night (2 am), bottom panel.

D4 Scenario # 2: Huizinge Earthquake M_w = 4 (50th percentile)

Scenario # 2 comprises a M_w = 4 earthquake with a hypocentral depth of 3km and an epicentre located at Huizinge. The earthquake is assumed to have a point source and median PGA ground motion values have been used. The distribution of PGA values at the building locations is shown in Figure D. 8. Note that the maximum PGA value for this scenario is <0.15 g and many houses experience very low PGA values (<0.05g).

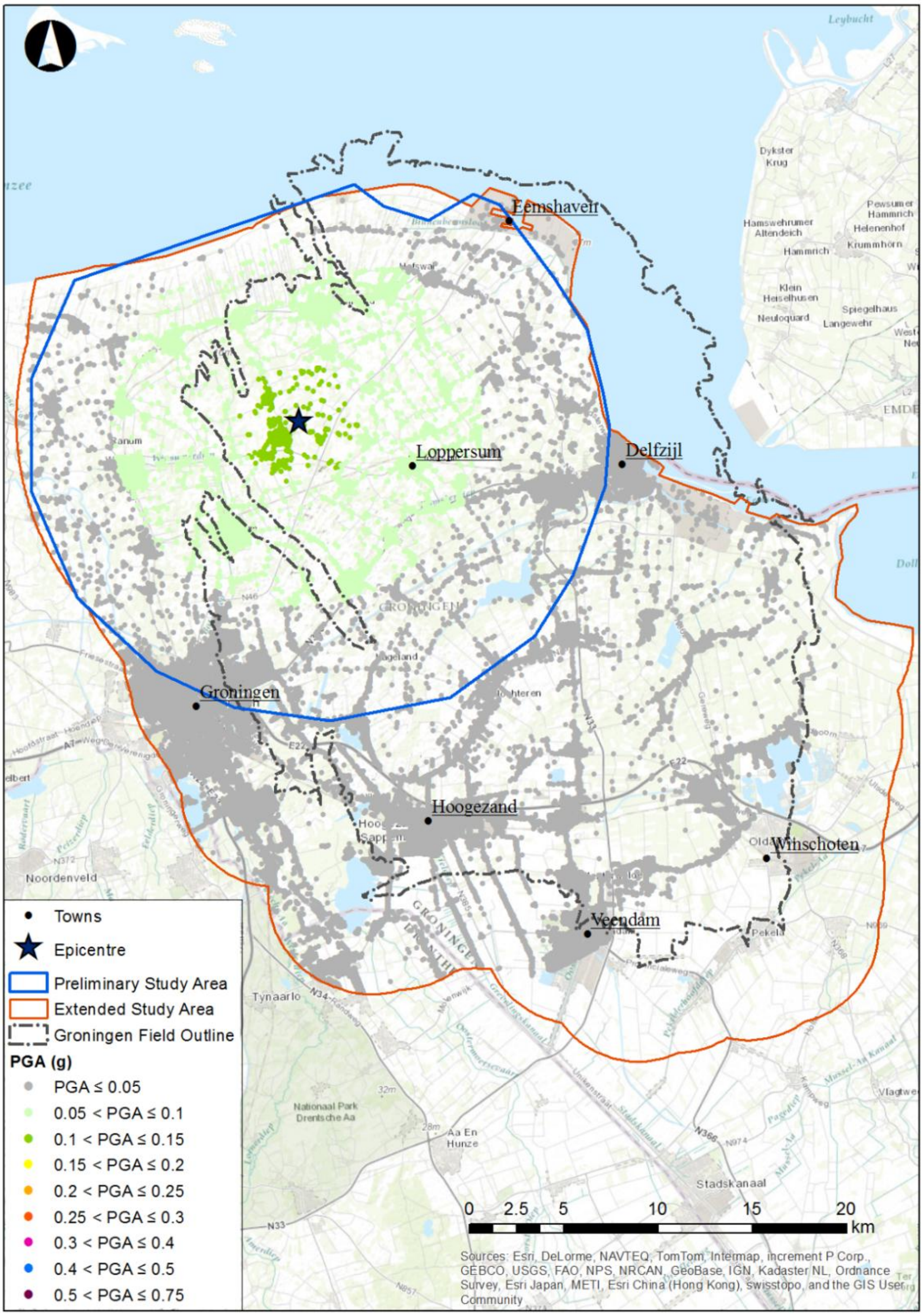

Figure D. 8 Median peak ground acceleration (PGA) estimated for an earthquake of M_w=4 and depth H=3 km with epicentre in Huizinge. The GMPE by Akkar et al. (2013) is used.

D4.1 Number of building exposed

The numbers of buildings that are subjected to different levels of ground motion, in terms of PGA, as a result at the M_w=4 earthquake scenario are summarised in Table D. 3.

Table D. 3 Number of buildings subjected to ground motion (*PGA* in g) in the Huizinge M_w = 4 earthquake scenario.

Building Type	$0 \leq PGA < 0.05$	$0.05 \leq PGA < 0.1$	$0.1 \leq PGA < 0.15$
URM: Pre 1920	20841	3059	348
URM: 1920-1960	70087	6505	528
URM: Post 1960	76507	10269	601
RC1	6055	724	33
RC2	3256	119	3
Wood	459	118	14
S1	1211	168	11
S2	184	4	2

D4.2 Building damage

The calculated numbers of buildings of different typologies damaged in this M_w=4 scenario are summarised in Table D. 4 and Figure D. 9. Only two buildings suffer complete damage while no building is estimated to collapse under a M_w=4 earthquake. Approximately 170 buildings are estimated to be slightly damaged, 40 moderately damaged, six extensively damaged and two building are completely damaged. No collapse is expected.

Table D. 4 Number of buildings damaged in Huizinge M_w = 4 earthquake scenario.

	DS1	DS2	DS3	DS4	DS5
Huizinge Scenario	173	39	6	2	0

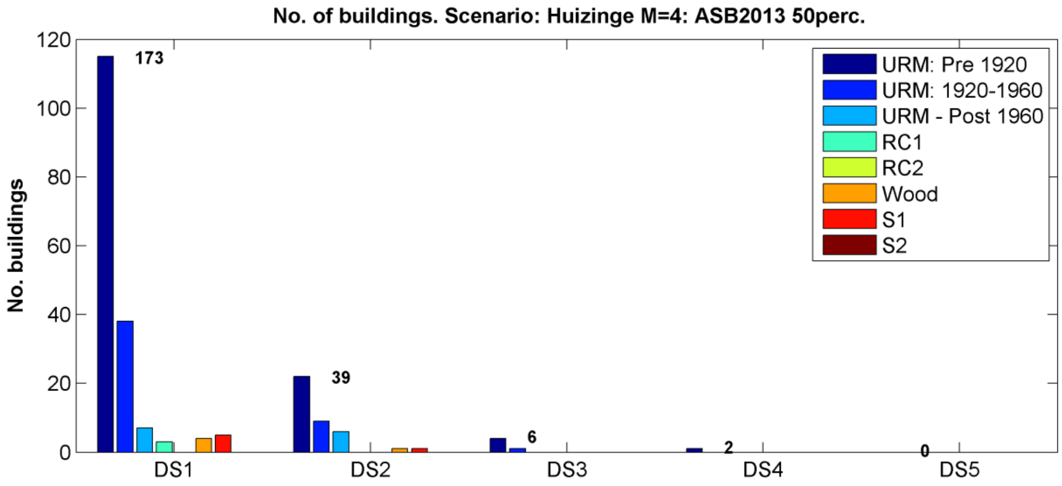

Figure D. 9 Number of buildings in damage state DS1, DS2, DS3, DS4 and DS5 according to their building class for the Huizinge M_w = 4 earthquake scenario.

D4.3 Casuality Estimation

Figure D. 10 presents the numbers of buildings in each damage state estimated for the M_w=4 earthquake scenario for the casualty estimation. Although the preliminary (15 km radius) building database has been used here, the numbers of damaged buildings are not different to the numbers of buildings estimated using the extended database (see Figure D. 9).

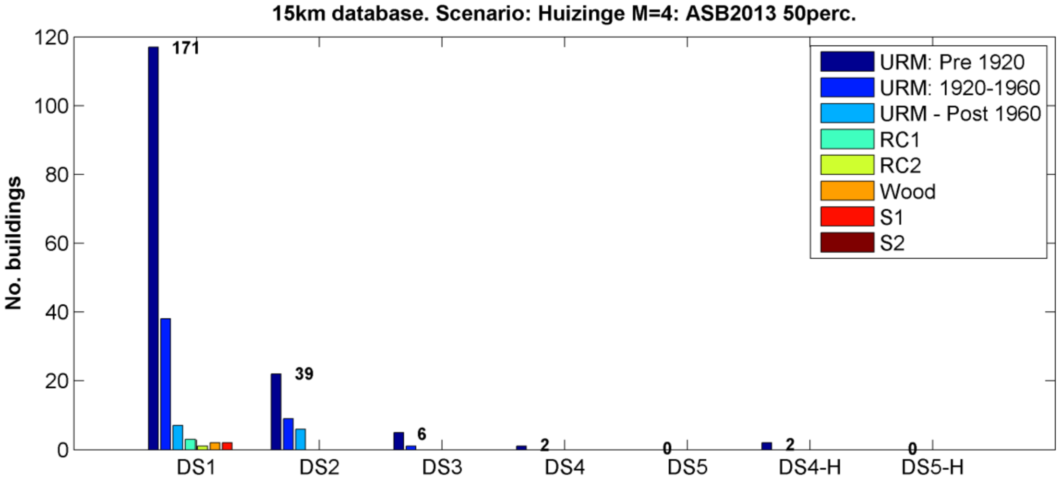

Figure D. 10 Number of buildings in damage state DS1, DS2, DS3, DS4 and DS5 according to their building class for the Huizinge M_w = 4 earthquake scenario. DS4 – H and DS5 – H represent the number of buildings computed using the HAZUS methodology for loss estimation purposes. Labels in the plot present the total number of buildings in each damage state.

One to two slight injuries are estimated with the M_w=4 earthquake scenario both if the earthquake occurs during the day or during the night. No fatalities are estimated to occur with this magnitude earthquake.

D5 Scenario # 3: Huizinge Earthquake of M_w = 4.5 (50th percentile)

Scenario # 3 comprises a M_w = 4.5 earthquake with a hypocentral depth of 3km and with an epicentre located at Huizinge. The distribution of ground motions in terms of peak ground acceleration caused by this scenario earthquake are shown in Figure D. 11.

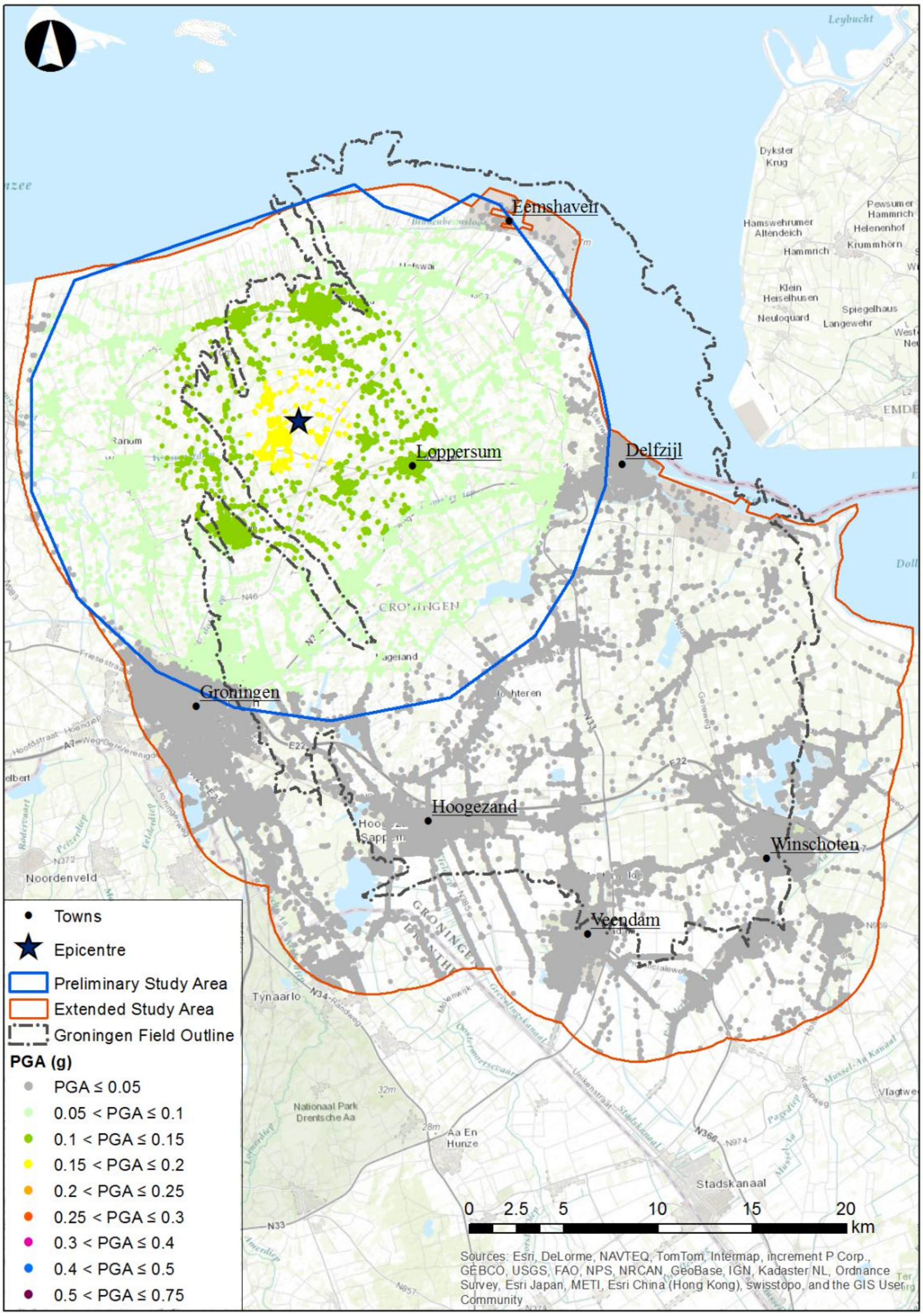

Figure D. 11 Median peak ground acceleration (PGA) estimated for an earthquake of M_w=4.5 and depth H=3 km with epicentre in Huizinge. The GMPE by Akkar et al. (2013) is used.

D5.1 Number of buildings exposed

The number of buildings that are subjected to different levels of ground motion, in terms of PGA as a result of the M_w=4.5 earthquake scenario, are summarised in Table D. 5.

Table D. 5 Number of buildings subjected to ground motion (*PGA* in g) in scenario #5 - Huizinge M_w = 4.5 earthquake

Building Type	**0 ≤ *PGA* < 0.05**	**0.05 ≤ *PGA* < 0.1**	**0.1 ≤ *PGA* < 0.15**	**0.15 ≤ *PGA* < 0.2**
URM: Pre 1920	18529	3789	1594	336
URM: 1920-1960	65292	7849	3453	525
URM: Post 1960	60128	21640	5009	599
RC1	4353	2074	352	33
RC2	2877	432	66	3
Wood	343	172	62	13
S1	1047	256	75	10
S2	173	14	1	2

D5.2 Building damage

The calculated number of buildings of different structural typologies damaged in this M_w=4.5 earthquake scenario are summarised in Table D. 6 and Figure D. 12. Approximately 750 buildings are estimated to be slightly damaged, 270 moderately damaged, 50 extensively damaged, approximately 20 completely damaged and 7 buildings are estimated to collapse.

Table D. 6 Number of buildings damaged in the Hoekdmeer M_w = 4.5 earthquake scenario.

	DS1	**DS2**	**DS3**	**DS4**	**DS5**
Hoeksmeer	753	269	54	18	7

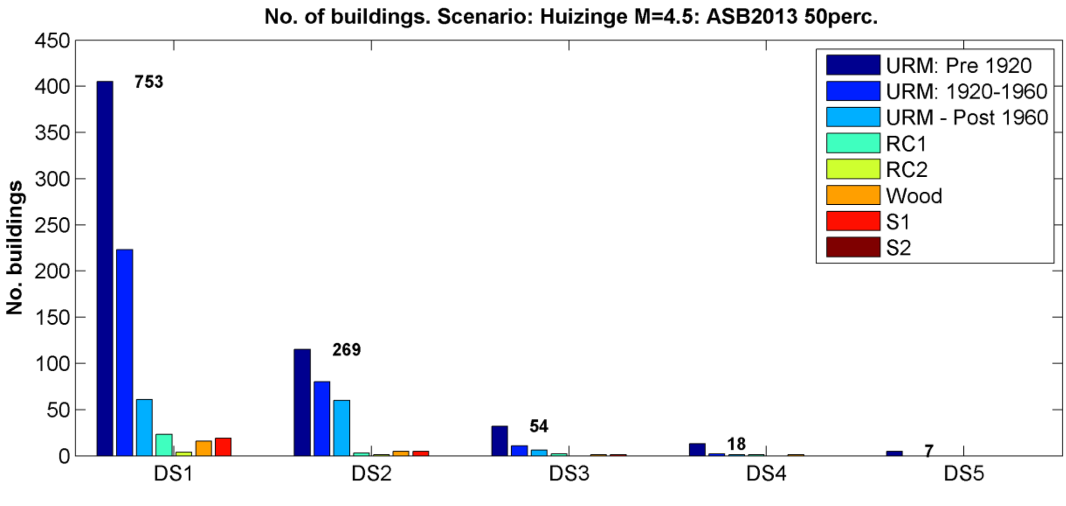

Figure D. 12 Number of buildings in damage states DS1, DS2, DS3, DS4 and DS5 according to their building class for the Huizinge M_w = 4.5 earthquake scenario.

D5.3 Casualty Estimation

Figure D. 13 presents the numbers of buildings in each damage state estimated for the M_w=4.5 earthquake scenario for casualty estimation purposes. In this case, the estimated number of collapsed buildings is four.

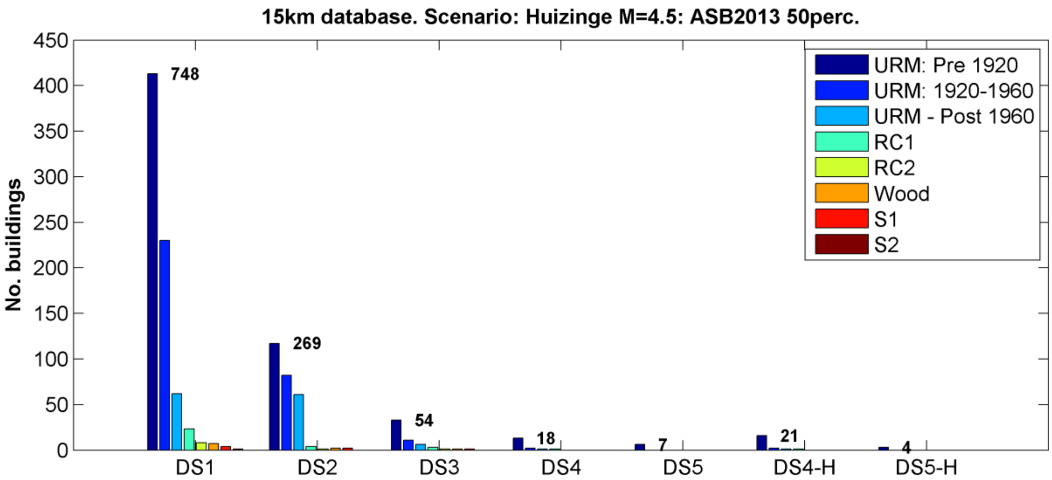

Figure D. 13 Number of buildings in damage state DS1, DS2, DS3, DS4 and DS5 according to their building class for the Huizinge M_w = 4.5 earthquake scenario computed with the 15 km radius database. DS4 – H and DS5 – H represent the number of buildings computed using the HAZUS methodology for loss estimation purposes. Labels in the plot present the total number of buildings in each damage state.

The numbers of casualties in terms of the severity of injury estimated for the M_w=4.5 earthquake scenario are summarised on the top panel of Figure D. 14for the occurrence of the Huizinge scenario event during the day and on the bottom panel for the occurrence of the event during the night. Approximately 23 people are estimated to be slightly-to-seriously injured with 1 potential fatality during the day and approximately 20 injured and 1 potential fatality during the night.

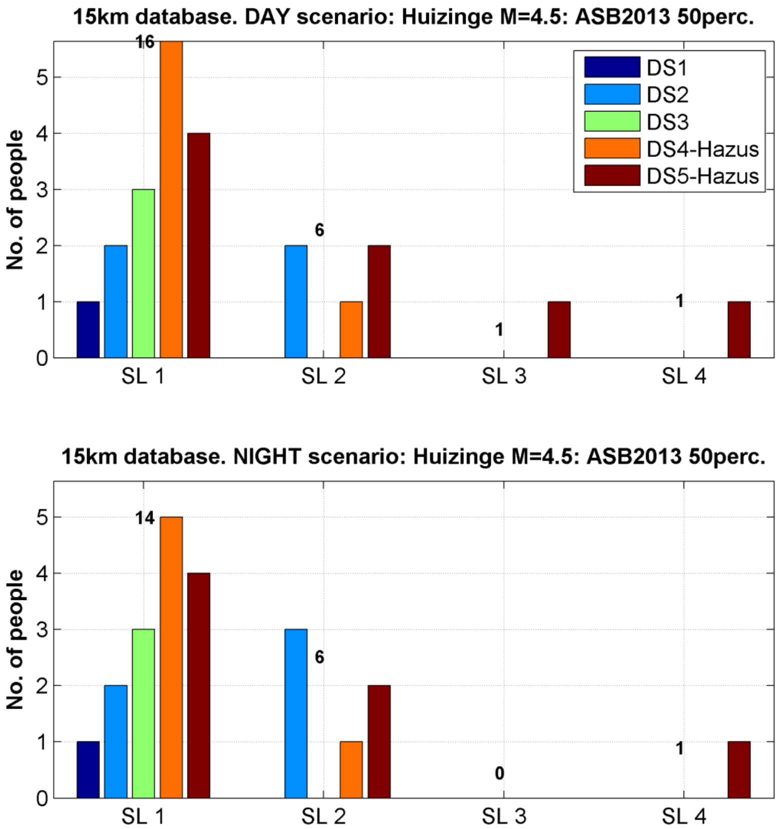

Figure D. 14 Estimated number of casualties in severity levels SL1, SL2, SL3 and SL4 associated with damage states DS1, DS2, DS3, DS4 and DS5, due to the occurrence of the Huizinge $M_w = 4.5$ earthquake scenario during the day (2 pm), top panel, and during the night (2 am), bottom panel.

D6 Scenario # 4: Zandeweer Earthquake M_w = 5

Scenario # 4 comprises a $M_w = 5$ earthquake with a hypocentral depth of 3km and an epicentre located at Zandeweer in the north of the Groningen region. The earthquake is assumed to have a point source and median ground motion values have been used. The distribution of ground motions in terms of peak ground acceleration caused by this scenario earthquake are shown in Figure D. 15. Note that almost all the buildings with significant PGA (>0.05g) fall inside the 15 km study area. For PGA< 0.05 g the probability of having slight damage in the fragility curves is interpreted to be extremely low.

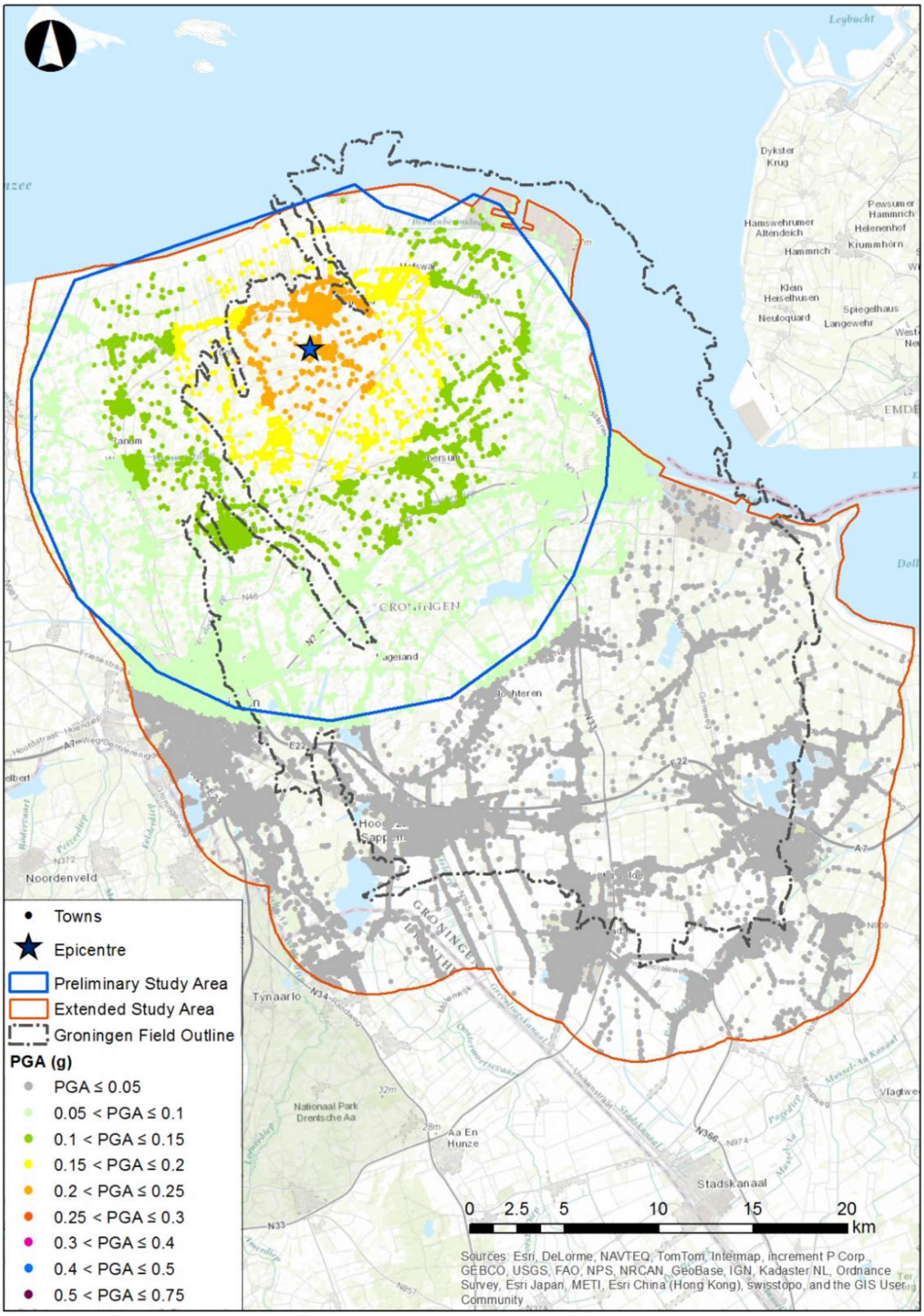

Figure D. 15 Median peak ground acceleration (PGA) estimated for an earthquake of M_w=5 and depth H=3 km with epicentre in Zandeweer. The GMPE by Akkar et al. (2013) is used.

D6.1 Number of building exposed

The number of buildings that are subjected to different levels of ground motion, in terms of PGA as a result of the M_w=5 Zandeweer earthquake scenario, are summarised in Table D. 7.

Table D. 7 Number of buildings subjected to ground motion (*PGA* in g) in the Zanderweer M_w = 5 earthquake scenario.

Building Type	$0 \leq PGA < 0.05$	$0.05 \leq PGA < 0.1$	$0.1 \leq PGA < 0.15$	$0.15 \leq PGA < 0.2$	$0.2 \leq PGA < 0.25$
URM: Pre 1920	11444	9284	1929	927	663
URM: 1920-1960	42017	28288	3720	1565	1530
URM: Post 1960	42060	36097	5964	1454	1800
RC1	2956	3253	366	77	161
RC2	1746	1545	40	12	35
Wood	293	158	75	39	25
S1	686	554	81	30	38
S2	118	68	1	2	2

D6.2 Building damage

The calculated number of buildings of different typologies damaged in the M_w=5 Zandeweer earthquake scenario are summarised in Table D. 8 and Figure D. 16. The numbers of damaged buildings are similar to those obtained for the M_w=5 Huizinge earthquake scenario (#1) with a few more buildings in the higher damage states. Over 1700 buildings are estimated to be slightly damaged, over 1000 moderately damaged, 280 extensively damaged, 114, completely damaged and 55 buildings are estimated to collapse with the M_w=5 Zandeweer earthquake scenario.

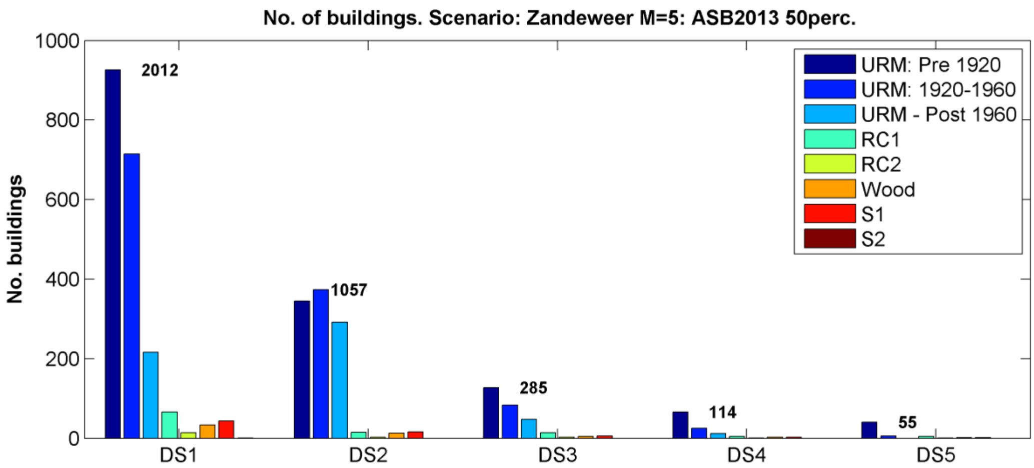

Figure D. 16 Number of buildings in damage state DS1, DS2, DS3, DS4 and DS5 according to their building class for the Zandeweer M_w = 5 earthquake scenario.

Table D. 8 Number of buildings damaged in Zandeweer M_w = 5 earthquake scenario.

	DS1	DS2	DS3	DS4	DS5
Zandeweer Scenario	2012	1057	285	114	55

D6.3 Casuality estimation

Figure D. 17 summarises the numbers of buildings in each damage state for the preliminary (15 km radius) building database. The numbers of buildings in DS1 and DS2 are slightly different than those presented for the extended building database, but almost all the buildings that suffer damage are included in the preliminary (15 km radius) study area.

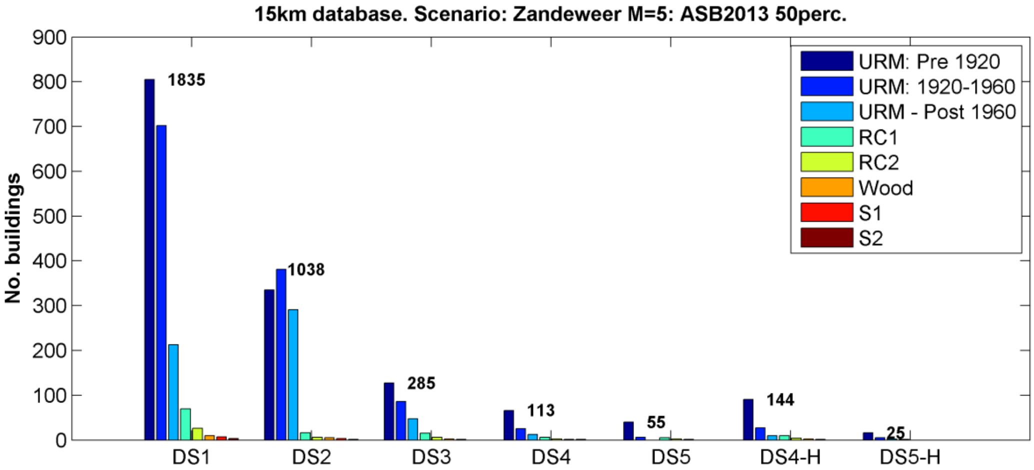

Figure D. 17 Number of buildings in damage state DS1, DS2, DS3, DS4 and DS5 according to their building class for the Zandeweer M_w = 5 earthquake scenario. DS4 – H and DS5 – H represent the number of buildings computed using the HAZUS methodology for loss estimation purposes. Labels in the plot present the total number of buildings in each damage state.

The numbers of casualties in terms of the severity of injury are summarised on the top panel of Figure D. 18 for the occurrence of the M_w=5 Zandeweer earthquake scenario during the day and on the bottom panel for the occurrence of the event during the night. The figures show the number of people that would suffer injury severity levels (SL) 1 to 4 in damage state DS1, DS2, DS3, DS4 (HAZUS) and DS5 (HAZUS). 125 people are estimated to be slightly-to-seriously injured with approximately 7 potential fatalities during the day and 114 injured and 6 potential fatalities during the night.

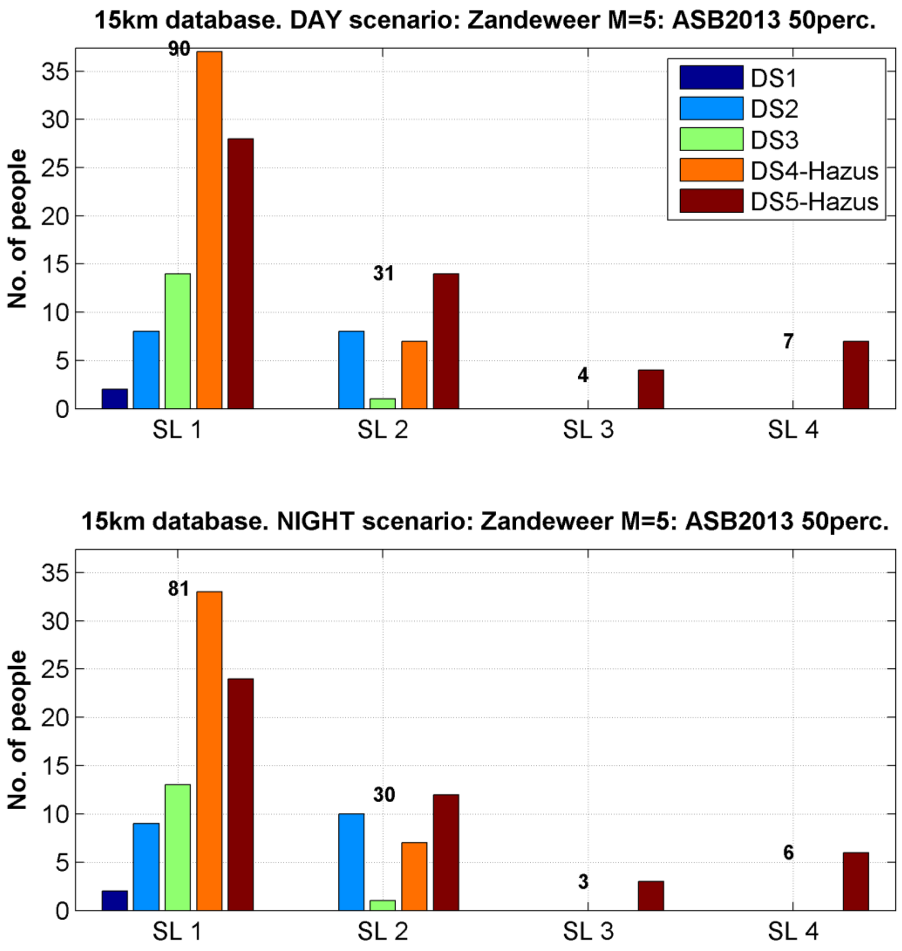

Figure D. 18 Estimated number of casualties in severity levels SL1, SL2, SL3 and SL4 associated with damage states DS1, DS2, DS3, DS4 and DS5, due to the occurrence of the Zandeweer $M_w = 5$ earthquake scenario during the day (2 pm), top panel, and during the night (2 am), bottom panel.

D7 Scenario # 5: Hoeksmeer Earthquake of $M_w = 5$

Scenario # 5 comprises a $M_w = 5$ earthquake with a hypocentral depth of 3km but with an epicentre located in the south of the Groningen region at Hoeksmeer. The earthquake is assumed to have a point source and median ground motion PGA values have been used as previously. The distribution of ground motions in terms of PGA caused by this scenario earthquake is shown in Figure D. 19. Note that many buildings with a non-negligible PGA value (>0.05 g) are located within the extended study area but outside the preliminary study area. This will affect the casualty estimation but not the building damage estimation as the extended building database is used for damage estimation.

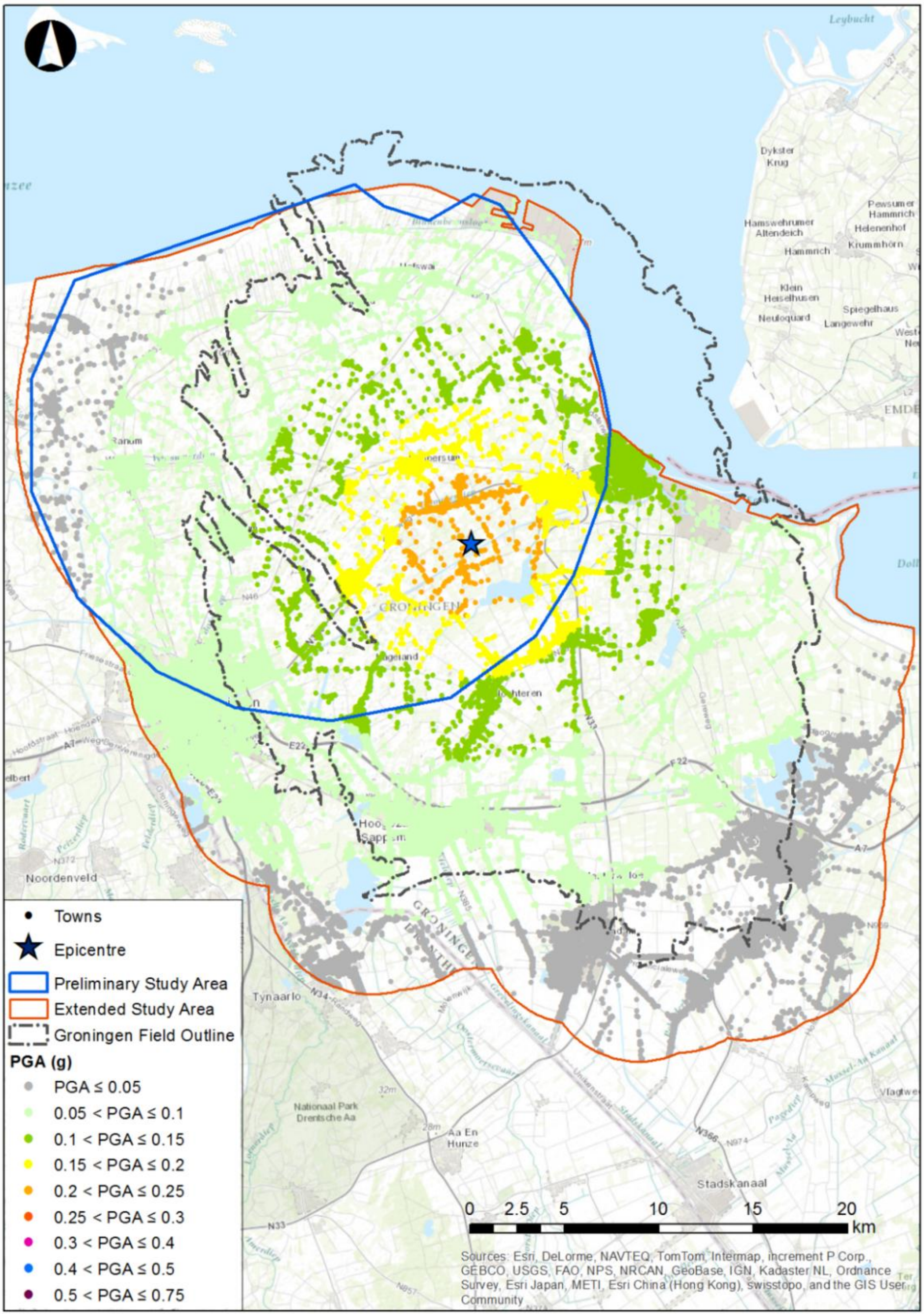

Figure D. 19 Median peak ground acceleration (PGA) estimated for an earthquake of M_w=5 and depth H=3 km with epicentre in Hoeksmeer. The GMPE by Akkar et al. (2013) is used.

D7.1 Number of buildings exposed

The number of buildings that are subjected to different levels of ground motion, in terms of PGA as a results of the M_w=5 Hoeksmeer earthquake scenario are summarised in Table D. 9.

Table D. 9 Number of buildings subjected to ground motion (*PGA* in g) in scenario #2 - Hoeksmeer M_w = 5 earthquake

Building Type	$0 \le PGA < 0.05$	$0.05 \le PGA < 0.1$	$0.1 \le PGA < 0.15$	$0.15 \le PGA < 0.2$	$0.2 \le PGA < 0.25$
URM: Pre 1920	2392	18274	1699	1599	284
URM: 1920-1960	10985	55417	6292	4070	356
URM: Post 1960	11276	61277	8445	6175	203
RC1	706	5209	507	380	12
RC2	218	2825	214	120	2
Wood	131	271	112	57	19
S1	194	978	127	84	7
S2	13	149	19	10	0

D7.2 Building damage

The calculated number of buildings of different structural typologies damaged in the M_w=5 Hoeksmeer earthquake scenario are summarised in Table D. 10 and Figure D. 20. The numbers are similar to those obtained in the Huizinge earthquake scenario and Zandeweer earthquake scenario. Over 2500 buildings are estimated to be slightly damaged, 1150 moderately damaged, 260 extensively damaged, 94 buildings completely damaged and 41 to collapse.

Table D. 10 Number of buildings damaged in the Hoeksmeer M_w = 5 earthquake scenario.

	DS1	DS2	DS3	DS4	DS5
Hoeksmeer	2620	1161	261	94	41

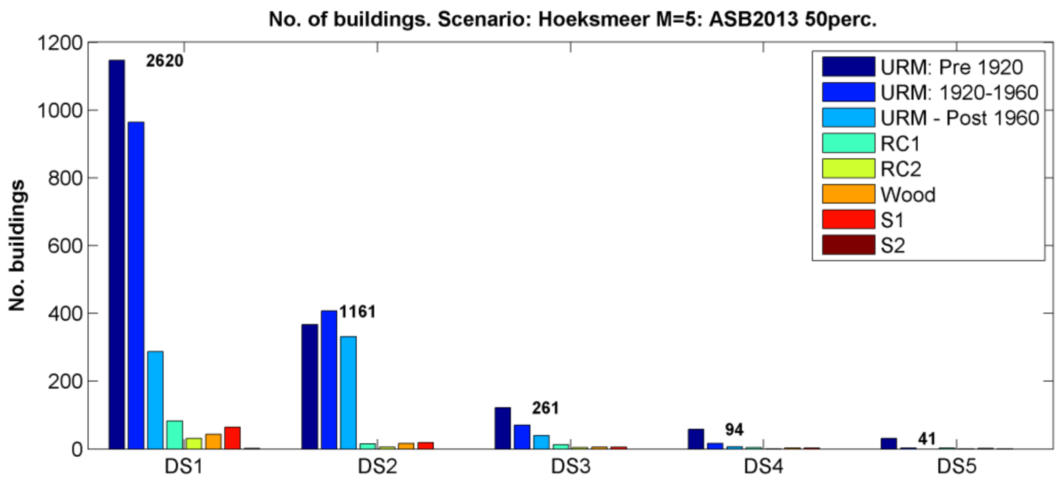

Figure D. 20 Number of buildings in damage states DS1, DS2, DS3, DS4 and DS5 according to their building class for the Hoeksmeer M_w = 5 earthquake scenario.

D7.3 Casualty Estimation

Figure D. 21 presents the numbers of buildings in each damage state for the preliminary (15 km radius) building database. Since the epicentre is close to the boundary of the initial study area the number of buildings that suffer damage is lower than that found with the extended database (Figure D. 20). Within the initial study area approximately 1600 buildings are estimated to be slightly damaged, 870 moderately damaged and 214 extensively damaged. For the casualty estimation the estimated number of buildings in DS4 is ~100 and in DS5 is 17.

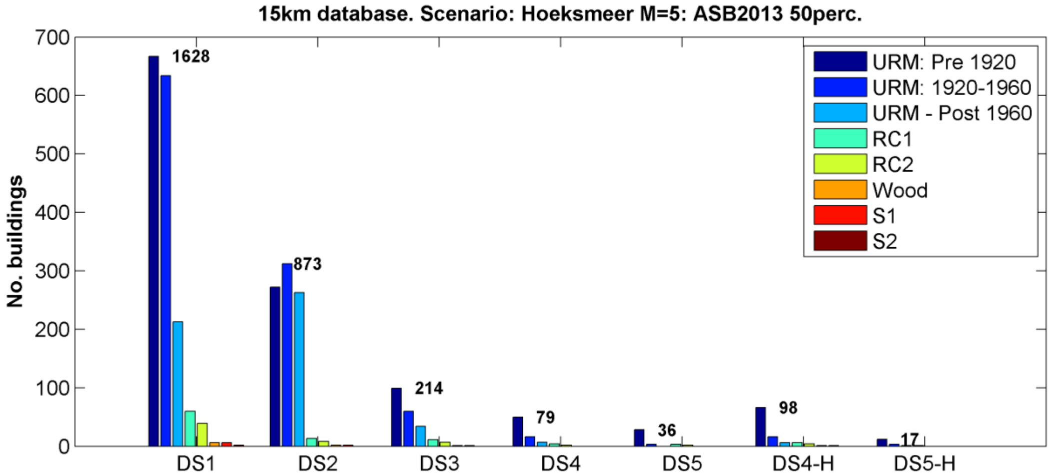

Figure D. 21 Number of buildings in damage state DS1, DS2, DS3, DS4 and DS5 according to their building class for the Hoeksmeer M_w = 5 earthquake scenario computed with the 15 km radius database. DS4 – H and DS5 – H represent the number of buildings computed using the HAZUS methodology for loss estimation purposes. Labels in the plot present the total number of buildings in each damage state.

The numbers of casualties in terms of the severity of injury are summarised on the top panel of Figure D. 22 for the occurrence of the M_w=5 Hoeksmeer earthquake scenario event during the day and on the bottom panel for the occurrence of the event during the night. The figures show the number of people that would suffer injury severity levels (SL) 1 to 4 in damage state DS1, DS2, DS3, DS4 (HAZUS) and DS5 (HAZUS). 91 people are estimated to be slightly-to-seriously injured with approximately 5 potential fatalities during the day and 82 injured and 4 potential fatalities during the night.

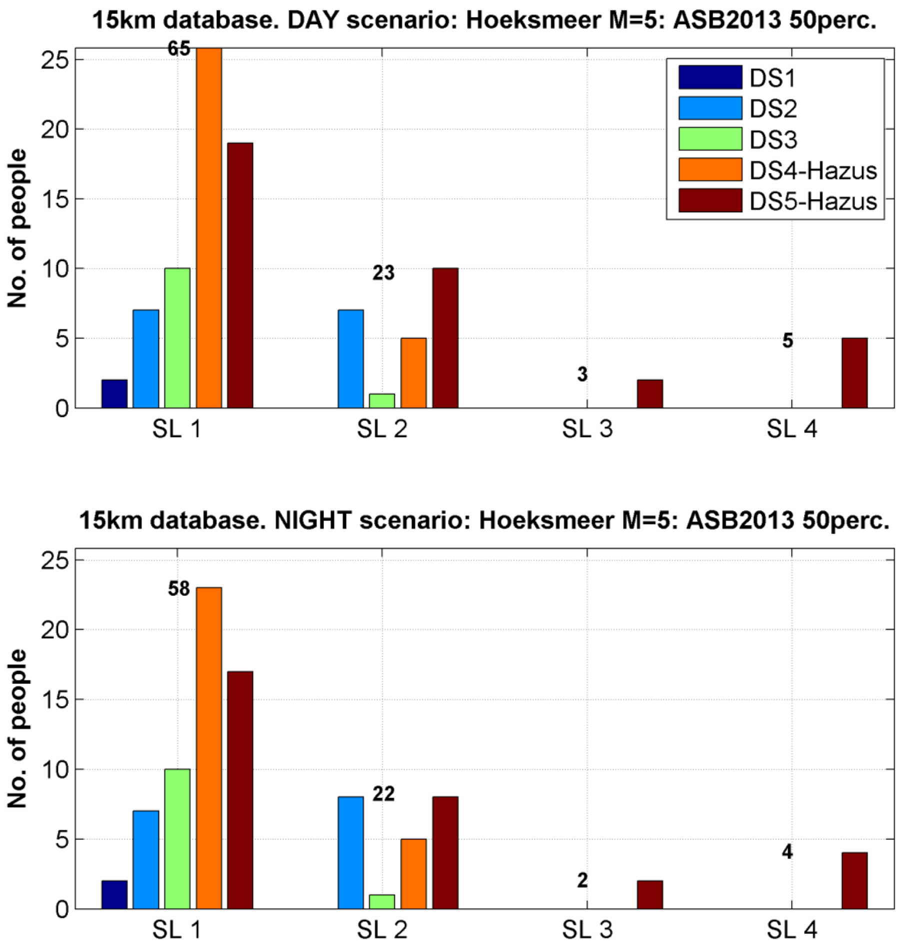

Figure D. 22 Estimated number of casualties in severity levels SL1, SL2, SL3 and SL4 associated with damage states DS1, DS2, DS3, DS4 and DS5, due to the occurrence of the Hoeksmeer $M_w = 5$ earthquake scenario during the day (2 pm), top panel, and during the night (2 am), bottom panel.

D8 Scenario # 6: Huizinge Earthquake M_w = 5 – Fragility Functions by Pinho and Crowley

D8.1 Building damage

The calculated numbers of buildings of different typologies damaged during a M_w =5 earthquake located in Huizinge but computed with the Pinho and Crowley “duration unmodified” fragility functions are summarised in Table D. 11 and Figure D. 23. Over 3000 buildings are slightly damaged, 360 moderately damaged, 208 extensively damaged, ~80 are completely damaged and 53 buildings are estimated to collapse.

Table D. 11 Number of buildings damaged in Huizinge M_w = 5 earthquake scenario using the Pinho and Crowley “duration unmodified” fragility functions.

	DS1	DS2	DS3	DS4	DS5
Huizinge Scenario	3075	363	208	77	53

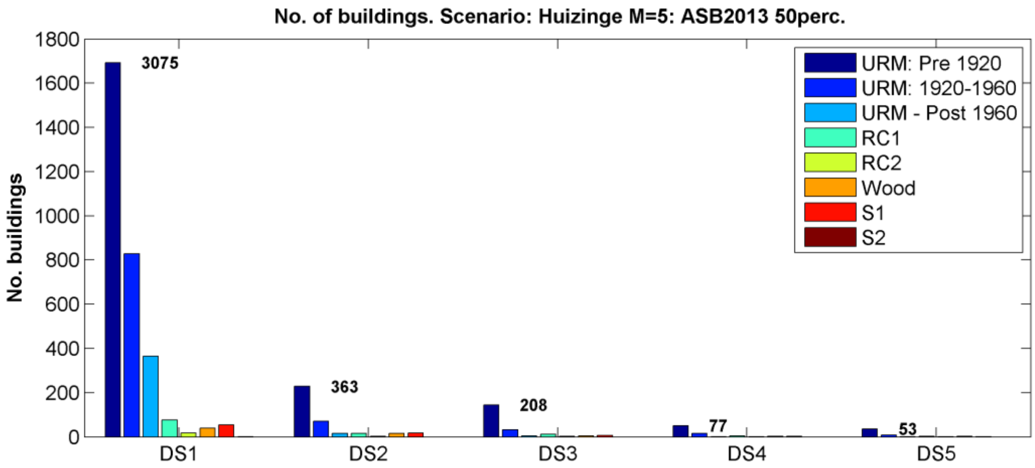

Figure D. 23 Number of buildings in damage state DS1, DS2, DS3, DS4 and DS5 according to their building class for the Huizinge M_w = 5 earthquake scenario computed with the Pinho and Crowley "duration unmodified" fragility functions.

D8.2 Casuality Estimation

Figure D. 24 presents the numbers of buildings in each damage state for the preliminary (15 km radius) building database.

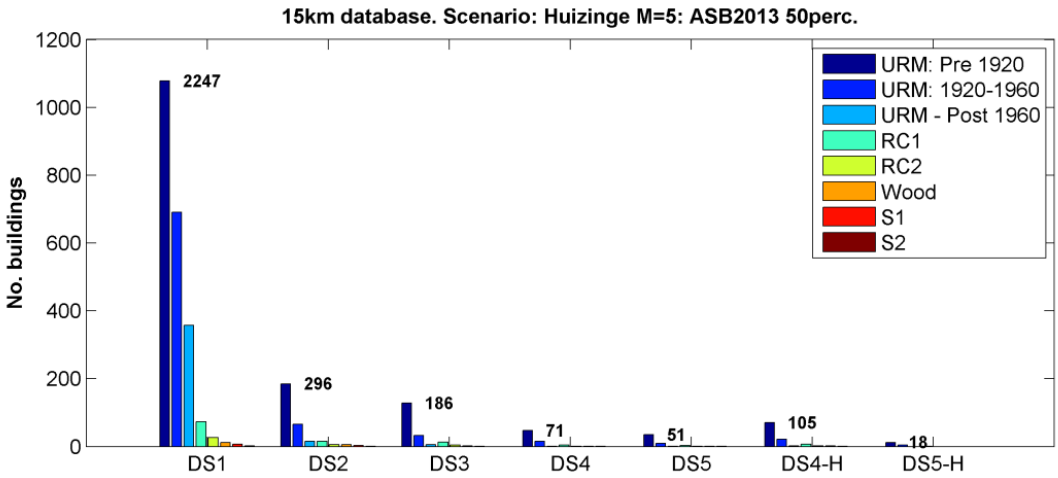

Figure D. 24 Number of buildings in damage state DS1, DS2, DS3, DS4 and DS5 according to their building class for the Huizinge M_w = 5 earthquake scenario, computed with the Pinho and Crowley "duration unmodified" fragility functions. DS4 – H and DS5 – H represent the number of buildings computed using the HAZUS methodology for loss estimation purposes. Labels in the plot present the total number of buildings in each damage state.

The numbers of casualties in terms of the severity of injury for this M_w=5 Huizinge earthquake scenario but using the Pinho and Crowley "duration unmodified" fragility functions are summarised in Figure D. 25.

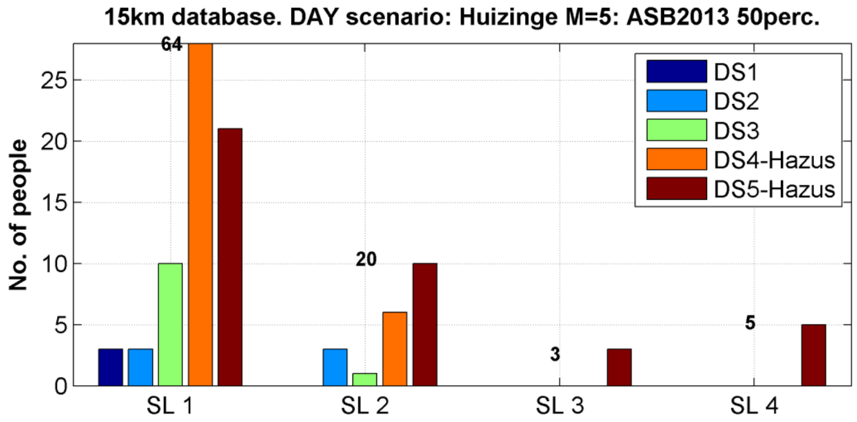

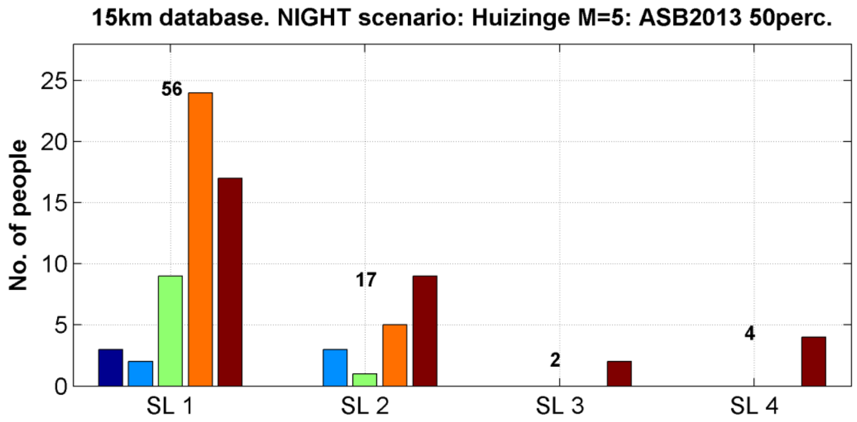

Figure D. 25 Estimated number of casualties in severity levels SL1, SL2, SL3 and SL4 associated with damage states DS1, DS2, DS3, DS4 and DS5, computed with the Pinho/Crowley “original” fragility functions, due to the occurrence of the Huizinge M_w = 5 earthquake during the day (2 pm), top panel, and during the night (2 am), bottom panel.

D9 Scenario # 7: Huizinge Earthquake M_w = 5 – Fragility Functions by Pinho and Crowley “duration”

D9.1 Building damage

The calculated number of buildings of different structural typologies damaged in the M_w=5 Huizinge earthquake scenario using the Pinho and Crowley “duration modified” fragility functions are summarised in Table D. 12 and Figure D. 26. 30 buildings are expected to be completely damaged and 10 to collapse.

Table D. 12 Number of buildings damaged in the Huizinge M_w = 5 earthquake scenario, computed with the Pinho and Crowley “duration modified” fragility functions..

	DS1	DS2	DS3	DS4	DS5
Pinho/Crowley “duration modified”	3263	349	124	29	10

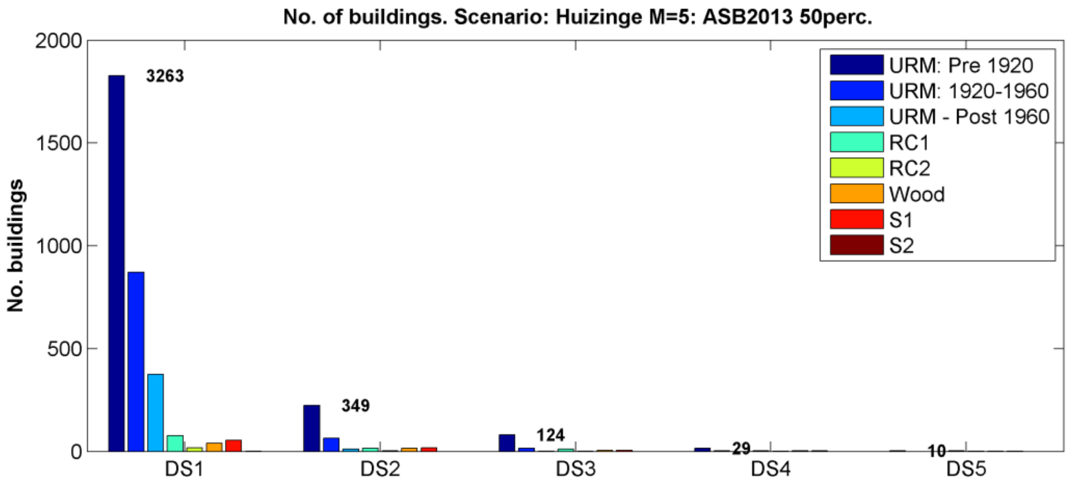

Figure 49: Number of buildings in damage states DS1, DS2, DS3, DS4 and DS5 according to their building class for the Huinzinge M_w = 5 earthquake scenario computed with the Pinho/Crowley "duration modified" fragility functions.

D9.2 Casualty Estimation

Figure D. 26 presents the numbers of buildings in each damage state for the preliminary (15 km radius) building database.

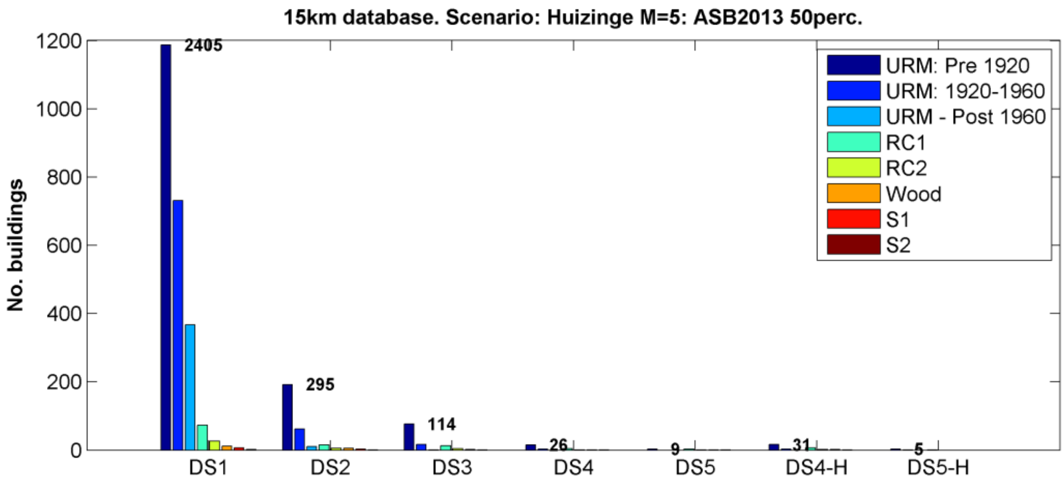

Figure D. 26 Number of buildings in damage state DS1, DS2, DS3, DS4 and DS5 according to their building class for the Huizinge M_w = 5 earthquake scenario computed with the Pinho/Crowley "duration modified" fragility functions using the preliminary (15 km radius) building database. DS4 – H and DS5 – H represent the number of buildings computed using the HAZUS methodology for loss estimation purposes. Labels in the plot present the total number of buildings in each damage state.

The numbers of casualties in terms of the severity of injury for the M_w=5 Huizinge earthquake scenario using the Pinho and Crowley "duration modified" fragility functions are summarised on the top panel of Figure D. 27 for the occurrence of the scenario event during the day and on the bottom panel for the occurrence of the event during the night. 41 people are estimated to be slightly-to-seriously injured with approximately 2 potential fatalities during the day and 29 injured and 1 potential fatality during the night.

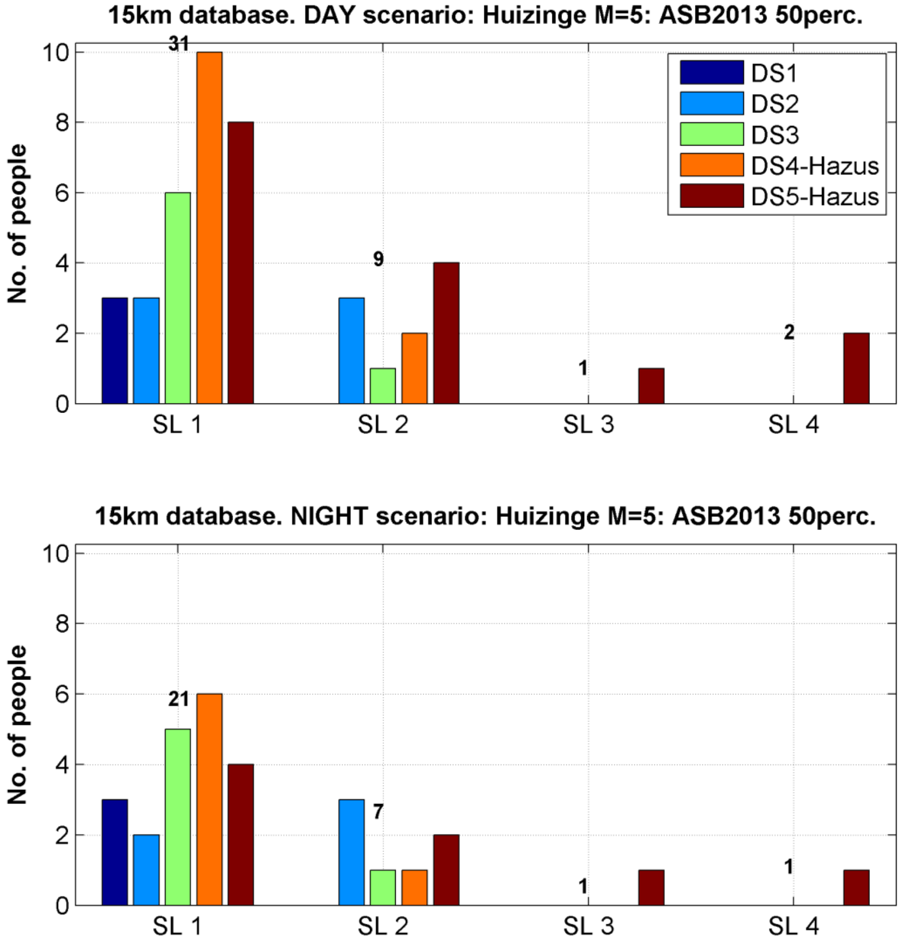

Figure D. 27 Estimated number of casualties in severity levels SL1, SL2, SL3 and SL4 associated with damage states DS1, DS2, DS3, DS4 and DS5, computed with the Pinho/Crowley "duration modified" fragility functions due to the occurrence of the Huizinge $M_w = 5$ earthquake scenario during the day (2 pm), top panel, and during the night (2 am), bottom panel.

D10 Comparison of the results using the 84th percentile PGA values

D10.1 Comparison of the Results Using the Three Families of Fragility Functions (84th percentile PGA values)

The risk results in terms of damaged buildings for the earthquake scenario computed with the three sets of fragility functions but using the 84th percentile PGA values are compared Table D. 13 and in Figure D. 28. Table D. 14 and Table D. 15 show the number of casualties.

Table D. 13 Comparison of the earthquake scenario of Huizinge M_w=5 using the three families of fragility functions in terms of number of buildings damaged to damage states DS1 to DS5.

Scenario	Location	Fragility functions	DS1	DS2	DS3	DS4	DS5
#1	Huizinge	Arup	11847	9210	3351	1841	1286
#6	Huizinge	Pinho/Crowley "duration unmodified"	15141	2471	1750	867	1038
#7	Huizinge	Pinho/Crowley "duration modified"	16373	2714	1362	497	320

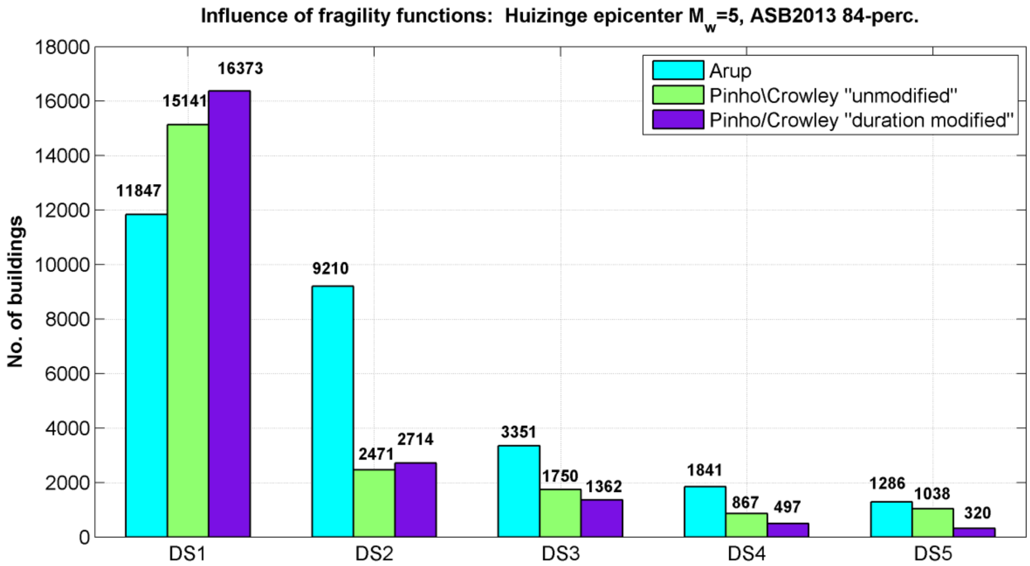

Figure D. 28 Comparison of the earthquake scenario of Huizinge M=5 using the three families of fragility functions in terms of number of buildings damaged to damage states DS1 to DS5.

The risk results between the Arup and Pinho and Crowley "duration unmodified" fragility functions are similar for the damage states DS1, DS2 and DS3 while for DS4 the duration adjustment leads to lower estimates. As a consequence the numbers of injured people drastically decrease when the Pinho and Crowley "duration modified" fragility functions are used.

The results highlight the large epistemic uncertainty involved in the loss estimation due to the selection of the set of fragility functions.

The estimated number of casualties using the Pinho and Crowley "duration modified" fragility functions is approximately one third (30%-40%) of the estimated casualties using the Arup fragility functions. The estimated number of casualties using the Pinho and Crowley "duration unmodified" fragility functions is approximately two thirds (60%-70%) of the estimated casualties using the Arup fragility functions.

Table D. 14 Comparison of the estimated number of casualties for the earthquake scenario of Huizinge M_w =5 using the 84th percentile and the three families of fragility functions, assuming the occurrence of the earthquake during the day.

Scenario	Location	Fragility functions	SL1	SL2	SL3	SL4
#1	Huizinge	Arup	1279	427	60	118
#6	Huizinge	Pinho/Crowley "duration unmodified"	790	251	39	77
#7	Huizinge	Pinho/Crowley "duration modified"	468	150	22	43

Table D. 15 Comparison of the estimated number of casualties for the earthquake scenario of Huizinge M_w=5 using the 84th percentile and the three families of fragility functions, assuming the occurrence of the earthquake during the night.

Scenario	Location	Fragility functions	SL1	SL2	SL3	SL4
#1	Huizinge	Arup	1205	407	54	106
#6	Huizinge	Pinho/Crowley "duration unmodified"	641	202	30	59
#7	Huizinge	Pinho/Crowley "duration modified"	290	93	12	23

D11 Investigating the Ground Motion Variability

This Section presents details of the analysis undertaken to better understand the influence of the ground motion variability on the risk estimation results illustrated in Section 6.4.

Figure D. 29 shows an example of one of the fully correlated Monte Carlo case for the M_w=5 Huizinge earthquake scenario but where the number of total standard deviations, ε, is taken to be $\varepsilon = -1$, while Figure D. 30 is a second example which illustrates the same scenario but where the ground motion is fully uncorrelated cases and the number of inter-event standard deviations, ε_τ, is taken to be $\varepsilon_\tau = -1$.

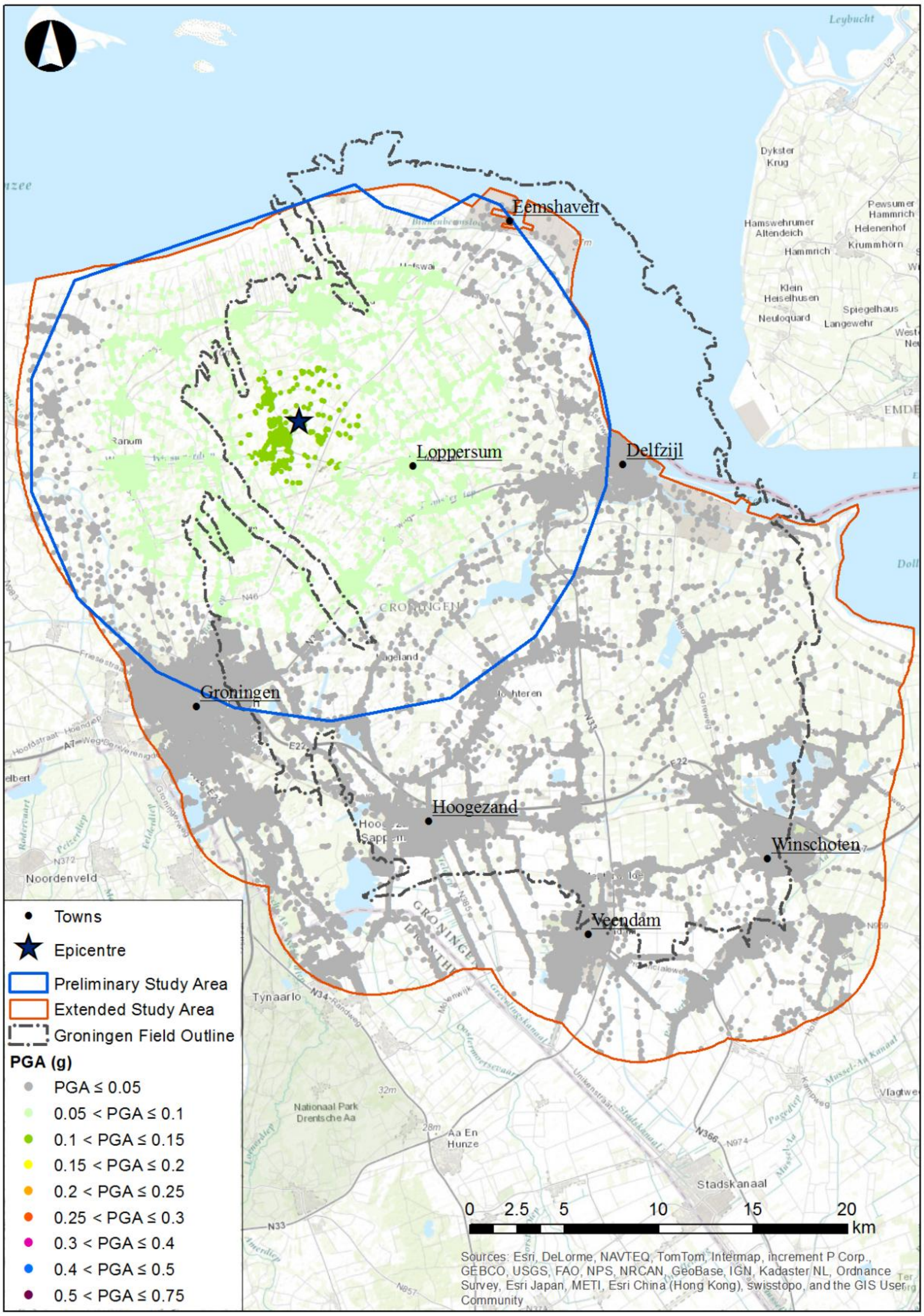

Figure D. 29 Fully correlated PGA values estimated for an earthquake of M_w=5 and depth H=3 km with epicentre in Huizinge with ε=−1.

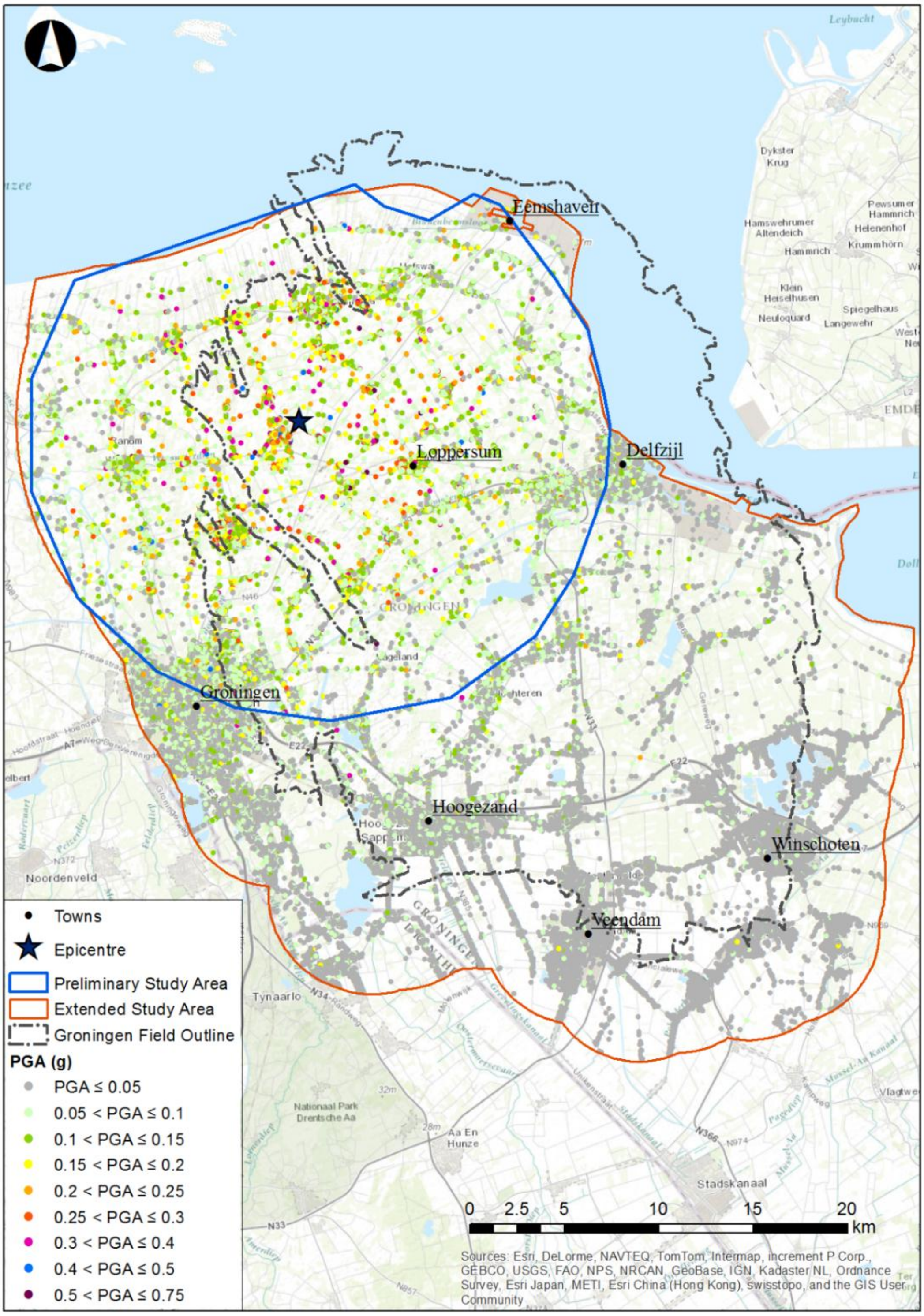

Figure D. 30 Fully uncorrelated PGA values estimated for an earthquake of M_w=5 and depth H=3 km with epicentre in Huizinge with ε_τ=−1.

As a first check on the number of sets of Monte Carlo simulations needed to have robust estimates for the risk estimations, the analysis is carried out using a number of sets of Monte Carlo simulations N_{sim}=50, 100, 1000, 2500, 5000 and 10000. The analysis is performed for the Huizinge earthquake scenario with M_w=5.

Figure D. 31 and Figure D. 32 show the median (50th percentile) and the 84th percentile) of the number of buildings in each damage state. Figure D. 33 shows for the mean and confidence intervals (16th and 84th percentiles interval is considered). Spatial correlation is taken into account by a parameter, ρ, between zero and one, where zero means no spatial correlation and one means full spatial correlation. All results are plotted as a function of the number of Monte Carlo simulations, N_{sim}, computed with the fully uncorrelated PGA values (ρ=0, green circles) and with the fully correlated PGA values (ρ=1, blue squares). For comparison, the red dashed lines represent the number of buildings computed in scenario #1 with the 50th percentile input PGA values while the magenta lines refer to the 84th percentile input PGA values. Note that care is needed to interpret these figures as the terms 50th and 84th percentiles are used to describe both the input PGA values and the output number of damaged buildings. A brief description of the statistical terms is provided in Appendix E.

Figure D. 31 shows that the estimated median (50th percentile) number of damaged buildings obtained with the fully correlated spatial distribution of PGA values as input to the Monte Carlo simulations (blue squares) are consistent with the number of damaged buildings estimated using the median (50th percentile) input PGA values of the GMPE (red dashed curves) as reported in Section 6.2. This result may be interpreted as a check on the reliability of the Monte Carlo simulations.

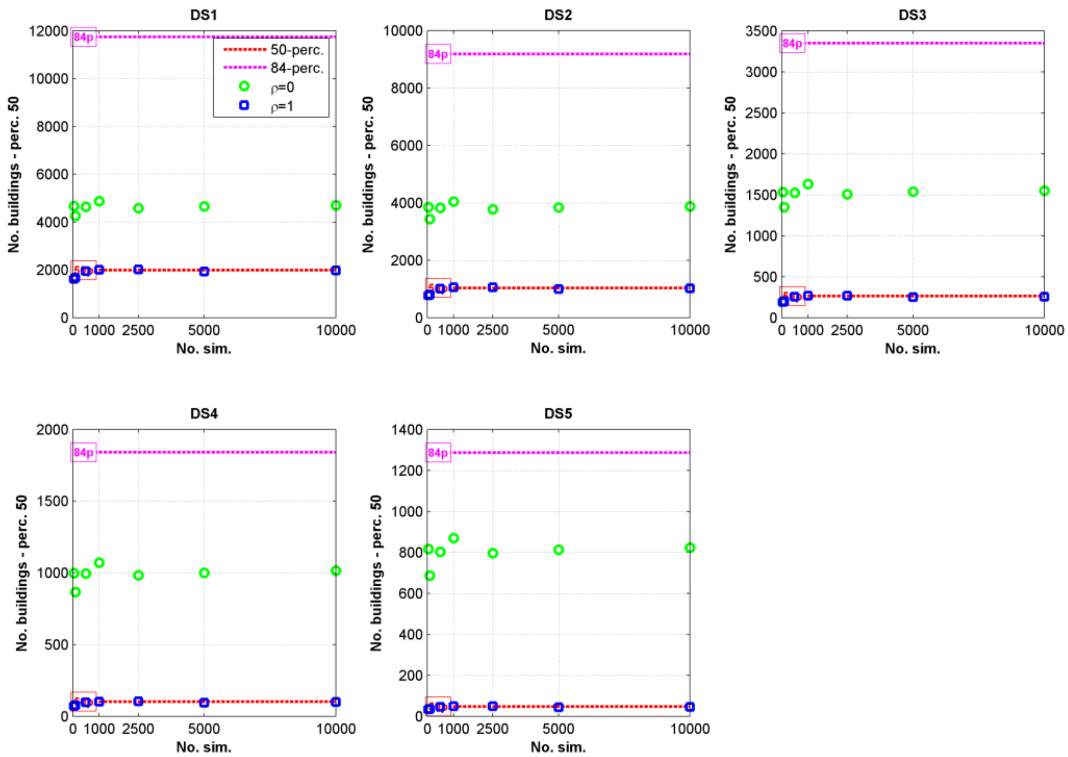

Figure D. 31 Summary plots of the 50th percentile of the number of buildings in each damage state as a function of the number of Monte Carlo simulations computed with the fully uncorrelated PGA values (ρ=0, green circles) and with the fully correlated PGA values (ρ=1, blue squares). For comparison, the red dashed lines represent the number of buildings computed in the M_w=5 Huizinge earthquake scenario with the 50th percentile PGA values while the magenta lines refer to the 84th percentile PGA input values.

Equivalently Figure D. 32 shows that the estimated 84th percentiles of the number of damaged buildings obtained with the fully correlated spatial distribution of PGA values as input of the Monte Carlo simulations (blue squares). The results are consistent with the numbers of damaged buildings estimated using the 84th percentile input PGA values of the GMPE (magenta dashed curves), as described in Section 6.3.1.

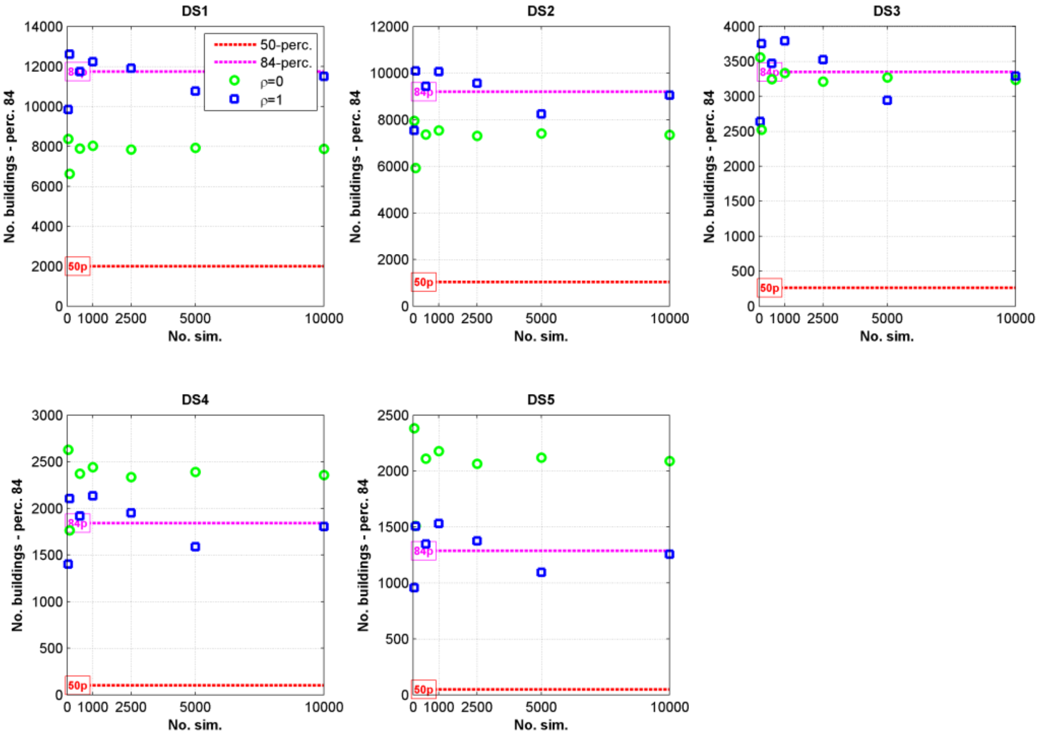

Figure D. 32 Summary plots of the 84th percentile of the number of buildings in each damage state as a function of the number of Monte Carlo simulations computed with the fully uncorrelated PGA values (ρ=0, green circles) and with the fully correlated PGA values (ρ=1, blue squares). For comparison, the red dashed lines represent the number of buildings computed in the M_w =5 Huizinge earthquake scenario with the 50th percentile PGA input values while the magenta lines refer to the 84th percentile PGA input values.

Figure D. 33 provides the summary of the results displaying the mean of the estimated numbers of damaged buildings and the confidence intervals of the estimated number of damaged buildings. The following observations can be made:

- The final results in terms of number of damaged buildings do not change for $N_{sim}\geq 2500$, and therefore calculations based on 2500 simulations may be considered to give a stable result.
- The mean numbers of buildings over the N_{sim} simulations obtained through the fully correlated and the fully uncorrelated spatial distribution cases are very similar.
- The mean results of the Monte Carlo simulations show that approximately 5100 buildings in DS1, 4500 in DS2, 2000 in DS3, 1400 in DS4 and 1250 collapsed buildings. The estimates for DS1 to DS4 are between the 50th and the 84th percentiles, whereas the DS5 mean number of buildings from the Monte Carlo simulations is close to the 84th percentile of the completely deterministic approach. This finding is consistent with the reporting of the risk

assessment results for both the 50th and the 84th percentiles input PGA values as presented in Section 6.2 of this report.

- The variability associated with these estimates shown as the confidence intervals between the 16th and 84th percentiles of the Monte Carlo simulations (error bars in the figure) is large, in particular when the fully correlated ground motion variability is used, as expected, since in this case all the buildings in the database may experience either a very large or a very low number of standard deviations above or below the median. The confidence intervals for 10th and 90th percentiles would of course be even larger if shown.

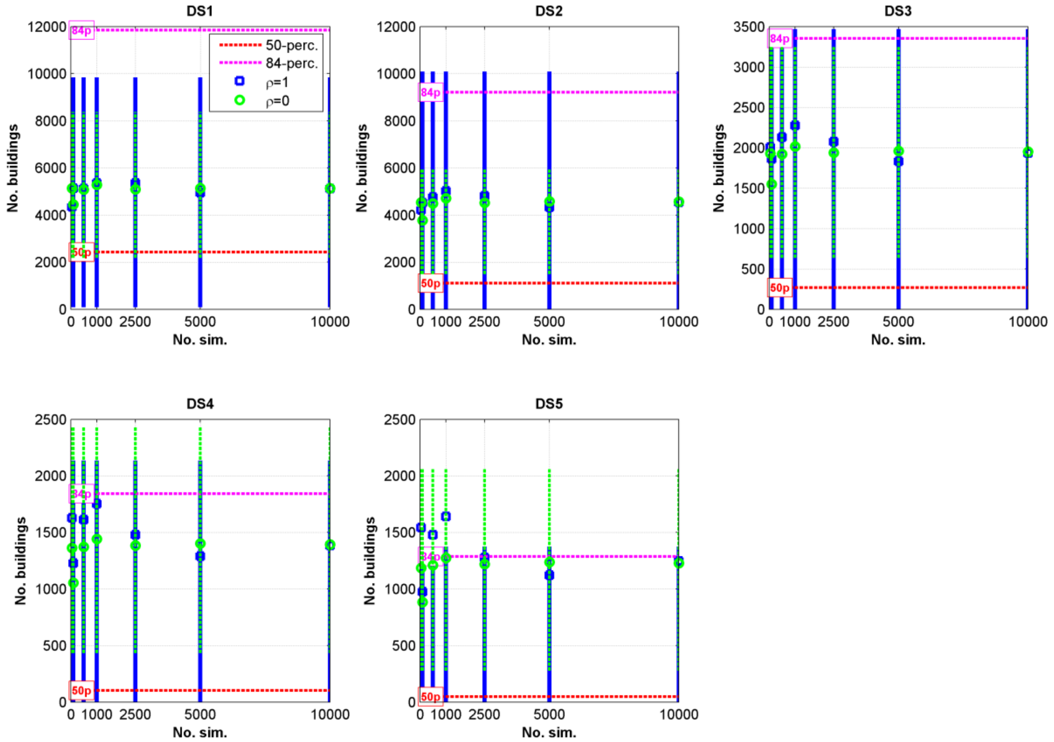

Figure D. 33 Summary plots of the mean and the confidence intervals of the number of buildings in each damage state as a function of the number of Monte Carlo simulations computed with the fully uncorrelated PGA values (ρ=0, green circles) and with the fully correlated PGA values (ρ=1, blue squares). For comparison, the red dashed lines represent the number of buildings computed in the M_w =5 Huizinge earthquake scenario with the 50th percentile PGA values while the magenta lines refer to the 84th percentile PGA input values.

The analysis shows that a relatively small number of Monte Carlo simulations (2500) is sufficient to obtain a good estimate of the numbers of damaged buildings. Hence, a set of 2500 Monte Carlo simulations is used to carry out the casualty estimation with the study area (15 km radius), for the case of fully uncorrelated ground motion variability.

Figure D. 34 compares the 16th percentile, 50th percentile (median), 84th percentile, and mean number of damaged buildings from the Monte Carlo simulations (left panel) with the number of damaged buildings estimated using the 16th percentile PGA values, 50th percentile PGA values, the mean PGA values and the 84th percentile PGA values (right). Figure D. 35 shows the same comparison but in terms of estimated number of casualties. It is noted that the results obtained using the 16th percentile PGA values as input are unconservative and are expected to be exceeded 84% of the time.

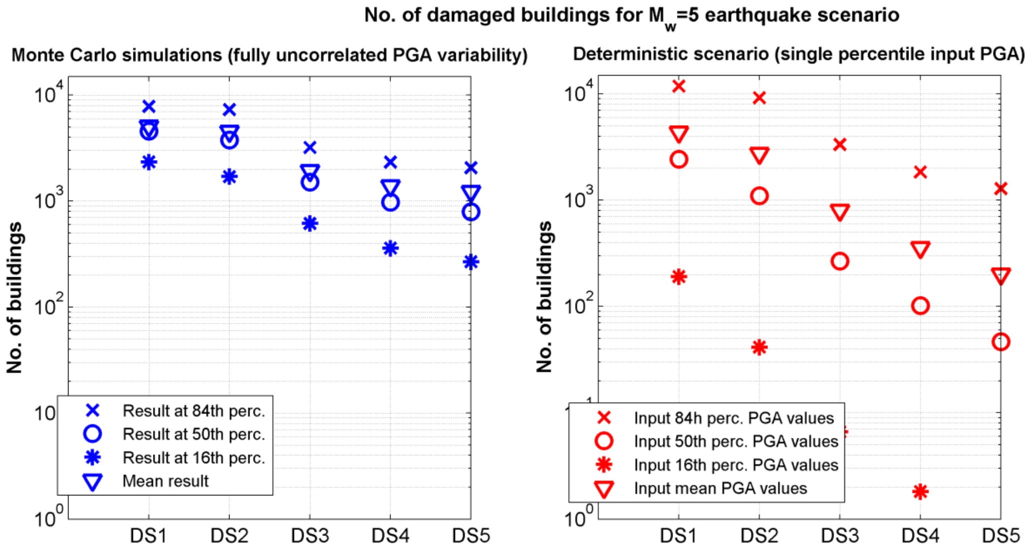

Figure D. 34 Summary of the numbers of damaged buildings obtained with the different approaches for the Huizinge earthquake scenario with M_w =5. Left: 16th, 50th (median), 84th, and mean number of damaged buildings from the Monte Carlo simulations. Right: number of damaged buildings estimated using the 16th percentile PGA values, 50th percentile PGA values, the mean PGA values and the 84th percentile PGA values.

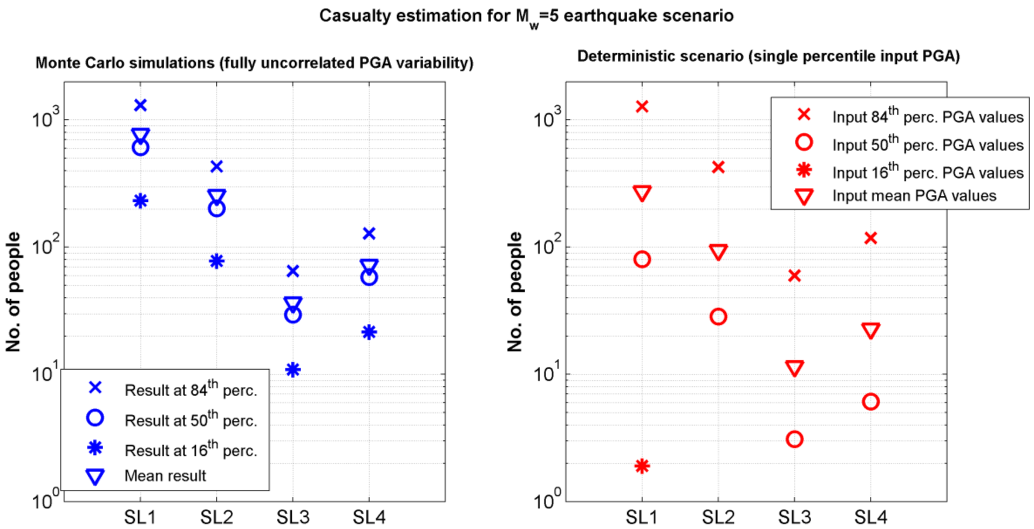

Figure D. 35 Summary of the numbers of casualties estimated with the different approaches for the Huizinge earthquake scenario with M_w=5. Left: 16th, 50th (median), 84th, and mean number of casualties from the Monte Carlo simulations. Right: number of casualties estimated using the 16th percentile PGA values, 50th percentile PGA values, the mean PGA values and the 84th percentile PGA values.

Appendix E

Statistical Definitions

E1 Mean, median and standard deviation of a distribution

In statistics the mean of a probability distribution is the expected value, i.e. the weighted average of all the possible values (x_i) that a random variable can assume. These weights are the probabilities (p_i) associated with each of these values, so that:

$$E[x] = \sum_{i-1}^{N} x_i p_i$$

The standard deviation, also called *sigma*, σ, is a measure of the dispersion and shows how much the data are spread with respect to the mean. A low sigma means that the data are very close while a high value indicates that the data are very disperse. The standard deviation is the square root of the variance, var, that is defined as:

$$\mathrm{var} = E\left[(x-\mu)^2\right]$$

Estimators of variance are:

$$\mathrm{var} = \frac{1}{N}\sum_{i-1}^{N}(x_i - \bar{x}) \quad \text{or} \quad \mathrm{var} = \frac{1}{N-1}\sum_{i-1}^{N}(x_i - \bar{x})$$

A percentile of a distribution is the value below which a certain percentage of observations falls. For example the 30th percentile is the value below which 30% of the observations can be found.

The median is the value that separates the higher half of a data sample from the lower half. Thus, given an ordered one-dimensional vector of data the median is the central value of the vector. The median is thus the 50th percentile of a distribution.

E2 Normal and Lognormal Distributions

The normal (or Gaussian) distribution is a continuous probability distribution. The probability distribution function is:

$$f(x) = \frac{1}{\sigma\sqrt{2\pi}} e^{\frac{-(x-\mu)^2}{2\sigma^2}}$$

where x is the real variable, μ is the mean of the distribution and σ the standard deviation. In the normal distribution mean and median coincide because the distribution is symmetric.

The lognormal distribution is a continuous distribution for which the logarithm of the random variable (Y) is normally distributed. Hence, if Y is lognormally distributed, X=log(Y) is normally distributed. Given μ and σ the mean and standard deviation of the associated normal distribution (X):

- The median (50th percentile) is $Median(Y) = e^{\mu_X}$; and
- The mean is $Mean(Y) = e^{\mu_X + \sigma_X{}^2/2}$.

A graphical description of the probability density functions of the two distributions is provided in Figure E. 1. The top panels show the changes in the distributions (normal on the left and corresponding lognormal on the right) for different sigma value while the bottom panels show the change due to different mean values. A larger sigma leads to a broader bell of the normal distribution and a shift toward left of the lognormal distribution. The change of the mean value instead does not change the shape of the normal distribution which is only shifted so that the peak of the bell coincides with the mean value. In the lognormal distribution these changes lead to a variation in the amplitude of the density function.

(a) Sensitivity to the standard deviation σ (μ=0)

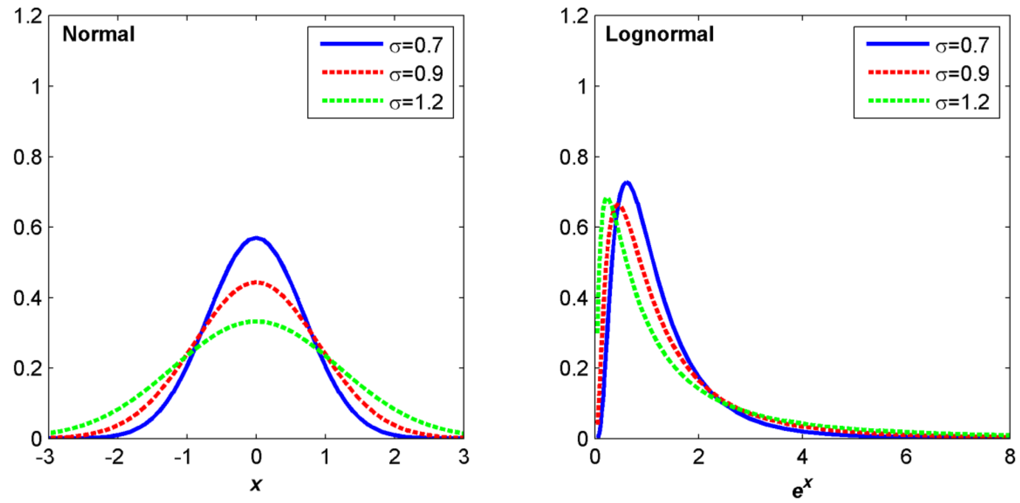

(b) Sensitivity to the mean μ (σ=0.7)

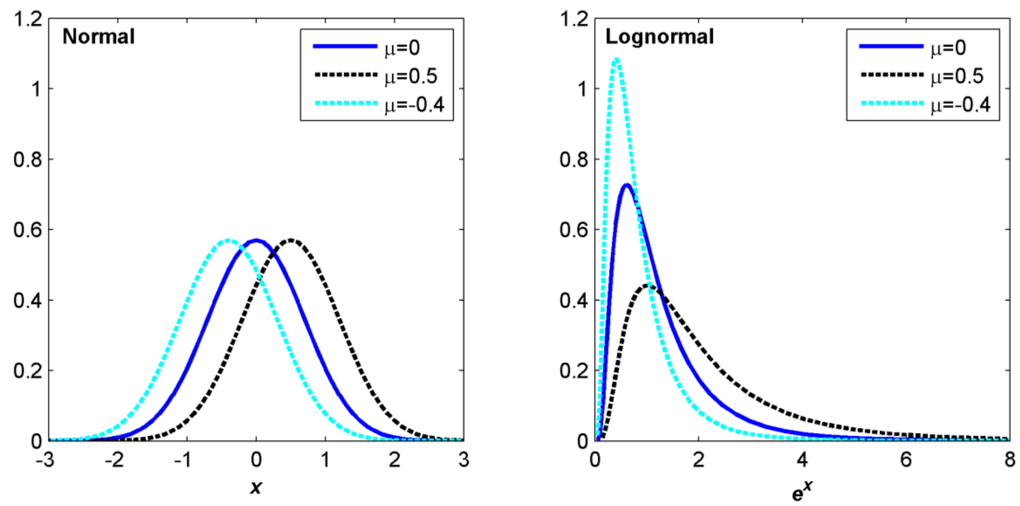

Figure E. 1 Sensitivity of the normal and lognormal distribution to the sigma (σ) value, top, and to the mean (μ), bottom.

Figure E. 2 shows the probability density functions (top) of the normal (left) and the lognormal (right) distribution and the corresponding cumulative density functions (bottom). The figure highlights the location of the mean and the median as well as 16th and 84th percentiles of the distributions. As said the mean and median in the normal distribution coincide while in the lognormal distribution they are different and the separation between the two values depend on the skewness of the distribution (i.e. on the sigma of the corresponding normal distribution).

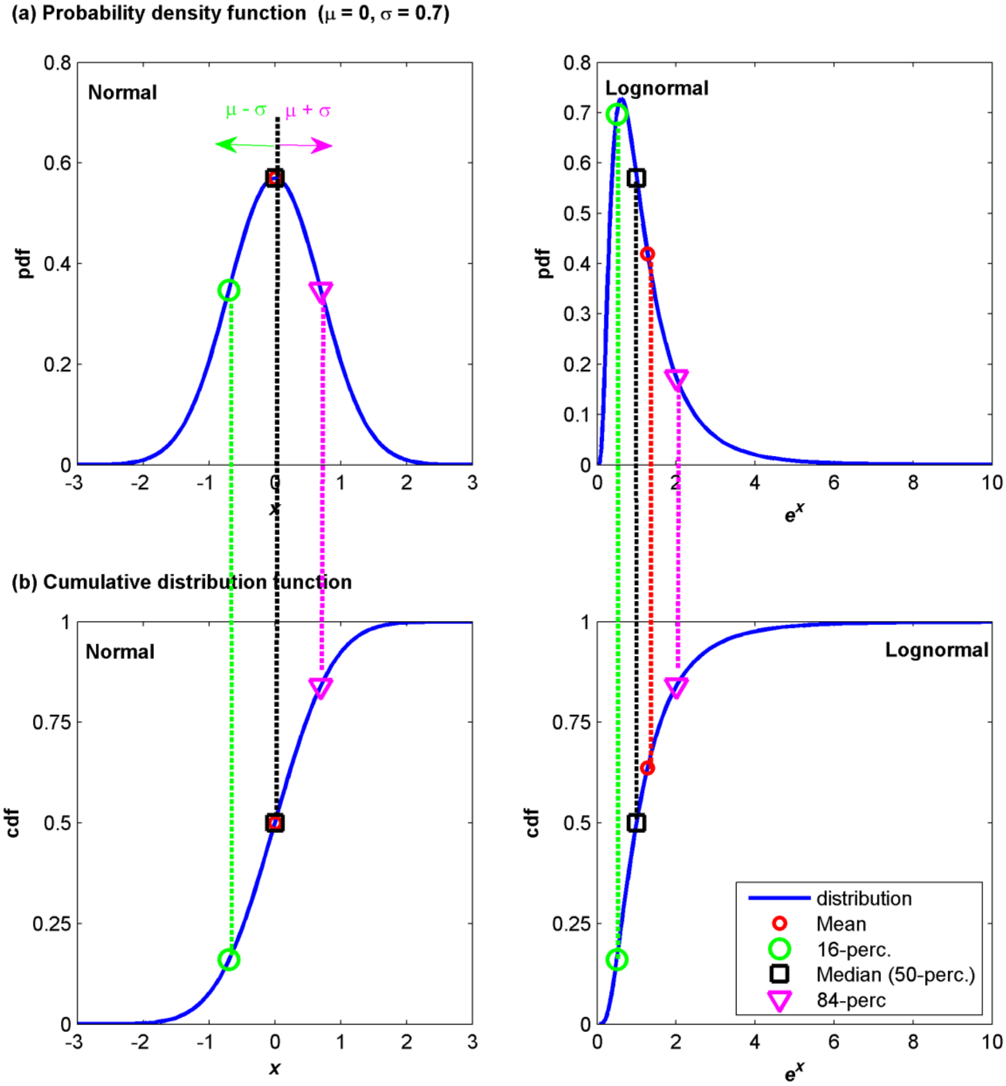

Figure E. 2 Definition of the 16th, 50th, 84th percentiles and mean for the normal (left) and lognormal (right) distribution. Note that for the normal distribution the mean and median values coincide but for the lognormal distribution they are separated.

Appendix F

Glossary

F1 General

Accelerogram: A record of acceleration versus time during an earthquake obtained from an accelerometer.

Accelerometer: An instrument used to measure ground accelerations caused by an earthquake.

Aleatory Variability: This is the natural randomness in a process. For discrete variables, the randomness is parameterised by the probability of each possible value. For continuous variables, the randomness is parameterised by the probability density function.

Attenuation: Decrease in seismic motions with respect to distance from the epicentre, depending on both geometric spreading and the damping characteristics of the ground.

Capacity: The amount of force or deformation an element or component is capable of sustaining.

Casualty classification: Severity levels (SL) are defined as:

SL 1: injuries that require basic medical aid and could be administered by paraprofessionals. They would need bandages or observations;

SL 2: injuries requiring a greater level of medical care and use of medical technology (x-rays or surgery) but not expected to progress to a life threatening status;

SL 3: injuries posing immediate life threatening conditions if not adequately treated; and

SL 4: instantaneously killed or mortally injured.

Collapse: For a given structure type, more than one failure mechanism can be identified as leading to collapse of different extents or parts of the total building envelope. Earthquake induced collapse of a masonry building is defined as failure of one or more exterior walls resulting in partial or complete failure of the roof and/or one or more floors. For an in-situ concrete building collapse is defined as failure of one or more floors or complete failure of part of the framed structure. For a steel frame building collapse refers to failure of the roof or one or more floors due to instability of the frame. For a multi-storey building, collapse refers to more than 50% volume reduction resulting from failure of the roof and one or more floors of the building.

Damage: Non-rehabilitating structural or aesthetic change following a seismic event.

Damage state classification: DS0: no damage;

DS1: negligible to slight damage (no structural damage, slight non-structural damage);

DS 2: moderate damage (slight structural damage, moderate non-structural damage);

DS 3: substantial to heavy damage (moderate structural damage, heavy non-structural damage);

DS 4: very heavy damage (heavy structural damage, very heavy non-structural damage); and

DS 5: destruction (very heavy structural damage).

Damping: A measure of energy dissipation. Damping in a structure is typically defined in terms of percent of critical damping.

Deformation: The amount by which an element or component changes from its initial shape.

Design Earthquake: A theoretical earthquake against which the building will be assessed.

Design Life: The period of time during which a facility or component is expected to perform according to the technical specifications to which it was produced.

Eurocode (EC): Standard suite of structural design guidance adopted across the European Union.

Focal Depth: The conceptual "depth" of an earthquake. If determined from high-frequency arrival-time data, this represents the depth of rupture initiation (the "hypocentre" depth).

Focus: See Hypocentre.

Free Field Ground Motion: The motion that would occur at a given point on the ground owing to an earthquake if vibratory characteristics were not affected by structures and facilities.

Frequency of Exceedance: The frequency at which a specified level of seismic hazard will be exceeded at a site or in a region within a specified time interval.

Geometric Mean: This is a type of mean or average, which indicates the central tendency or typical value of a set of numbers. The geometric mean of two numbers is given by the root square of the product of the numbers. Many GMPEs are derived for the Geometric Mean.

Ground Motion Prediction Equation (GMPE): Also known as “attenuation relationships”, these correlations estimate the ground motion due to an earthquake of a given magnitude at a specific distance. It can also consider the tectonic regime, fault characteristics, focal depth and soil conditions.

Hypocentre: Point in the earth where the seismic disturbance (earthquake) originates. Also known as focus.

In-Plane: In the direction parallel to the plane created by the element's largest dimensions.

KNMI: Koninklijk Nederlands Meteorologisch Instituut.

Large Seismic Event: A seismic event of M5.5 or greater.

Longitudinal Direction: Direction which is parallel to the plane created by the largest two dimensions of an element.

Magnitude: A logarithmic scale of earthquake size, based on seismograph records. A number of different magnitude scales exist, including Richter or local (M_L), surface wave (M_S), body wave (m_b) and duration (M_d) magnitudes. The most common magnitude scale now used is moment magnitude (M_W), which measures the size of earthquakes in terms of the energy released.

Masonry Pier: Vertical element between openings in a masonry wall.

Modal Response: An analytical tool for assessing the dynamic response of a structure's response to vibration (typically taking into account the structures mass and stiffness).

Mode: The specific behaviour of a structure under a defined frequency.

NPR: Nationale Praktijkrichtlijn (Dutch national codes of practice).

NEN: Nederlands Normalisatie-Instituut

NAM: Nederlandse Aardolie Maatschappij

Non-Linear Analysis : Analysis which accounts for deformations in an element or yielding of the material.

Out-of-Plane: In the direction perpendicular to the plane created by the element's largest dimensions.

Peak Ground Acceleration (PGA): The maximum absolute value of ground acceleration displayed on an accelerogram; the greatest ground acceleration produced by an earthquake at a site.

Probabilistic Seismic Hazard Analysis (PSHA): An assessment of the seismic hazard at a given site, taking into account in a probabilistic framework the seismic sources in the area, how often earthquakes of different magnitudes are produced by those sources, what the expected shaking at the site would be under different magnitudes (see “attenuation”) and all the uncertainties in each of these aspects.

Reference Period: A period of time over which a probability calculation is made; for example a reference period for seismic hazard may be the design life of the structure.

Response Spectrum: The plot of structural period against peak response (absolute acceleration, relative velocity or relative displacement) of an elastic, single degree of freedom system, for a specified earthquake ground motion and percentage of critical damping. Relative motions are measured with respect to the ground.

Return Period: The inverse of the annual frequency of occurrence. For example, the ground motion which has a 1% chance of being exceeded at a given point each year has a return period of (1/0.01) or 100 years.

Seismic Action: See Base Shear.

Seismic Hazard: The frequency with which a specified level of ground motion (for instance 20% of ground acceleration) is exceeded during a specified period of time.

Seismic Response: The behaviour of the structure with regards to the base shear and modal response.

Seismicity: The frequency and size of earthquake activity of an area.

Serviceability Limit State (SLS): The combination of loads which relate to the assessment of the building for the functioning or appearance of the structure or comfort of people.

Site Response: The behaviour of a rock or soil column at a site under a prescribed ground motion.

TNO: Nederlandse Organisatie voor Toegepast Natuurwetenschappelijk Onderzoek (Dutch organisation for applied scientific research).

Transverse Direction: Direction which is perpendicular to the plane created by the largest two dimensions of the element.

Ultimate Limit State (ULS): The combination of loads which relate to the assessment of the building for the safety of people, structure or contents.

Uniform Hazard Response Spectrum (UHRS): This is a multi-parameter description of ground motion that can be generated from a probabilistic seismic hazard assessment. It is composed of a number of points which each have an equal likelihood of being exceeded in a given time period.

Unreinforced Masonry (URM): Masonry which does not contain any additional element to strengthen the masonry beyond masonry units and mortar.

Unusable: A damage state whereby a building cannot be used for its primary function – e.g. for residences, the building is not safe to occupy and for hospitals the facilities cannot be used for post-earthquake treatment.

Viscous Damping: Dissipation of seismic energy considered to be proportional to velocities in the structure. Commonly used as a mathematical model to represent sources of energy dissipation that are not explicitly accounted for in the modelling of structural elements, such as cracking in partitions or radiation energy into the soil.

Wall Ties: Objects which connect one leaf of masonry to another object (typically the internal masonry leaf).

F2 Eurocode 8

Capacity Assessment Method: Design method in which elements of the structural system are chosen and suitably designed and detailed for energy dissipation under severe deformations while all other structural elements are provided with sufficient strength so that the chosen means of energy dissipation can be maintained.

Damage Limitation (DL): Structure is only lightly damaged, with structural elements prevented from significant yielding and retaining their strength and stiffness properties. Non-structural components, such as partitions and infills, may show distributed cracking, but the damage could be economically repaired. Permanent drifts are negligible. The structure does not need any repair measures.

Elastic Response: Behaviour of the structure when subject to the design spectrum for elastic analysis.

Lateral Force Method: A simplified linear-elastic analysis method which applies a horizontal load to each storey. This method is only applicable to buildings which are regular in elevation and is within a limiting fundamental period.

Modal Response Spectrum Analysis: A linear-elastic analysis method which applies lateral load depending on the combined modal responses of the specific structure. This method is applicable to buildings which do not meet the Lateral Force Method criteria.

Near Collapse (NC): Structure is heavily damaged, with low residual lateral strength and stiffness, although vertical elements are still capable of sustaining vertical loads. Most non-structural components have collapsed. Large permanent drifts are present. The structure is near collapse and would probably not survive another earthquake, even of moderate intensity.

Non-structural Element: Architectural, mechanical or electrical element, system and component which, whether due to lack of strength or to the way it is connected to the structure, is not considered in the seismic design as load carrying element.

Significant Damage (SD): Structure is significantly damaged, with some residual lateral strength and stiffness, and vertical elements are capable of sustaining vertical loads. Non-structural components are damaged, although partitions and infills have not failed out-of-plane. Moderate permanent drifts are present. The structure can sustain after-shocks of moderate intensity. The structure is likely to be uneconomic to repair.

F3 ASCE 41-13

Acceptance criteria: Limiting values of properties such as drift, strength demand and inelastic deformation used to determine the acceptability of a component at a given performance level (See also performance levels).

Collapse Prevention (S-5): Post-earthquake damage state in which the building is on the verge of partial or total collapse. Substantial damage to the structure has occurred, potentially including significant degradation in the stiffness and strength of the lateral-force-resisting system, large permanent lateral deformation of the structure, and - to a more limited extent - degradation in vertical-load-carrying capacity. However, all significant components of the gravity-load-resisting system must continue to carry their gravity loads. Significant risk of injury due to falling hazards from structural debris might exist. The structure might not be technically practical to repair and is not safe for re-occupancy, as aftershock activity could induce collapse.

Damage Control (S-2): Midway point between Life Safety and Immediate Occupancy. It is intended to provide a structure with a greater reliability of resisting collapse and being less damaged than a typical structure, but not to the extent required of facility structure designed to meet the Immediate Occupancy performance level.

Demand: The amount of force or deformation imposed on an element or component.

Diaphragm: A horizontal (or nearly horizontal) structural element used to transfer inertial lateral forces to vertical elements of the lateral-force-resisting system.

Drift: Horizontal deflection at the top of the storey relative to the bottom of the storey.

Flexible Diaphragm: A diaphragm with horizontal deformation along its length twice or more than twice the average storey drift.

Fundamental Period: The natural period of the building in the direction under consideration which has the greatest mass participation.

Immediate Occupancy (S-1): Post-earthquake damage state in which only very limited structural damage has occurred. The basic vertical- and lateral-force-resisting systems of the building retain nearly all of their pre-earthquake strength and stiffness. The risk of life-threatening injury as a result of structural damage is very low, and although some minor structural repairs might be appropriate, these would generally not be required prior to re-occupancy. Continued use of the building will not be limited by its structural condition, but might be limited by damage or disruption to non-structural elements of the building, furnishings, or equipment and availability of external utility services.

Life Safety (S-3): Post-earthquake damage state in which significant damage to the structure has occurred but some margin against either partial or total structural collapse remains. Some structural elements and components are severely damaged but this has not resulted in large falling debris hazards, either inside or outside the building. Injuries might occur during the earthquake; however, the overall risk of life-threatening injury as a result of structural damage is expected to be low. It should be possible to repair the structure; however, for economic reasons this might not be practical. Although the damaged structure is not an imminent collapse risk, it would be prudent to implement structural repairs or install temporary bracing prior to re-occupancy.

Limited Safety (S-4): Midway point between Life Safety and Collapse Prevention. It is intended to provide a structure with a greater reliability of resisting collapse than a structure that only meets the collapse prevention performance, but not to the full level of safety that the life safety performance level would imply.

Load Duration: The period of continuous application of a given load, or the cumulative period of intermittent applications of load.

Probability of Exceedance: The probability that a specified level of ground motion or specified social or economic consequences of earthquakes will be exceeded at a site or in a region during a specified period of time.

Rigid Diaphragm: A diaphragm with horizontal deformation along its length less than half the average storey drift.

Shear Wall: A wall that resists lateral forces applied parallel with its plane. Also known as an in-plane wall.

Stiff Diaphragm: A diaphragm that is neither flexible nor rigid.

Target Displacement: An estimate of the maximum expected displacement of the roof of a building calculated for the design earthquake.